



**Chemical and functional analyses of the plant cuticle as leaf
transpiration barrier**

**Chemie-Funktionsanalysen der pflanzlichen Kutikula als
Transpirationsbarriere**

Doctoral thesis for a doctoral degree
at the Graduate School of Life Sciences,
Julius-Maximilians-Universität Würzburg,
Section Integrative Biology

submitted by
Ann-Christin Schuster
from Ingolstadt

Würzburg 2016

Submitted on:

Members of the *Promotionskomitee*:

Chairperson:	Prof. Dr. Thomas Müller
Primary Supervisor:	Prof. Dr. Markus Riederer
Supervisor (Second):	Prof. Dr. Dirk Becker
Supervisor (Third):	Dr. Adrian Friedmann
Supervisor (Fourth):	Dr. Markus Burghardt

Date of Public Defence:

Date of Receipt of Certificates:

Table of contents

Introduction	1
1 The plant cuticle	2
1.1 Cutin polymer	3
1.2 Cuticular waxes	4
1.3 Biosynthetic origin of cutin and cuticular waxes	7
2 The plant cuticle as transpiration barrier	8
2.1 Definition of transport parameters	8
2.2 The plant cuticle as transpiration barrier	10
3 Aim of the present study	13
Materials and methods	16
1 Leaf characteristics	16
1.1 Plant material and leaf harvest	16
1.2 Saturated fresh weight, dry weight and relative water deficit	17
1.3 Leaf area	18
1.4 Degree of succulence, specific leaf area and leaf water content	18
1.5 Stomata density	19
1.6 Leaf surface properties by scanning electron microscopy	19
2 Leaf thermal tolerance and leaf dehydration tolerance	19
3 Leaf area shrinkage and leaf water potential to correct transpiration rates and conductances	20
4 Transpiration rate and minimum conductance	21
5 Transpiration rate and cuticular permeance	23
6 Temperature effect on minimum conductance and cuticular permeance	24
7 Gravimetric and chemical analysis of the cuticular components	25
7.1 Isolation of cuticular membranes	25
7.2 Gravimetric analysis of the cuticular components	26
7.3 Extraction of the cuticular waxes for chemical analysis	26
7.4 Extraction of the cutin monomers for chemical analysis	27
7.5 Chemical analysis of the cuticular waxes and the cutin monomers	27
7.6 Average carbon chain length	28
8 Statistical analyses	29

Chapter I. The leaf minimum conductance and the temperature effect on the cuticular transpiration barrier of the desert plant

***Rhazya stricta*..... 30**

1 Introduction 30

2 Results 33

 2.1 Leaf characteristics of *Rhazya stricta* 33

 2.2 Leaf thermal tolerance and leaf dehydration tolerance 34

 2.3 Leaf area shrinkage and leaf water potential to correct transpiration rates and conductances 35

 2.4 Leaf drying curve, minimum conductance and temperature effect on minimum conductance 37

 2.5 Gravimetric and chemical analysis of the cuticular components 40

 2.5.1 Chemical analysis of the cuticular leaf wax 40

 2.5.2 Chemical analysis of the cutin monomers 43

3 Discussion..... 45

 3.1 Measurement of the minimum conductance: evaluation and correction 45

 3.2 Classification of the minimum conductance 46

 3.3 Cuticular wax chemistry and minimum water permeability..... 49

 3.4 Conclusion 52

Chapter II. Comparison of the temperature effect on the minimum conductance and the cuticular permeance of the Mediterranean

sclerophyll *Nerium oleander* 53

1 Introduction 53

2 Results 55

 2.1 Leaf characteristics of *Nerium oleander*..... 55

 2.2 Leaf thermal tolerance 56

 2.3 Cuticular permeance and temperature effect on cuticular permeance 56

 2.4 Leaf drying curve, minimum conductance and temperature effect on minimum conductance 58

 2.5 Gravimetric and chemical analysis of the cuticular components 61

 2.5.1 Chemical analysis of the cuticular leaf wax 61

 2.5.2 Chemical analysis of the cutin monomers 64

3 Discussion..... 66

3.1	Classification and comparison of the minimum conductance and the cuticular permeance.....	66
3.2	Temperature effect on the minimum conductance and the cuticular permeance	68
3.3	Shift of relative water deficit at stomatal closure at elevated temperatures	70
3.4	Cuticular wax chemistry and minimum or cuticular water permeability	71
3.5	Conclusion	72
Chapter III. Temperature effect on the cuticular permeance of		
<i>Prunus laurocerasus</i>		
74		
1	Introduction	74
2	Results	76
2.1	Leaf thermal tolerance	76
2.2	Cuticular permeance and temperature effect on cuticular permeance	76
3	Discussion.....	80
3.1	Classification and comparison of the cuticular permeance	80
3.2	Temperature effect on the cuticular permeance.....	82
3.3	Conclusion	85
Chapter IV. Cuticular barrier properties and thermal tolerances of		
plants in hot and dry environments.....		
86		
1	Introduction	86
2	Results	89
2.1	Leaf characteristics and minimum conductance	89
2.2	Leaf thermal tolerance	93
2.3	Leaf thermal tolerance and minimum conductance.....	94
2.4	Chemical analysis of the cuticular leaf wax.....	95
2.4.1	Cuticular leaf wax from <i>Hippocrepis comosa</i>	95
2.4.2	Cuticular leaf wax from <i>Helianthemum apenninum</i>	98
2.4.3	Cuticular leaf wax from <i>Geranium sanguineum</i>	101
2.4.4	Cuticular leaf wax from <i>Sanguisorba minor</i>	105
2.4.5	Cuticular leaf wax from <i>Sesleria albicans</i>	108
2.4.6	Cuticular leaf wax from <i>Pulsatilla vulgaris</i>	110
2.4.7	Cuticular leaf wax from <i>Teucrium chamaedrys</i>	112
2.4.8	Cuticular leaf wax from <i>Salvia pratensis</i>	114
2.4.9	Cuticular leaf wax from <i>Plantago lanceolata</i>	117

2.5	Cuticular wax chemistry and minimum water permeability.....	120
3	Discussion.....	121
3.1	Leaf characteristics and minimum conductance	121
3.2	Leaf thermal tolerance	123
3.3	Leaf thermal tolerance and minimum conductance.....	124
3.4	Cuticular wax chemistry and minimum water permeability.....	125
3.5	Conclusion	127
Chapter V. Chemical and functional analyses of the plant cuticle as leaf transpiration barrier.....		129
1	Introduction	129
2	Results	131
2.1	Minimum conductance and cuticular permeance	131
2.2	Chemical analysis of the cuticular leaf wax.....	132
2.2.1	Cuticular leaf wax from <i>Solanum lycopersicum</i>	132
2.2.2	Cuticular leaf wax from <i>Solanum surratense</i>	134
2.2.3	Cuticular leaf wax from <i>Vanilla planifolia</i>	137
2.2.4	Cuticular leaf wax from <i>Juglans regia</i>	140
2.2.5	Cuticular leaf wax from <i>Prunus laurocerasus</i>	142
2.2.6	Cuticular leaf wax from <i>Olea europaea</i>	145
2.3	Cuticular wax chemistry and minimum or cuticular water permeability	147
3	Discussion.....	153
3.1	Classification of the minimum conductance and the cuticular permeance	153
3.2	Chemistry of the plant cuticle	154
3.3	Cuticular wax chemistry and minimum or cuticular water permeability	155
3.4	Conclusion	160
Summarising discussion.....		162
1	Temperature effect on the minimum or cuticular water permeability	162
2	The plant cuticle as leaf transpiration barrier	165
Summary.....		168
Zusammenfassung		170
References.....		172
Annex.....		188
Publications and presentations		198

Curriculum vitae.....	199
Acknowledgements	200
Affidavit	201
Eidesstattliche Erklärung	201

Introduction

The epidermis of all aerial primary plant organs is covered with a continuous extracellular membrane, the plant cuticle. The main function of the plant cuticle is to protect the plant against uncontrolled non-stomatal water loss from the interior of leaves, fruits, stems and flowers into the surrounding atmosphere (Kerstiens 1996b, Riederer and Schreiber 2001). Stomatal and cuticular transpiration are two different processes that account for water loss. The majority of water diffuses through stomatal pores, whose closure can be regulated to minimise stomatal water loss. The remaining water transpiration occurs through the cuticular membrane.

The plant cuticle is a multifunctional barrier, which plays a role in the physiology, ecology and development of the plant (Kerstiens 1996a, Riederer 2006a, Yeats and Rose 2013). Cuticular membranes attenuate ultraviolet radiation (Krauss *et al.* 1997) and enhance the reflectance of both UV and photosynthetically active wavelength radiation (Holmes and Keiller 2002). The maintenance of the structural integrity and stability, in addition to being flexible enough to accommodate externally applied forces such as wind, rain, dust, snow and leaf-to-leaf contact, is of upmost mechanical importance (Bargel *et al.* 2006, Shepherd and Griffiths 2006). Plant cuticular membranes are typically viscoelastic, which is thought to reduce the risk of mechanical failure, such as fruit cracking (Matas *et al.* 2004), and to facilitate the expansion and/or shrinkage of leaves (Edelmann *et al.* 2005). Cuticular membranes form mechanical barriers against pests and pathogens (Eigenbrode and Espelie 1995, Müller 2006). This can affect the foraging behaviour of predators (Gentry and Barbosa 2006) and determine fungal pathogen development (Hansjakob *et al.* 2011). Additionally, the plant phyllosphere hosts microbial communities (Leveau 2006, Reisberg *et al.* 2013). The plant cuticle enables a self-cleaning mechanism (lotus effect) in many plant species, with the adhesion of contaminating particles being reduced due to water repellence (Barthlott and Neinhuis 1997, Bargel *et al.* 2006). During plant development the cuticle seems to play an important role in preventing organ fusion (Smirnova *et al.* 2013, Yeats and Rose 2013).

1 The plant cuticle

Plant cuticles are commonly composed of two major hydrophobic constituents: the insoluble polymer cutin and the solvent-soluble cuticular waxes. Another major lipid polymer which is often present in plant cuticles is cutan. Polysaccharides, such as pectin and cellulose, are also described as cuticle constituents (Holloway 1982a, Jeffree 1996, López-Casado *et al.* 2007). Plant cuticles are heterogeneous in both composition and structure, differing between layers that are chemically characterised by different components. The proposed structure of the layered cuticle differs between the outer cuticle proper and the inner cuticle layer. The thin cuticle proper is rich in cutin and embedded cuticular waxes. The cuticle layer contains cutin, cuticular waxes and polysaccharides. The cuticular waxes are embedded within the cutin matrix (intracuticular wax) and additionally deposited in the outermost layer, as either wax crystals and/or wax films (epicuticular wax; Figure 1; Holloway 1982a, Jeffree 1996, 2006).

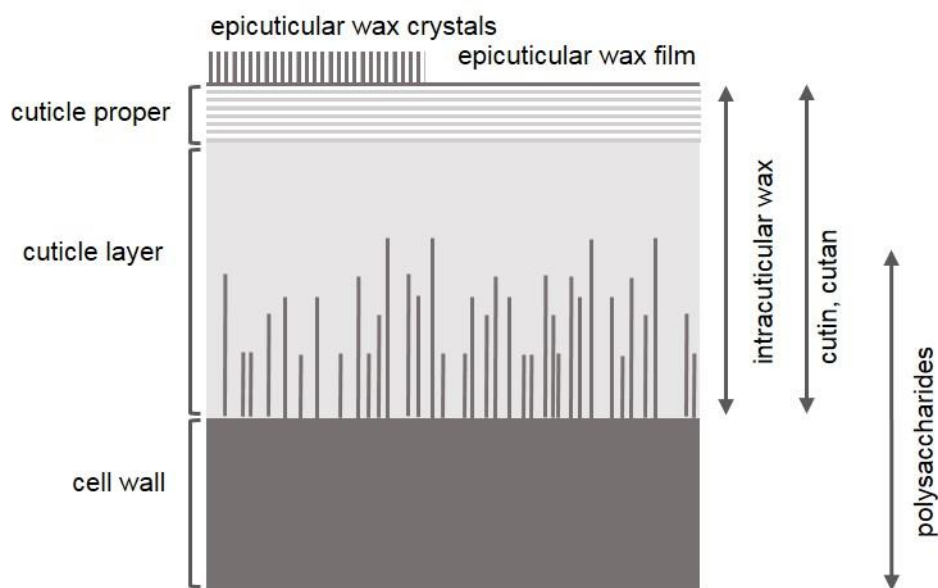
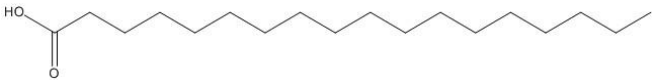
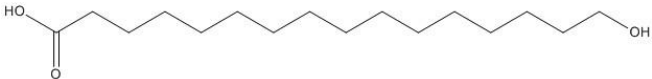
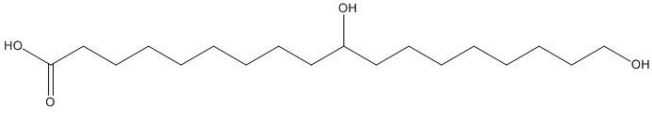
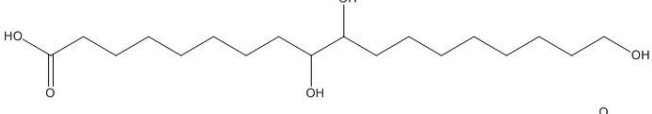
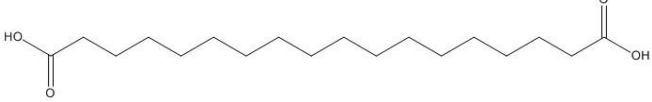
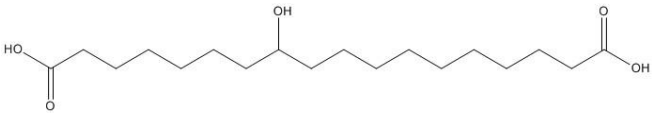
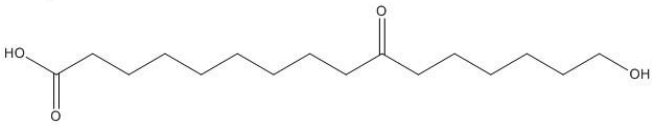
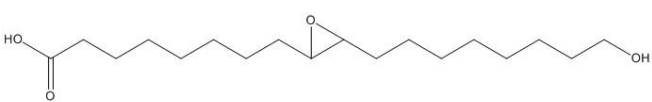


Figure 1. Structural features of a simplified cross section of a plant cuticle and the major chemical components of the different layers (according to Holloway 1994, Bargel *et al.* 2006). Thickness varies from 0.02 μm in *Arabidopsis thaliana* leaves (Franke *et al.* 2005) to 225 μm in *Ariocarpus fissuratus* stems (Loza-Cornejo and Terrazas 2003).

1.1 Cutin polymer

The cutin polymer is typically composed of substituted C₁₆ and C₁₈ alkanolic acid monomers. Common monomers include hydroxyalkanoic acids and alkandioic acids and often contain additional hydroxy, carboxylic, epoxy and oxo groups in secondary, mostly mid-chain positions (Table 1). Other cutin components are glycerol and phenolic acids (Kolattukudy 1980, Graça *et al.* 2002, Franke *et al.* 2005, Leide *et al.* 2007). Cutin types can be classified into three groups according to the main monomer composition: C₁₆, C₁₈ or a mixture of C₁₆ and C₁₈ (Holloway 1982b).

Table 1. Representative structures of common cutin monomers (Pollard *et al.* 2008, Yeats and Rose 2013). The cutin quantity varies between 0.4 µg cm⁻² in *Arabidopsis thaliana* leaves (Franke *et al.* 2005) and 1500 µg cm⁻² in red ripe tomato fruits (*Solanum lycopersicum*; Leide *et al.* 2011).

	common cutin monomer types	carbon chain length
alkanoic acids		18
hydroxyalkanoic acids		16
dihydroxyalkanoic acids		18
trihydroxyalkanoic acids		18
alkandioic acids		18
hydroxyalkandioic acids		18
hydroxyoxoalkanoic acids		16
epoxyhydroxyalkanoic acids		18


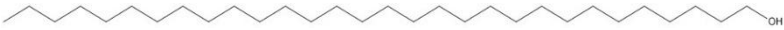



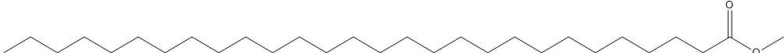
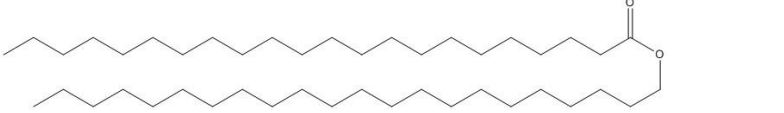
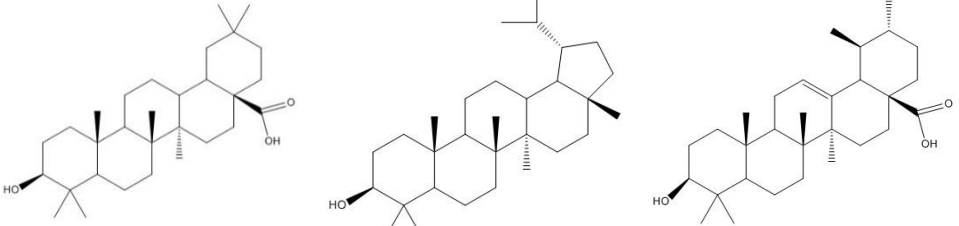
The proposed structure of the cutin polymer is a three-dimensional network of ester-linked cutin monomers. Most of the primary hydroxy groups of the alkanolic acids are ester-linked, which creates linear structures. On the other hand, the secondary mid-chain groups are only partially esterified, which generates cross-linked or branched structures (Kolattukudy 1980, Deshmukh *et al.* 2003).

After de-esterification of the cutin, a highly resistant residue often remains, known as the cuticle polymer cutan. The structure and function of cutan is still unknown. Series of *n*-alkanes, alkenes, alkadienes, alkanolic acids, alkanedioic acids and trihydroxybenzene moieties (Nip *et al.* 1986, McKinney *et al.* 1996, Shouten *et al.* 1997) are part of the polymer and are mainly ether-linked, which forms a three-dimensional network (Villena *et al.* 1999). Cuticular membranes without cutan (*Solanum lycopersicum*, *Citrus limon*), without cutin (*Beta vulgaris*) and with mixed cutin/cutan polymers (*Agave americana*, *Clivia miniata*) have been described (Nip *et al.* 1986, Jeffree 1996, Gupta *et al.* 2006).

1.2 Cuticular waxes

The cuticular waxes are typically mixtures of very-long-chain acyclic hydrocarbon backbones, the common component classes being *n*-alkanes, primary alkanols, alkanolic acids, alkanals and alkyl esters. Other very-long-chain acyclic cuticular wax component classes are branched alkanes, secondary alkanols, alkanol acetates, alkanones and methyl esters (Table 2). Common homologous series have carbon chain lengths of C₂₀ up to C₃₇ (Kolattukudy 1970, Martin and Juniper 1970, Bianchi *et al.* 1995, Jetter *et al.* 2006). Even-numbered carbon chain lengths dominate the alkanolic acids, the primary alkanols and the alkanals and odd-numbered carbon chain lengths dominate the *n*-alkanes, the secondary alkanols and the alkanones (Jetter *et al.* 2006). Alkyl esters have carbon chain lengths of C₃₆ up to C₅₂ and are composed of alkanolic acids esterified with primary alkanols (Gülz *et al.* 1994). Pentacyclic triterpenoids, mainly of the oleanane, lupane and ursane type, are common cyclic components of the cuticular waxes (Table 2). β -Amyrin, erythrodiol and oleanolic acid are common structures of the oleanane type. Representative structures of the lupane type are lupeol, betulin and betulinic acid. α -Amyrin, uvaol and ursolic acid represent the ursane type. Other cyclic components detected in cuticular waxes are tocopherols and phytosterols. However, phytosterols might be solvent-extracted from inner tissues (Kolattukudy 1970, Martin and Juniper 1970, Bianchi *et al.* 1995, Jetter *et al.* 2006).

Table 2. Representative structures of common cuticular very-long-chain acyclic and cyclic wax components.

	common cuticular wax component classes	carbon chain length
<i>n</i> -alkanes		29
primary alkanols		30
alkanol acetates		30
alkanoic acids		30
alkanals		30
methyl esters		28
alkyl esters		44
pentacyclic triterpenoid types		
	<div style="display: flex; justify-content: space-around;"> <div style="text-align: center;"> <p>oleanane example: oleanolic acid</p> </div> <div style="text-align: center;"> <p>lupane example: lupeol</p> </div> <div style="text-align: center;"> <p>ursane example: ursolic acid</p> </div> </div>	

The proposed structure of the cuticular waxes differs between three fractions, each with different degrees of order and composition. Cuticular waxes are partially present as highly ordered orthorhombic crystalline fractions (Basson and Reynhardt 1988, Reynhardt and Riederer 1991, Reynhardt and Riederer 1994, Merk *et al.* 1998). The middle portions of the very-long-chain acyclic wax components align (orthorhombic crystal lattice) with the vertical orientation towards the leaf surface. These crystalline fractions form flakes with probable parallel orientation to the outer surface of the cuticle. The chain ends of the very-long-chain acyclic wax components form a second, less ordered amorphous fraction. Short-chain components and cyclic components are

excluded from the crystalline fraction and contribute to the amorphous fraction or form, if present in sufficiently high quantities, another amorphous fraction (Figure 2; Riederer and Schreiber 1995).

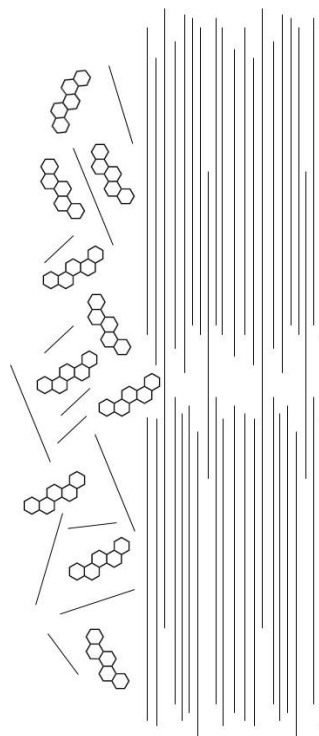


Figure 2. Molecular features of a simplified order of the cuticular waxes. The major chemical very-long-chain acyclic and cyclic wax components are shown (according to Riederer and Schreiber 1995).

The cuticular waxes are heterogeneous in both quantity and quality. This heterogeneity is evident when looking at different plant species (Schreiber and Riederer 1996, Belge *et al.* 2014), organ types, tissues (Jetter *et al.* 2000, Vogg *et al.* 2004, Szakiel *et al.* 2012, 2013), developmental stages (Hauke and Schreiber 1998, Jetter and Schäffer 2001, Leide *et al.* 2007, Pensec *et al.* 2014) and environmental growth conditions (Baker 1974, Giese 1975, Riederer and Schneider 1990, Hauke and Schreiber 1998, Bouzoubaâ *et al.* 2006, Cordeiro *et al.* 2011, Szakiel *et al.* 2012).

Leaf cuticular wax coverage varies strongly between plant species. Minor wax coverages reported vary between $0.4 \mu\text{g cm}^{-2}$ (*Morus alba* leaves; Mamrutha *et al.* 2010) and $0.8 \mu\text{g cm}^{-2}$ (*Arabidopsis thaliana* leaves; Aharoni *et al.* 2004). Medium wax coverages are in the range between $8.0 \mu\text{g cm}^{-2}$ (*Hordeum vulgare* leaves; Hansjakob *et al.* 2010) and $28.0 \mu\text{g cm}^{-2}$ (*Ligustrum vulgare* leaves; Buschhaus *et al.* 2007b). Major wax coverages reported are between $72.0 \mu\text{g cm}^{-2}$ (*Ziziphus joazeiro* leaves;

Oliveira and Salatino 2000) and $160.0 \mu\text{g cm}^{-2}$ (*Argania spinosa* leaves; Bouzoubaâ *et al.* 2006).

The diverse heterogeneity is once again evident when the focus lies on different wax compositions among different plant species. A diverse mixture of component classes is common for some plant species (Aharoni *et al.* 2004, Szafranek and Synak 2006), while one single component or a dominating component class is found in other cuticular waxes (Ji and Jetter 2007, Hansjakob *et al.* 2010, Oliveira and Salatino 2000).

Epicuticular and intracuticular waxes can be mechanically and chemically separated in different layers. The epicuticular waxes from *Prunus laurocerasus* leaves are entirely composed of very-long-chain acyclic cuticular wax components, whereas pentacyclic triterpenoids comprise 63% of the intracuticular waxes (Jetter *et al.* 2000). The predominant accumulation of pentacyclic triterpenoids in the intracuticular wax layer has been confirmed in both *Ligustrum vulgare* and *Rosa canina* leaves (Buschhaus *et al.* 2007a, b, Buschhaus and Jetter 2011).

Epicuticular waxes are deposited on the surface as either wax crystals and/or wax films, with both possibilities exhibiting considerable variation in microstructures. Barthlott *et al.* (1998) classified 23 epicuticular wax types, differing between films, layers, crusts and crystals. Common wax types are associated with certain major chemical components. For example, primary alkanols typically form platelets (Koch *et al.* 2009).

1.3 Biosynthetic origin of cutin and cuticular waxes

Genetic studies with *Arabidopsis* and tomatoes have improved the understanding of both cutin and cuticular wax biosynthesis. In plastids of epidermal cells, C_{16} and C_{18} alkanolic acid precursors are derived from *de novo* synthesis and are catalysed by a fatty acid synthase (FAS) enzyme complex (Ohlrogge and Browse 1995, Post-Beittenmiller 1996). The alkanolic acid precursors are converted to coenzyme A (CoA) thioesters by long-chain acyl-coenzyme A synthases (LACS1 and LACS2) and transported into the endoplasmic reticulum (Schnurr *et al.* 2002, Lee and Suh 2013). The C_{16} -CoA and C_{18} -CoA are the precursors for both cutin and wax biosynthesis.

Three major protein groups are important for cutin synthesis: the long-chain acyl-coenzyme A synthases (LACS), hydroxylases (CYP86 and CYP77 subfamily of cytochrome P450) and acyltransferases (GPAT, glycerol-3-phosphate acyltransferase; Yeats and Rose 2013). The sequential order is still unknown; however, there is evidence that the end-chain hydroxylation of the cutin monomers precedes the mid-

chain hydroxylation (Li-Beisson *et al.* 2009). The acyltransferases esterify acyl groups (Yang *et al.* 2010), linking cutin precursors to glycerols and producing acylglycerols. This transfer to glycerol is probably occurring after the end-chain hydroxylation (Yang *et al.* 2012). The polymerization site of the precursors remains uncertain. Recently, Yeats *et al.* (2012) found a cutin synthase (CD1) localized in the developing cuticle.

The cuticular wax biosynthesis continues in the endoplasmic reticulum through the elongation of the long-chain alkanolic acids, with the successive addition of two carbon units per cycle derived from malonyl-CoA via the fatty acid elongase (FAE) enzyme complex, to very-long-chain alkanolic acids (VLCFA, $\geq C_{20}$; Joubes *et al.* 2008). Three distinct pathways play a role in producing the typical wax components. The decarbonylation pathway forms alkanes through alkanals as intermediate products. Secondary alkanols and alkanones are derived from alkanes. The acyl-reduction pathway forms primary alkanols. The primary alkanols can be esterified to alkanolic acids to form wax esters. Additionally, free alkanolic acids are released (Millar *et al.* 1999, Samuels *et al.* 2008, Yeats and Rose 2013).

The cuticular wax and cutin components need to be transported through the plasma membrane and the polysaccharide cell wall to the cuticular membrane. ATP-binding cassette (ABC) transporters (McFarlane *et al.* 2010) and lipid transfer proteins (Kim *et al.* 2012) play a role in cutin and wax export.

2 The plant cuticle as transpiration barrier

2.1 Definition of transport parameters

The transpiration rate (J) characterises the water movement across plant cuticles and is calculated as the amount of water transpired per time ($\Delta W \Delta t^{-1}$) and exposed area (A).

$$J = \frac{\Delta W}{\Delta t \cdot A}$$

From the transpiration rate two important transport parameters, the minimum conductance (g_{\min}) and the cuticular permeance (P), are calculated. Both describe the diffusion of water through plant cuticles and consider the driving force. The driving

force is the concentration difference of water between the leaf and the atmosphere, that is the density of water (ρ_w) and water activity (a ; Burghardt and Riederer 2006).

$$J = g_{min \text{ or } P} \cdot \rho_w \cdot \Delta a$$

The minimum conductance is the lowest conductance a leaf can reach with completely closed stomata as a result of desiccation stress (Körner 1995). The term cuticular permeance refers to the permeance measured in stomata-free systems (Kerstiens 1996b).

The calculations of the minimum conductance and the cuticular permeance are either based on the water density in the liquid state or the water density in the vapour state. For the calculation based on the water density in the liquid state 0.9971 g cm^{-3} (ρ_w^{liquid} at $25 \text{ }^\circ\text{C}$; Nobel 2009) is used to calculate g_{min} or P .

$$g_{min \text{ or } P} = \frac{J}{\rho_w^{\text{liquid}} (a_{\text{leaf}} - a_{\text{air}})}$$

For the calculation based on the water density in the vapour state, the water vapour content of air at saturation is used to calculate g_{min} or P ($c_{wv}^* = 23.07 \text{ g m}^{-3}$ at $25 \text{ }^\circ\text{C}$; Burghardt and Riederer 2006, Nobel 2009).

$$g_{min \text{ or } P} = \frac{J}{c_{wv}^* (a_{\text{leaf}} - a_{\text{air}})}$$

Cuticular permeances referenced to the water vapour are by the conversion factor 43384 times greater than cuticular permeances referenced to the liquid state (at $25 \text{ }^\circ\text{C}$ and standard pressure; Kerstiens 2006). The water vapour based g_{min} or P are advantageous when analysing temperature effects on cuticular permeabilities (Kerstiens 1996b).

A third option often encountered in literature is the mole fraction based conductance (g_{mol}), which uses the vapour pressure difference ($P_{wv}^* = 3.169 \text{ kPa}$ at $25 \text{ }^\circ\text{C}$; Nobel 2009) and the atmospheric pressure ($P_A = 101.3 \text{ kPa}$, standard conditions) as driving force (Burghardt and Riederer 2006).

$$J_{mol} = g_{mol} \frac{\Delta P_{wv}^*}{P_A} = g_{mol} \frac{\Delta P_{wv}^* (a_{leaf} - a_{air})}{P_A}$$

The conversion factor is g_{min} or P of $1.00 \cdot 10^{-5} \text{ m s}^{-1}$ to an equivalent of $0.41 \text{ mmol m}^{-2} \text{ s}^{-1}$ (standard conditions; Kerstiens 1996b).

2.2 The plant cuticle as transpiration barrier

The main function of the plant cuticle is the protection against uncontrolled non-stomatal diffusion of water into the atmosphere (Kerstiens 1996b, Riederer and Schreiber 2001). Together, with the hydrophobic cutin, the cuticular waxes constitute the lipophilic pathway. Water, as a small, polar, non-ionic molecule, diffuses through the lipophilic pathway, which is reserved for lipophilic non-ionised substances (Niederl *et al.* 1998, Buchholz 2006, Schreiber 2006). A second parallel pathway, the polar pathway, is formed by hydrated polar domains and is reserved for ionised substances, such as inorganic ions, charged and uncharged organic molecules. Water molecules are able to diffuse through both the lipophilic and the polar pathway (Schönherr 2000, 2006, Schreiber *et al.* 2001, Schreiber 2005).

Separate functional analysis of the two major hydrophobic components, conducted with enzymatically isolated cuticular membranes, proved the establishment of the main transport-limiting barrier by the cuticular waxes. Removal of the cuticular waxes with organic solvents led to an increased cuticular water permeability and, thus, an increased cuticular permeance (Schönherr 1982, Schreiber 2002).

Thick cuticular membranes do not establish more efficient transpiration barriers (Kamp 1930, Schreiber and Riederer 1996, Riederer and Schreiber 2001, Anfodillo *et al.* 2002). Fruits, for example, exhibit thick cuticles associated with high cuticular permeances (Schreiber and Riederer 1996). Given that there are strong indications that cuticular waxes form the main transport-limiting barrier, these are assumed to play a role in regulating cuticular transpiration. There is no simple relationship between the wax quantity and cuticular water permeability. The gravimetrically obtained wax amount of plant species from different habitats indicated no correlation between the wax quantity and the cuticular permeance (Schreiber and Riederer 1996).

The chemical composition of the cuticular waxes was consequently proposed as a regulating factor. *Citrus aurantium* leaves grown under different environmental conditions had variable wax quantities of the major component classes (Riederer and Schneider 1990). The cuticular permeance was not significantly influenced by the

different environmental conditions (Geyer and Schönherr 1990) and there was no correlation between wax quantity, wax composition and cuticular water permeability. However, both the average carbon chain length of the aliphatic wax components and the dispersion around the average value did not differ among the different growing conditions. This might explain the missing effect on the cuticular permeance. It is proposed that waxes with high values of the average carbon chain length and small dispersions around the average value establish more efficient barriers and would enhance the crystalline volume fraction (Riederer and Schneider 1990, Riederer 1991). Hauke and Schreiber (1998) partially confirmed this hypothesis. The average carbon chain length of ivy leaves (*Hedera helix*) increased from C₂₇ to C₃₃ during development, in accordance with a decrease of cuticular transpiration.

The highly ordered orthorhombic crystalline fractions of the cuticular waxes are impermeable to water molecules. Water diffuses through the less ordered intercrystalline amorphous fractions. The crystalline volume fraction and the spatial arrangement of very-long-chain acyclic components are proposed to increase the tortuosity of the path and impede the transport (Riederer and Schneider 1990, Riederer and Schreiber 1995, Schreiber et al. 1997).

When comparing the cuticular permeance and the chemical composition, tomato fruits (*Solanum lycopersicum*) and its *cer6* mutant exhibit considerable differences. This mutant had a distinct decrease of the very-long-chain acyclic components (*n*-alkanes of carbon chain length > C₂₈), which probably explains the observed increase in cuticular water permeability, and a concomitant increase in pentacyclic triterpenoids (Vogg *et al.* 2004, Leide *et al.* 2007). Similarly, *positional sterile* mutants of tomato fruits were characterised by a decrease in *n*-alkanes and alkanals, an increase in triterpenoids and an increased cuticular permeance (Leide *et al.* 2011). Buschhaus and Jetter (2012) compared the water loss of *Arabidopsis thaliana* leaves with and without triterpenoids as cuticular wax constituents. Triterpenoid accumulation caused a reduction of the water barrier effectiveness. The water permeability of component classes was compared through the use of impregnated discs of Whatman paper with different cuticular wax constituents. *N*-alkanes (C₂₇-C₃₃) were the most efficient constituents to reduce the water permeability, while a triterpenoid (ursolic acid) and an alkanone (hentriacontan-16-one) formed less efficient barriers (Oliveira *et al.* 2003).

Plants exposed to dehydration periods often exhibit increased wax coverage (Cameron *et al.* 2006, Jenks *et al.* 2001, Kim *et al.* 2007, Kosma *et al.* 2009, Sánchez

et al. 2001). This increase has been attributed to either one component class (*n*-alkanes; Kosma *et al.* 2009), several component classes (*n*-alkanes and alkanals; Kim *et al.* 2007) or no alteration of the component classes (Cameron *et al.* 2006). *Lepidium sativum* leaves exposed to ABA application did not differ in total cuticular wax quantities compared to the control plants, instead the ABA-treated plants contained higher proportions of very-long-chain acyclic components ($> C_{26}$; Macková *et al.* 2013). After the dehydration periods, a reduction of the weight loss and/or chlorophyll leaching of the leaves is observed (Cameron *et al.* 2006, Kosma *et al.* 2009). In these studies, the mass loss through transpiration is referenced to the fresh weight rather than the surface area. According to Kerstiens *et al.* (2006), this might lead to seemingly different water loss rates across leaf surfaces when the leaf thickness differs, even when the water loss rates are not different when referenced to the surface area. Kerstiens *et al.* (2006) furthermore states that, in order to allow a comparison, rates of water loss should always be referenced to the surface area across which water transport has been measured. One study that indicated the water loss rate per unit surface area did not detect a correlation between cuticular transpiration rate and wax quantity (Sánchez *et al.* 2001).

Mutants with reduced cuticular wax coverages have been associated with increased water loss referenced to either the dry weight or fresh weight (Jenks *et al.* 1994, Chen *et al.* 2003, Zhang *et al.* 2005). For example, *eceriferum* (*cer1*) mutants from *Arabidopsis thaliana* demonstrated a lack of very-long-chain *n*-alkanes and derivatives, while the *cer1* overexpression increased the production of *n*-alkanes and branched alkanes. The wax coverage was lowest in the *cer1* mutant compared to the wildtype. The overexpression mutant had the highest wax quantity. The water loss rates were lowest in the overexpression mutant and the highest for *cer1* mutants compared to the wildtype. This result was confirmed with chlorophyll extraction rates (Bourdenx *et al.* 2011). Nevertheless, plant mutants with a higher wax coverage have been associated with increased water loss, referenced to either the dry weight or fresh weight, or increased chlorophyll extraction rates (Kurdyukov *et al.* 2006, Ristic and Jenks 2002, Schnurr *et al.* 2004). For example, the *Arabidopsis thaliana* mutant *shine* (*shn*) demonstrated a six-fold higher wax level compared to the wildtype. Chlorophyll leaching and weight loss experiments indicated an increased cuticular water permeability (Aharoni *et al.* 2004).

Several mutants with altered cutin quantity, cutin composition and disorganized ultrastructure, probably due to defective cross-linking of cutin monomers, had a seemingly increased cuticle permeability (Goodwin and Jenks 2005, Kurdyukov *et al.* 2006). Therefore, it was proposed that cutin and the corresponding ester-linkage play a major role in establishing barrier properties by providing the framework in which the cuticular waxes are arranged (Goodwin and Jenks 2005, Kosma and Jenks 2007). However, after the analysis of cutin-deficient mutants (*cd*) of tomato fruits, Isaacson *et al.* (2009) suggested that there is no correlation between the cutin amount and the cuticular water permeability.

3 Aim of the present study

The relation between wax composition, wax coverage and the cuticular water permeability remains to be elucidated (Kerstiens 2006). Cuticular permeances from 57 plant species were categorised according to leaf anatomy and habitat (Riederer and Schreiber 2001). A wide range of cuticular permeances, between $0.04 \cdot 10^{-5} \text{ m s}^{-1}$ (*Vanilla planifolia*) and $14.40 \cdot 10^{-5} \text{ m s}^{-1}$ (*Abies alba*), was detected. A tendency was observed that the lowest cuticular permeances occurred for evergreen leaves from epiphytic or climbing plants naturally growing in tropical climates. Mesomorphic leaves from deciduous species growing in temperate climates had cuticles with high cuticular permeances. Intermediate cuticular permeances from xeromorphic plants typically growing in Mediterranean climates demonstrated a great range of overlap between these three groups.

In order to deduce principles connecting the chemistry, the structure and the function of plant cuticles, one plant species was usually analysed under different conditions, such as drought exposure (Cameron *et al.* 2006), different developmental stages (Hauke and Schreiber 1998) or different environmental conditions (Riederer and Schneider 1990). In the present work, from a wide range of plant species the cuticular wax coverage, wax composition and the cuticular transpiration barrier properties were analysed. The total wax coverage, the amount of acyclic and cyclic components and the average carbon chain lengths were compared with the cuticular water permeability. High average carbon chain lengths and their role in enhancing the crystalline volume fractions and reducing the cuticular water permeability were analysed (Riederer and Schneider 1990, Riederer 1991). Additionally, it was hypothesised that not the total wax coverage but the amount of acyclic very-long-chain

components strongly influenced the cuticular transpiration barrier, given that cyclic triterpenoids seem to establish less efficient barriers than acyclic very-long-chain components (Oliveira *et al.* 2003, Vogg *et al.* 2004, Leide *et al.* 2007, 2011, Buschhaus and Jetter 2012).

Temperature influences the cuticular transpiration. A slight increase of the cuticular permeance was described following a slight increase of temperature (from 10 °C to 35 °C) and a drastic increase at higher temperatures was noted (Schreiber 2001, Riederer 2006b). In Chapter I the temperature effect on the minimum water permeability of a desert plant was analysed. The survey of cuticular permeances from 57 plant species presented by Riederer and Schreiber (2001) does not include desert plant species. The minimum water permeability of the desert plant *Rhazya stricta* was compared with the available literature data.

Chapter II focused on the temperature-dependent cuticular water permeability of *Nerium oleander*, a Mediterranean plant species. The temperature effect on the cuticular transpiration barrier of intact leaves is still unknown (Kerstiens 2006). Few studies have focused on the comparison between minimum conductance and cuticular permeance (Burghardt and Riederer 2003, Burghardt *et al.* 2008). In this study, the temperature-dependent cuticular permeance of astomatous, isolated plant cuticles and the temperature-dependent minimum conductance of intact, stomatous leaves were compared.

In Chapter III different experimental approaches were used to compare the temperature-dependent leaf cuticular permeance of the model plant *Prunus laurocerasus*. It was discussed if all approaches were similarly appropriate to determine the temperature-dependent cuticular water permeability.

In Chapter IV the cuticular wax chemistry and the minimum water permeability of nine characteristic plant species from a xeric limestone growing site were investigated. Additionally, the problem of water saving at elevated temperatures was addressed. It was hypothesised that plant species with efficient transpiration barriers are more heat tolerant.

In Chapter V a wide range of plant species, including tropical (*Vanilla planifolia*), temperate (*Juglans regia*) and Mediterranean (*Olea europaea*) plant species, were used for chemical analysis of the cuticular waxes. The corresponding minimum conductances and, if applicable, the cuticular permeances were determined. Chemical

and functional analyses attempted to clarify the still unsolved relationship between wax coverage, wax composition and cuticular water permeability.

Materials and methods

1 Leaf characteristics

1.1 Plant material and leaf harvest

Leaves of *Rhazya stricta* Decne. were obtained from native growing sites located about 100 km north-east of Riyadh, Saudi Arabia (25°24'35.51"N, 47°14'32.61"E and 25°22'53.80"N, 47°14'20.52"E). The area has been classified as arid desert (hot) by the Köppen-Geiger climate classification system (Peel *et al.* 2007). Macroclimatic data are available from a standard meteorological weather station at Riyadh. Annual average rainfall reported is 88.9 mm (1979 - 2009; Almazroui *et al.* 2012). Annual average temperature is 26.8 °C (1984 - 2013), the average maximum of the warmest month August is 43.7 °C (Krishna 2014). Whole shoots were harvested from November to February (2012 - 2014).

Leaves of *Nerium oleander* L. were obtained from potted plants grown at the Botanical Garden in Würzburg, Germany. In winter plants were kept in the greenhouse, in summer outdoors. Leaves were harvested in October 2013 (cuticle isolation, storage time: air-dried several days) and October 2014.

Leaves of *Prunus laurocerasus* L. were obtained at an outdoor growing site at the Botanical Garden. Leaves were harvested from September to November 2012.

Leaves of *Hippocrepis comosa* L., *Helianthemum apenninum* (L.) Mill., *Geranium sanguineum* L., *Sanguisorba minor* Scop., *Sesleria albicans* Kit., *Pulsatilla vulgaris* Mill. and *Teucrium chamaedrys* L. were harvested at a xeric limestone outdoor growing site (xerophytic grassland of the class Festuco-Brometea) at the Botanical Garden, while leaves of *Salvia pratensis* L. and *Plantago lanceolata* L. were harvested at a mesic outdoor growing site (mesophytic grassland of the class Molinio-Arrhenatheretea). Leaves of the dwarf form of *Salvia pratensis* were harvested at the natural growing site (xerophytic grassland of the class Festuco-Brometea, nature protection area "Grainberg-Kalbenstein und Saupurzel", located about 25 km north of Würzburg). Leaves were harvested in September 2011, May - June 2012, July - August 2013, September - October 2014 and April - May 2015.

Leaves of *Solanum lycopersicum* L. cultivar MicroTom, leaves of *Solanum surratense* L. (February - April 2014) and *Vanilla planifolia* Jacks. ex Andrews leaves (December - March 2014) were grown in the green house at the Botanical Garden.

Juglans regia L. leaves were harvested at the Botanical Garden in Würzburg. Isolated cuticular membranes were stored for several months. Measurements were conducted from October to December 2014. Leaves of *Olea europaea* L. cultivar Arbequina were obtained from an olive orchard close to Lleida, Spain. Leaves were harvested in November 2014.

The dominant climate type in Germany is temperate to cold, no dry seasons and warm summers (Köppen-Geiger climate classification system; Peel *et al.* 2007). Macroclimatic data are available from a standard meteorological weather station at Würzburg (German Weather Service, Deutscher Wetterdienst). Annual average rainfall reported is 601.0 mm (1981 - 2010). Annual average temperature is 9.6 °C (1981 - 2010), the average temperature of the warmest month is 19.2 °C (1981 - 2010).

Intact, fully developed leaves were harvested by detaching at the petiole base or by harvesting whole shoots. Leaves were put into plastic bags and transported to the laboratory.

1.2 Saturated fresh weight, dry weight and relative water deficit

The saturated fresh weight was determined after leaf rehydration in humid chambers with the cut petioles submerged in water (minimum 6 hours; Garnier *et al.* 2001). Gravimetry was conducted using a laboratory analytical balance (Sartorius MC-1 AC210S or Kern ARJ 220-4M) or a microbalance for small leaves (Sartorius MC-5). The length of rehydration period was determined for several species by measuring the fresh weight whilst rehydrating (Figure 3). *Rhazya stricta* leaves were fully saturated within 5 hours, *Prunus laurocerasus* leaves within 6 hours and *Hippocrepis comosa* as well as *Geranium sanguineum* leaves within 2.5 hours.

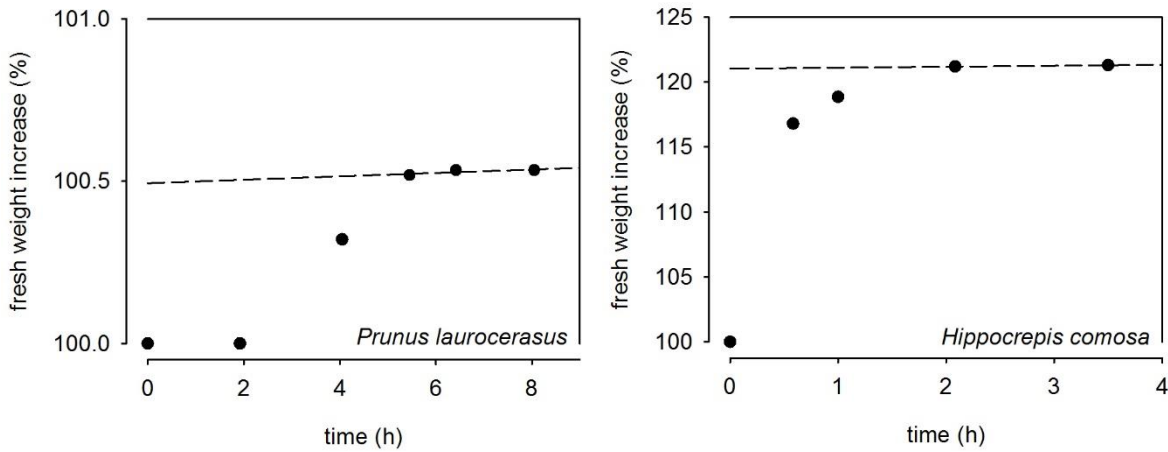


Figure 3. Length of rehydration period as percentage fresh weight increase of one leaf. Extrapolation to the y-axis of the constant values indicated the saturated fresh weight.

The dry weight (DW) was determined after oven drying the leaves at 90 °C (approximately 24 h) or microwave drying, until constant mass was reached. The relative water content (RWC) and relative water deficit (RWD) were calculated using the actual fresh weight (FW), the saturated fresh weight (FW_{sat}) and the dry weight (DW) and indicate the actual water content of a leaf in relation to the maximum water content.

$$RWD = 1 - RWC = 1 - \frac{FW - DW}{FW_{sat} - DW}$$

1.3 Leaf area

For the leaf area determination, saturated leaves were scanned with a flatbed scanner. The projected leaf area was determined using an image analysis software (Adobe Photoshop). Following the recommendation of Kerstiens (1996b) the whole leaf area was defined as the dual projected leaf area (LA).

1.4 Degree of succulence, specific leaf area and leaf water content

The water content at saturation ($FW_{sat} - DW$) divided by the dual projected leaf area (LA) was the degree of succulence (SU; Barkman 1988). The specific leaf area (SLA) was obtained by dividing the one-sided leaf area of a fresh leaf by its dry weight (DW);

Cornelissen *et al.* 2003). The leaf water content (LWC) was calculated on the fresh mass basis ($1 - DW / FW_{sat}^{-1}$; Vendramini *et al.* 2002).

1.5 Stomata density

The stomata density was determined from leaf surface imprints. A thin film of colourless nail polish was applied on the leaf surface, removed after desiccation and visualised under a microscope (Leica DMR, Leica Microsystems) with a connected digital camera (AxioCam MRc, Zeiss). The number of stomata per area was counted from the digital images using an image analysis software (AxioVision, Zeiss).

1.6 Leaf surface properties by scanning electron microscopy

The fine structure of the leaf cuticular surface was characterised by scanning electron microscopy. Small air-dried leaf samples were mounted on aluminium stubs and sputter-coated with gold palladium (150 s, 25 mA, partial argon pressure 0.05 mbar, SCD 005 Sputter Coater, Bal-Tec). The samples were examined with a field emission scanning electron microscope (5.0 kV, WD 10.0 mm JSM-7500F, JEOL).

2 Leaf thermal tolerance and leaf dehydration tolerance

Chlorophyll fluorescence was used to determine the photosynthetic thermal tolerance of leaves (Knight and Ackerly 2003). The maximum quantum yield of the photosystem II of dark adapted leaves (F_v / F_m^{-1}) was measured using the ratio of the minimum fluorescence level of dark adapted leaves and the maximum fluorescence following an actinic light pulse (Schreiber *et al.* 1995) with a pulse-amplitude modulated fluorometer (Junior PAM, Walz). Leaves were exposed to a temperature treatment in the range of 25 °C to 65 °C at 2.5 °C intervals in the dark. Leaves were immersed in an agitated water bath increasing the temperature with 1 °C min⁻¹, measuring F_v / F_m^{-1} every 2.5 minutes. The same leaves were used for each temperature level. Two threshold temperatures for the leaf thermal tolerance were determined. Regression lines were fitted to the two linear portions of the plot. The critical temperature (T_{crit}) indicated the onset of a substantial decrease of F_v / F_m^{-1} and was identified as the intersection point of both regression lines. The T_{50} is the temperature at which F_v / F_m^{-1} declined to 50% of the maximum at the non-stressed level (Knight and Ackerly 2003, Curtis *et al.* 2014). From the mean F_v / F_m^{-1} value at the non-stressed level the 50% value was calculated, inserted in the linear equation of the decreasing branch and the corresponding temperature (T_{50}) was calculated.

Chlorophyll fluorescence was used to determine the dehydration tolerance of leaves. Saturated leaves were progressively dried on the bench in the dark and $F_v F_m^{-1}$ was measured for the different dehydration levels. Two threshold water deficits for leaf dehydration tolerance were determined. The critical relative water deficit (RWD_{crit}) indicated the start of the strong decrease of $F_v F_m^{-1}$. The RWD_{50} is the relative water deficit at which $F_v F_m^{-1}$ declined to 50% of the maximum value for the water saturated status of the leaves. Parameters were calculated in accordance with the photosynthetic thermal tolerance parameters.

3 Leaf area shrinkage and leaf water potential to correct transpiration rates and conductances

The transpiration rate of intact *Rhazya stricta* leaves was corrected for the leaf area shrinkage at each dehydration level. Water vapour conductances were corrected for the actual leaf temperatures, the water activity in the leaf for each dehydration level and the boundary layer conductance to water vapour.

Leaf area shrinkage (percentage loss of area, PLA) during leaf dehydration was measured for different dehydration levels using the leaf area at actual fresh weight (LA_{FW}) and the leaf area at saturated fresh weight (LA_{sat}).

$$PLA = \left(1 - \frac{LA_{FW}}{LA_{sat}}\right) \cdot 100$$

Between the measurements, the leaves were allowed to desiccate on the bench. The maximum area shrinkage is given by the percentage loss of area in a dry leaf (Scoffoni *et al.* 2014). The transpiration rate of *Rhazya stricta* leaves was corrected for the leaf area shrinkage at each dehydration level.

A pressure chamber (PMS Instrument Company) was used to determine leaf water potential (Turner 1988). Saturated leaves were progressively dried on the bench. Water potential was measured repeatedly for different dehydration levels and corresponding fresh weights were determined immediately before and after water potential measurements. Water relation parameter were obtained from pressure-volume analysis (Bartlett *et al.* 2012). The leaf water potential (Ψ_{leaf}) represents the sum of the pressure potential (Ψ_P) and the osmotic potential (Ψ_{π}). For the construction of pressure-volume curves, the negative reciprocal value of the leaf water potential is

plotted against the relative water deficit. The turgor loss point is visible as the inflection point at which the pressure potential becomes zero, the osmotic potential equals the leaf water potential and the osmotic potential is linearly related to the relative water deficit. The interception with the y-axis gives the osmotic potential at full saturation (π_0). The symplastic water fraction is obtained from the interception with the x-axis, the apoplastic water fraction (a_r) can be calculated accordingly (1 - symplastic water fraction). The pressure potential can be calculated as the difference between the measured water potential and the extrapolated osmotic potential. The plot of the pressure potential (Ψ_P) versus the symplastic relative water content (RWC_{sym}) gives the modulus of elasticity (ϵ) as slope.

$$\epsilon = \frac{\Delta\Psi_P}{\Delta RWC_{sym}}$$

The water activity in the leaf for each dehydration level was deduced from pressure-volume analysis of water potential. Leaf water potential (Ψ_{leaf}) can be converted to leaf water activity (a_{leaf}) with the gas constant (R), the absolute temperature (T) and the molar volume of water (V_w ; Nobel 2009).

$$\Psi_{leaf} = \frac{R \times T}{V_w} \times \ln a_{leaf}$$

Boundary layer conductance to water vapour was determined with wet filter paper. The conductance was $6 \cdot 10^{-3} \text{ m s}^{-1}$ and was not temperature-dependent. The boundary layer acts as resistance in series and leaf conductances were corrected accordingly (Pearcy *et al.* 1989).

4 Transpiration rate and minimum conductance

The transpiration rate was obtained from the mass loss of desiccating leaves in the dark at low humidity (Burghardt and Riederer 2003). The cut petioles of saturated leaves were sealed with a high melting paraffin wax (melting point 68 °C; Fluka). The leaves were freely exposed to transpirational water loss in a climate incubator (temperature control; IPP110, Memmert) over silica gel (humidity control; Applichem). The fresh weight of the desiccating leaves was repeatedly weighed at regular time

intervals (Figure 4). The water loss (ΔFW) per time (Δt) and per dual projected leaf area (LA) is the transpiration rate (J).

$$J = \frac{\Delta FW}{\Delta t \cdot LA}$$

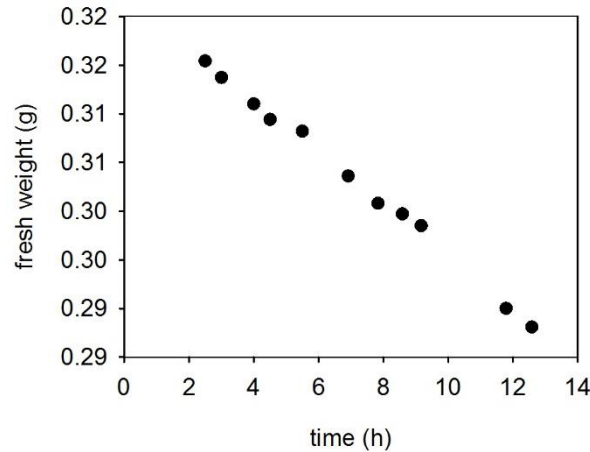


Figure 4. Fresh weight as a function of time of one *Rhazya stricta* leaf. The water loss per time and per dual projected leaf area is the transpiration rate.

The conductance (g) was calculated from the transpiration rate (J) divided by the driving force of transpiration. The driving force is the concentration difference of water vapour between the leaf and the surrounding atmosphere. The water vapour content of air at saturation is 23.07 g m^{-3} at $25 \text{ }^\circ\text{C}$ (c_{wv}^* ; Nobel 2009).

$$g = \frac{J}{c_{wv}^* (a_{leaf} - a_{air})} = \frac{J}{c_{wv}^{leaf} \cdot a_{leaf} - c_{wv}^{air} \cdot a_{air}}$$

Air water activity (a_{air}) and hence air water vapour concentration (c_{wv}^{air}) over silica gel is close to zero. The water activity in the leaf (a_{leaf}) was assumed to be unity according to Burghardt and Riederer (2003). The water vapour saturation concentration in the leaf (c_{wv}^{leaf}) is given by leaf temperature, the corresponding values were derived from Nobel (2009). Leaf temperature was measured with a leaf temperature sensor (Walz) and with an infrared thermometer (Scantemp Pro440, Dostmann electronic).

The relative water deficit at the point of complete stomatal closure was determined from the plot of the leaf conductance versus the relative water deficit. An initial decline of conductance indicated progressive stomatal closure. After complete stomatal closure, the conductance reached a constant and low value referred to as minimum conductance (g_{\min}). The minimum conductance is the lowest conductance a leaf can reach with completely closed stomata as a result of desiccation stress (Körner 1995). The point of complete stomatal closure was derived from the transition point between the declining phase and the plateau phase.

5 Transpiration rate and cuticular permeance

Stainless steel transpiration chambers were used to measure the water vapour based cuticular permeance of stomata-free plant cuticles (Schönherr and Lenzian 1981). Isolated cuticles or leaf discs were mounted in transpiration chambers, the physiological inner surface of the cuticle facing the chamber interior (donor compartment). To ensure a continuous water flow in the leaf discs, the abaxial leaf surface was removed with a scalpel. A stainless steel ring, teflon paste (PTFE, Roth) and adhesive tape were used to seal the chambers. The donor compartment was filled with 0.5 ml deionised water. Placement of the transpiration chambers in plastic containers over silica gel (humidity control; Applichem) in a climate incubator (temperature control; IPP110, Memmert) was upside down (liquid water - cuticular membrane - vapour). Prior to the measurement the mounted chambers were equilibrated overnight.

The weight of the transpiration chambers was repeatedly determined at regular time intervals (Figure 5). The weight loss (ΔW) per time (Δt) and per exposed area (A , 1.13 cm²) is the transpiration rate (J).

$$J = \frac{\Delta W}{\Delta t \cdot A}$$

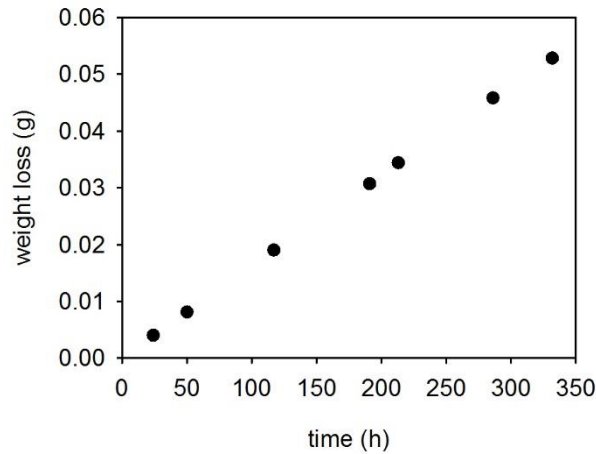


Figure 5. Accumulated weight loss as a function of time of one isolated cuticular membrane of *Nerium oleander* in a transpiration chamber. The water loss per time and per exposed area is the transpiration rate.

The cuticular permeance (P) was calculated from the transpiration rate (J) divided by the driving force of transpiration.

$$P = \frac{J}{c_{wv}^* (a_{chamber} - a_{air})}$$

Air water activity (a_{air}) over silica gel is close to zero. The water activity in the chamber ($a_{chamber}$) is unity, hence the donor compartment is filled with pure water. The water vapour saturation concentration (water vapour content of air at saturation, c_{wv}^*) was derived from Nobel (2009).

Additionally, cuticular permeance was measured from whole leaves by sealing the stomatal surface with a high melting paraffin wax (melting point 68 °C; Fluka) and from leaf envelopes with self-adhesive aluminium foil. Leaf envelopes were modified after Hoad *et al.* (1996). The transpirational water loss was measured from a defined, adaxial, astomatous leaf surface. In contrast to Hoad *et al.* (1996) no additional water supply was provided and whole leaves were used for the experimental approach.

6 Temperature effect on minimum conductance and cuticular permeance

The measurement of transpirational water loss in a climate incubator enabled temperature control. Leaves, transpiration chambers and leaf envelopes were exposed

to temperatures between 15 °C and 55 °C (at 5 °C intervals). The air temperature was verified with a digital thermometer (Testoterm 6010, Testo). Fresh leaf samples were used for each temperature level, the transpiration chambers were subsequently heated. The difference between the leaf and air temperature ($\Delta T_{\text{leaf}-T_{\text{air}}}$) of intact leaf material (leaf drying curves, leaf envelopes) was recorded at all temperatures (Figure 6). The minimum conductances and the cuticular permeances from the intact leaf material were corrected accordingly.

The effect of temperature on the minimum conductance and the cuticular permeance was analysed by Arrhenius plots. The natural logarithm was plotted versus the reciprocal of the absolute temperature. The activation energy was obtained from the slope of the regression line multiplied with the gas constant (Schreiber 2001, Riederer 2006b).

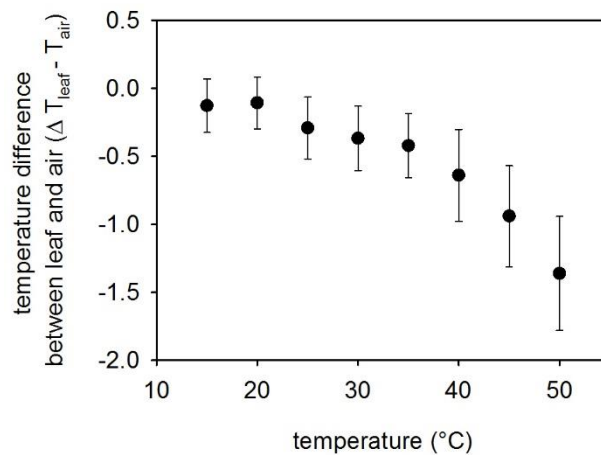


Figure 6. Leaf temperature (T_{leaf}) to air temperature (T_{air}) difference of *Rhazya stricta* leaves as a function of temperature during the phase of maximum stomatal closure as a result of desiccation stress (mean value \pm SD, $n \geq 11$).

7 Gravimetric and chemical analysis of the cuticular components

7.1 Isolation of cuticular membranes

Cuticular membranes of leaves were enzymatically isolated, using punched-out leaf discs. The discs were submerged and vacuum-infiltrated in a solution containing pectinase (1%; Trenolin Super DF, Erbslöh) and cellulase (1%; Celluclast, Novozymes, NCBE) in citrate buffer (0.01 mol l⁻¹, pH 3.0; citric acid monohydrate, Applichem). Additionally, the enzymatic solution contained sodium azide (0.1%, 1 mol l⁻¹ solution; Sigma-Aldrich). The isolated cuticular membranes were washed with aqueous borax

buffer at pH 9 for 24 h (0.01 mol l^{-1} ; disodium tetraborate decahydrate, Applichem). After subsequent washing with deionized water the cuticular membranes were dried before storage.

7.2 Gravimetric analysis of the cuticular components

Cuticular membranes were gravimetrically analysed (microbalance Sartorius MC5) before and after extracting the cuticular wax components. The gravimetric amount of the cuticular membrane, the wax-free matrix membrane and the wax coverage per unit area were obtained.

7.3 Extraction of the cuticular waxes for chemical analysis

To analyse the chemical composition, total wax mixtures were extracted by incubating isolated cuticular membranes in chloroform (5 ml, room temperature; $\geq 99.9\%$, Roth) in two subsequent dippings for 5 min. Total wax mixtures were extracted from intact leaves by dipping the leaves twice for 30 sec in chloroform (1 - 25 ml, room temperature; $\geq 99.9\%$, Roth), the cut end of the petiole protruding from the solvent. Solvent amount varied with leaf size. Immediately after extraction a determined amount of internal standard (*n*-tetracosane, Sigma-Aldrich) was added to all extracts. The extracts were compressed to dryness in reaction vials by evaporation of chloroform under a gentle flow of nitrogen.

Additional extraction steps revealed that dipping twice in chloroform was sufficient to obtain the maximum of the wax coverage. The first extraction steps yielded approximately 90% of the cuticular wax coverage (Figure 7). From *Prunus laurocerasus* isolated cuticular membranes the first extraction yielded 95.9% of the cuticular wax. From *Nerium oleander* isolated cuticular membranes 88.4% of the cuticular wax were obtained within the first extraction.

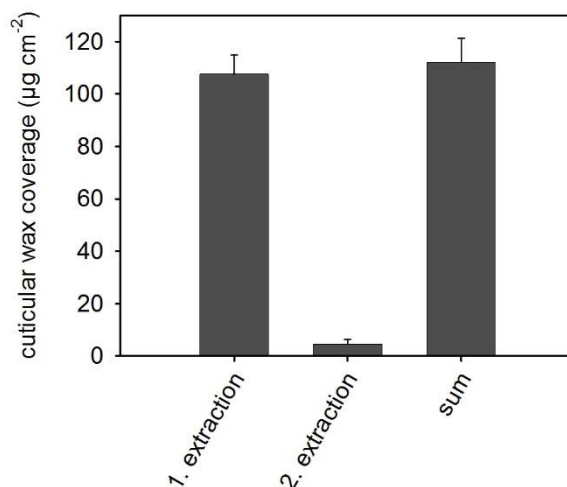


Figure 7. Total wax coverage of two subsequent extraction steps. From *Prunus laurocerasus* isolated cuticular membranes the first extraction yielded 95.9% of the cuticular wax (mean value \pm SD, $n = 3$).

7.4 Extraction of the cutin monomers for chemical analysis

To analyse the chemical composition of the cutin monomers, the wax-free matrix membranes were transesterified with BF_3 -methanol (approximately 1.3 mol l^{-1} ; boron trifluoride in methanol, Fluka) overnight at 70°C . The transesterification depolymerises the cutin, releasing methyl esters of cutin acid monomers and phenolic acids. To the transesterified cutin monomers a saturated aqueous solution of sodium chloride (Applichem) and a determined amount of internal standard (*n*-dotriacontane, Sigma-Aldrich) were added, this mixture was extracted three times with chloroform. The combined chloroform extracts were dried over sodium sulfate (anhydrous, Applichem), filtered and subsequently compressed to dryness in reaction vials by evaporation of chloroform under a gentle flow of nitrogen.

7.5 Chemical analysis of the cuticular waxes and the cutin monomers

Wax and cutin samples were derivatised for gas chromatography into the corresponding trimethylsilyl derivatives by reaction with BSTFA (N,O-bis(trimethylsilyl)trifluoroacetamide, Marchery-Nagel) in dry pyridine (Roth) and subsequent heating (70°C , 30 min).

Quantitative analysis was carried out with a gas chromatograph equipped with a flame ionisation detector (7890A, GC System, Agilent Technologies). Separation of

components was achieved by cool-on-column injection of 1 µl extract on a fused silica capillary column (DB1-ms, 30 m length x 0.32 mm ID, 0.1 µm film, Agilent Technologies) with hydrogen as carrier gas. The temperature program for the wax analysis was: injection at 50 °C, after 2 min with 40 °C min⁻¹ to 200 °C, after 2 min with 3 °C min⁻¹ to 320 °C remaining stable for 30 min. The pressure at injection was 50 kPa, after 5 min with 3 kPa min⁻¹ to 150 kPa remaining stable for 40 min. The temperature program for the cutin analysis was: injection at 50 °C, after 1 min with 10 °C min⁻¹ to 150 °C, after 2 min with 3 °C min⁻¹ to 320 °C remaining stable for 30 min. The pressure at injection was 50 kPa, after 60 min with 10 kPa min⁻¹ to 150 kPa remaining stable for 30 min.

The quantitative, area-based amount of the cuticular components (m_c) was calculated using the amount of the internal standard (m_{st}), the corresponding peak area (A_{st}), the peak area of the components (A_c) and the extracted area (A_{ex}) of the isolated cuticular membranes or leaves.

$$m_c = \frac{A_c \cdot m_{st}}{A_{st} \cdot A_{ex}}$$

Qualitative analysis was carried out with a gas chromatograph (6890N Network GC System, Agilent Technologies) equipped with a mass spectrometric detector (70 eV, m/z 50 - 750, 5975 inert Mass Selective Detector, Agilent Technologies) under the same gas chromatographic conditions, except that helium was used as carrier gas. Cuticular components were identified using authentic standards and literature data.

7.6 Average carbon chain length

The weighted average carbon chain length (ACL) was calculated from the chain length (x_i) and the mass fraction (w_i) of the component (i) with the standard deviation (ΔACL) as a measure of dispersion (Galassi *et al.* 2015). The average carbon chain length was calculated based on the wax amount coverage ($\mu\text{g cm}^{-2}$) and based on the molar wax coverage ($\mu\text{mol m}^{-2}$). Based on the wax amount ACL and ΔACL were additionally calculated separately for the low chain length range ($\leq C_{37}$) and the high chain length range ($\geq C_{38}$).

$$ACL = \frac{\sum_i x_i \cdot w_i}{\sum_i w_i}$$

$$\Delta ACL = \sqrt{\frac{\sum_i w_i \cdot (ACL - x_i)^2}{(\sum_i w_i) - 1}}$$

8 Statistical analyses

The cuticular permeances and minimum conductances were analysed for normal distribution by the Shapiro-Wilk normality test (p value to reject 0.05). Normally distributed data was given as mean values with the corresponding standard deviation (SD). Data that was not normally distributed was given as median values with the corresponding interquartile range (IQR = Q75 (75% quartile) - Q25 (25% quartile)). Comparisons between minimum conductances and cuticular permeances within plant species were tested for significance with Student's t-test or Mann-Whitney U-test (level of significance $p < 0.05$) and when comparing more than two groups with Kruskal-Wallis one way analysis of variance (ANOVA) on ranks. Slopes of Arrhenius plots were compared using the "significance of the difference between two slopes calculator" (Soper 2016). Pearson product moment correlation for normally distributed data and Spearman rank order correlation for not normally distributed data was used to calculate the Pearson correlation coefficient (PCC) or Spearman correlation coefficient (SCC; level of significance $p < 0.05$). Statistical analyses were performed with SigmaPlot 12.5 (Systat Software).

Chapter I. The leaf minimum conductance and the temperature effect on the cuticular transpiration barrier of the desert plant *Rhazya stricta*

1 Introduction

During evolution, land plants have acquired properties and strategies allowing them to cope with scarce water supplies. The efficient control of water loss to the atmosphere is proposed as one of the foremost prerequisites for plant survival in arid environments. The optimisation of this purpose depends on the coordinated interplay between stomatal regulation and the water loss over the rest of the plant surface area. During dry periods, plants reduce the transpiration by stomatal closure. Under such conditions, plant life depends on the efficacy of a thin membrane covering all aerial primary tissues of terrestrial plants - the cuticle. The water permeability of the cuticle determines the minimum and unavoidable water loss under conditions of complete stomatal closure. A low cuticular water permeability can be considered as crucial for the survival and viability of plants under scarce water supply.

Leaf cuticles from some plant species can be enzymatically isolated and directly used for permeability measurements. Cuticular water permeability differs widely among species. A survey of experimental data for the water permeability of astomatous, isolated cuticles from 57 plant species has shown that the corresponding values are in the range from $0.04 \cdot 10^{-5} \text{ m s}^{-1}$ (*Vanilla planifolia*) to $14.40 \cdot 10^{-5} \text{ m s}^{-1}$ (*Abies alba*). A tendency can be observed that the lowest cuticular water permeabilities occur for evergreen leaves from epiphytic or climbing plants in tropical climates. Scleromorphic leaves from plants growing in Mediterranean-type climates show higher water permeabilities. The cuticular water permeability is highest for deciduous species with mesomorphic leaves growing in temperate climates. Though the species tend to cluster according to life-form and climate of origin, there is a great range of overlapping values between these three groups (Riederer and Schreiber 2001).

The plant cuticles are lipid in nature consisting of a cutin matrix (ester-linked C₁₆ and C₁₈ alkanolic acids and hydroxyalkanoic acids, often with additional hydroxy, carboxylic, epoxy and oxo groups in secondary mostly mid-chain positions) with cuticular waxes embedded within or deposited on its surface (Pollard *et al.* 2008, Yeats and Rose 2013). Typical compounds of plant cuticular waxes are very-long-chain

aliphatics and cyclic molecules especially pentacyclic triterpenoids (Jetter *et al.* 2006). The barrier properties of cuticular membranes are almost completely determined by the presence of cuticular waxes, since the extraction of waxes with organic solvents leads to a considerable increase of the cuticular water permeability (Schönherr 1976, Schönherr and Lenzian 1981). Thick cuticular membranes do not provide more efficient transpiration barriers (Kamp 1930, Schreiber and Riederer 1996, Riederer and Schreiber 2001, Anfodillo *et al.* 2002). Even though cuticular waxes represent the main transport-limiting barrier of plant cuticles, the relationship between wax composition and cuticular water permeability has remained as yet unsolved (Schönherr 1982, Kerstiens 2006).

Temperature has a significant effect on the cuticular water permeability. For plant species studied so far, a slight increase of the cuticular permeances is described following a slight increase of temperature (from 10 °C to 35 °C). A drastic increase of the cuticular permeances at temperatures ranging from 35 °C to 55 °C is noted (Schreiber 2001, Riederer 2006b). The abrupt decline of the efficacy of the barrier against water diffusion, which can be analysed by Arrhenius plots, is interpreted as a phase transition of the cuticular membrane leading to structural changes in the transport-limiting barrier. Hence, the cuticular waxes form the main transport-limiting barrier, the phase transition has been attributed to the waxes (Eckl and Gruler 1980). Merk *et al.* (1998) investigated the phase behaviour of cuticular waxes and found extended melting ranges, indicating structural changes. On the other hand, the phase transition is explained by micro-defects and cracks in the cuticular wax barrier caused by volume expansions of the cutin polymer and/or the wax-free matrix membrane (Schreiber and Schönherr 1990, Schreiber 2001). Finally, it is argued that the steep increase of water permeabilities is due to swelling of the polysaccharide material and opening up new regions of the polysaccharides for the water diffusion (Riederer 2006b).

The occurrence of a phase transition of plant cuticles is an important finding, especially when the ecological consequences for desert plants are considered, since their above-ground parts reach extreme temperatures (up to 50 °C; Smith 1978) through high air temperatures, strong irradiation and reduced or absent transpirational cooling. As stated by Goodwin and Jenks (2005), it is difficult to reconcile the finding of a phase transition of plant cuticles with the successful adaptation of many xerophytes to high-temperature climates. The question arises whether the cuticles of

plants adapted to hot and dry environments have peculiar wax and/or cutin compositions to limit water loss during periods of high temperature. Up to date, there is no study on the temperature dependence of cuticular water permeability of desert plants and its link to cuticle chemistry. Therefore, studies are needed to elucidate the cuticle composition and structure of xeromorphic leaves and their association with temperature-dependent water permeability (Goodwin and Jenks 2005).

Rhazya stricta Decne. (Apocynaceae) is a non-succulent, perennial shrub commonly distributed in the desert vegetation of the Arabian Peninsula ranging into Iran, southern Afghanistan and Pakistan (Abd El-Ghani 1997, Emad El-Deen 2005, Al-Khamis *et al.* 2012) and it is described as a widespread sand-binding and nebkha-forming shrub (Quets *et al.* 2014). *Rhazya stricta* has been recently identified as a plant species with a photosynthetic physiology able to function well under typical desert conditions of daily extremes of heat, high light intensity and low humidity. Field studies in the native habitat proved a high temperature tolerance of *Rhazya stricta* with no decrease in photosynthetic capacity observed up to leaf temperatures of 45 °C (Lawson *et al.* 2013, Yates *et al.* 2014). These studies confirm that *Rhazya stricta* experiences indeed high leaf temperatures during the day course, which exceed the phase transition temperatures of cuticles reported for non-desert plants (Schreiber 2001, Riederer 2006b). Therefore, *Rhazya stricta* is a suitable candidate to investigate potential adaptations to heat and drought on the level of the cuticular transpiration barrier. The minimum water permeability and its temperature dependence were determined and compared with the available literature data. It was hypothesised that an efficient cuticular transpiration barrier enables plant survival in arid environments. Additionally, the relationship between the minimum water permeability and the cuticle chemistry was investigated.

2 Results

2.1 Leaf characteristics of *Rhazya stricta*

Leaf characteristics of *Rhazya stricta* were determined. The leaf saturated fresh weight was 0.43 ± 0.15 g, the dry weight was 0.11 ± 0.04 g and the dual projected leaf area was $1.44 \pm 0.45 \cdot 10^{-3}$ m². Characteristic leaf traits were calculated from the leaf properties. The leaf water content was $0.75 (\pm 0.02)$ g g⁻¹, the specific leaf area was $6.76 (\pm 0.53)$ m² kg⁻¹ and the degree of succulence was 223.26 ± 24.57 g m⁻² (mean value \pm SD, n = 66). Stomata occurred on both leaf surfaces (Figure 8). Stomata density was 121.95 ± 34.42 mm⁻² for the adaxial surface and 111.47 ± 33.49 mm⁻² for the abaxial leaf surface (mean value \pm SD, n = 12). The fine structure of the cuticular surface showed a grainy, amorphous epicuticular wax.

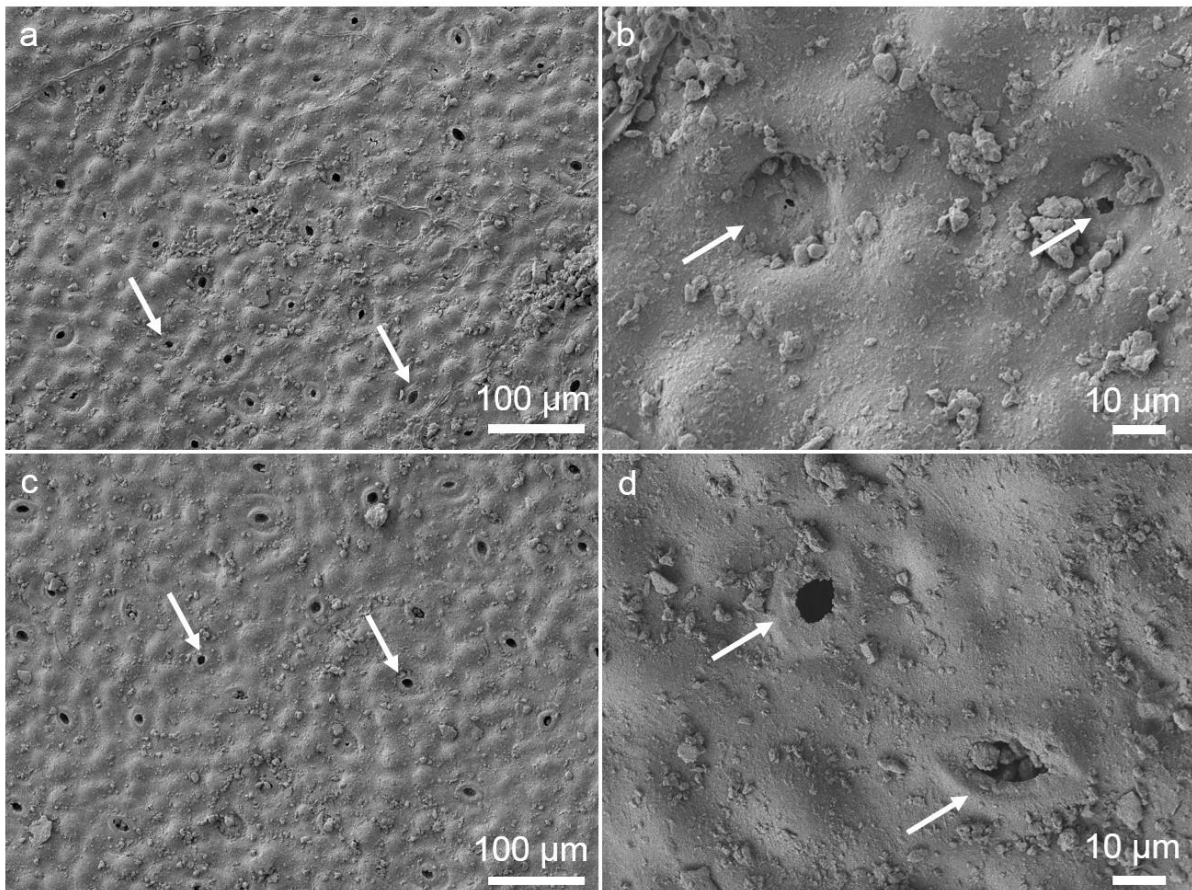


Figure 8. The native adaxial (a,b) and abaxial (c,d) leaf surface of *Rhazya stricta*. Stomata occurred on both leaf surfaces and are indicated by arrows. The epicuticular waxes had an amorphous and grainy structure.

2.2 Leaf thermal tolerance and leaf dehydration tolerance

The photosynthetic leaf thermal tolerance and the leaf dehydration tolerance were measured with chlorophyll fluorescence. The decline of the maximum quantum yield of photosystem II ($F_v F_m^{-1}$) indicates the occurrence of damage to the photosynthetic apparatus (Maxwell and Johnson 2000, Lichtenthaler *et al.* 2005) and provides an appropriate method to assess the limits of whole leaf survival in response to high temperature stress and/or dehydration stress.

The leaf thermal tolerance of *Rhazya stricta* leaves was determined (Figure 9). Heat exposure was applied for 1 °C per min and, subsequently, the maximum quantum yield of photosystem II in the dark adapted state ($F_v F_m^{-1}$) was measured without recovery time every 2.5 min. $F_v F_m^{-1}$ was only slightly affected by temperature treatments between 25.0 °C and 42.5 °C, whereas a strong decrease at temperatures higher than 45.0 °C occurred. The intersection point of the fitted regression lines indicated the critical temperature (T_{crit}) and T_{crit} was 44.31 ± 2.14 °C. T_{50} indicated a decline of $F_v F_m^{-1}$ to 50% of the maximum at the non-stressed level. T_{50} was 51.46 ± 1.33 °C (mean value \pm SD, $n = 9$).

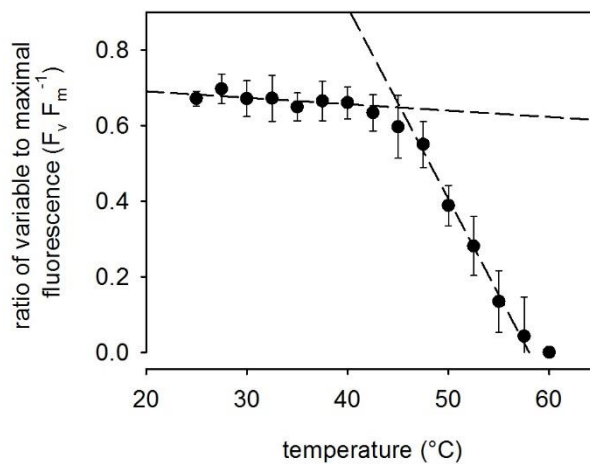


Figure 9. Effect of temperature on the maximum quantum yield of the photosystem II ($F_v F_m^{-1}$) of dark adapted *Rhazya stricta* leaves (mean value \pm SD, $n = 9$).

The leaf dehydration tolerance was measured with chlorophyll fluorescence. Leaves were desiccated and the maximum quantum yield of photosystem II in the dark adapted state ($F_v F_m^{-1}$) was measured at different dehydration levels. The relative water deficit (RWD) was calculated for each dehydration level. $F_v F_m^{-1}$ during leaf dehydration remained high and stable provided that the water status dropped not far below a

relative water deficit of 0.5 (Figure 10). $F_v F_m^{-1}$ started to decline at higher values of relative water deficit. The intersection point of the fitted regression lines indicated the critical relative water deficit (RWD_{crit}). RWD_{crit} was 0.55. RWD_{50} indicated a decline of $F_v F_m^{-1}$ to 50% of the maximum value for the water saturated status of the leaves and was 0.75.

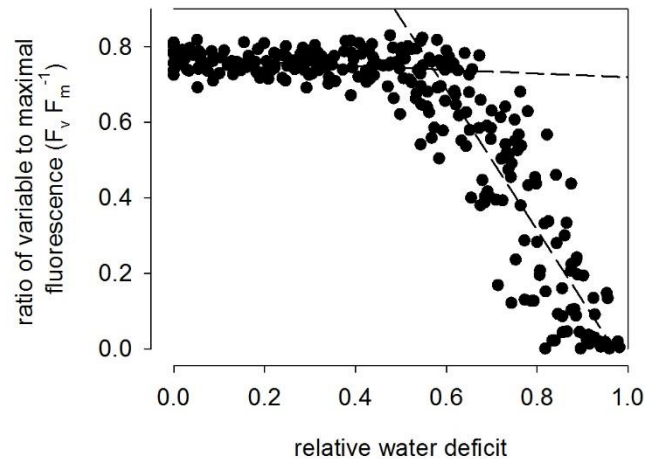


Figure 10. Effect of relative water deficit on the maximum quantum yield of the photosystem II ($F_v F_m^{-1}$) of dark adapted *Rhazya stricta* leaves ($n = 18$).

2.3 Leaf area shrinkage and leaf water potential to correct transpiration rates and conductances

The transpiration rate of *Rhazya stricta* leaves was corrected for the leaf area shrinkage at each dehydration level (Figure 11). Water vapour conductances were corrected for the actual leaf temperatures (Figure 6). Additionally, the conductances were corrected for the water activity in the leaf at each dehydration level (Figure 12) and the boundary layer conductance to water vapour.

The leaf area of *Rhazya stricta* shrank continuously with leaf dehydration (Figure 11). Distinct slopes of the shrinkage curve were identified. Starting from a fully turgid leaf, shrinkage amounted to 1.8% at a relative water deficit of 0.09. The percentage loss of leaf area (PLA) up to this relative water deficit was described by the regression equation: $PLA = 20.140 \cdot RWD + 0.033$ ($r^2 = 0.928$; $n = 8$). The leaf area was further reduced to 4.8% at a relative water deficit of 0.60 described by the regression equation: $PLA = 5.880 \cdot RWD + 1.273$ ($r^2 = 0.715$; $n = 15$). The two equations were used to correct the leaf area when calculating the transpiration rate of *Rhazya stricta* leaves.

At relative water deficits higher than 0.60, area shrinkage became more pronounced. At full dehydration, the maximum shrinkage of dry leaves reached 14.6% ($\pm 2.1\%$; mean \pm SD, $n = 23$).

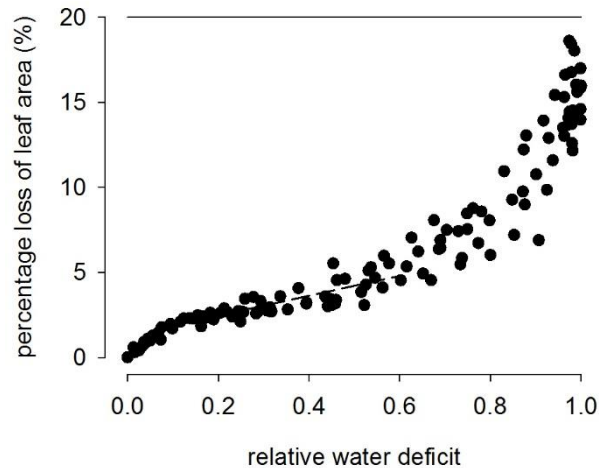


Figure 11. Percentage loss of leaf area (PLA) as a function of relative water deficit ($n = 16$).

Leaf water potential (Ψ_{leaf}) declined with leaf dehydration and its dependence on relative water deficit (RWD) was described by pressure-volume analysis (Figure 12). The regression equation $\Psi_{\pi}^{-1} = -0.878 \cdot \text{RWD} + 0.670$ ($r^2 = 0.785$; $n = 17$) was obtained for the osmotic potential (Ψ_{π}) and the regression equation $\Psi_P = 12.690 \cdot \text{RWC} - 11.470$ for the pressure potential (Ψ_P ; $r^2 = 0.880$; $n = 14$). The following parameters were derived from pressure-volume analysis: the relative water deficit at the turgor loss point (RWD_{TLP}) was 0.10, the osmotic potential at the turgor loss point (π_{TLP}) was -1.72 MPa, the osmotic potential at full saturation (π_0) was -1.49 MPa, the apoplastic water fraction (a_i) was 0.24 and the modulus of elasticity (ϵ) was 9.68 MPa.

The determined boundary layer conductance was $6 \cdot 10^{-3} \text{ m s}^{-1}$ and was not temperature-dependent.

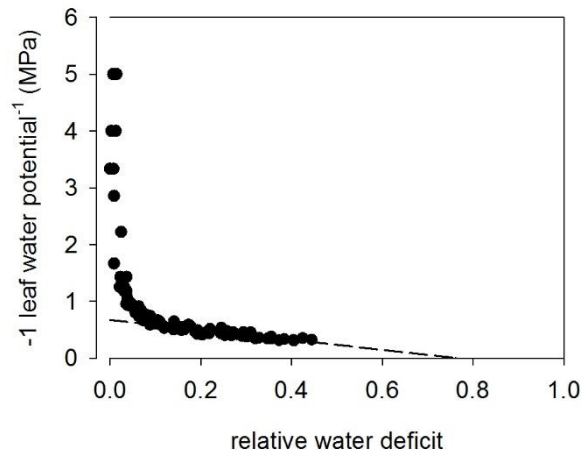


Figure 12. Pressure-volume curve of *Rhazya stricta* leaves. The negative reciprocal value of the leaf water potential (Ψ_{leaf}) is plotted against the relative water deficit ($n = 18$). Ψ_{leaf} is the sum of the pressure potential (Ψ_{P}) and the osmotic potential (Ψ_{T}). The turgor loss point is visible as the inflection point at which Ψ_{P} becomes zero, Ψ_{T} equals Ψ_{leaf} and Ψ_{T} is linearly related to RWD (fitted line).

2.4 Leaf drying curve, minimum conductance and temperature effect on minimum conductance

Leaf drying curves were conducted to obtain the leaf minimum conductance with maximum stomatal closure. The initial phase of leaf drying curves was characterised by high conductances. Conductances declined with leaf dehydration until a plateau of constant and low values was reached, the minimum conductance at maximum stomatal closure. The point of complete stomatal closure was derived from the transition between the declining phase and the plateau phase (Figure 13).

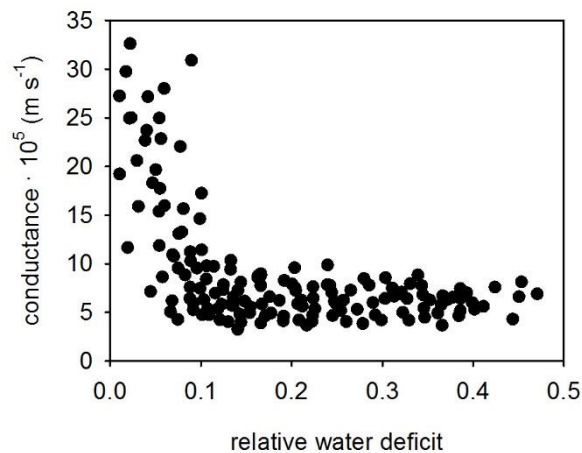


Figure 13. The leaf conductance of *Rhazya stricta* at 30 °C as a function of relative water deficit exemplarily represents the obtained leaf drying curves ($n = 12$).

Leaf drying curves were carried out in the temperature range from 15 °C to 50 °C. Minimum conductances increased with elevation of air temperatures by a factor of 2.4 between 15 °C and 50 °C from $4.27 \pm 1.03 \cdot 10^{-5} \text{ m s}^{-1}$ to $10.30 \pm 2.48 \cdot 10^{-5} \text{ m s}^{-1}$ (Table 3).

Table 3. Minimum conductance (g_{\min}) of *Rhazya stricta* leaves as a function of temperature (T) obtained from leaf drying curves (mean value \pm SD, $n \geq 17$).

T (°C)	$g_{\min} \cdot 10^5$ (m s^{-1})
15	4.27 \pm 1.03
20	5.08 \pm 1.15
25	5.41 \pm 1.36
30	5.96 \pm 1.30
35	6.87 \pm 1.86
40	7.74 \pm 2.21
45	8.72 \pm 2.09
50	10.30 \pm 2.48

Leaf temperatures were only slightly lower at moderate air temperatures. The leaf-air temperature difference ($\Delta T_{\text{leaf-Tair}}$) increased progressively with increasing air temperatures. The highest leaf-air temperature difference of -1.36 °C was detected at air temperature 50 °C (Figure 6). Maximum stomatal closure occurred at relative water deficits between 0.1 and 0.2 in the temperature range between 15 °C and 40 °C. At higher temperatures (> 40 °C), the point of maximum stomatal closure shifted to higher

water deficits and amounted to a relative water deficit of 0.45 ± 0.09 at $50\text{ }^{\circ}\text{C}$ (Figure 14).

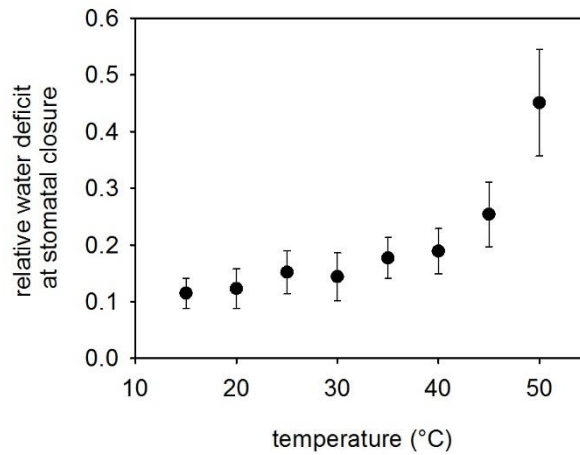


Figure 14. The relative water deficit of *Rhazya stricta* leaves at which maximum stomatal closure occurred as a function of temperature (mean value \pm SD, $n \geq 17$).

The temperature dependence of the minimum conductances was analysed by an Arrhenius plot. An activation energy for the permeation of water of 18.5 kJ mol^{-1} (from $15\text{ }^{\circ}\text{C}$ to $50\text{ }^{\circ}\text{C}$) was calculated from the slope of the regression line (Figure 15). In addition, activation energies were separately calculated for the lower temperature range (16.4 kJ mol^{-1} ; from $15\text{ }^{\circ}\text{C}$ to $35\text{ }^{\circ}\text{C}$) and the higher temperature range (22.1 kJ mol^{-1} ; from $35\text{ }^{\circ}\text{C}$ to $50\text{ }^{\circ}\text{C}$).

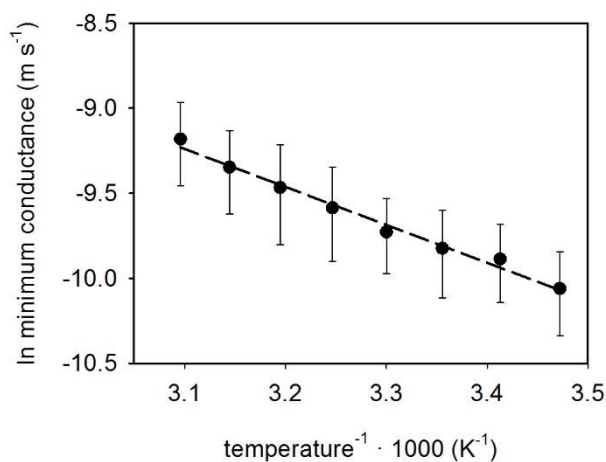


Figure 15. Arrhenius plot of the natural logarithm of the minimum conductance and the inverse absolute temperature (mean value \pm SD, $n \geq 17$; Pearson correlation coefficient (PCC) = -0.994 , $p < 0.001$).

2.5 Gravimetric and chemical analysis of the cuticular components

Enzymatically isolated cuticular membranes had a total weight of $1015.26 \pm 150.46 \mu\text{g cm}^{-2}$. After extraction of the cuticular waxes, the wax-free matrix membranes had a weight of $702.99 \pm 126.54 \mu\text{g cm}^{-2}$. From the weight loss before and after extraction, the extracted wax coverage was calculated ($312.27 \pm 47.44 \mu\text{g cm}^{-2}$; mean value \pm SD, $n = 12$). From the total cuticular membranes 30.8% were extractable components.

2.5.1 Chemical analysis of the cuticular leaf wax

The cuticular waxes were analysed quantitatively by gas chromatograph equipped with a flame ionisation detector and the qualitative analysis by gas chromatograph equipped with a mass spectrometric detector. Total cuticular leaf wax coverage of *Rhazya stricta* was $251.41 \pm 38.97 \mu\text{g cm}^{-2}$ (mean value \pm SD, $n = 5$). The leaf wax composed of a major portion of cyclic components (85.2%, $214.12 \pm 31.20 \mu\text{g cm}^{-2}$) and a minor portion of very-long-chain acyclic component classes (3.4%, $8.56 \pm 2.93 \mu\text{g cm}^{-2}$).

N-alkanes were the most prominent acyclic component class (2.5%, $6.30 \pm 2.15 \mu\text{g cm}^{-2}$), followed by primary alkanols (0.7%, $1.78 \pm 0.78 \mu\text{g cm}^{-2}$) and alkanoic acids (0.2%, $0.48 \pm 0.12 \mu\text{g cm}^{-2}$). Carbon chain lengths ranged from C_{20} to C_{33} , the most abundant chain lengths were C_{31} and C_{33} (Figure 16). *N*-hentriacontane (0.9%, $2.38 \pm 0.75 \mu\text{g cm}^{-2}$) and *n*-tritriacontane (0.7%, $1.76 \pm 0.72 \mu\text{g cm}^{-2}$) dominated the acyclic components. The average carbon chain length (ACL) of the very-long-chain acyclic wax components was 28.52.

The main cyclic component was ursolic acid with a coverage of $102.69 \pm 12.73 \mu\text{g cm}^{-2}$ (40.8%), followed by echinocystic acid (20.9%, $52.56 \pm 12.57 \mu\text{g cm}^{-2}$) and oleanolic acid (19.1%, $48.05 \pm 6.18 \mu\text{g cm}^{-2}$; Table 4).

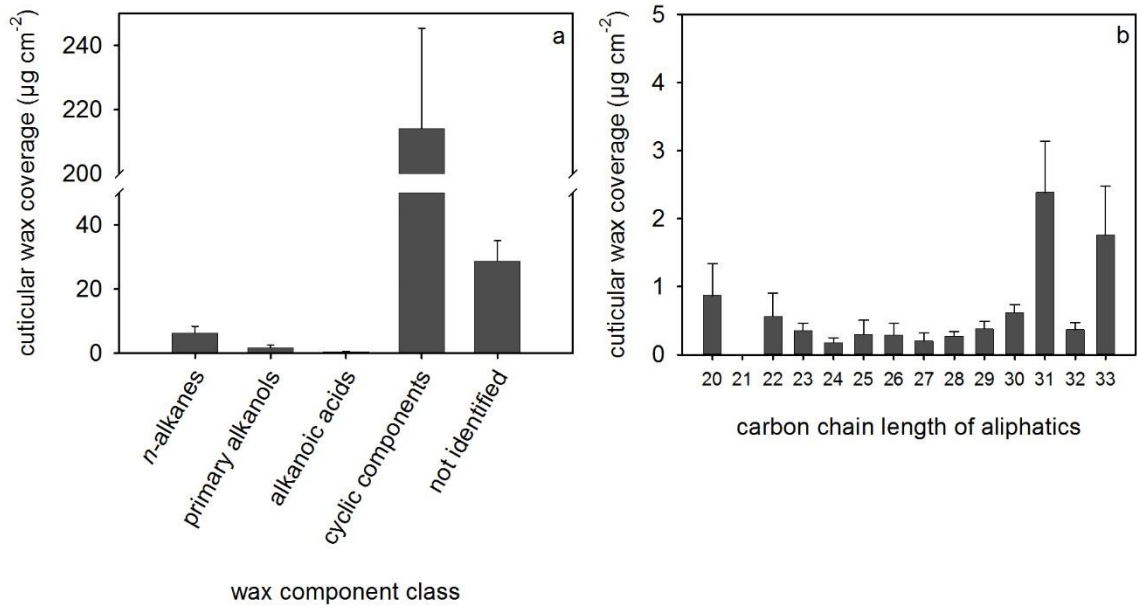


Figure 16. Cuticular wax composition of *Rhazya stricta* leaves. (a) Cuticular wax coverage arranged according to the component classes and (b) the carbon chain length distribution of the acyclic components (mean value \pm SD, n = 5).

Table 4. The cuticular wax coverage and components of isolated cuticular membranes of *Rhazya stricta* leaves (mean value \pm SD, n = 5).

	carbon chain length	wax coverage ($\mu\text{g cm}^{-2}$)		
<i>n</i> -alkanes	23	0.36	\pm	0.11
	25	0.30	\pm	0.20
	26	0.29	\pm	0.17
	27	0.20	\pm	0.12
	28	0.13	\pm	0.07
	29	0.28	\pm	0.11
	30	0.22	\pm	0.04
	31	2.38	\pm	0.75
	32	0.37	\pm	0.10
	33	1.76	\pm	0.72
primary alkanols	20	0.64	\pm	0.43
	22	0.42	\pm	0.31
	24	0.07	\pm	0.02
	28	0.14	\pm	0.03
	29	0.10	\pm	0.01
	30	0.40	\pm	0.10
alkanoic acids	20	0.23	\pm	0.04
	22	0.14	\pm	0.05
	24	0.11	\pm	0.05
sum acyclic components (3.4%)		8.56	\pm	2.93
α -amyrin		0.27	\pm	0.07
taraxerol		0.95	\pm	0.19
erythrodiol		2.60	\pm	1.26
uvaol		2.27	\pm	0.32
oleanolic acid		48.05	\pm	6.18
betulinic acid		2.47	\pm	1.09
ursolic acid		102.69	\pm	12.73
echinocystic acid		52.56	\pm	12.57
hederagenin		2.26	\pm	0.60
sum cyclic components (85.2%)		214.12	\pm	31.20
not identified		28.72	\pm	6.34
sum acyclic, cyclic and not identified cuticular wax components (100.0%)		251.41	\pm	38.97

2.5.2 Chemical analysis of the cutin monomers

The total amount of cutin monomers was $340.60 \pm 33.14 \mu\text{g cm}^{-2}$ (mean value \pm SD, $n = 5$). The cutin polymer composed of a major portion of aliphatic acid components (87.0%, $296.18 \pm 28.39 \mu\text{g cm}^{-2}$) and a minor portion of phenolic acid components (8.7%, $29.70 \pm 3.13 \mu\text{g cm}^{-2}$).

Carbon chain lengths ranged from C₁₅ to C₂₂, the most abundant chain lengths were C₁₆ (54.0%, $183.88 \pm 19.31 \mu\text{g cm}^{-2}$) and C₁₈ (31.7%, $107.98 \pm 11.21 \mu\text{g cm}^{-2}$). The ratio between the C₁₆/C₁₈ carbon chain length components was 1.7. The aliphatic acid components were dominated by 9/10,16-dihydroxyhexadecanoic acid (49.7%, $169.11 \pm 22.95 \mu\text{g cm}^{-2}$), followed by 9,10-epoxy-18-hydroxyoctadecanoic acid (22.3%, $75.88 \pm 10.02 \mu\text{g cm}^{-2}$) and 9,10,18-trihydroxyoctadecanoic acid (4.3%, $14.77 \pm 7.52 \mu\text{g cm}^{-2}$).

The phenolic acid components were dominated by *trans*-coumaric acid (4.5%, $15.23 \pm 1.27 \mu\text{g cm}^{-2}$). Two coumaric acid derivatives (I and II) were not identified further in detail (Table 5).

The ratio between the total wax coverage and the total amount of cutin monomers was 0.7 and the ratio between the cyclic wax components and the total amount of cutin monomers was 0.6.

Table 5. The cutin coverage and monomers of isolated cuticular membranes of *Rhazya stricta* leaves (mean value \pm SD, n = 5).

cutin monomers	carbon chain length	cutin coverage ($\mu\text{g cm}^{-2}$)		
9/10,15-dihydropentadecanoic acid	15	2.34	\pm	0.15
hexadecanoic acid	16	1.13	\pm	0.30
hexadecane-1,16-dioic acid	16	0.76	\pm	0.22
16-hydroxyhexadec-9-enoic acid	16:1	0.61	\pm	0.27
16-hydroxyhexadecanoic acid	16	1.71	\pm	0.22
16-hydroxy-9/10-oxo-hexadecanoic acid	16	6.19	\pm	2.15
7/8-hydroxyhexadecane-1,16-dioic acid	16	4.37	\pm	2.21
9/10,16-dihydroxyhexadecanoic acid	16	169.11	\pm	22.95
9/10,17-dihydroxyheptadecanoic acid	17	1.03	\pm	0.24
octadec-9-enoic acid	18:1	0.71	\pm	0.32
octadecanoic acid	18	0.79	\pm	1.09
octadecane-1,18-dioic acid	18	traces		
18-hydroxyoctadeca-9,12-dienoic acid	18:2	2.77	\pm	0.18
7/8-hydroxyoctadecane-1,18-dioic acid	18	2.76	\pm	0.42
9/10,18-dihydroxyoctadecanoic acid	18	7.19	\pm	0.89
9,10-epoxy-18-hydroxyoctadec-12-enoic acid	18:1	2.46	\pm	0.56
9,10-epoxy-18-hydroxyoctadecanoic acid	18	75.88	\pm	10.02
9,10,18-trihydroxyoctadec-12-enoic acid	18:1	0.12	\pm	0.20
9,10,18-trihydroxyoctadecanoic acid	18	14.77	\pm	7.52
7/8,9/10-dihydroxyoctadec-12-ene-1,18-dioic acid	18	0.51	\pm	0.07
nonadec-10-enoic acid	19:1	0.63	\pm	0.24
9/10,19-dihydroxynonadecanoic acid	19	traces		
eicosanoic acid	20	traces		
docosanoic acid	22	0.33	\pm	0.31
sum aliphatic acid components (87.0%)		296.18	\pm	28.39
<i>cis</i> -coumaric acid		0.38	\pm	0.08
<i>trans</i> -coumaric acid		15.23	\pm	1.27
coumaric acid derivative I		10.41	\pm	2.62
coumaric acid derivative II		3.68	\pm	0.73
sum phenolic acid components (8.7%)		29.70	\pm	3.13
glycerol		0.23	\pm	0.03
not identified		14.49	\pm	2.97
sum total cutin monomers (100.0%)		340.60	\pm	33.14

3 Discussion

3.1 Measurement of the minimum conductance: evaluation and correction

The amount of knowledge on transpiration control by cuticular features of desert plants is astonishingly limited. This might be due to the fact that leaves of woody, non-succulent desert plants are generally amphistomatic with each surface having very similar stomatal densities (Kummerow 1973, Gibson 1996, 1998). The stomatal density and distribution of *Rhazya stricta* leaves confirmed this finding (Figure 8). Cuticular permeances for water vapour are determined by the measurement of the water vapour flux across astomatous cuticular membranes (Kerstiens 1996b), but this experimental technique is not available for desert shrubs that have stomata on both leaf sides, such as *Rhazya stricta*. The measurement of water loss of detached and desiccating leaves under conditions of complete stomatal closure is a technique traditionally used to obtain the minimum conductance of amphistomatic leaves (Körner 1995, Kerstiens 2006). The minimum value for the leaf water vapour conductance at fully closed stomata is often assumed to be essentially equal to the cuticular permeance (Nobel 2009), but residual stomatal transpiration and leakiness of incompletely closed stomata cannot be excluded (Kerstiens 1996b).

Leaves of *Rhazya stricta* demonstrated the characteristic shape of a leaf drying curve (Figure 13). Stomata are at least partially open in the initial phase at full water saturation and the conductance is high. Stomata are successively closed with ongoing leaf dehydration leading to a decline of conductance. The conductance reaches a constant and minimum value at maximum stomatal closure in the final phase (Pisek and Berger 1938, Burghardt and Riederer 2003, Walden-Coleman *et al.* 2013). A slight decrease of the minimum transpiration rate might occur even after the point of maximum stomatal closure. This led to speculations that cuticular water permeability declines with decreasing leaf water content due to a deswelling of the cuticle (Pisek and Berger 1938, Van Gardingen and Grace 1992, Anfodillo *et al.* 2002). The minimum conductance of *Rhazya stricta* remained constant at a low value after stomatal closure (Figure 13). This might be due to the fact that the transpiration rates of *Rhazya stricta* leaves were corrected for the leaf area shrinkage (Figure 11) and the conductances were corrected for the water potential decline during leaf dehydration (Figure 12). The minimum conductances were also corrected for the actual leaf temperatures (Figure 6) and the boundary layer conductance to water vapour. However, the correction of the water activity of the leaf (leaf water potential) and the leaf area shrinkage had minor

influences on the minimum conductances of *Rhazya stricta* leaves. At the turgor loss point the leaf water activity was 0.99 and at the critical relative water deficit 0.96 ($RWD_{crit} = 0.55$). At the critical relative water deficit a leaf area shrinkage of 4.5% occurred. The determined boundary layer conductance was $6 \cdot 10^{-3} \text{ m s}^{-1}$ and the influence on the minimum conductance was minor. The leaf temperature correction was most influential at elevated temperatures.

Temperatures up to 55 °C (Schreiber 2001, Riederer 2006b) or even 65 °C (Schönherr *et al.* 1979, Schönherr and Mérida 1981) were applied when the effect of temperature on cuticular water permeability was studied. For the interpretation of leaf drying curves in the present study, the lethal limits of heat and drought stress were considered. Chlorophyll fluorescence is a widely-used technique to measure the ability of leaves to tolerate environmental stresses. The most frequently applied parameter is the maximum quantum yield of photosystem II in the dark adapted state ($F_v F_m^{-1}$), since it is easy, non-invasive and fast to determine. The decline of $F_v F_m^{-1}$ indicates the occurrence of damage to the photosynthetic apparatus (Maxwell and Johnson 2000, Lichtenthaler *et al.* 2005) and provides an appropriate method to assess the limits of whole leaf survival in response to high temperature and drought stress. The decline of $F_v F_m^{-1}$ below 50% of the maximum value of unstressed leaves can be taken as threshold for viability with the onset of irreversible damage (Woo *et al.* 2008, Curtis *et al.* 2014). Correspondingly, minimum conductances of *Rhazya stricta* leaves (Table 3) were measured in the range of leaf temperatures below the lethal limit for heat stress ($T_{50} = 51.13 \text{ °C}$) and in the range of water deficits below the lethal limit for drought stress ($RWD_{50} = 0.75$).

3.2 Classification of the minimum conductance

Thick plant cuticles are often considered as a prominent feature of desert plants, generally concluding that desert plants possess an effective cuticular transpiration barrier as an important drought survival mechanism (Oppenheimer 1960, De Micco and Aronne 2012). The minimum conductance to water vapour of *Rhazya stricta* leaves amounted to $5.41 \cdot 10^{-5} \text{ m s}^{-1}$ at 25 °C (Table 3) and ranged within the upper scale of the ranking of cuticular permeances from 57 plant species (Riederer and Schreiber 2001). Many deciduous plant species with mesomorphic leaves growing in temperate climates have a comparable high cuticular water permeability as the minimum conductance of *Rhazya stricta* (Riederer and Schreiber 2001). Only little information on minimum conductances of desert plants is available. Körner (1994, 1995) reported

a mean value of $6.4 \cdot 10^{-5} \text{ m s}^{-1}$ for seven evergreen desert shrubs, representing only a very rough estimation. Nevertheless, the minimum conductance of *Rhazya stricta* is in good accordance with this approximate value.

A model, which allows the prediction of minimum conductances, was reported recently (Scoffoni *et al.* 2014). The predictive model is based on the relationship between the modulus of elasticity and the maximum amount of leaf area shrinkage, which is most directly linked to the minimum conductance. Plant species with less rigid and more elastic leaves are characterised by a lower modulus of elasticity, a higher maximum leaf area shrinkage and a higher minimum conductance. The validity of this hypothesis was tested on *Rhazya stricta* as model plant. The modulus of elasticity (ϵ) of *Rhazya stricta* obtained from pressure-volume analysis (Figure 12) amounted to 9.68 MPa. Insertion of this value into the prediction equation ($\text{PLA}_{\text{dry}} = 757 \cdot \epsilon^{-1.7}$; $g_{\text{min}} = 0.27 \cdot \text{PLA}_{\text{dry}} - 0.08$; Scoffoni *et al.* 2014) led to an estimation for the maximum leaf area shrinkage (PLA_{dry}) of 15.4% and an estimation for the minimum conductance of $4.08 \text{ mmol m}^{-2} \text{ s}^{-1}$, which amounts to $4.97 \cdot 10^{-5} \text{ m s}^{-1}$ by conversion from the mole fraction based conductance to the water vapour based conductance and by consideration of the total (two-sided) leaf area as reference for leaf transpiration (Körner 1995, Burghardt and Riederer 2006, Nobel 2009). The experimental data for the maximum area shrinkage (14.6%) and for the minimum conductance ($5.41 \cdot 10^{-5} \text{ m s}^{-1}$) of *Rhazya stricta* are in agreement with the predicted values according to Scoffoni *et al.* (2014).

Cuticular water permeability increases with temperature. For all plant species investigated so far, a phase transition at temperatures above 35 °C with a sharp increase of cuticular permeances was detected. Above the phase transition temperature, the reduced cuticular barrier properties, presumably caused by structural changes, are accompanied by high activation energies for water permeability in the range from 52 kJ mol^{-1} to 122 kJ mol^{-1} (Schreiber 2001, Riederer 2006b). In contrast, the Arrhenius plot for minimum conductances of *Rhazya stricta* revealed no phase transition (Figure 15). The low activation energy of 18.5 kJ mol^{-1} indicates that the structural integrity of the transpiration barrier was maintained over the whole temperature range up to 50 °C. Therefore, a strong reduction of transpiration as adaptation of desert plants might become relevant and evident only for the exposure of leaves to high temperatures. The minimum conductance to water vapour of *Rhazya stricta* leaves is $10.30 \cdot 10^{-5} \text{ m s}^{-1}$ at 50 °C (Table 3). However, almost all plant species

investigated by Riederer (2006b) exhibited cuticular permeances lower than $10.00 \cdot 10^{-5} \text{ m s}^{-1}$ at $50 \text{ }^{\circ}\text{C}$ (Figure 17).

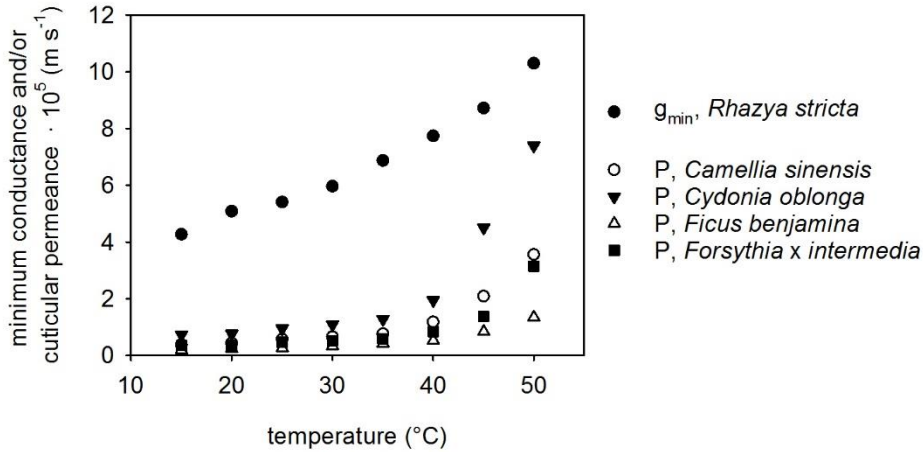


Figure 17. Comparison of the temperature effect on the minimum conductance (●, g_{\min}) of *Rhazya stricta* leaves with the cuticular permeances (P) from four plant species (○ ▼ △ ■, Riederer 2006b).

The importance of the cuticular transpiration barrier of *Rhazya stricta* leaves was assessed by calculating the leaf survival time, a parameter used to estimate the ability of plants to withstand drought stress. The survival time is defined as the quotient between the water supply available for cuticular transpiration when stomata are closed and the minimum transpiration rate (Pisek and Winkler 1953, Burghardt and Riederer 2003, Burghardt *et al.* 2008). The water supply is determined by subtracting the water content at critical dehydration level ($\text{RWD}_{\text{crit}} = 0.55$) or the water content at 50% of the maximum dehydration level ($\text{RWD}_{50} = 0.75$) from the water content at the stomatal closure point (Figure 14) and by multiplication with the degree of succulence (223.26 g m^{-2}). The minimum transpiration rate is calculated from the minimum conductance (Table 3) and the driving force. The model calculation of the leaf survival time of *Rhazya stricta* using RWD_{crit} as threshold value amounts to 25.3 h at $25 \text{ }^{\circ}\text{C}$ and 20% relative humidity. At higher temperatures the leaf survival time (20% relative humidity) decreases strongly to 4.3 h ($45 \text{ }^{\circ}\text{C}$) and 1.0 h ($50 \text{ }^{\circ}\text{C}$). Correspondingly, with RWD_{50} as threshold value, leaves have a survival time of 37.9 h at $25 \text{ }^{\circ}\text{C}$ and 20% relative humidity. The survival time decreases strongly at elevated temperature levels (7.1 h at $45 \text{ }^{\circ}\text{C}$ and 2.9 h at $50 \text{ }^{\circ}\text{C}$, 20% relative humidity). The short leaf survival times at $45 \text{ }^{\circ}\text{C}$ and $50 \text{ }^{\circ}\text{C}$ demonstrate that *Rhazya stricta* leaves lack the ability to withstand longer periods of drought without water uptake from the soil.

Stomatal closure is related to leaf water potential and the turgor loss point is considered as an important threshold value (Brodribb and Holbrook 2003, Burghardt and Riederer 2003). Generally, the turgor loss point is not uniquely associated with stomatal closure and falls between the initial phase and the final stage of stomatal closure (Brodribb *et al.* 2003). Complete stomatal closure (Figure 14) occurred for *Rhazya stricta* at lower relative water deficits than the turgor loss point (Figure 12). At moderate temperatures (< 40 °C), stomata were shut near the turgor loss point. In the high temperature range, especially at 45 °C and 50 °C, the point of stomatal closure shifted to distinct higher water deficits. Gibson (1998) proposed that non-succulent desert plants have the capability to open stomata at very low leaf water potentials and under extreme water stress, predisposing survival in arid climates.

The comparable high minimum conductances of *Rhazya stricta* leaves, the short leaf survival times and the late points of stomatal closure at elevated temperatures contradict the assumption that desert plants have an extraordinary effective transpiration barrier when stomata are closed in order to survive in arid climates. Gibson (1998) proposed that saving water is not as central for desert plants as formerly thought. Even more important is maximising of net photosynthesis and regulation of leaf energy balance for the maintenance of a favourable leaf temperature (Maximov 1931, Gibson 1998, Sandquist 2014).

3.3 Cuticular wax chemistry and minimum water permeability

The minimum conductance of the desert plant *Rhazya stricta* was in the upper range of cuticular permeances of stomatous, isolated cuticular membranes (Riederer and Schreiber 2001). Minimum conductances were not subjected to a phase transition with increasing temperature (Figure 15) as it is the case for isolated cuticular membranes (Schreiber 2001, Riederer 2006b). However, the 14 plant species investigated by Riederer (2006b) exhibited cuticular permeances lower than the obtained minimum conductances for *Rhazya stricta* (Table 3). The question rises whether the effectiveness of the transpiration barrier of *Rhazya stricta* leaves under the assumption of complete stomatal closure can be related to the amount and/or chemical composition of the cuticle.

The chemical composition of the cuticular leaf wax of *Rhazya stricta* showed the predominance of cyclic components, namely pentacyclic triterpenoids (85.2%) and a minor fraction of very-long-chain acyclic components (3.4%). The acyclic fraction (*n*-alkanes, primary alkanols and alkanolic acids) are common component classes often

present in cuticular leaf waxes. The detected carbon chain lengths of the aliphatic compounds are ubiquitously found (Figure 16; Jetter *et al.* 2006). Pentacyclic triterpenoids, for example ursolic acid and oleanolic acid, can accumulate in very high amounts in the cuticular wax of fruits and leaves (Bianchi *et al.* 1992, Casado and Heredia 1999, Oliveira and Salatino 2000, Tsubaki *et al.* 2013). For instance, the cuticular wax of *Aspidosperma tomentosum* (Apocynaceae) leaves is mainly composed of pentacyclic triterpenoids (69.4%; Oliveira and Salatino 2000). Chemical analysis of cutin monomers of *Rhazya stricta* leaves showed a typical profile of cutin monomers with dominating C₁₆ and C₁₈ hydroxyalkanoic acids with mid-chain hydroxy and epoxy groups. 9/10,16-dihydroxyhexadecanoic acid and 9,10-epoxy-18-hydroxyoctadecanoic acid as major monomers (Table 5) are commonly described for leaf cuticles (Holloway 1982b, Pollard *et al.* 2008). The chemical composition of cuticles from *Rhazya stricta* leaves contradicts the assumption that desert plants have a special cuticle chemistry in order to survive in arid climates. *Rhazya stricta* leaves had a high leaf wax quantity, in comparison to reported leaf wax quantities ranging from 0.4 µg cm⁻² to 160.0 µg cm⁻² (Mamrutha *et al.* 2010, Bouzoubaâ *et al.* 2006).

There are strong indications that cuticular waxes act as the main transport-limiting barrier of plant cuticles against uncontrolled water loss, whereas the contribution of the cutin matrix is still uncertain (Goodwin and Jenks 2005). *Rhazya stricta* leaves exhibited, in comparison to other plant species (Oliveira and Salatino 2000, Bouzoubaâ *et al.* 2006), a high wax coverage of 251.41 µg cm⁻² originating mainly from the accumulation of triterpenoids (Table 4). From reconstitution experiments of cuticular waxes on artificial membranes (Grncarevic and Radler 1967, Oliveira *et al.* 2003) and from experiments with mutants of tomato fruits (Vogg *et al.* 2004, Leide *et al.* 2011) and *Arabidopsis thaliana* leaves (Buschhaus and Jetter 2012), it is known that triterpenoid constituents do not establish as efficient transpiration barriers as aliphatic components. These findings seem reasonable, if the knowledge about the molecular structure of cuticular waxes is considered (Riederer and Schneider 1990, Riederer and Schreiber 1995). Aliphatic wax compounds are arranged in highly ordered, crystalline zones. Permeation is restricted to amorphous zones between the crystalline fractions. The amorphous zones are made up by chain ends, functional groups and short-chain aliphatics. The structural arrangement of cyclic wax compounds, such as pentacyclic triterpenoids, is characterised by a low molecular ordering (Casado and Heredia 1999, Tsubaki *et al.* 2013) and triterpenoids form amorphous zones, which are accessible to

permeating water molecules (Riederer and Schreiber 1995). Therefore, it can be assumed that the aliphatic fraction of cuticular waxes contributes to the main formation of an efficient cuticular barrier against water loss. The leaf cuticle of *Citrus aurantium* as example has a comparable small wax amount of $9.84 \mu\text{g cm}^{-2}$, exclusively aliphatic compounds, that is sufficient to establish a cuticular permeance of $4.71 \cdot 10^{-5} \text{ m s}^{-1}$ (Haas and Schönherr 1979). For *Rhazya stricta*, the amount of aliphatic wax components was $8.56 \mu\text{g cm}^{-2}$ (Table 4) and the minimum conductance was $5.41 \cdot 10^{-5} \text{ m s}^{-1}$ (Table 3). Consequently, it is proposed that the additional accumulation of very high amounts of triterpenoids in the cuticle of *Rhazya stricta* leaves ($214.12 \mu\text{g cm}^{-2}$) did not contribute to the formation of a particularly effective transpiration barrier. The major triterpenoid composition might be beneficial in high light intensity environments due to the UV-adsorbing characteristic of triterpenoids (Shepherd and Griffiths 2006).

The temperature-dependent minimum conductances of *Rhazya stricta* leaves reveal no phase transition at high temperatures. Residual stomatal transpiration and leakiness of incompletely closed stomata cannot be excluded (Kerstiens 1996b). An undetected stomatal effect might cover a phase transition of the cuticular permeance. Hence, the cuticular waxes form the main transport-limiting barrier, the phase transition has been attributed to the melting ranges of cuticular waxes (Eckl and Gruler 1980, Merk *et al.* 1998). However, triterpenoids have high melting points and the structural arrangement remains unaffected up to temperatures of $100 \text{ }^\circ\text{C}$ (Casado and Heredia 1999). Possible melting of the cuticular wax might occur at temperatures that are not ecologically relevant. The phase transition is also attributed to micro-defects and cracks in the cuticular wax barrier caused by a volume expansion of the cutin polymer and/or the wax-free matrix membrane (Schönherr *et al.* 1979, Schreiber and Schönherr 1990). This volume expansion was measured with isolated cuticular membranes and might be suppressed due to the cell wall stabilising the cuticular membrane in intact leaves. Pentacyclic triterpenoids are proposed to endow the toughness of the cuticle by functioning as nanofillers in the cutin matrix (Tsubaki *et al.* 2013). Such a function might be assumed for *Rhazya stricta* due to the presence of high amounts of triterpenoids ($214.12 \mu\text{g cm}^{-2}$) in relation to the amounts of cutin monomers ($340.60 \mu\text{g cm}^{-2}$). Strengthening of the cutin matrix by triterpenoids potentially reduces the extensibility of the cuticle and might prevent cuticular cracks suppressing the occurrence of a phase transition.

3.4 Conclusion

Functional cuticular membranes and, thus, low cuticular water permeabilities are considered as important mechanisms to enable plant survival under drought conditions. Only little information on cuticular water permeabilities of desert plants is available. Potential adaptations of the desert plant *Rhazya stricta* to heat and drought on the level of cuticular transpiration and cuticular chemistry were investigated.

Based on the current knowledge, it is known that triterpenoid compounds in cuticular waxes do not constitute as efficient transpiration barriers as for example *n*-alkanes (Oliveira *et al.* 2003). Due to the comparison with literature values, it can be deduced that small aliphatic wax coverages ($9.84 \mu\text{g cm}^{-2}$; Haas and Schönherr 1979) are sufficient to build transpiration barriers with similar efficiency as the transpiration barrier of *Rhazya stricta* leaves. The aliphatic wax coverage of $8.56 \mu\text{g cm}^{-2}$ is proposed to establish the main transport-limiting barrier, whereas cyclic components might fulfil other functions, such as protection of high light intensity and/or strengthen the cutin matrix.

Over the whole temperature range from 15 °C to 50 °C the minimum conductances are in the upper range of previously reported cuticular permeances (Riederer and Schreiber 2001, Riederer 2006b). The comparable high minimum conductance of *Rhazya stricta* leaves at 25 °C, the short leaf survival times and the late points of stomatal closure at elevated temperatures (> 40 °C) contradict the assumption that desert plants need an extraordinary efficient transpiration barrier when stomata are closed in order to survive in arid climates.

The minimum conductances were not subjected to a phase transition with increasing temperature as described for cuticular permeances of stomatous, isolated cuticular membranes (Riederer 2006b). It is proposed that the absence of a phase transition is due to (1) the cell wall stabilising the cuticular membrane, (2) residual stomatal transpiration, (3) melting of the wax components at temperatures that are not ecologically relevant and/or (4) triterpenoids strengthening the cutin matrix.

Chapter II. Comparison of the temperature effect on the minimum conductance and the cuticular permeance of the Mediterranean sclerophyll *Nerium oleander*

1 Introduction

Limited water availability induces stomatal closure and, thus, the stomatal transpiration is minimised. The remaining much lower water transpiration occurs through the plant cuticle, a continuous membrane that covers the epidermis of all aerial primary plant organs. A fundamental function of the plant cuticle is to reduce the uncontrolled water loss from the plant into the surrounding atmosphere. A low cuticular water permeability can be considered as crucial for plant survival under environmental conditions with limited water supply.

Plant cuticles are composed of a cutin matrix with cuticular waxes embedded within or deposited on its surface (Yeats and Rose 2013). Typical constituents of the cuticular waxes are very-long-chain aliphatic components and pentacyclic triterpenoids (Jetter *et al.* 2006). The cuticular waxes establish the main transport-limiting barrier (Schönherr 1976, Schönherr and Lenzian 1981). However, the relationship between wax coverage, wax composition and cuticular water permeability has remained unsolved (Schönherr 1982, Kerstiens 2006). Thick cuticular membranes do not provide more efficient transpiration barriers (Kamp 1930, Schreiber and Riederer 1996, Riederer and Schreiber 2001, Anfodillo *et al.* 2002). It is known that triterpenoid constituents do not establish as efficient transpiration barriers as aliphatic components (Grncarevic and Radler 1967, Oliveira *et al.* 2003, Vogg *et al.* 2004, Leide *et al.* 2011, Buschhaus and Jetter 2012).

The cuticular water permeability is frequently determined from astomatous, enzymatically isolated cuticular membranes. A wide literature survey of cuticular permeances of astomatous, isolated leaf cuticles from 57 plant species indicated a range between $0.04 \cdot 10^{-5} \text{ m s}^{-1}$ and $14.40 \cdot 10^{-5} \text{ m s}^{-1}$ (Riederer and Schreiber 2001). The measurement of water loss of detached and desiccating leaves under conditions of complete stomatal closure is a technique traditionally used to obtain the minimum water permeability of amphistomatic leaves (Körner 1995, Kerstiens 2006). The minimum value for the leaf water vapour conductance at fully closed stomata is often assumed to be essentially equal to the cuticular permeance (Nobel 2009). However,

the assumption of complete stomatal closure is described as a highly uncertain one and residual stomatal transpiration that influences the minimum conductance cannot be ruled out (Kerstiens 1996, 2006). Measurements comparing the cuticular permeance (astomatous system) with the minimum conductance (stomatous system) are rare. Nonetheless, for several plant species it was shown that the minimum conductance and cuticular permeance did not differ (Burghardt and Riederer 2003, Burghardt *et al.* 2008).

In hot and dry environments, plant species need to cope with drought periods often occurring simultaneously with high temperatures. The temperature effect on the cuticular water permeability of isolated cuticular membranes showed a slight increase of water permeabilities in the temperature range below 35 °C. At elevated temperatures (≥ 35 °C) a steep increase of the cuticular water permeability indicated an abrupt decline of the barrier properties, often described as a phase transition of the cuticular membrane (Schreiber 2001, Riederer 2006b). The analysis of intact stomatous leaves and the temperature effect on the minimum conductance of the desert plant *Rhazya stricta* revealed no such phase transition (Chapter I). However, little is known about the temperature dependence of the cuticular permeability of intact plant systems (Kerstiens 2006). The cell wall stabilising the cuticular membrane might prevent the phase transition. Additionally, residual stomatal transpiration that influences the minimum conductance cannot be excluded.

Nerium oleander (Apocynaceae) is a non-succulent, evergreen, hypostomatic shrub native to the Mediterranean region ranging into North Africa and South-West Asia (Kummerow 1973, Badger *et al.* 1982, Meletiou-Christou and Rhizopoulou 2012). The hypostomatic leaves enable a comparison between minimum conductance measured with intact, stomatous leaves and cuticular permeance measured with astomatous, isolated cuticular membranes. Possible influence on the minimum conductance due to residual stomatal transpiration and/or the cell wall stabilising the plant cuticle were addressed. The temperature effect on the minimum conductance and the cuticular permeance was compared. The question whether both experimental approaches were adequate to determine the temperature dependence of the minimum or cuticular water permeability was analysed. In addition, the cuticle chemistry and its relationship with the cuticular water permeability was investigated.

2 Results

2.1 Leaf characteristics of *Nerium oleander*

Leaf characteristics of *Nerium oleander* were determined. The leaf saturated fresh weight was 0.83 ± 0.21 g, the dry weight was 0.30 ± 0.08 g and the dual projected leaf area was $31.13 \pm 7.19 \cdot 10^{-4}$ m². Characteristic leaf traits were calculated from the leaf properties. The leaf water content was $0.64 (\pm 0.04)$ g g⁻¹, the specific leaf area was $5.32 (\pm 1.09)$ m² kg⁻¹ and the degree of succulence was 169.76 ± 19.70 g m⁻² (mean value \pm SD, n = 45). Stomata occurred on the abaxial leaf surface and were localised in crypts. Both leaf surfaces were covered with non-glandular foliar trichomes (Figure 18; Kummerow 1973, Gabr *et al.* 2015).

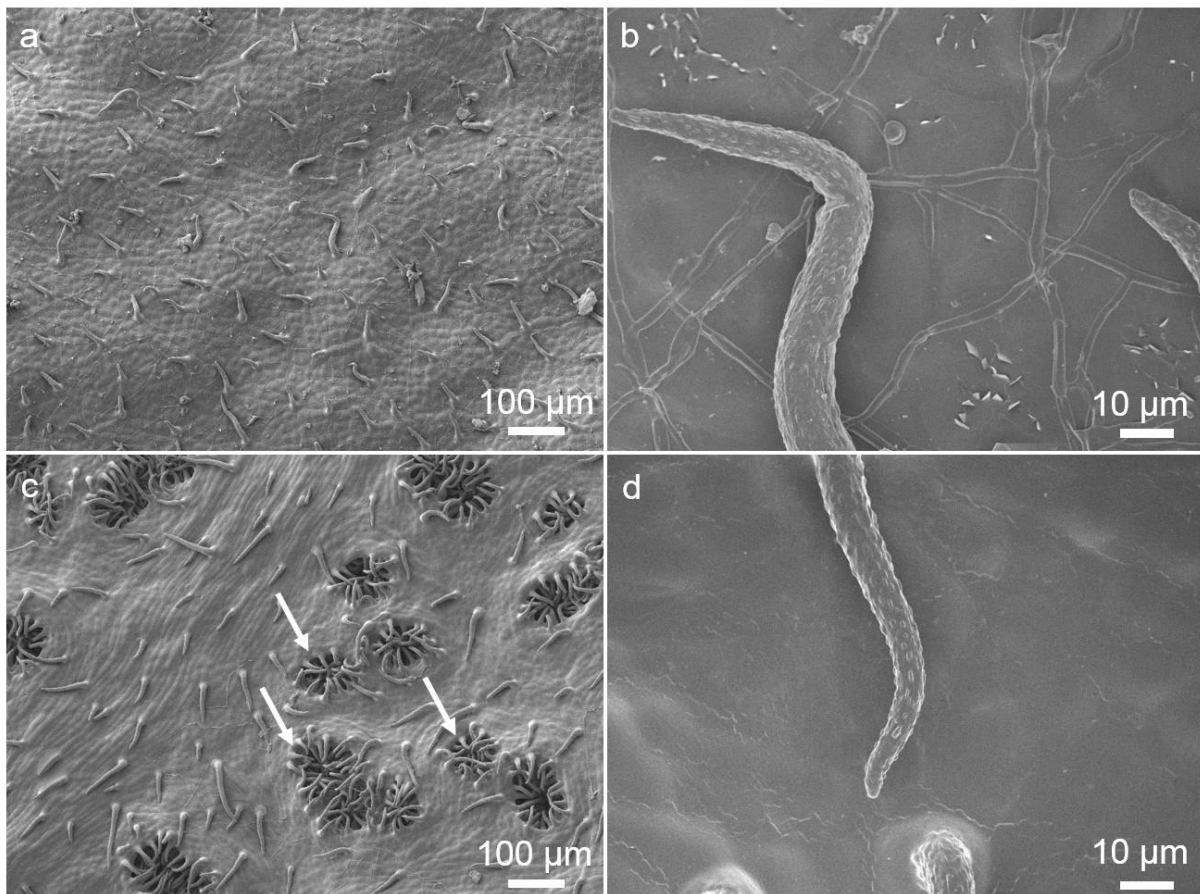


Figure 18. The native adaxial (a,b) and abaxial (c,d) leaf surface of *Nerium oleander*. Stomata occurred on the abaxial leaf surface, localised in crypts and are indicated by arrows. Both leaf surfaces showed foliar trichomes.

2.2 Leaf thermal tolerance

The leaf thermal tolerance of *Nerium oleander* leaves was determined (Figure 19). Heat exposure was applied for 1 °C per min and, subsequently, the maximum quantum yield of photosystem II in the dark adapted state ($F_v F_m^{-1}$) was measured without recovery time every 2.5 min. $F_v F_m^{-1}$ was only slightly affected by temperature treatments between 25.0 °C and 42.5 °C, whereas a strong decrease at temperatures higher than 45.0 °C occurred. The intersection point of the fitted regression lines indicated the critical temperature, T_{crit} was 42.57 ± 1.48 °C for dark adapted *Nerium oleander* leaves. T_{50} indicated a decline of $F_v F_m^{-1}$ to 50% of the maximum at the non-stressed level and was 51.78 ± 1.90 °C (mean value \pm SD, $n = 10$).

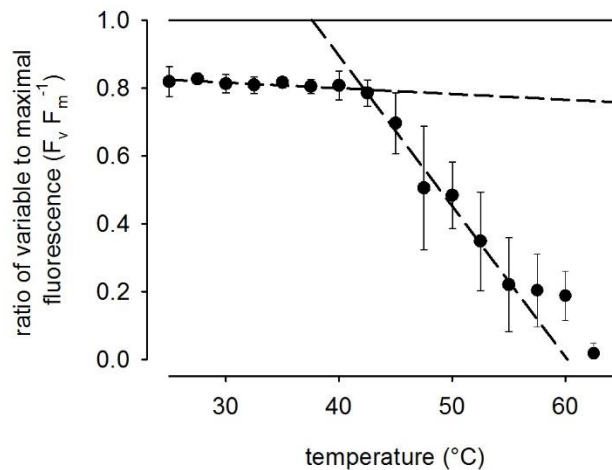


Figure 19. Effect of temperature on the maximum quantum yield of the photosystem II ($F_v F_m^{-1}$) of dark adapted *Nerium oleander* leaves (mean value \pm SD, $n = 10$).

2.3 Cuticular permeance and temperature effect on cuticular permeance

The cuticular permeance of isolated cuticular membranes inserted in transpiration chambers was measured in the temperature range from 15 °C to 55 °C. At 25 °C the cuticular permeance was $1.77 (1.53 - 1.83) \cdot 10^{-5} \text{ m s}^{-1}$ (median value (25% quartile - 75% quartile) and the median and non-parametric statistics were applied because data was not normally distributed. Cuticular permeances increased with elevation of temperatures by a factor of 3.4 between 15 °C and 55 °C from $1.35 (1.14 - 1.41) \cdot 10^{-5} \text{ m s}^{-1}$ to $4.62 (4.12 - 4.92) \cdot 10^{-5} \text{ m s}^{-1}$ (Table 6).

Table 6. The cuticular permeance (P) of *Nerium oleander* isolated cuticular membranes as a function of temperature (T) given as the median value with the 25% and 75% quartiles (Q25 - Q75, n = 10).

T (°C)	P · 10 ⁵ (m s ⁻¹)	
	median value (Q25 - Q75)	
15	1.35	(1.14 - 1.41)
20	1.27	(1.04 - 1.34)
25	1.77	(1.53 - 1.83)
30	2.57	(2.23 - 2.64)
35	2.69	(2.39 - 2.80)
40	3.05	(2.73 - 3.13)
45	3.20	(3.03 - 3.42)
50	3.78	(3.30 - 4.02)
55	4.62	(4.12 - 4.92)

The temperature dependence of the cuticular permeance was analysed by an Arrhenius plot (Figure 20). An activation energy for the permeation of water of 26.9 kJ mol⁻¹ (from 15 °C to 55 °C) was calculated from the slope of the regression line. In addition, activation energies were separately calculated for the lower temperature range (31.4 kJ mol⁻¹; from 15 °C to 35 °C) and the higher temperature range (23.4 kJ mol⁻¹; from 35 °C to 55 °C).

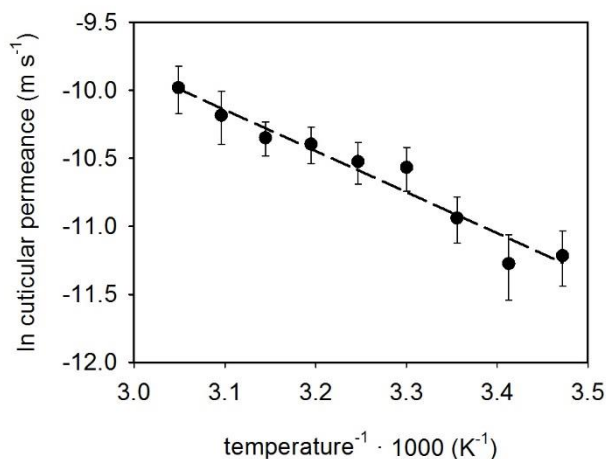


Figure 20. Arrhenius plot of the natural logarithm of the cuticular permeance and the inverse absolute temperature (median value ± interquartile range (IQR), n = 10; Spearman correlation coefficient (SCC) = -0.983, p < 0.001).

2.4 Leaf drying curve, minimum conductance and temperature effect on minimum conductance

Leaf drying curves were conducted to obtain the leaf minimum conductance with maximum stomatal closure. The initial phase of the leaf drying curves was characterised by high conductances. Conductances declined with leaf dehydration until a plateau of constant and low values was reached, the minimum conductance at maximum stomatal closure (Figure 21). The relative water deficit at the point of complete stomatal closure was derived from the transition between the declining phase and the plateau phase. At 25 °C the minimum conductance was $2.16 \pm 0.58 \cdot 10^{-5} \text{ m s}^{-1}$ and the relative water deficit at stomatal closure was 0.11 ± 0.02 (mean value \pm SD).

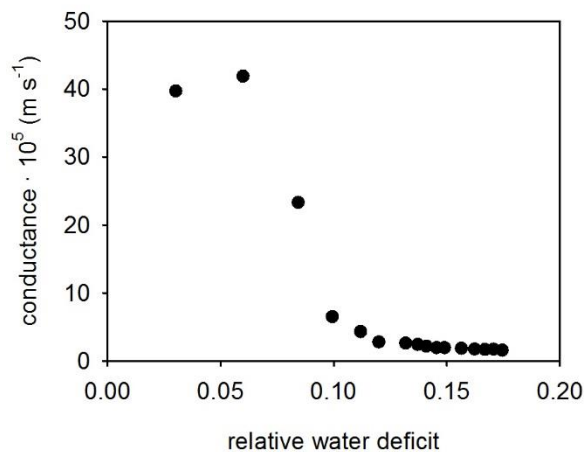


Figure 21. The leaf conductance of *Nerium oleander* at 25 °C as a function of relative water deficit exemplarily represents the obtained leaf drying curves ($n = 1$).

Leaf drying curves were carried out in the temperature range from 15 °C to 55 °C. Minimum conductances increased with elevation of temperatures by a factor of 2.7 between 15 °C and 55 °C from $1.95 \pm 0.57 \cdot 10^{-5} \text{ m s}^{-1}$ to $5.18 \pm 1.29 \cdot 10^{-5} \text{ m s}^{-1}$ (Table 7).

Table 7. The minimum conductance (g_{\min}) of *Nerium oleander* leaves as a function of temperature (T) obtained from leaf drying curves (mean value \pm SD, $n \geq 5$), the ratio between g_{\min} and the cuticular permeance (P, Table 6). Statistical differences between P and g_{\min} were analysed by Mann-Whitney U-tests.

T (°C)	$g_{\min} \cdot 10^5$ (m s^{-1})	ratio g_{\min}/P	p-values
15	1.95 \pm 0.57	1.56	$p = 0.03$
20	2.24 \pm 0.70	1.88	$p = 0.02$
25	2.16 \pm 0.58	1.31	$p = 0.12$
35	2.66 \pm 0.89	1.05	$p = 0.50$
40	2.74 \pm 0.53	0.96	$p = 0.50$
45	4.10 \pm 1.16	1.22	$p = 0.43$
50	4.02 \pm 0.67	1.12	$p = 0.58$
55	5.18 \pm 1.29	1.16	$p = 0.36$

Maximum stomatal closure occurred at relative water deficits between 0.1 and 0.2 in the temperature range between 15 °C and 45 °C. At higher temperatures (> 45 °C), the point of maximum stomatal closure was shifted to higher water deficits and amounted to a relative water deficit of 0.63 ± 0.03 at 55 °C (Figure 22).

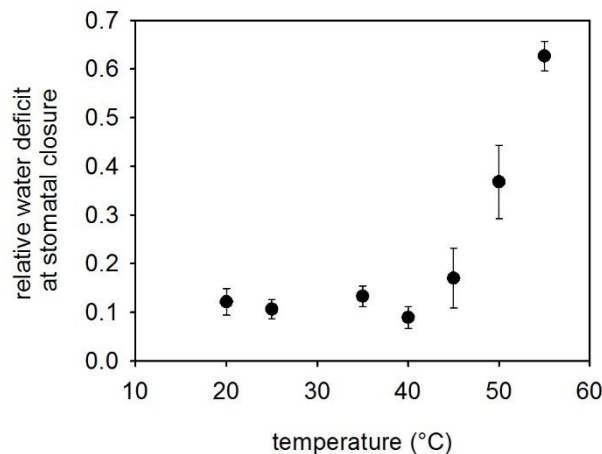


Figure 22. The relative water deficit of *Nerium oleander* leaves at which maximum stomatal closure occurred as a function of temperature (mean value \pm SD, $n \geq 5$).

To confirm the shift of the relative water deficit at stomatal closure at elevated temperatures, leaves of *Nerium oleander* were dehydrated at 25 °C until stomatal closure by a decrease of conductance was determined. Upon maximum stomatal closure the leaves were exposed to elevated temperatures (55 °C). A novel increase of the conductance confirmed stomatal closure at relative water deficits above $RWD = 0.6$ (Figure 23).

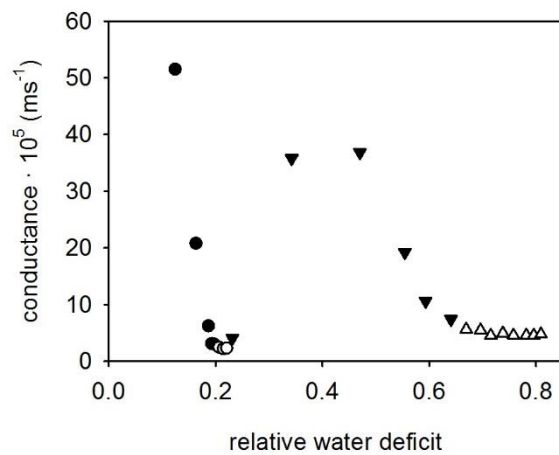


Figure 23. The leaf conductance of *Nerium oleander* as a function of the relative water deficit: conductance at 25 °C (●), minimum conductance at 25 °C (○), conductance at 55 °C (▼) and minimum conductance at 55 °C (△; n = 1).

The temperature dependence of the minimum conductance was analysed by an Arrhenius plot (Figure 24). An activation energy for the permeation of water of 18.2 kJ mol⁻¹ (from 15 °C to 55 °C) was calculated from the slope of the regression line. In addition, activation energies were separately calculated for the lower temperature range (10.5 kJ mol⁻¹; from 15 °C to 35 °C) and the higher temperature range (28.8 kJ mol⁻¹; from 35 °C to 50 °C). Slopes of Arrhenius plots were compared (Soper 2016). Slopes of the Arrhenius plots of the natural logarithm of the minimum conductance or the cuticular permeance and the inverse absolute temperature did not differ significantly from each other ($p = 0.06$).

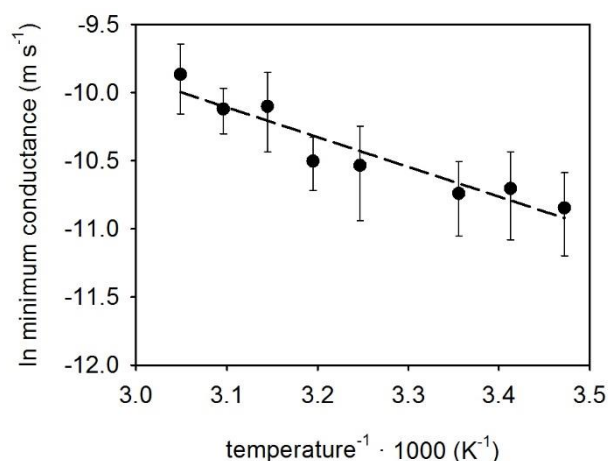


Figure 24. Arrhenius plot of the natural logarithm of the minimum conductance and the inverse absolute temperature (mean value \pm SD, $n \geq 5$; Pearson correlation coefficient (PCC) = -0.946, $p < 0.001$).

2.5 Gravimetric and chemical analysis of the cuticular components

Enzymatically isolated cuticular membranes had a total weight of $1912.50 \pm 265.71 \mu\text{g cm}^{-2}$. After extraction of the cuticular waxes, the wax-free matrix membranes had a weight of $1400.69 \pm 201.16 \mu\text{g cm}^{-2}$. From the weight loss before and after extraction, the extracted wax coverage was calculated ($511.82 \pm 69.15 \mu\text{g cm}^{-2}$; mean value \pm SD, $n = 5$). From the total cuticular membranes 26.8% were extractable components.

2.5.1 Chemical analysis of the cuticular leaf wax

The cuticular waxes were analysed quantitatively by gas chromatograph equipped with a flame ionisation detector and the qualitative analysis by gas chromatograph equipped with a mass spectrometric detector. Total cuticular adaxial leaf wax coverage of *Nerium oleander* was $336.93 \pm 63.73 \mu\text{g cm}^{-2}$ (mean value \pm SD, $n = 6$). The leaf wax composed of a major portion of cyclic components (83.7%, $281.96 \pm 52.76 \mu\text{g cm}^{-2}$) and a minor portion of very-long-chain acyclic component classes (10.1%, $34.08 \pm 5.87 \mu\text{g cm}^{-2}$).

N-alkanes were the most prominent acyclic component class (9.3%, $31.35 \pm 5.26 \mu\text{g cm}^{-2}$), followed by primary and secondary alkanols (0.7%, $2.44 \pm 0.73 \mu\text{g cm}^{-2}$) and alkanolic acids (0.1%, $0.28 \pm 0.12 \mu\text{g cm}^{-2}$). Carbon chain lengths ranged from C_{20} to C_{37} , the most abundant chain lengths were C_{29} , C_{31} and C_{33} (Figure 25). *N*-nonacosane (2.0%, $6.81 \pm 1.45 \mu\text{g cm}^{-2}$), *n*-hentriacontane (2.8%, $9.34 \pm 2.02 \mu\text{g cm}^{-2}$) and *n*-

tritriacontane (2.0%, $6.78 \pm 1.17 \mu\text{g cm}^{-2}$) dominated the acyclic components. The average carbon chain length (ACL) of the very-long-chain acyclic wax components was 31.33.

The main cyclic component was ursolic acid with a cuticular wax coverage of $199.80 \pm 35.08 \mu\text{g cm}^{-2}$ (59.3%), followed by oleanolic acid (20.8%, $70.12 \pm 12.97 \mu\text{g cm}^{-2}$; Table 8).

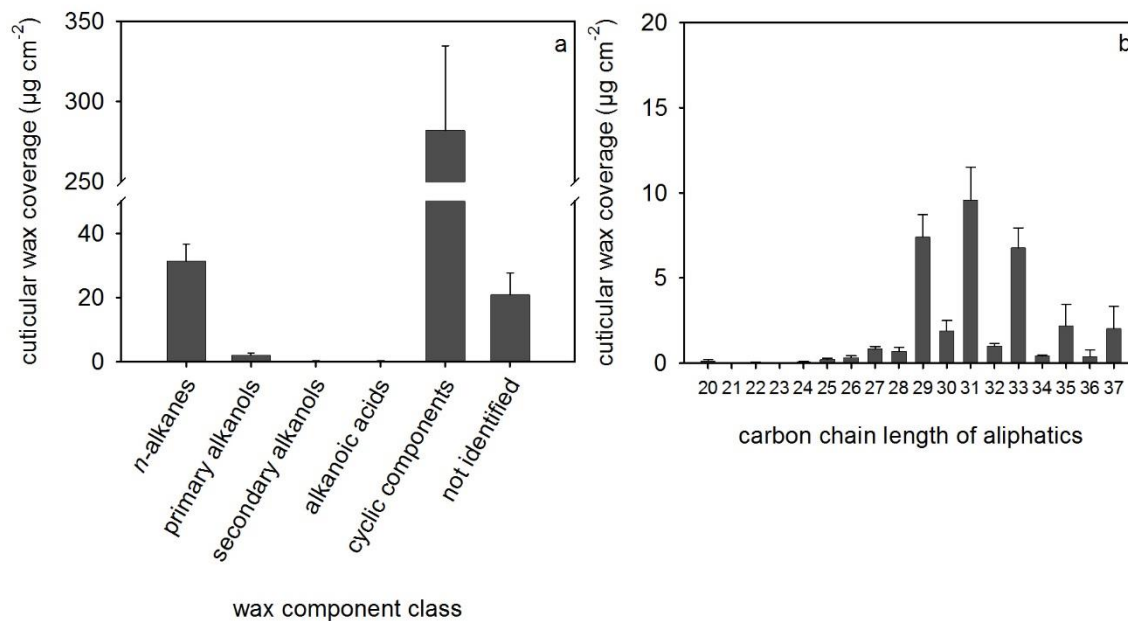


Figure 25. Adaxial cuticular wax composition of *Nerium oleander* leaves. (a) Cuticular wax coverage arranged according to the component classes and (b) the carbon chain length distribution of the acyclic components (mean value \pm SD, $n = 6$).

Table 8. The cuticular wax coverage and components of isolated adaxial cuticular membranes of *Nerium oleander* leaves (mean value \pm SD, n = 6).

		carbon chain length	wax coverage ($\mu\text{g cm}^{-2}$)		
<i>n</i> -alkanes		25	0.14	\pm	0.09
		26	0.15	\pm	0.11
		27	0.60	\pm	0.14
		28	0.42	\pm	0.11
		29	6.81	\pm	1.45
		30	1.07	\pm	0.22
		31	9.34	\pm	2.02
		32	1.01	\pm	0.16
		33	6.78	\pm	1.17
		34	0.41	\pm	0.09
		35	2.20	\pm	1.27
		36	0.40	\pm	0.37
		37	2.03	\pm	1.32
primary alkanols		24	0.02	\pm	0.01
		25	0.09	\pm	0.03
		26	0.11	\pm	0.04
		27	0.23	\pm	0.04
		28	0.29	\pm	0.12
		29	0.51	\pm	0.34
		30	0.84	\pm	0.41
secondary alkanols	pos. 2	29	0.10	\pm	0.02
	pos. 2	31	0.24	\pm	0.12
alkanoic acids		20	0.13	\pm	0.10
		22	0.04	\pm	0.02
		24	0.05	\pm	0.02
		26	0.06	\pm	0.02
sum acyclic components (10.1%)			34.08	\pm	5.87
α -amyrin			0.23	\pm	0.10
erythrodiol			0.87	\pm	0.37
uvaol			3.08	\pm	1.01
oleanolic acid			70.12	\pm	12.97
betulinic acid			5.55	\pm	4.23
ursolic acid			199.80	\pm	35.08
hederagenin			2.00	\pm	1.18
β -sitosterol			0.19	\pm	0.10
stigmasterol			0.12	\pm	0.11
sum cyclic components (83.7%)			281.96	\pm	52.76
not identified			20.90	\pm	6.78
sum acyclic, cyclic and not identified cuticular wax components (100.0%)			336.93	\pm	63.73

2.5.2 Chemical analysis of the cutin monomers

The total amount of adaxial cutin monomers was $483.52 \pm 76.94 \mu\text{g cm}^{-2}$ (mean value \pm SD, $n = 5$). The cutin polymer composed a major portion of aliphatic acid components (88.8%, $429.26 \pm 60.62 \mu\text{g cm}^{-2}$) and a minor portion of phenolic acid components (3.0%, $14.67 \pm 5.10 \mu\text{g cm}^{-2}$).

Carbon chain lengths ranged from C₁₄ to C₂₂, the most abundant chain lengths were C₁₆ (26.1%, $126.08 \pm 17.86 \mu\text{g cm}^{-2}$) and C₁₈ (61.3%, $296.24 \pm 42.54 \mu\text{g cm}^{-2}$). The ratio between the C₁₆/C₁₈ carbon chain length components was 0.4. The aliphatic acid components were dominated by 9,10-epoxy-18-hydroxyoctadecanoic acid (50.9%, $246.03 \pm 27.05 \mu\text{g cm}^{-2}$) and 9/10,16-dihydroxyhexadecanoic acid (24.3%, $117.33 \pm 17.47 \mu\text{g cm}^{-2}$).

The phenolic acid components were dominated by *trans*-coumaric acid (1.8%, $8.53 \pm 3.60 \mu\text{g cm}^{-2}$). Two coumaric acid derivatives (I and II) were not identified further in detail (Table 9).

The ratio between the total wax coverage and the total amount of cutin monomers was 0.7 and the ratio between the cyclic wax components and the total amount of cutin monomers was 0.6.

Table 9. The cutin coverage and monomers of adaxial isolated cuticular membranes of *Nerium oleander* leaves (mean value \pm SD, n = 5).

cutin monomers	carbon chain length	cutin coverage ($\mu\text{g cm}^{-2}$)		
tetradecanoic acid	14	0.39	\pm	0.06
hexadecanoic acid	16	0.85	\pm	0.17
hexadecane-1,16-dioic acid	16	0.52	\pm	0.07
16-hydroxyhexadec-9-enoic acid	16:1	traces		
16-hydroxyhexadecanoic acid	16	2.11	\pm	0.18
16-hydroxy-9/10-oxo-hexadecanoic acid	16	0.48	\pm	0.18
7/8-hydroxyhexadecane-1,16-dioic acid	16	4.76	\pm	0.64
9/10,16-dihydroxyhexadecanoic acid	16	117.33	\pm	17.47
9/10,16-dihydroxyheptadecanoic acid	17	0.85	\pm	0.11
octadec-9-enoic acid	18:1	0.28	\pm	0.08
octadecanoic acid	18	0.22	\pm	0.07
octadecane-1,18-dioic acid	18	1.01	\pm	0.15
18-hydroxyoctadeca-9,12-dienoic acid	18:2	7.45	\pm	1.09
9/10-hydroxyoctadec-12-ene-1,18-dioic acid	18:1	4.06	\pm	2.23
7/8-hydroxyoctadecane-1,18-dioic acid	18	1.05	\pm	0.34
9/10,18-dihydroxyoctadecanoic acid	18	11.88	\pm	1.97
9,10-epoxy-18-hydroxyoctadec-12-enoic acid	18:1	2.97	\pm	0.28
9,10-epoxy-18-hydroxyoctadecanoic acid	18	246.03	\pm	27.05
9,10,18-trihydroxyoctadec-12-enoic acid	18:1	1.04	\pm	1.04
9,10,18-trihydroxyoctadecanoic acid	18	19.42	\pm	10.57
7/8,9/10-dihydroxyoctadec-12-ene-1,18-dioic acid	18	0.83	\pm	0.59
nonadec-10-enoic acid	19:1	3.10	\pm	0.24
9/10,19-dihydroxynonadecanoic acid	19	traces		
eicosanoic acid	20	0.24	\pm	0.21
9/10,20-dihydroxyeicosanoic acid	20	1.91	\pm	0.85
docosanoic acid	22	0.44	\pm	0.12
sum aliphatic acid components (88.8%)		429.26	\pm	60.62
<i>cis</i> -coumaric acid		0.34	\pm	0.05
<i>trans</i> -coumaric acid		8.53	\pm	3.60
coumaric acid derivative I		4.36	\pm	1.23
coumaric acid derivative II		1.43	\pm	0.59
sum phenolic acid components (3.0%)		14.67	\pm	5.10
glycerin		0.20	\pm	0.03
not identified		39.40	\pm	13.08
sum total cutin monomers (100.0%)		483.52	\pm	76.94

3 Discussion

3.1 Classification and comparison of the minimum conductance and the cuticular permeance

The adaxial leaf surface of *Nerium oleander* is astomatous (Figure 18) and the cuticular membranes can be enzymatically isolated. These facts enable the measurement of both the cuticular permeance of isolated cuticular membranes and the minimum conductance of intact leaves and the comparison of both parameters. The minimum conductance ($2.16 \cdot 10^{-5} \text{ m s}^{-1}$) and the adaxial cuticular permeance ($1.77 \cdot 10^{-5} \text{ m s}^{-1}$) of *Nerium oleander* leaves were not significantly different at 25 °C. The minimum conductance of leaves with fully closed stomata and the astomatous cuticular permeance are often considered to be equal (Nobel 2009). However, assuming complete stomatal closure is described as a highly uncertain presumption (Kerstiens 2006). Residual stomatal conductance might exceed the values for cuticular permeances, even if stomata would be regarded as completely closed (Kerstiens 1996b). In the case for *Nerium oleander* leaves the residual stomatal conductance after complete stomatal closure was negligible. Similar results were obtained for leaves of *Acer campestre*, *Fagus sylvatica*, *Quercus petraea*, *Ilex aquifolium* and *Teucrium chamaedrys* (Burghardt and Riederer 2003, Burghardt *et al.* 2008). Currently, only one plant species, *Hedera helix*, is described to have a significantly higher minimum conductance than cuticular permeance. The minimum conductance is the sum of residual stomatal conductance and cuticular permeance. In the case of *Hedera helix* the residual stomatal conductance contributed 67.0% ($4.90 \cdot 10^{-6} \text{ m s}^{-1}$) to the minimum conductance (Burghardt and Riederer 2003). Assuming a statistical difference between the minimum conductance and the cuticular permeance of *Nerium oleander* leaves, the residual stomatal conductance would amount to $3.90 \cdot 10^{-6} \text{ m s}^{-1}$ and contribute 18.1% to the minimum conductance.

An asymmetrical distribution is reported for the cuticular permeances measured from astomatous, isolated cuticular membranes (Geyer and Schönherr 1990, Schreiber and Riederer 1996, Niederl *et al.* 1998). Geyer and Schönherr (1990) excluded the outliers that caused the tailing due to isolation procedures probably damaging cuticular membranes. Schreiber and Riederer (1996) regarded all measured cuticular permeances and opted for using the median with 25% and 75% quartiles. Another option is the log transformation and, therefore, obtaining a log-normal distribution of data (Baur 1997, Niederl *et al.* 1998). An asymmetrical distribution was

obtained for the cuticular permeances of *Nerium oleander* adaxial, astomatous, isolated cuticular membranes (Figure 26). Due to the symmetrical distribution of the minimum conductances and the good accordance between minimum conductance and cuticular permeance at 25 °C isolation damage to the cuticular membranes can be excluded in the case of *Nerium oleander*. The cuticular permeances were given as median values and quartiles and non-parametric statistics were used for the comparison.

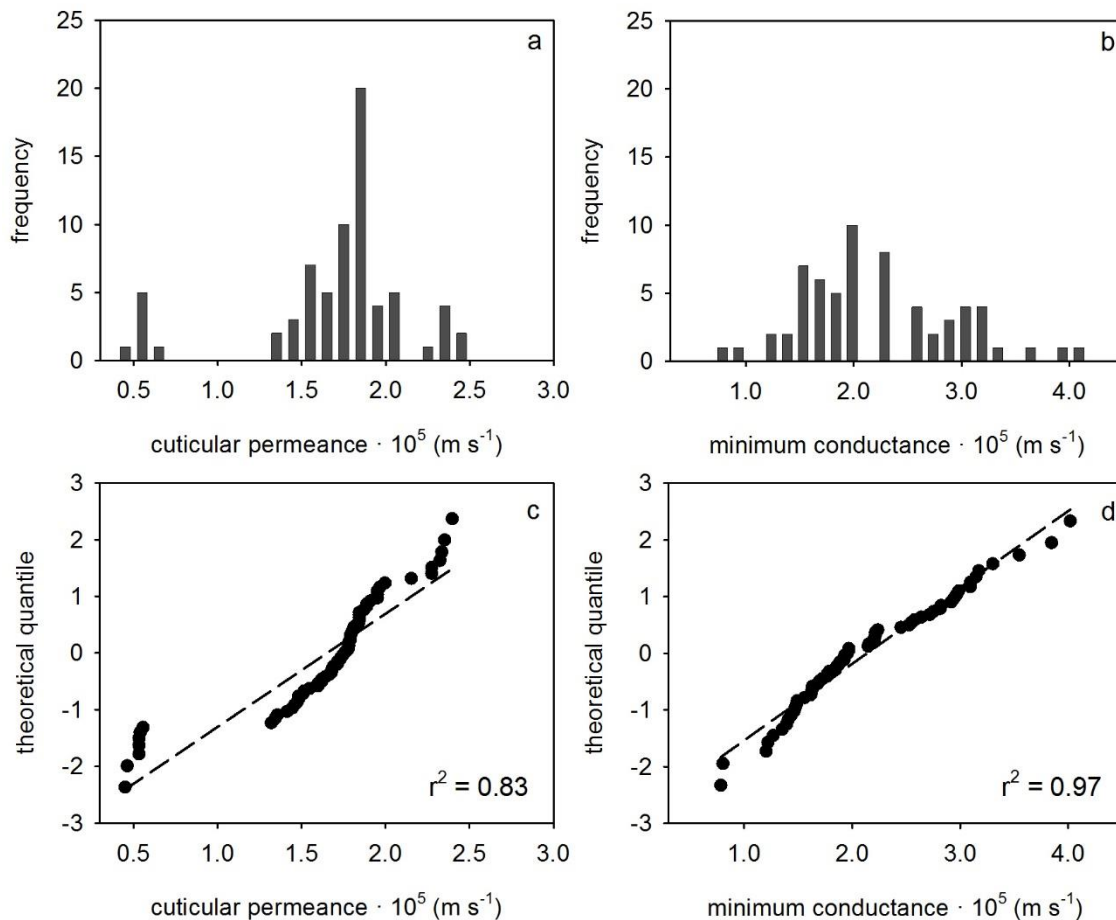


Figure 26. Frequency distribution histogram (a,b) and the corresponding quantile-quantile plots (c,d). (a,c) Cuticular permeance of isolated cuticular membranes from *Nerium oleander* leaves at 25 °C (n = 10). (c,d) Minimum conductance of intact *Nerium oleander* leaves at 25 °C (n = 10).

The minimum conductance to water vapour of *Nerium oleander* leaves amounted to $2.16 \cdot 10^{-5} \text{ m s}^{-1}$ and the cuticular permeance was $1.77 \cdot 10^{-5} \text{ m s}^{-1}$ (25 °C). The cuticular permeances of xeromorphic plant species from Mediterranean climates reported by Riederer and Schreiber (2001) vary from $0.05 \cdot 10^{-5} \text{ m s}^{-1}$ to $10.00 \cdot 10^{-5} \text{ m s}^{-1}$. Both the minimum conductance and the cuticular permeance of *Nerium oleander* leaves are

in the upper medium scale of this ranking of cuticular permeances. Ample information on the cuticular permeance at 25 °C of *Nerium oleander* leaves is available. Cuticular permeances of $0.3 \cdot 10^{-5} \text{ m s}^{-1}$ are reported for astomatous, isolated *Nerium oleander* cuticular membranes (Becker *et al.* 1986, Riederer 2006b). On the other hand, cuticular permeances and minimum conductances in the range of $2.0 \cdot 10^{-5} \text{ m s}^{-1}$ are described (Schreiber and Riederer 1996, Burghardt and Riederer 2006). These literature data differs by a factor of 6.7. Underestimation of the cuticular permeance might possibly be induced by the reduction of cuticular permeances during the storage of isolated cuticular membranes (Geyer and Schönherr 1990, Kerstiens 1996b, Schreiber and Schönherr 2009). Storage time is not always clearly indicated. Only, Schreiber and Riederer (1996) documented a storage time of several weeks. In the case of the *Nerium oleander* leaves used in this study, the isolated cuticular membranes were air-dried for several days. The cuticular permeances are in good accordance with the values obtained by Schreiber and Riederer (1996) and Burghardt and Riederer (2006). Differences comparing the available literature values and measured values could be due to different cultivars and/or different growth conditions. Due to the congruence of the cuticular permeance and the minimum conductance ($\geq 25 \text{ °C}$; Table 7) it is concluded that, for *Nerium oleander* leaves both measurement systems are appropriate.

3.2 Temperature effect on the minimum conductance and the cuticular permeance

The lethal limit of heat stress of *Nerium oleander* leaves was 51.78 °C (T_{50}) and indicated a decline of the maximum quantum yield of photosystem II in the dark adapted state ($F_v F_m^{-1}$) below 50% of the maximum value of unstressed leaves. This value is used as a threshold value for viability with the onset of irreversible damage to the photosynthetic apparatus (Woo *et al.* 2008, Curtis *et al.* 2014). The limit of whole leaf survival in response to high temperature stress was assessed. This indicated that the measurement temperature of 55 °C is above the lethal limit of heat stress and should be interpreted carefully.

The cuticular permeances of many plant species increase steeply at temperatures above 35 °C (Schreiber 2001, Riederer 2006b). The temperature dependence can be quantified by the activation energy from the slope of the regression line in Arrhenius plots. The isolated cuticular membranes of for example *Citrus aurantium* leaves had a low activation energy of 23.6 kJ mol⁻¹ (from 15 °C to 35 °C) and 52.2 kJ mol⁻¹ (from 35

°C to 55 °C). A substantial increase is reported for the activation energy of *Forsythia intermedia*, with 21.7 kJ mol⁻¹ from 15 °C to 35 °C and 105.2 kJ mol⁻¹ from 35 °C to 55 °C. *Nerium oleander* isolated cuticular membranes had an activation energy of 15.2 kJ mol⁻¹ (from 15 °C to 35 °C) and 89.9 kJ mol⁻¹ (from 35 °C to 55 °C; Riederer 2006b). In contrast to the literature, the Arrhenius plot in the present study analysing the temperature effect on cuticular permeances and minimum conductances of *Nerium oleander* leaves revealed no phase transition (Figure 20, Figure 24). The activation energies from 15 °C to 35 °C were 31.4 kJ mol⁻¹ and 10.5 kJ mol⁻¹ and from 35 °C to 55 °C the activation energies were 23.4 kJ mol⁻¹ and 28.8 kJ mol⁻¹ (cuticular permeances and minimum conductances, respectively). The minimum conductance did not differ significantly from the cuticular permeance at temperatures ≥ 25 °C, indicating the same temperature effect on isolated cuticular membranes as well as on intact leaves.

Studies comparing the minimum conductance of intact leaves with the cuticular permeance of stomatous leaf surfaces at 25 °C are scarce in the literature (Burghardt and Riederer 2003, Burghardt *et al.* 2008). Data of the temperature effect on both the minimum conductance and the cuticular permeance from one plant species are not published so far. This is the first study comparing the temperature effect on isolated cuticular membranes as well as intact leaves of *Nerium oleander* as model plant species. Only one study available compared the temperature effect on the cuticular permeances of isolated cuticular membranes and punched-out leaf discs inserted in modified transpiration chambers from the same plant species (Schreiber 2001). However, Schreiber (2001) referenced the permeance for water to the liquid phase and, by this, the temperature effect might be overestimated (Kerstiens 1996b). Additionally, the activation energy should exceed the latent heat of vaporisation if referenced to the water density in the liquid state based permeance (Kerstiens 2006). This is not the case with some of the activation energies indicated by Schreiber (2001).

The temperature effect on cuticular permeances and minimum conductances of *Nerium oleander* leaves revealed no phase transition. The cell wall might act stabilising on the cuticular membranes and, thus, suppress the volume expansion of the cutin polymer and/or wax-free membrane described by Schönherr *et al.* (1979) and Schreiber and Schönherr (1990) for isolated cuticular membranes. The influence of the cell wall on the cuticular water permeability can be excluded by comparing the cuticular permeance of isolated cuticular membranes and the minimum conductance of intact

leaves from *Nerium oleander* leaves. Both systems are adequate to determine the temperature dependence of the minimum or cuticular water permeability. Furthermore, residual stomatal transpiration affecting the minimum conductance is not deducible.

3.3 Shift of relative water deficit at stomatal closure at elevated temperatures

The relative water deficit of *Nerium oleander* leaves at which maximum stomatal closure occurred was shifted to higher water deficits at elevated temperatures (Figure 22). In the high temperature range, especially at 45 °C, 50 °C and 55 °C, the point of stomatal closure shifted to distinct higher water deficits. This shift of RWD_{SC} was also detected when analysing the temperature effect on the minimum conductance of *Rhazya stricta* (Chapter I). For *Nerium oleander* leaves, an anew increase of leaf conductance after complete stomatal closure at 25 °C with leaf exposure to high temperatures was observed (Figure 23). The increase of the leaf conductance after stomatal closure might indicate a stomatal opening at elevated temperatures after complete stomatal closure.

Plant species are often exposed to drought and elevated temperatures simultaneously. Antagonistic effects of drought and heat on stomata have been described. Stomatal closure upon leaf dehydration is a widely accepted stomatal reaction. In contrast, stomatal aperture upon temperature elevation was described (Feller 2006, Reynolds-Henne *et al.* 2010). Feller (2006) described a stomatal aperture increase from 0.66 μm at 23 °C to 4.47 μm at 45 °C for *Phaseolus vulgaris* leaf segments. Reynolds-Henne *et al.* (2010) suggested by means of thermal imaging that two analysed plant species (*Phaseolus vulgaris* and *Trifolium pratense*) close the stomata under moderate water stress prioritising water relations, while at high temperature stress the stomatal conductance is increased, even under drought, protecting the photosynthetic apparatus from heat. Similarly, a stomatal opening above the approximate lethal leaf temperatures (above 40 °C) has been reported by Lösch (1978, 2001) and Brunner and Eller (1974). According to Lösch (2001), the stomatal opening is accompanied by an increase of conductance and indicates an increased transpirational cooling. The increase of the leaf conductance of *Nerium oleander* at high temperatures might demonstrate an enhanced leaf cooling under heat impact, as proposed by Lösch (2001) and Feller (2006).

3.4 Cuticular wax chemistry and minimum or cuticular water permeability

The question arises whether the effectiveness of the cuticular transpiration barrier of *Nerium oleander* leaves can be related to the chemical composition of the cuticle. Both the minimum conductances and cuticular permeances were not subjected to a phase transition with increasing temperature.

The chemical composition of the cuticular leaf waxes showed the predominance of cyclic components, namely pentacyclic triterpenoids (83.7%), and a minor portion of very-long-chain acyclic components (10.1%). Similarly, Merk (1998) found that cuticles of *Nerium oleander* leaves are mainly composed of pentacyclic triterpenoids (79.0%). The acyclic very-long-chain component classes from the *Nerium oleander* leaf wax are common wax components such as *n*-alkanes, primary and secondary alkanols and alkanolic acids. The carbon chain lengths of the aliphatic compounds were typical homologous series of wax components ranging from C₂₀ to almost C₄₀ (Figure 25; Jetter *et al.* 2006). The chemical analysis of the cutin monomers of *Nerium oleander* showed a typical profile of cutin monomers with dominating C₁₆ and C₁₈ hydroxyalkanoic acids with mid-chain hydroxy and epoxy groups (Pollard *et al.* 2008). 9,10-epoxy-18-hydroxyoctadecanoic acid and 9/10,16-dihydroxy-hexadecanoic acid were the dominating monomer components (Table 9). *Nerium oleander* leaves had a high leaf wax quantity, in comparison to reported leaf wax quantities ranging from 0.4 µg cm⁻², 160.0 µg cm⁻² (Mamrutha *et al.* 2010, Bouzoubaâ *et al.* 2006) up to 251.4 µg cm⁻² (Chapter I).

The cuticular waxes establish the main transport-limiting barrier (Schönherr 1976, Schönherr and Lenzian 1981) and are commonly composed of very-long-chain aliphatic components and cyclic constituents. Cyclic components, such as triterpenoids, do not establish as efficient transpiration barriers as very-long-chain acyclic components (Grncarevic and Radler 1967, Oliveira *et al.* 2003, Vogg *et al.* 2004, Leide *et al.* 2011, Buschhaus and Jetter 2012). The very-long-chain aliphatic components form crystalline fractions that are not available for the water diffusion. Between the crystalline fractions, amorphous zones enable the water diffusion (Riederer and Schreiber 1995). Triterpenoids have low molecular ordering (Casado and Heredia 1999, Tsubaki *et al.* 2013) and form amorphous zones. The main barrier function of plant cuticles might be primarily established by the very-long-chain aliphatic components. However, no relationship between structure and property on a quantitative level has been established (Burghardt and Riederer 2006).

The minimum conductance to water vapour of *Nerium oleander* leaves amounted to $2.16 \cdot 10^{-5} \text{ m s}^{-1}$ and the aliphatic leaf wax coverage was $34.08 \mu\text{g cm}^{-2}$. For *Rhazya stricta*, the amount of aliphatic wax components was lower ($8.56 \mu\text{g cm}^{-2}$) and the minimum conductance was higher ($5.41 \cdot 10^{-5} \text{ m s}^{-1}$). The average carbon chain length (ACL) was 28.52 for the very-long-chain acyclic components of *Rhazya stricta* and 31.33 for *Nerium oleander* very-long-chain acyclic components. Higher ACL values were proposed to enhance the crystalline volume fractions and, thus, reduce the cuticular water permeability (Riederer and Schneider 1990, Riederer 1991). Accordingly, it is hypothesised that higher aliphatic wax coverages and higher ACL values form more efficient transpiration barriers. It is also proposed that the additional accumulation of very high amounts of triterpenoids in the cuticle of *Nerium oleander* leaves ($281.96 \mu\text{g cm}^{-2}$) did not contribute to the formation of a particularly efficient transpiration barrier. The major triterpenoid composition might be beneficial in high light intensity environments due to the UV-adsorbing characteristic of triterpenoids (Shepherd and Griffiths 2006).

The temperature dependence of the cuticular water permeability and the cuticular chemistry might be related. The decline of the barrier properties at elevated temperatures has been attributed to the decrease of aliphatic crystallinity (Eckl and Gruler 1980, Merk *et al.* 1998). However, triterpenoids have high melting points and the structural arrangement remains unaffected up to temperatures of $100 \text{ }^\circ\text{C}$ (Casado and Heredia 1999). *Nerium oleander* cuticles had a high amount of triterpenoids ($281.96 \mu\text{g cm}^{-2}$) in relation to the amount of cutin monomers ($483.52 \mu\text{g cm}^{-2}$). A ratio of 0.6 was calculated for the cyclic wax components and cutin monomer coverage of *Nerium oleander* cuticular membranes. As proposed for *Rhazya stricta* (Chapter I), the high amount of triterpenoids in relation to the amount of cutin monomers might strengthen the cutin matrix by endowing the toughness of the cuticle and, thus, preventing the phase transition (Tsubaki *et al.* 2013). The reduced extensibility might avoid micro-defects and/or cracks of the cuticular wax barrier, as proposed by Schreiber and Schönherr (1990), due to differential volume expansions of the matrix membrane and the waxes.

3.5 Conclusion

Studies comparing the minimum conductance of stomatous, intact leaves with the cuticular permeance of astomatous leaf surfaces at $25 \text{ }^\circ\text{C}$ are scarce in literature (Burghardt and Riederer 2003, Burghardt *et al.* 2008) and the temperature

dependence of the cuticular permeability of intact plants is still unresolved (Kerstiens 2006). The hypostomatic leaves of *Nerium oleander* enabled a comparison between the temperature-dependent minimum conductances, measured with intact leaves, and cuticular permeances, measured with isolated cuticular membranes. No significant differences between the minimum conductances and the cuticular permeances from 25 °C to 55 °C were detected. It can be concluded that for *Nerium oleander* leaves the residual stomatal transpiration after complete stomatal closure was negligible. Both experimental approaches are adequate to determine the temperature effect on the minimum or cuticular water permeability of *Nerium oleander* leaves.

The minimum conductances and cuticular permeances were not subjected to a phase transition with increasing temperature, as previously described for cuticular permeances of astomatous, isolated cuticular membranes (Riederer 2006b). It can be excluded that the absence of a phase transition in *Nerium oleander* leaves is an effect of the cell wall, which might stabilise the cuticular membrane, or residual stomatal transpiration. The absence of the phase transition is proposed to be due to melting of the wax components at temperatures that are not ecologically relevant and/or triterpenoids strengthening the cutin matrix.

Based on the current knowledge, it is known that triterpenoid constituents in cuticular waxes do not constitute as efficient transpiration barriers as aliphatic components (Grncarevic and Radler 1967, Oliveira *et al.* 2003, Vogg *et al.* 2004, Leide *et al.* 2011, Buschhaus and Jetter 2012). The higher aliphatic cuticular wax coverage, the higher average carbon chain length of the aliphatic components (ACL) and the lower cuticular water permeability of *Nerium oleander* leaves when compared to *Rhazya stricta* (Chapter I), led to the hypothesis that the aliphatic wax coverage establishes the main transport-limiting barrier, whereas cyclic components might fulfil other functions, such as protection of high light intensity and/or strengthening of the cutin matrix.

Chapter III. Temperature effect on the cuticular permeance of *Prunus laurocerasus*

1 Introduction

Leaf surfaces are covered by the plant cuticle, a continuous extracellular membrane composed of the cutin polymer and the cuticular waxes. The cuticular waxes are constituted of very-long-chain aliphatic and cyclic components embedded within the cutin matrix and/or deposited on the surface as either epicuticular wax films or wax crystals (Yeats and Rose 2013). The main function of the plant cuticle is the minimisation of uncontrolled water loss under conditions when stomata are closed, such as drought.

Elevated temperatures often occur in parallel with water limitation. The temperature effect on the cuticular water permeability of leaves is described with a drastic increase of the permeability at temperatures above 35 °C for the plant species reported so far (Schönherr *et al.* 1979, Schönherr and Mérida 1981, Schreiber 2001, Riederer 2006b). Analysis of the temperature-dependent water permeability as Arrhenius plots showed this phase transition, which is attributed to structural changes of the plant cuticle and indicates a substantial decline of the barrier properties. The structural alterations are ascribed to the melting behaviour of the cuticular waxes (Eckl and Gruler 1980, Merk *et al.* 1998), micro-defects and cracks in the cuticular wax barrier caused by volume expansions of the wax-free matrix membrane (Schreiber and Schönherr 1990) and swelling of the polysaccharide material and, thus, opening up new regions of the polysaccharides for the water diffusion (Riederer 2006b).

The abrupt decline of the cuticular barrier properties at elevated temperatures (≥ 35 °C) is shown for stomatous, enzymatically isolated plant cuticles (Schreiber 2001, Riederer 2006b). However, the temperature effect on cuticular water permeabilities of intact leaf material in comparison to enzymatically isolated plant cuticles is an ecophysiologicaly relevant question still unanswered (Kerstiens 2006). The first plant species analysed were *Rhazya stricta* and *Nerium oleander*. The temperature-dependent minimum water permeabilities of stomatous, intact leaves did not indicate structural changes of the transpiration barrier (Chapter I - II). The minimum water permeability of stomatous systems is the minimum conductance. Stomatal closure is induced by desiccation of leaves. However, even though the minimum conductance

determines the cuticular water permeability of amphistomatic leaves, residual stomatal transpiration due to incomplete stomatal closure cannot be excluded (Kerstiens 2006). Therefore, the temperature-dependent cuticular water permeability of astomatous, isolated plant cuticles of *Nerium oleander* leaves was analysed (Chapter II). The cuticular permeance did not increase steeply at temperatures above 35 °C and no structural changes of the barrier properties were detected. It was proposed that the high amount of triterpenoids in relation to the amount of cutin monomers might strengthen the cutin matrix by endowing the toughness of the cuticle and, thus, preventing the phase transition (Chapter I - II; Tsubaki *et al.* 2013).

Little is known about the temperature dependence of the cuticular water permeability of intact plant systems. Hence, in addition the question arises whether the structural changes might be due to isolation of the cuticular membranes, also because the phase transition is mostly reported for isolated plant cuticles inserted in transpiration chambers (Riederer 2006b). Alternatively, cuticular permeances can be assessed by inserting leaf discs in transpiration chambers (Schreiber 2001, Burghardt and Riederer 2003), by coating the stomatous surface with paraffin wax (Burghardt and Riederer 2003) or by insertion of leaf discs in leaf envelopes (Hoad *et al.* 1996).

In this study, the question whether structural integrity over the measured temperature range of intact leaves is due to the cell wall, which might have a stabilising influence, and/or the chemical components of the cuticle, was addressed by comparing the temperature effect on the cuticular permeance of intact leaves and isolated cuticles. As model plant species, the evergreen, laurophyllic, hypostomatic *Prunus laurocerasus* L. was chosen. *Prunus laurocerasus* is frequently used as model plant species when the cuticular water permeability is analysed (Kerstiens and Lenzian 1989, Schreiber and Riederer 1996, Kirsch *et al.* 1997, Niederl *et al.* 1998, Schreiber 2001, Riederer 2006b, Zeisler and Schreiber 2015). To avoid residual stomatal transpiration, three different, astomatous experimental approaches were used to compare the temperature effect on the cuticular water permeance of *Prunus laurocerasus* leaves. Enzymatically isolated cuticular membranes and punched-out leaf discs inserted in transpiration chambers were compared with constructed leaf envelopes (modified after Hoad *et al.* 1996). Leaf discs and leaf envelopes represented intact leaf systems.

2 Results

2.1 Leaf thermal tolerance

The leaf thermal tolerance of *Prunus laurocerasus* leaves was determined (Figure 27). Heat exposure was applied for 1 °C per min and, subsequently, the maximum quantum yield of photosystem II in the dark adapted state ($F_v F_m^{-1}$) was measured without recovery time every 2.5 min. $F_v F_m^{-1}$ was only slightly affected by temperature treatments between 25.0 °C and 40.0 °C, whereas a strong decrease at temperatures higher than 42.5 °C occurred. The intersection point of the fitted regression lines indicated the critical temperature, T_{crit} was 40.07 ± 2.90 °C for dark adapted *Prunus laurocerasus* leaves. T_{50} indicated a decline of $F_v F_m^{-1}$ to 50% of the maximum at the non-stressed level and was 53.16 ± 1.76 °C (mean value \pm SD, $n = 10$).

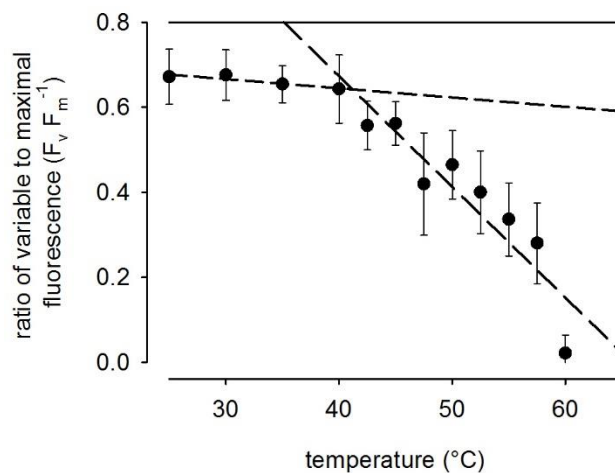


Figure 27. Effect of temperature on the maximum quantum yield of the photosystem II ($F_v F_m^{-1}$) of dark adapted *Prunus laurocerasus* leaves (mean value \pm SD, $n = 10$).

2.2 Cuticular permeance and temperature effect on cuticular permeance

The cuticular permeances of isolated cuticular membranes and leaf discs, inserted in transpiration chambers, and of leaf envelopes were measured in a temperature range from 15.0 °C and 55.0 °C. Cuticular permeances of isolated leaf cuticles of *Prunus laurocerasus* increased by a factor of 17.0 from $0.75 \cdot 10^{-5} \text{ m s}^{-1}$ to $12.74 \cdot 10^{-5} \text{ m s}^{-1}$ with elevation of temperatures. The cuticular permeance of the leaf discs rose by factor 9.6 (from $0.64 \cdot 10^{-5} \text{ m s}^{-1}$ to $6.14 \cdot 10^{-5} \text{ m s}^{-1}$) and the cuticular permeance of leaf envelopes by factor 5.5 (from $0.78 \cdot 10^{-5} \text{ m s}^{-1}$ to $4.26 \cdot 10^{-5} \text{ m s}^{-1}$; Table 10).

Cuticular permeances of isolated cuticular membranes and leaf discs are indicated as median values (25% quartile - 75% quartile) and non-parametric statistics were applied because data was not normally distributed.

Table 10. The cuticular permeances (P) of *Prunus laurocerasus* isolated cuticular membranes, leaf discs and leaf envelopes as a function of temperature (T). Cuticular permeances of isolated cuticular membranes and leaf discs are given as the median value with the 25% and 75% quartiles (Q25 - Q75) and cuticular permeances of leaf envelopes are given as mean value \pm SD ($n \geq 14$). Statistical differences between the cuticular permeances were analysed by ANOVA on ranks (ns = not significant, * $p < 0.05$, ** $p < 0.01$, *** $p < 0.001$).

T (°C)	P · 10 ⁵ (m s ⁻¹) leaf disc median			P · 10 ⁵ (m s ⁻¹) isolated cuticle median			P · 10 ⁵ (m s ⁻¹) leaf envelope mean		
	15	0.64	(0.35 - 0.99)	ns	0.75	(0.63 - 1.05)	ns	0.78	\pm 0.23
20	0.77	(0.59 - 1.30)	*	0.44	(0.39 - 0.59)	***	1.10	\pm 0.37	
25	1.11	(0.96 - 1.41)	ns	0.77	(0.62 - 1.39)	ns	1.04	\pm 0.37	
30	1.27	(1.01 - 1.98)	ns	1.26	(0.94 - 2.11)	ns	1.64	\pm 0.49	
35	1.36	(1.08 - 2.00)	ns	1.52	(1.23 - 2.41)	ns	1.60	\pm 0.56	
40	1.48	(1.21 - 2.09)	ns	1.96	(1.78 - 2.82)	ns	1.93	\pm 0.64	
45	1.88	(1.55 - 2.71)	***	4.01	(2.76 - 5.23)	***	2.06	\pm 0.72	
50	2.90	(2.50 - 4.45)	**	6.62	(4.12 - 8.04)	***	2.73	\pm 0.85	
55	6.14	(4.08 - 9.96)	**	12.74	(10.07 - 14.00)	***	4.26	\pm 0.85	

No statistical differences between P of all three measurement systems at 15 °C, 25 °C, 30 °C, 35 °C, and 40 °C. No statistical differences between P of leaf discs and leaf envelopes over the whole temperature range.

The temperature dependence of the cuticular permeance was analysed by Arrhenius plots (Figure 28). The activation energies for the permeation of water were calculated from the slope of the regression line for the cuticular permeance over the whole temperature range (from 15 °C to 55 °C). In addition, activation energies were separately calculated for the lower temperature range (from 15 °C to 35 °C) and the higher temperature range (from 35 °C to 50 °C; Table 11). Slopes of Arrhenius plots were compared (Soper 2016). Slopes of the Arrhenius plots of the natural logarithm of the cuticular permeance of leaf discs and leaf envelopes and the inverse absolute temperature did not differ significantly from each other ($p = 0.21$). In contrast, differed the slope of the Arrhenius plots of the natural logarithm of the cuticular permeance of isolated cuticles significantly from the slope of leaf discs ($p = 0.02$) and from the slope of leaf envelopes ($p < 0.001$).

Table 11. Activation energies calculated from the slope of the regression line of the Arrhenius plots for the whole temperature range (15 °C to 55 °C), the lower temperature range (from 15 °C to 35 °C) and the higher temperature range (from 35 °C to 50 °C).

	activation energy (kJ mol ⁻¹)		
	15 °C to 55 °C	15 °C to 35 °C	35 °C to 55 °C
isolated cuticle	54.9	38.1	82.9
leaf disc	38.4	36.1	57.8
leaf envelope	29.4	27.6	39.0

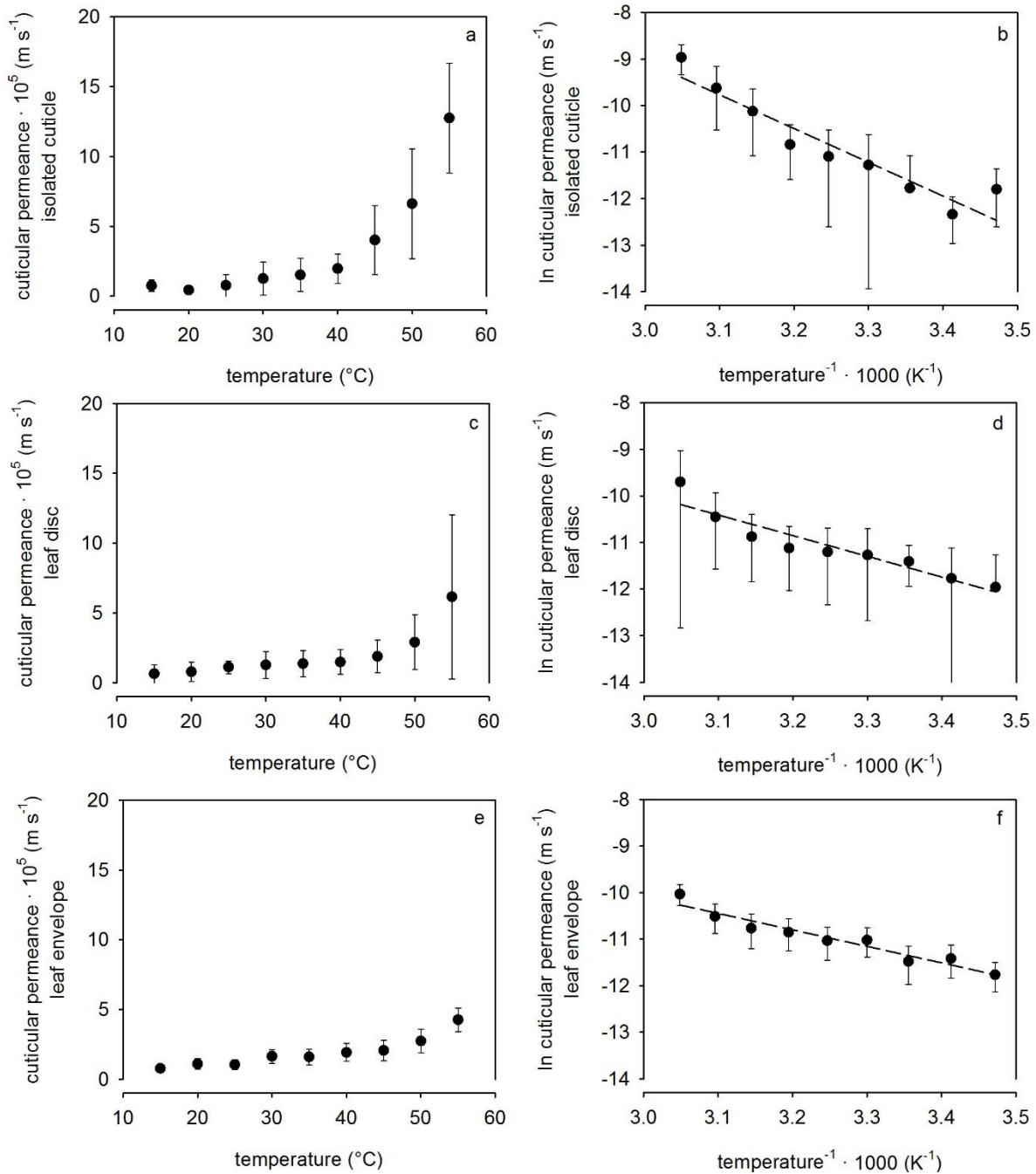


Figure 28. The temperature dependence of cuticular permeances ($n \geq 14$) of (a) isolated cuticular membranes (median value \pm interquartile range (IQR)), (c) leaf discs (median value \pm IQR) and (e) leaf envelopes (mean value \pm SD). Arrhenius plot of the natural logarithm of the cuticular permeances and the inverse absolute temperature of (b) isolated cuticular membranes ($r^2 = 0.917$; Spearman correlation coefficient (SCC) = -0.938 , $p < 0.001$), (d) leaf discs ($r^2 = 0.886$; SCC = -1.000 , $p < 0.001$) and (f) leaf envelopes ($r^2 = 0.934$; PCC = -0.966 , $p < 0.001$).

3 Discussion

3.1 Classification and comparison of the cuticular permeance

Cuticular permeances are frequently determined from isolated cuticular membranes mounted in transpiration chambers (Schönherr and Lenzian 1981, Schreiber und Riederer 1996, Riederer 2006b). An advantage is the ability to measure stomata-free systems without residual stomatal transpiration. Another experimental setting is the insertion of punched-out leaf discs in modified transpiration chambers (Schreiber 2001). In this study, in addition to the measurement of isolated leaf cuticles and leaf discs mounted in transpiration chambers, the cuticular transpiration from leaf envelopes was determined. The leaf envelopes were modified after Hoad *et al.* (1996), the whole leaves were wrapped with self-adhesive aluminium foil, with the transpirational water loss over a defined, stomata-free area. *Prunus laurocerasus* leaves were used as model plant. The cuticular permeance and the temperature effect on the cuticular permeance of isolated cuticles and leaf discs has been reported (Schreiber 2001, Riederer 2006b). The cuticular permeance and the temperature effect on the cuticular permeance of leaf envelopes has not yet been investigated. In the case of *Prunus laurocerasus* leaves, no significant difference of the cuticular permeances at 25 °C between the three experimental settings was detected (Table 10).

Due to the asymmetrical distribution of the cuticular permeances determined from isolated cuticular membranes and leaf discs, the median values (25% quartile - 75% quartile) and non-parametric statistics were applied. The cuticular permeances of isolated cuticular membranes of *Prunus laurocerasus* at 25 °C had an asymmetrical distribution with pronounced tailing on the right side. This has been commonly reported when regarding the frequency distribution histogram of cuticular permeances from isolated cuticular membranes (Geyer and Schönherr 1990, Schreiber and Riederer 1996, Niederl *et al.* 1998). The cuticular permeances of the leaf discs had an asymmetrical distribution. Only the cuticular permeances of the leaf envelopes was symmetrically distributed (Figure 29). Isolation procedures damaging the cuticular membranes (Geyer and Schönherr 1990) can be excluded in the case of *Prunus laurocerasus* due to the similarity of all three cuticular permeances at 25 °C.

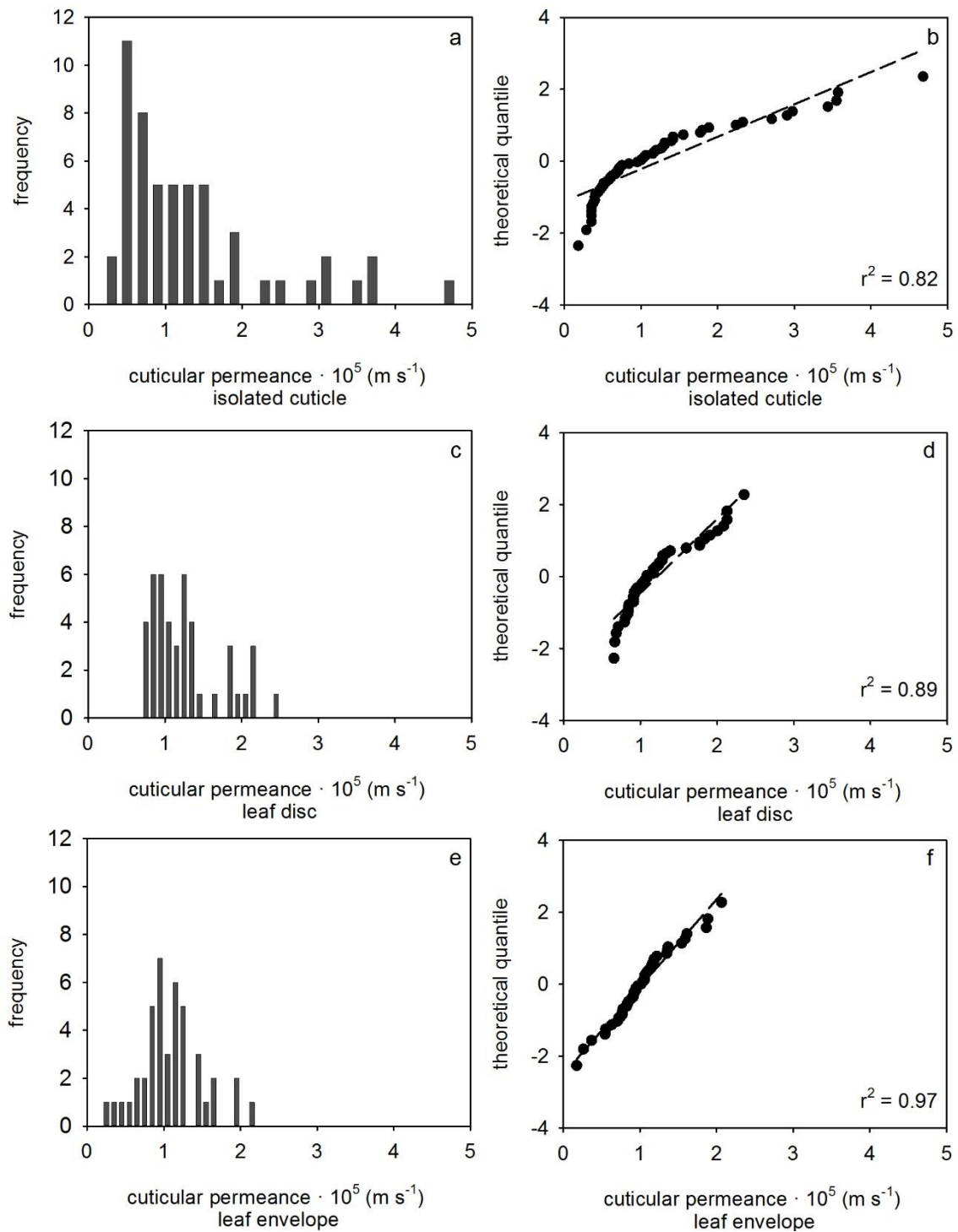


Figure 29. Frequency distribution histogram (a,c,e) and the corresponding quantile-quantile plots (b,d,f). Cuticular permeances of *Prunus laurocerasus* leaves at 25 °C measured with (a,b) isolated cuticles ($n = 22$), (c,d) leaf discs ($n = 16$) and (e,f) leaf envelopes ($n = 23$).

The cuticular permeance to water vapour of *Prunus laurocerasus* adaxial side of leaves ranged from $0.8 \cdot 10^{-5} \text{ m s}^{-1}$ to $1.1 \cdot 10^{-5} \text{ m s}^{-1}$ at 25 °C (Table 10). Schreiber and Riederer (1996) reported a cuticular permeance of $0.6 \cdot 10^{-5} \text{ m s}^{-1}$ for isolated cuticular membranes of *Prunus laurocerasus*. Similar values for the cuticular permeances of isolated cuticular membranes of *Prunus laurocerasus* were obtained by Kerstiens and Lenzian (1989; $1.7 \cdot 10^{-5} \text{ m s}^{-1}$) and Riederer (2006b; $1.1 \cdot 10^{-5} \text{ m s}^{-1}$). Schreiber (2001) compared isolated cuticular membranes and leaf discs, the cuticular permeances were $2.0 \cdot 10^{-5} \text{ m s}^{-1}$ for isolated cuticles and $1.2 \cdot 10^{-5} \text{ m s}^{-1}$ for leaf discs, respectively. Thus, the reported and measured cuticular permeances of *Prunus laurocerasus* at 25 °C are in the same order of magnitude. The given slight variances might be due to different cultivars, developmental stages and harvest dates (Hauke and Schreiber 1998, Maguire and Banks 2000, Leide *et al.* 2011, Peschel and Knoche 2012). This enabled the conclusion that leaf envelopes with self-adhesive aluminium foil are suitable to determine the cuticular water permeability of intact leaves by sealing the lower leaf surface, too. Moreover, it can be concluded that the three measurement systems are appropriate to determine the cuticular permeance at 25 °C for *Prunus laurocerasus* leaves.

3.2 Temperature effect on the cuticular permeance

The limit of whole leaf survival in response to high temperature stress was assessed. The lethal limit of heat stress of *Prunus laurocerasus* leaves was 53.16 °C (T_{50}). T_{50} , which is indicated by a decline of the maximum quantum yield of photosystem II in the dark adapted state ($F_v F_m^{-1}$) below 50% of the maximum value of unstressed leaves, is used as a threshold value for viability with the onset of irreversible damage to the photosynthetic apparatus (Woo *et al.* 2008, Curtis *et al.* 2014). Hence, the measurement temperature of 55 °C is above the lethal limit of heat stress and should be interpreted carefully.

The analysis of temperature-dependent cuticular permeances of isolated cuticular membranes was described with a slight increase of the cuticular permeances in the temperature range from 15 °C to 35 °C and a drastic increase in the temperature range from 35 °C to 55 °C (Schreiber 2001, Riederer 2006b). The steep increase of cuticular permeances at elevated temperatures is interpreted as a phase transition and indicates structural changes of the cuticular membranes. The temperature dependence of the cuticular permeances can be quantified by the activation energy, which is calculated from the slope of the regression line in Arrhenius plots. A strong

temperature dependence of water permeation is indicated by a higher activation energy (Kerstiens 2006).

Schreiber (2001) compared the temperature-dependent cuticular water permeability of isolated cuticular membranes and leaf discs mounted in modified transpiration chambers. The cuticular transpiration was measured with tritiated water. The cuticular permeance of isolated cuticular membranes from *Prunus laurocerasus* increased by factor 62.2 from 10 °C to 55 °C. The cuticular permeance of leaf discs rose by factor 82.5. Below the phase transition temperature (36.9 °C) an activation energy of 49.6 kJ mol⁻¹ and above the phase transition an energy of 89.3 kJ mol⁻¹ were reported for isolated cuticular membranes. The activation energy of leaf discs below the transition temperature (32.3 °C) was 36.9 kJ mol⁻¹ and above the transition temperature 120.5 kJ mol⁻¹. Regarding the results obtained by Schreiber (2001) using the density of liquid water as driving force might lead to an overestimation of the temperature effect (Kerstiens 1996b). Kerstiens (2006) even describes the results as “impossible” due to activation energies that were lower than the latent heat of vaporisation.

In this study, the cuticular permeances of isolated cuticular membranes from *Prunus laurocerasus* increased by factor 17.0 from 15 °C to 55 °C. The corresponding activation energies were 38.1 kJ mol⁻¹ (from 15 °C to 35 °C) and 82.9 kJ mol⁻¹ the higher temperature range (from 35 °C to 55 °C). The activation energies indicate a steep increase of the cuticular water permeability at elevated temperatures. The obtained values are in good accordance with the literature data. Riederer (2006b) reported an increase by a factor of 12.7 from 25 °C to 55 °C ($1.1 \cdot 10^{-5} \text{ m s}^{-1}$ to $14.0 \cdot 10^{-5} \text{ m s}^{-1}$). According to this, the activation energy rose from 34.1 kJ mol⁻¹ (from 10 °C to 35 °C) up to 101.1 kJ mol⁻¹ (from 35 °C to 55 °C).

Compared to the isolated cuticles, the cuticular permeances of the intact leaf systems had a smaller overall increase by a factor of 9.6 and 5.5, leaf discs and leaf envelopes, respectively (from 15 °C to 55 °C). Correspondingly, smaller activation energies were obtained at the higher temperature range of the cuticular permeances of leaf discs (57.8 kJ mol⁻¹) and of leaf envelopes (39.0 kJ mol⁻¹) compared to the activation energy of the isolated cuticular membranes. The cuticular permeances of leaf discs and leaf envelopes, representing astomatous, intact leaf systems, did not increase steeply in the higher temperature range (Figure 28). In contrast, the cuticular

permeances of the astomatous, isolated cuticular membranes had a steep increase at elevated temperatures (Figure 30).

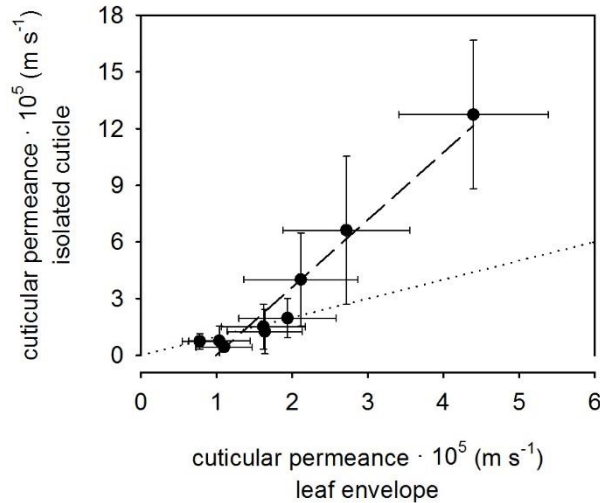


Figure 30. The cuticular permeance ($n \geq 14$) of isolated cuticular membranes (median value \pm IQR) plotted against the cuticular permeance of leaf envelopes from *Prunus laurocerasus* leaves (mean value \pm SD; $r^2 = 0.948$).

The phase transition and the decline of the barrier properties has been attributed to different structural changes of the plant cuticles. The structural alterations have been ascribed to melting of the cuticular waxes (Eckl and Gruler 1980, Merk *et al.* 1998), micro-defects and cracks in the cuticular wax barrier (Schreiber and Schönherr 1990) and swelling of the polysaccharide (Riederer 2006b). For cuticular waxes extracted from *Prunus laurocerasus* leaves a melting range from 50 °C to 83 °C with the midpoint of the melting range at 74 °C was reported (Merk 1998). This melting of the cuticular waxes, which might influence the barrier properties, occurred at temperatures above the ecological relevance. Schreiber and Schönherr (1990) proposed that an increased volume expansion of the wax-free matrix membrane exceeds the expansion coefficient of the cuticular waxes at temperatures above 40 °C. This volume expansion is proposed to affect the wax barrier and, thus, enhance the cuticular water permeability. The volume expansion was determined from isolated cuticular membranes of different plant species, such as *Citrus aurantium* and *Nerium oleander*. For *Prunus laurocerasus* intact leaves, a steep increase of the cuticular water permeability at elevated temperatures might be suppressed due to the cell wall stabilising the cuticular membrane. However, no comparably steep increase was detected when analysing the cuticular permeances of *Nerium oleander* isolated cuticular membranes (Chapter II).

The influence of elevated temperatures on the cuticular permeances of isolated *Nerium oleander* cuticles might be minimised, given that scleromorphic leaves, such as *Nerium oleander* and *Olea europaea*, had low volume expansions of isolated cuticular membranes. Schreiber and Schönherr (1990) propose an ecological adaptation to dry and warm environments, due to the fact that a low volume expansion might reduce the negative influence of structural changes on the cuticular water permeability at elevated temperatures.

3.3 Conclusion

The temperature dependence of the cuticular water permeability of intact plant systems is still unresolved (Kerstiens 2006). The cuticular permeance of *Prunus laurocerasus* leaves was determined for isolated cuticles, leaf discs and leaf envelopes, respectively. To avoid residual stomatal transpiration, intact leaves were enclosed in leaf envelopes with self-adhesive aluminium foil. Astomatous and adaxial leaf surfaces, as isolated cuticles and leaf discs, were inserted in transpiration chambers to measure the cuticular transpiration. At 25 °C no statistically significant difference between the three experimental settings was obtained. This leads to the conclusion that leaf envelopes are also suitable to determine the cuticular water permeability of intact leaves by sealing the lower leaf surface. Moreover, it can be concluded that all three measurement systems are adequate to determine the cuticular permeance at 25 °C for *Prunus laurocerasus* leaves.

However, the temperature effect on the cuticular permeance proved significant differences between the experimental approaches. The cuticular permeances of the leaf envelopes and leaf discs, representing astomatous, intact leaves, indicated no structural changes at elevated temperatures, which are detected by a steeper increase of the cuticular permeance and, thus, higher activation energies. In contrast, the cuticular permeances of the isolated cuticular membranes are in good accordance with literature values. Due to the higher activation energy at elevated temperatures, structural changes of the isolated cuticular barrier might influence the water permeability. When measuring *Prunus laurocerasus* intact leaves the steep increase of the cuticular permeance might be suppressed by the cell wall stabilising the cuticle.

Chapter IV. Cuticular barrier properties and thermal tolerances of plants in hot and dry environments

1 Introduction

The loss of water vapour from plants differs between stomatal and cuticular transpiration. The water vapour diffuses predominantly through stomatal pores. Stomatal closure minimises the stomatal water loss and the remaining much lower water transpiration occurs through the plant cuticle. Functionally similar groups of plant species had minimum leaf conductances, measured when stomata are completely closed as a result of desiccation stress, 20 to 300 times lower than maximum conductances with stomata open (Körner 1994, 1995). Drought induces stomatal closure. The effectuated limited water loss during drought periods is proposed to prolong plant survival. Drought often coincides with high temperatures. Heat has been shown to induce stomatal opening (Feller 2006, Reynolds-Henne *et al.* 2010). The higher stomatal transpiration is proposed to allow an efficient cooling of leaves (Feller 2006). There might be a trade-off between reducing heat stress through transpirational cooling or reducing drought stress through reduced water loss (Feller 2006, Crawford *et al.* 2012).

A fundamental function of the plant cuticle is to minimise the uncontrolled non-stomatal water loss from the interior of the plants into the surrounding atmosphere. The main transport-limiting barrier properties of cuticles are established by the cuticular waxes, since the extraction of waxes with organic solvents leads to a considerable increase of the cuticular water permeability (Schönherr 1982, Schreiber 2002). Thick cuticular membranes and high wax coverages, respectively, do not establish more efficient transpiration barriers (Kamp 1930, Schreiber and Riederer 1996, Riederer and Schreiber 2001, Anfodillo *et al.* 2002). The chemical wax composition differs widely among species. Common components of the cuticular waxes are very-long-chain aliphatics and cyclic constituents, such as pentacyclic triterpenoids. Cyclic wax components do not establish as efficient transpiration barriers as aliphatic components (Grncarevic and Radler 1967, Oliveira *et al.* 2003, Vogg *et al.* 2004, Leide *et al.* 2011, Buschhaus and Jetter 2012). Additionally, higher average carbon chain lengths are proposed to enhance the crystalline volume fractions of the cuticular wax and reduce the cuticular water permeability (Riederer and Schneider 1990, Riederer 1991).

The specific leaf area (SLA) is an accepted key leaf trait and often positively correlated to the relative growth rate and negatively with leaf life span. The leaf water content (LWC) is a rough indicator of leaf density (Garnier 1992, Lambers and Poorter 1992, Garnier and Laurent 1994, Vendramini *et al.* 2002, Cornelissen *et al.* 2003). Leaves of slow-growing plant species with a low SLA and a low LWC are described as sclerophyllous leaves. Commonly, sclerophyllous leaves have thick epidermal cell walls and cuticles. Fast-growing plant species with tender leaves were described to have a high SLA and high LWC (Lambers and Poorter 1992, Vendramini *et al.* 2002). Recently, Scoffoni *et al.* (2014) proposed that the leaf density and the leaf mass per area (reciprocal of SLA; Cornelissen *et al.* 2003) are positively correlated with the modulus of elasticity. The modulus of elasticity in turn is negatively correlated with the maximum area shrinkage and, thus, influences the minimum conductance. In addition, in atmospheric bromeliads a relationship between low SLA, high degree of succulence (SU) and low epidermal water loss was established and interpreted as drought avoidance strategies to tolerate water limitations by Woods (2013). In contrast, plant species that were drought deciduous, such as ferns, had high SLA, low SU and high epidermal water loss.

Xeric limestone sites naturally located in Franconia (Southern Germany) are characterised by extreme microclimatic and edaphic conditions. Above the weathered limestone the fine soil proportion is only a few centimetres thick. The growing sites are extremely dry and the edaphic drought is enhanced due to wind and sun exposure (Kraus 1906, 1911, Lösch 1980). Dwarfing of several plant species, such as *Salvia pratensis* and *Sanguisorba minor*, was described as a result of the edaphic dryness. A normal growth of plants from dwarf seeds was observed on garden mould (Kraus 1906).

In this study, the minimum conductance with maximum stomatal closure of nine typical and characteristic plant species from xeric limestone sites was determined from leaf drying curves. Low minimum conductance is used as an indicator of efficient cuticular transpiration barriers enabling dehydration avoidance (Muchow and Sinclair 1989, Smith *et al.* 2006). It is hypothesised that plant species with efficient transpiration barriers have a higher leaf thermal tolerance. The photosynthetic leaf thermal tolerance was assessed with chlorophyll fluorescence (Knight and Ackerly 2003). The parameter indicates the ability of leaves to tolerate environmental stresses. The decline of the maximum quantum yield of photosystem II ($F_v F_m^{-1}$) indicates the occurrence of

damage to the photosynthetic apparatus (Maxwell and Johnson 2000, Lichtenthaler *et al.* 2005) and provides an appropriate, non-invasive method to assess the limits of whole leaf survival in response to high temperature stress. In addition, relationships between minimum conductance, specific leaf area (SLA), leaf water content (LWC) and the degree of succulence (SU) of characteristic plant species from xeric limestone sites were analysed. Chemistry and function analyses of the leaf cuticular wax chemistry and the corresponding minimum conductances with the typical plant species from the hot and dry environment were conducted.

2 Results

2.1 Leaf characteristics and minimum conductance

Characteristic plant species from xeric limestone sites naturally located in Franconia (Southern Germany) were chosen. Xerophytic grassland plant species (class Festuco-Brometea) were *Hippocrepis comosa*, *Helianthemum apenninum*, *Geranium sanguineum*, *Sanguisorba minor*, *Sesleria albicans*, *Pulsatilla vulgaris*, *Teucrium chamaedrys* and *Salvia pratensis*. In addition, a mesophytic plant species associated with xeric limestone sites, *Plantago lanceolata*, was investigated. From *Salvia pratensis*, the dwarf form from xeric limestone sites and additionally the mesophytic *Salvia pratensis* (class Molinio-Arrhenatheretea) was analysed.

Minimum conductances of the xerophytic plant species ranged between $4.32 \cdot 10^{-5} \text{ m s}^{-1}$ for *Teucrium chamaedrys* leaves and $10.10 \pm 3.39 \cdot 10^{-5} \text{ m s}^{-1}$ for *Helianthemum apenninum* leaves. The minimum conductance of the *Salvia pratensis* leaves was $8.21 \cdot 10^{-5} \text{ m s}^{-1}$ (xerophytic) and $6.41 \cdot 10^{-5} \text{ m s}^{-1}$ (mesophytic). The minimum conductance of *Plantago lanceolata* leaves was $9.35 \cdot 10^{-5} \text{ m s}^{-1}$.

Temperature differences between the leaf and air temperature ($\Delta T_{\text{leaf}} - T_{\text{air}}$) were smallest for *Teucrium chamaedrys* ($-0.29 \text{ }^{\circ}\text{C}$) and highest for *Sanguisorba minor* ($-0.66 \text{ }^{\circ}\text{C}$). From the saturated fresh weight (FW_{sat}), the dry weight (DW) and the dual projected leaf area (LA) were calculated the degree of succulence (SU), the specific leaf area (SLA) and the leaf water content (LWC; Table 12).

Table 12. Leaf minimum conductance (g_{\min}), the difference between the leaf and air temperature ($\Delta T_{\text{leaf}} - T_{\text{air}}$), the saturated fresh weight (FW_{sat}), the dry weight (DW), the dual projected leaf surface area (LA), the degree of succulence (SU, water content LA^{-1}), the specific leaf area (SLA, one-sided $LA DW^{-1}$) and the leaf water content (LWC, fresh weight basis, $1 - DW FW_{\text{sat}}^{-1}$) of nine plant species (mean value \pm SD, $n = 7 - 25$).

plant species (family)	$g_{\min} \cdot 10^5$ ($m s^{-1}$)	$\Delta T_{\text{leaf}} -$ T_{air} ($^{\circ}C$)	FW_{sat} (g)	DW (g)	$LA \cdot 10^4$ (m^2)	SU ($g m^{-2}$)	SLA ($m^2 kg^{-1}$)	LWC ($g g^{-1}$)
<i>Hippocrepis comosa</i> (Fabaceae)	6.92 ± 3.52	-0.5 ± 0.2	0.15 ± 0.05	0.04 ± 0.02	8.4 ± 2.9	127.5 ± 19.7	11.5 ± 2.6	0.74 ± 0.04
<i>Helianthemum apenninum</i> (Cistaceae)	10.10 ± 3.39	-0.6 ± 0.2	0.05 ± 0.01	0.02 ± 0.00	2.0 ± 0.3	155.7 ± 17.8	6.9 ± 1.4	0.66 ± 0.04
<i>Geranium sanguineum</i> (Geraniaceae)	5.25 ± 0.54	-	0.12 ± 0.02	0.03 ± 0.01	10.9 ± 1.4	82.0 ± 3.9	16.8 ± 1.3	0.73 ± 0.02
<i>Sanguisorba minor</i> (Rosaceae)	7.30 ± 1.77	-0.7 ± 0.2	0.07 ± 0.01	0.02 ± 0.00	6.7 ± 1.2	61.1 ± 3.8	14.4 ± 2.1	0.63 ± 0.04
<i>Sesleria albicans</i> (Poaceae)	5.76 ± 2.00	-0.4 ± 0.1	0.06 ± 0.02	0.02 ± 0.01	6.5 ± 1.3	64.3 ± 8.0	15.4 ± 1.7	0.66 ± 0.02
<i>Pulsatilla vulgaris</i> (Ranunculaceae)	7.69 ± 1.86	-0.6 ± 0.1	0.18 ± 0.03	0.05 ± 0.01	10.1 ± 1.8	143.5 ± 31.5	10.6 ± 0.5	0.74 ± 0.01
<i>Teucrium chamaedrys</i> (Lamiaceae)	4.32 ± 0.97	-0.3 ± 0.1	0.03 ± 0.01	0.01 ± 0.00	1.7 ± 0.4	82.0 ± 5.0	5.8 ± 1.0	0.48 ± 0.04
<i>Salvia pratensis</i> (Lamiaceae, xerophytic)	8.21 ± 1.72	-	0.53 ± 0.16	0.13 ± 0.03	26.5 ± 7.0	150.6 ± 14.5	10.6 ± 1.6	0.76 ± 0.03
<i>Salvia pratensis</i> (Lamiaceae, mesophytic)	6.41 ± 2.55	-	1.55 ± 0.49	0.31 ± 0.11	104.8 ± 29.6	118.0 ± 14.0	17.3 ± 1.9	0.80 ± 0.03
<i>Plantago lanceolata</i> (Plantaginaceae)	9.35 ± 2.30	-0.6 ± 0.1	0.66 ± 0.25	0.11 ± 0.05	40.0 ± 12.2	140.2 ± 18.8	20.6 ± 5.7	0.84 ± 0.04

SLA and LWC of all plant species were significantly positively correlated. There was no correlation between SLA and SU (Figure 31). The minimum conductance of all plant species did not correlate with SLA, LWC or ($\Delta T_{\text{leaf}} - T_{\text{air}}$). The minimum conductance and SU were significantly positively correlated (Figure 32).

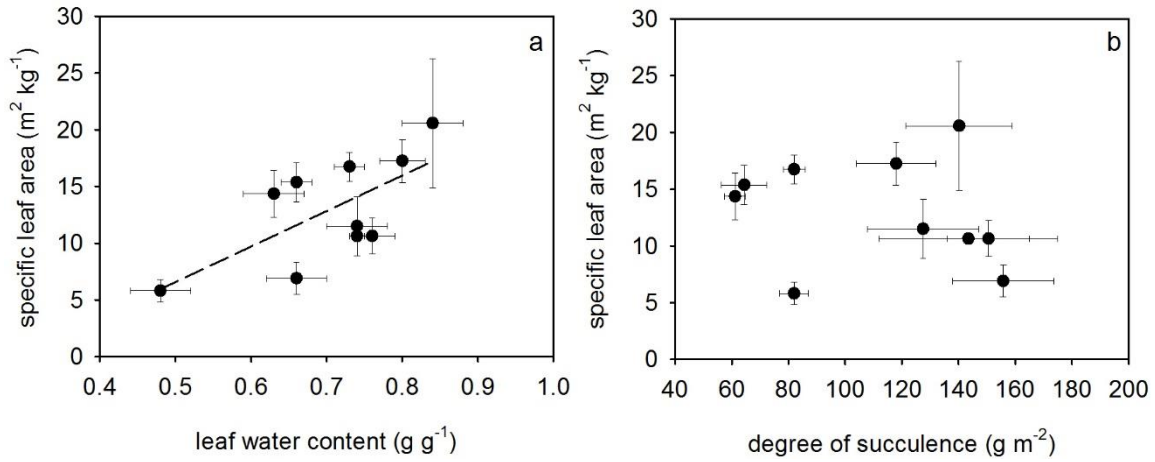


Figure 31. Specific leaf area (SLA) as a function of (a) leaf water content (LWC) and (b) degree of succulence (SU; mean values \pm SD). The specific leaf area increases with the leaf water content ($r^2 = 0.463$; Pearson correlation coefficient (PCC) = 0.680, $p = 0.030$).

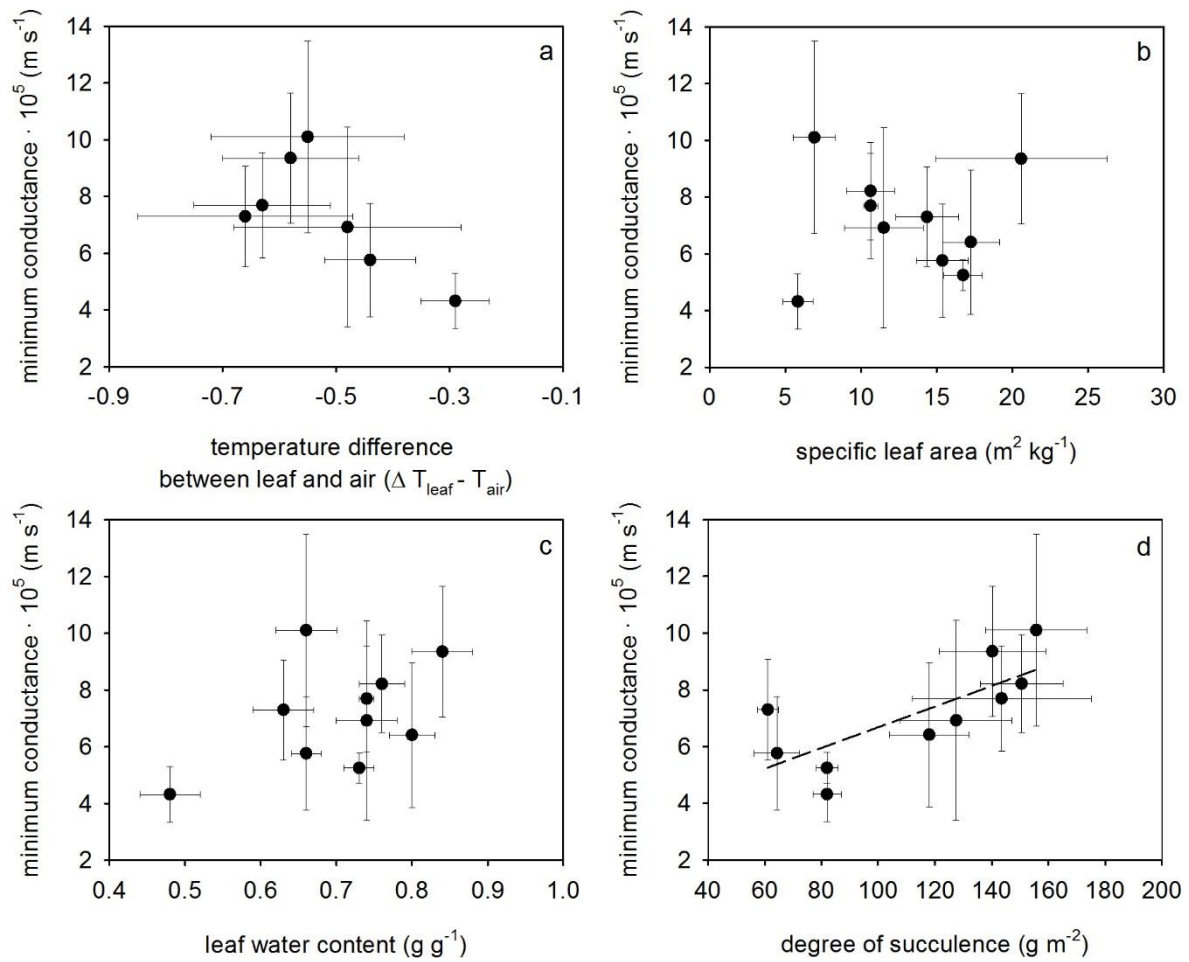


Figure 32. Minimum conductances as a function of (a) the difference between the leaf and air temperature ($\Delta T_{\text{leaf}} - T_{\text{air}}$), (b) specific leaf area (SLA), (c) leaf water content (LWC) and (d) degree of succulence (SU; mean values \pm SD). The minimum conductance increases with the degree of succulence ($r^2 = 0.552$; PCC = 0.743, $p = 0.014$).

2.2 Leaf thermal tolerance

Leaf thermal tolerances were determined from nine characteristic plant species from xeric limestone sites. Heat exposure was applied for 1 °C per min and, subsequently, the maximum quantum yield of photosystem II in the dark adapted state ($F_v F_m^{-1}$) was measured without recovery time every 2.5 min. $F_v F_m^{-1}$ was plotted against the air temperature and two regression lines were fitted to the graph. The intersection point of the fitted regression lines between non-stressed and decreasing branch indicated the critical temperature (T_{crit}). Critical temperatures of the xerophytic plant species ranged between 39.29 °C for *Helianthemum apenninum* leaves and 43.76 °C for *Teucrium chamaedrys* leaves. The critical temperature of *Salvia pratensis* leaves was 41.38 °C (xerophytic) and 40.43 °C (mesophytic). The critical temperature of *Plantago lanceolata* leaves was 37.85 °C (Table 13).

Table 13. Leaf critical temperature (T_{crit}) calculated from the maximum quantum yield of photosystem II ($F_v F_m^{-1}$) in the dark adapted state (mean value \pm SD, n = 8 - 25).

plant species	T_{crit} (°C)		
<i>Hippocrepis comosa</i>	40.14	\pm	1.13
<i>Helianthemum apenninum</i>	39.29	\pm	1.38
<i>Geranium sanguineum</i>	41.60	\pm	1.38
<i>Sanguisorba minor</i>	41.22	\pm	1.22
<i>Sesleria albicans</i>	41.24	\pm	1.07
<i>Pulsatilla vulgaris</i>	41.79	\pm	1.65
<i>Teucrium chamaedrys</i>	43.76	\pm	1.11
<i>Salvia pratensis</i> (xerophytic)	41.38	\pm	0.78
<i>Salvia pratensis</i> (mesophytic)	40.43	\pm	1.52
<i>Plantago lanceolata</i>	37.85	\pm	2.77

2.3 Leaf thermal tolerance and minimum conductance

Minimum conductances were significantly negatively correlated with leaf thermal tolerances. The regression equation $g_{\min} = (-8.764 \cdot 10^{-6}) \cdot T_{\text{crit}} + 4.295 \cdot 10^{-4}$ was obtained ($r^2 = 0.596$; Figure 33).

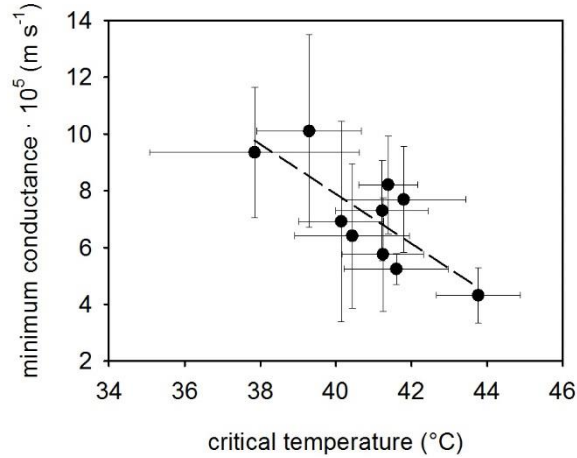


Figure 33. Minimum conductances as a function of the critical temperature (T_{crit}) calculated from the maximum quantum yield of photosystem II of dark adapted leaves ($F_v F_m^{-1}$). Minimum conductances decrease with increasing critical temperatures (mean values \pm SD; $r^2 = 0.596$; PCC = -0.772, $p = 0.009$).

2.4 Chemical analysis of the cuticular leaf wax

2.4.1 Cuticular leaf wax from *Hippocrepis comosa*

The cuticular waxes were analysed quantitatively by gas chromatograph equipped with a flame ionisation detector and the qualitative analysis by gas chromatograph equipped with a mass spectrometric detector. Total cuticular leaf wax coverage of *Hippocrepis comosa* was $13.71 \pm 1.71 \mu\text{g cm}^{-2}$ (mean value \pm SD, $n = 5$). The leaf wax composed of a major portion of very-long-chain acyclic component classes (90.5%, $12.41 \pm 1.73 \mu\text{g cm}^{-2}$) and a minor portion of cyclic components (1.9%, $0.26 \pm 0.05 \mu\text{g cm}^{-2}$).

Primary alkanols were the most prominent acyclic component class (60.0%, $8.23 \pm 1.35 \mu\text{g cm}^{-2}$), followed by alkanals (15.6%, $2.14 \pm 0.28 \mu\text{g cm}^{-2}$) and alkyl esters (6.3%, $0.87 \pm 0.07 \mu\text{g cm}^{-2}$). Additional component classes detected in the cuticular wax were *n*-alkanes, alkanolic acids and methyl esters. Carbon chain lengths ranged from C₂₀ to C₅₂, the most abundant chain lengths were C₂₆, C₂₈ and C₃₀ (Figure 34). Hexacosanol (26.5%, $3.63 \pm 0.65 \mu\text{g cm}^{-2}$), octacosanol (9.8%, $1.34 \pm 0.12 \mu\text{g cm}^{-2}$) and triacontanol (19.5%, $2.67 \pm 0.57 \mu\text{g cm}^{-2}$) dominated the acyclic components. The average carbon chain length (ACL) of the very-long-chain acyclic wax components was 29.15.

The main cyclic component was α -amyrin with a cuticular wax coverage of $0.14 \pm 0.06 \mu\text{g cm}^{-2}$ (1.0%), followed by β -amyrin (0.7%, $0.10 \pm 0.01 \mu\text{g cm}^{-2}$). In addition, a minor fraction of monoglycerides was detected (Table 14).

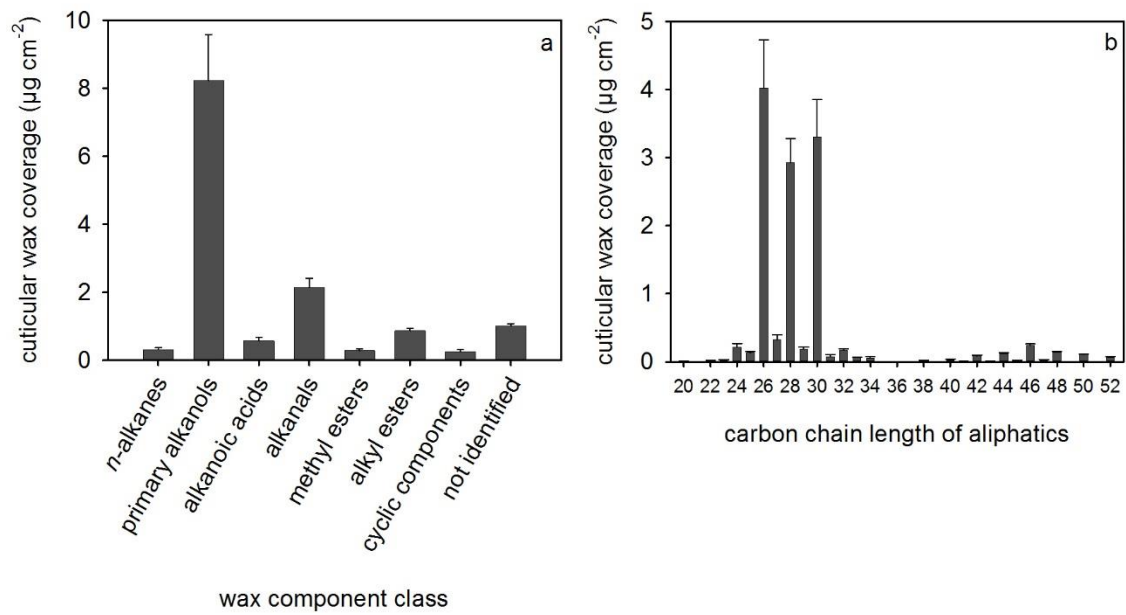


Figure 34. Cuticular wax composition of *Hippocrepis comosa* leaves. (a) Cuticular wax coverage arranged according to the component classes and (b) the carbon chain length distribution of the acyclic components (mean value \pm SD, $n = 5$).

Table 14. The cuticular wax coverage and components of *Hippocrepis comosa* leaves (mean value \pm SD, n = 5).

	carbon chain length	wax coverage ($\mu\text{g cm}^{-2}$)		
<i>n</i> -alkanes	23	0.01	\pm	0.00
	25	0.02	\pm	0.00
	27	0.05	\pm	0.02
	28	0.01	\pm	0.00
	29	0.08	\pm	0.01
	30	0.02	\pm	0.00
	31	0.04	\pm	0.03
	32	0.01	\pm	0.00
	33	0.07	\pm	0.00
primary alkanols	20,22,23	traces		
	24	0.09	\pm	0.02
	25	0.03	\pm	0.01
	26	3.63	\pm	0.65
	27	0.23	\pm	0.04
	28	1.34	\pm	0.12
	29	0.08	\pm	0.01
	30	2.67	\pm	0.57
	31	0.03	\pm	0.01
	32	0.09	\pm	0.02
alkanoic acids	34	0.01	\pm	0.01
	20	0.01	\pm	0.00
	22	0.01	\pm	0.00
	23	0.01	\pm	0.00
	24	0.07	\pm	0.02
	25	0.01	\pm	0.00
	26	0.20	\pm	0.03
	27	0.02	\pm	0.01
	28	0.12	\pm	0.04
	29	0.02	\pm	0.01
	30	0.06	\pm	0.03
alkanals	32	0.01	\pm	0.01
	34	0.04	\pm	0.02
	24	0.01	\pm	0.01
	26	0.09	\pm	0.05
	27	traces		
	28	1.40	\pm	0.23
	29	0.01	\pm	0.01
methyl esters	30	0.56	\pm	0.08
	32	0.06	\pm	0.01
	24	0.05	\pm	0.01
	25	0.07	\pm	0.03
	26	0.10	\pm	0.02
	28	0.06	\pm	0.02

(continued)

	carbon chain length	wax coverage ($\mu\text{g cm}^{-2}$)		
alkyl esters	38	0.01	±	0.01
	40	0.03	±	0.01
	41	0.01	±	0.00
	42	0.09	±	0.01
	43	0.01	±	0.00
	44	0.12	±	0.01
	45	0.02	±	0.00
	46	0.24	±	0.02
	47	0.03	±	0.00
	48	0.14	±	0.01
		50	0.11	±
	52	0.07	±	0.01
sum acyclic components (90.5%)		12.41	±	1.73
α -amyrin		0.14	±	0.06
β -amyrin		0.10	±	0.01
friedelin		0.01	±	0.01
ursolic acid		0.01	±	0.01
cholesterol		0.01	±	0.00
sum cyclic components (1.9%)		0.26	±	0.05
monoglycerides	16	0.01	±	0.00
	18	0.01	±	0.00
not identified		1.02	±	0.06
sum acyclic, cyclic and not identified cuticular wax components (100.0%)		13.71	±	1.71

2.4.2 Cuticular leaf wax from *Helianthemum apenninum*

Total cuticular leaf wax coverage of *Helianthemum apenninum* was $15.68 \pm 3.91 \mu\text{g cm}^{-2}$ (mean value \pm SD, $n = 5$). The leaf wax composed of a major portion of very-long-chain acyclic component classes (90.7%, $14.22 \pm 3.56 \mu\text{g cm}^{-2}$) and a minor portion of cyclic components (2.9%, $0.46 \pm 0.12 \mu\text{g cm}^{-2}$).

Alkyl esters were the most prominent acyclic component class (64.1%, $10.05 \pm 2.55 \mu\text{g cm}^{-2}$), followed by *n*-alkanes (11.6%, $1.82 \pm 0.49 \mu\text{g cm}^{-2}$) and primary alkanols (8.0%, $1.25 \pm 0.35 \mu\text{g cm}^{-2}$). Additional component classes detected in the cuticular wax were branched alkanes, alkanolic acids and alkanals. Carbon chain lengths ranged from C₂₀ to C₅₂, the most abundant chain lengths were C₄₄, C₄₆ and C₄₈ (Figure 35). C₄₄, C₄₆ and C₄₈ esters dominated the acyclic components with a total amount of $1.76 \pm 0.49 \mu\text{g cm}^{-2}$ (11.2%), $1.93 \pm 0.48 \mu\text{g cm}^{-2}$ (12.3%) and $1.58 \pm 0.37 \mu\text{g cm}^{-2}$ (10.1%),

respectively. The average carbon chain length (ACL) of the very-long-chain acyclic wax components was 41.15.

The main cyclic component was β -amyrin with a cuticular wax coverage of $0.09 \pm 0.04 \mu\text{g cm}^{-2}$ (0.6%), followed by α -amyrin (0.5%, $0.08 \pm 0.02 \mu\text{g cm}^{-2}$). In addition, a minor fraction of coumaric acid esters was detected (Table 15).

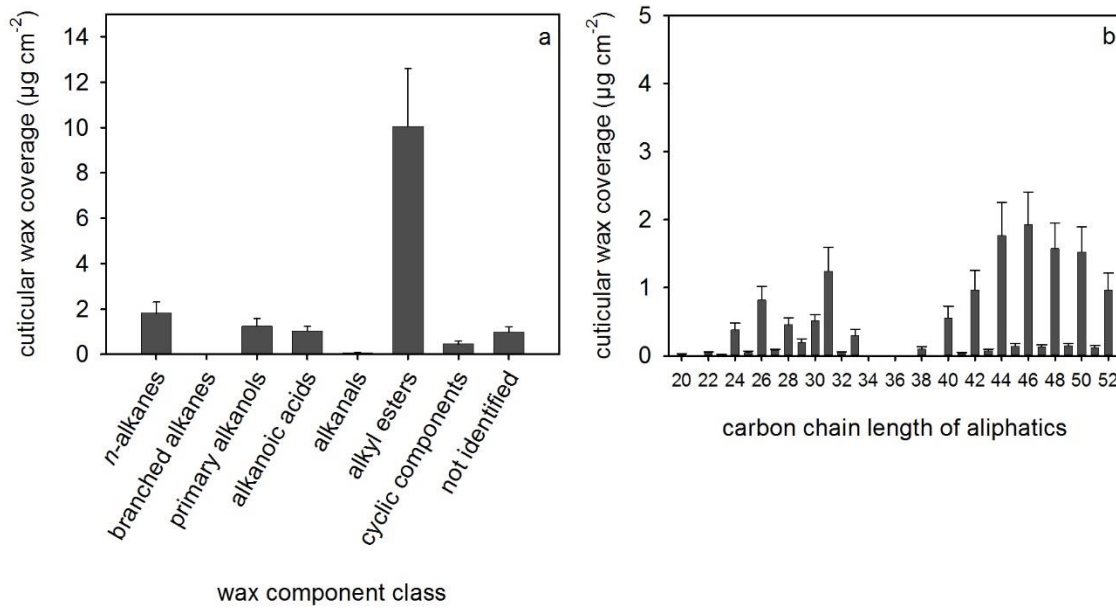


Figure 35. Cuticular wax composition of *Helianthemum apenninum* leaves. (a) Cuticular wax coverage arranged according to the component classes and (b) the carbon chain length distribution of the acyclic components (mean value \pm SD, $n = 5$).

Table 15. The cuticular wax coverage and components of *Helianthemum apenninum* leaves (mean value \pm SD, n = 5).

	carbon chain length	wax coverage ($\mu\text{g cm}^{-2}$)		
<i>n</i> -alkanes	23	0.01	\pm	0.00
	25	0.01	\pm	0.00
	26	0.02	\pm	0.00
	27	0.04	\pm	0.01
	28	0.03	\pm	0.00
	29	0.20	\pm	0.05
	30	0.04	\pm	0.01
	31	1.14	\pm	0.33
	32	0.03	\pm	0.00
	33	0.30	\pm	0.09
<i>iso</i> - and <i>anteiso</i> -alkanes	27	0.01	\pm	0.00
primary alkanols	20	traces		
	22	0.03	\pm	0.01
	23	traces		
	24	0.21	\pm	0.06
	25	0.03	\pm	0.01
	26	0.41	\pm	0.12
	27	0.03	\pm	0.00
	28	0.27	\pm	0.08
	30	0.15	\pm	0.04
	31	0.10	\pm	0.03
	32	0.01	\pm	0.00
	alkanoic acids	20	0.02	\pm
22		0.02	\pm	0.00
23		traces		
24		0.16	\pm	0.04
25		traces		
26		0.38	\pm	0.09
27		0.01	\pm	0.00
28		0.15	\pm	0.04
30		0.27	\pm	0.05
32		0.01	\pm	0.00
alkanals	24	traces		
	26	0.01	\pm	0.01
	28	0.01	\pm	0.00
	30	0.05	\pm	0.01
alkyl esters	38	0.10	\pm	0.03
	40	0.55	\pm	0.17
	41	0.04	\pm	0.01
	42	0.97	\pm	0.29
	43	0.08	\pm	0.02
	44	1.76	\pm	0.49
	45	0.14	\pm	0.04
	46	1.93	\pm	0.48

(continued)

	carbon chain length	wax coverage ($\mu\text{g cm}^{-2}$)		
alkyl esters	47	0.13	±	0.03
	48	1.58	±	0.37
	49	0.15	±	0.03
	50	1.53	±	0.37
	51	0.12	±	0.03
	52	0.97	±	0.24
sum acyclic components (90.7%)		14.22	±	3.56
α -amyirin		0.08	±	0.02
β -amyirin		0.09	±	0.04
β -amyirin acetate		traces		
amyirin derivative		0.05	±	0.01
uvaol		0.04	±	0.02
friedelin		0.05	±	0.01
oleanolic acid		0.06	±	0.01
ursolic acid		0.05	±	0.02
β -sitosterol		0.04	±	0.01
cholesterol		traces		
sum cyclic components (2.9%)		0.46	±	0.12
coumaric acid esters	26	traces		
not identified		0.99	±	0.22
sum acyclic, cyclic and not identified cuticular wax components (100.0%)		15.68	±	3.91

2.4.3 Cuticular leaf wax from *Geranium sanguineum*

Total cuticular leaf wax coverage of *Geranium sanguineum* was $8.35 \pm 2.13 \mu\text{g cm}^{-2}$ (mean value \pm SD, $n = 5$). The leaf wax composed of a major portion of very-long-chain acyclic component classes (65.3%, $5.45 \pm 1.31 \mu\text{g cm}^{-2}$) and a minor portion of cyclic components (22.4%, $1.87 \pm 0.60 \mu\text{g cm}^{-2}$).

N-alkanes were the most prominent acyclic component class (40.0%, $3.32 \pm 0.81 \mu\text{g cm}^{-2}$), followed by primary alkanols (9.8%, $0.82 \pm 0.34 \mu\text{g cm}^{-2}$) and alkyl esters (6.0%, $0.50 \pm 0.14 \mu\text{g cm}^{-2}$). Additional component classes detected in the cuticular wax were secondary alkanols, alkanol acetates, alkanolic acids, alkanals and methyl esters. Carbon chain lengths ranged from C_{20} to C_{52} , the most abundant chain lengths were C_{29} , C_{31} and C_{35} (Figure 36). *N*-nonacosane (5.9%, $0.49 \pm 0.13 \mu\text{g cm}^{-2}$), *n*-hentriacontane (10.9%, $0.91 \pm 0.26 \mu\text{g cm}^{-2}$) and *n*-pentatriacontane (10.7%, $0.89 \pm$

0.25 $\mu\text{g cm}^{-2}$) dominated the acyclic components. The average carbon chain length (ACL) of the very-long-chain acyclic wax components was 32.55.

The main cyclic component was α -amyrin with a cuticular wax coverage of $0.58 \pm 0.20 \mu\text{g cm}^{-2}$ (6.9%), followed by β -amyrin (6.5%, $0.54 \pm 0.44 \mu\text{g cm}^{-2}$; Table 16).

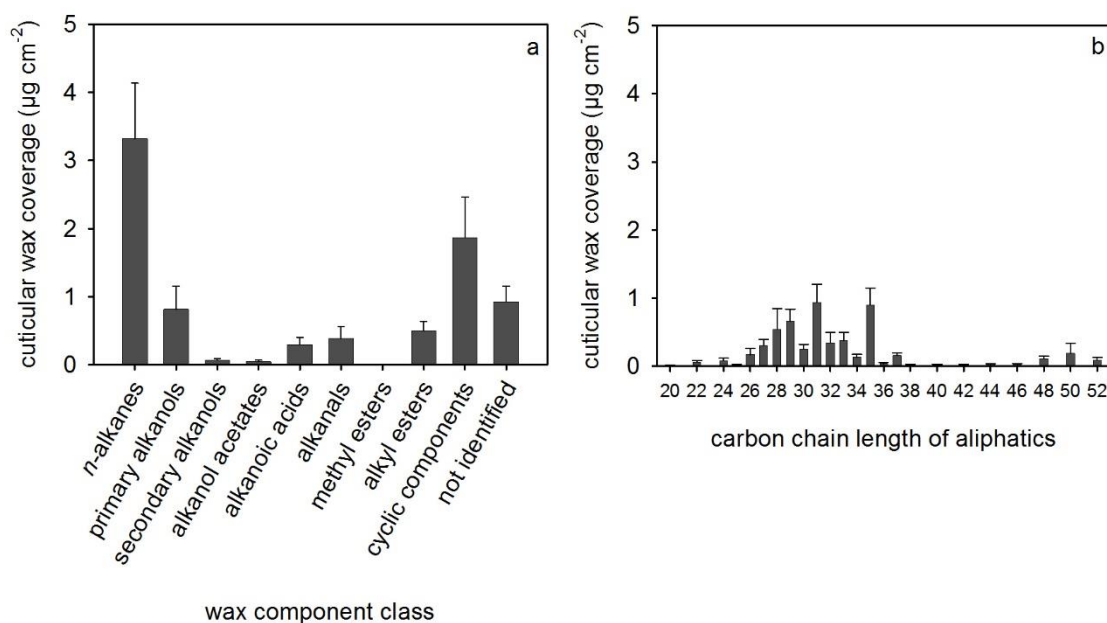


Figure 36. Cuticular wax composition of *Geranium sanguineum* leaves. (a) Cuticular wax coverage arranged according to the component classes and (b) the carbon chain length distribution of the acyclic components (mean value \pm SD, $n = 5$).

Table 16. The cuticular wax coverage and components of *Geranium sanguineum* leaves (mean value \pm SD, $n = 5$).

	carbon chain length	wax coverage ($\mu\text{g cm}^{-2}$)		
<i>n</i> -alkanes	23	0.00	\pm	0.00
	25	0.01	\pm	0.00
	26	0.01	\pm	0.00
	27	0.24	\pm	0.07
	28	0.02	\pm	0.01
	29	0.49	\pm	0.13
	30	0.03	\pm	0.01
	31	0.91	\pm	0.26
	32	0.12	\pm	0.09
	33	0.36	\pm	0.12
	34	0.09	\pm	0.03
	35	0.89	\pm	0.25
	36	0.04	\pm	0.01
	37	0.12	\pm	0.03

(continued)

		carbon chain length	wax coverage ($\mu\text{g cm}^{-2}$)		
primary alkanols		20	0.00	±	0.00
		21	0.00	±	0.00
		22	0.05	±	0.02
		23	0.00	±	0.00
		24	0.06	±	0.03
		25	0.01	±	0.00
		26	0.07	±	0.04
		27	0.02	±	0.01
		28	0.32	±	0.21
		29	0.16	±	0.06
		30	0.07	±	0.02
		31	0.01	±	0.01
		32	0.02	±	0.01
		33	0.01	±	0.00
34	0.02	±	0.00		
secondary alkanols		pos. 2 25	0.00	±	0.00
		pos. 2 27	0.00	±	0.00
		pos. 2 31	0.00	±	0.00
		pos. 2 33	0.00	±	0.00
		pos. 11/12/13 35	0.01	±	0.00
		pos. 11/12/13 37	0.03	±	0.01
		pos. 11/12/13 39	0.01	±	0.00
alkanol acetates		25	0.00	±	0.00
		26	0.01	±	0.01
		27	0.00	±	0.00
		28	0.01	±	0.01
		30	0.01	±	0.01
		32	0.01	±	0.00
alkanoic acids		20	0.01	±	0.01
		22	0.01	±	0.01
		23	0.00	±	0.00
		24	0.02	±	0.01
		25	0.00	±	0.00
		26	0.03	±	0.01
		27	0.01	±	0.01
		28	0.08	±	0.05
		29	0.01	±	0.01
		30	0.06	±	0.03
		31	0.01	±	0.00
32	0.04	±	0.02		
alkanals		24	0.01	±	0.00
		26	0.02	±	0.01
		27	0.03	±	0.02
		28	0.08	±	0.07

(continued)

	carbon chain length	wax coverage ($\mu\text{g cm}^{-2}$)		
	30	0.08	±	0.03
	32	0.15	±	0.13
	34	0.03	±	0.02
methyl esters	22	0.00	±	0.00
	24	0.00	±	0.00
alkyl esters	38	0.01	±	0.01
	40	0.02	±	0.01
	42	0.02	±	0.01
	44	0.03	±	0.01
	46	0.03	±	0.01
	48	0.11	±	0.04
	50	0.19	±	0.14
	52	0.09	±	0.04
sum acyclic components (65.3%)		5.45	±	1.31
α -amyrin		0.58	±	0.20
β -amyrin		0.54	±	0.44
β -amyrinon		0.03	±	0.01
amyrin derivatives		0.24	±	0.10
α -tocopherol		0.22	±	0.21
β -tocopherol		0.01	±	0.00
γ -tocopherol		0.00	±	0.00
taraxerol		0.10	±	0.05
lupeol		0.01	±	0.00
lupenon		0.07	±	0.03
uvaol		0.01	±	0.00
friedelin		0.01	±	0.01
β -sitosterol		0.05	±	0.02
sum cyclic components (22.4%)		1.87	±	0.60
phenylmethyl esters	26	0.03	±	0.02
	28	0.03	±	0.01
	30	0.00	±	0.00
coumaric acid esters	26	0.01	±	0.01
	28	0.03	±	0.01
not identified		0.93	±	0.23
sum acyclic, cyclic and not identified cuticular wax components (100.0%)		8.35	±	2.13

2.4.4 Cuticular leaf wax from *Sanguisorba minor*

Total cuticular leaf wax coverage of *Sanguisorba minor* was $23.26 \pm 4.31 \mu\text{g cm}^{-2}$ (mean value \pm SD, $n = 6$). The leaf wax composed of a major portion of very-long-chain acyclic component classes (80.7%, $18.77 \pm 3.12 \mu\text{g cm}^{-2}$) and a minor portion of cyclic components (5.5%, $1.29 \pm 0.82 \mu\text{g cm}^{-2}$).

N-alkanes were the most prominent acyclic component class (39.1%, $9.09 \pm 1.67 \mu\text{g cm}^{-2}$), followed by primary alkanols (15.4%, $3.59 \pm 0.57 \mu\text{g cm}^{-2}$) and alkyl esters (9.5%, $2.21 \pm 0.24 \mu\text{g cm}^{-2}$). Additional component classes detected in the cuticular wax were secondary alkanols, alkanolic acids, alkanals and methyl esters. Carbon chain lengths ranged from C_{20} to C_{50} , the most abundant chain lengths were C_{26} , C_{31} and C_{33} (Figure 37). Hexacosanol (7.7%, $1.79 \pm 0.33 \mu\text{g cm}^{-2}$), *n*-hentriacontane (11.0%, $2.55 \pm 0.77 \mu\text{g cm}^{-2}$) and *n*-tritriacontane (25.8%, $6.01 \pm 0.80 \mu\text{g cm}^{-2}$) dominated the acyclic components. The average carbon chain length (ACL) of the very-long-chain acyclic wax components was 31.79.

The main cyclic component was ursolic acid with a cuticular wax coverage of $1.03 \pm 0.67 \mu\text{g cm}^{-2}$ (4.4%). In addition, a minor fraction of monoglycerides was detected (Table 17).

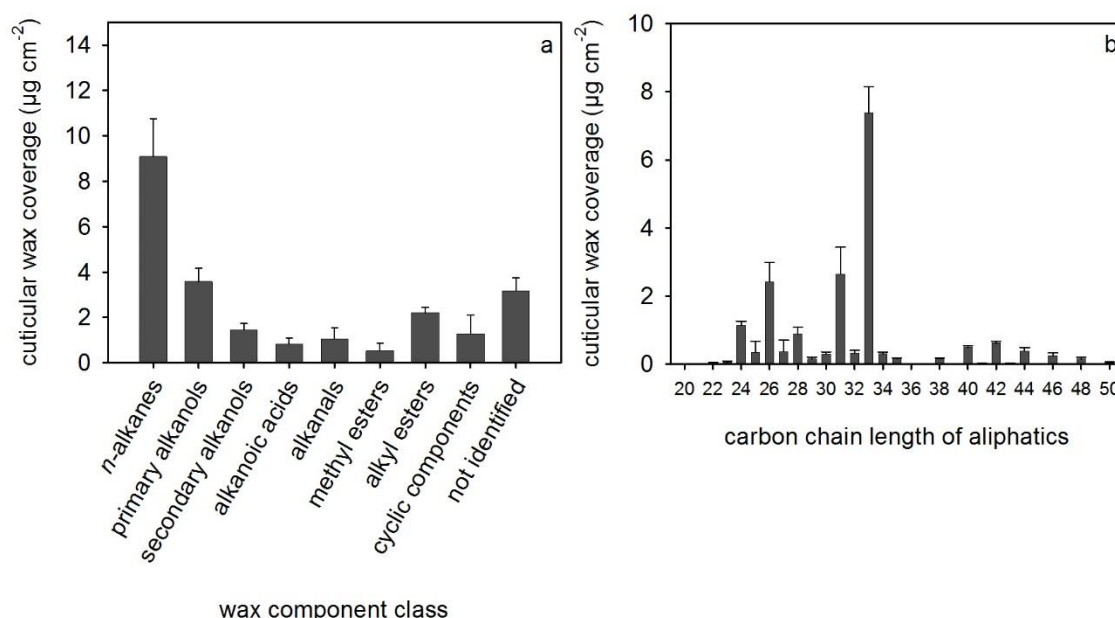


Figure 37. Cuticular wax composition of *Sanguisorba minor* leaves. (a) Cuticular wax coverage arranged according to the component classes and (b) the carbon chain length distribution of the acyclic components (mean value \pm SD, $n = 6$).

Table 17. The cuticular wax coverage and components of *Sanguisorba minor* leaves (mean value \pm SD, n = 6).

		carbon chain length	wax coverage ($\mu\text{g cm}^{-2}$)		
<i>n</i> -alkanes		23	0.01	\pm	0.00
		25	0.02	\pm	0.02
		26	0.01	\pm	0.00
		27	0.06	\pm	0.04
		28	0.01	\pm	0.00
		29	0.15	\pm	0.06
		30	0.02	\pm	0.01
		31	2.55	\pm	0.77
		32	0.09	\pm	0.02
		33	6.01	\pm	0.80
		34	0.03	\pm	0.00
		35	0.13	\pm	0.01
primary alkanols		20	traces		
		22	0.03	\pm	0.01
		23	0.01	\pm	0.00
		24	0.50	\pm	0.09
		25	0.05	\pm	0.03
		26	1.79	\pm	0.33
		27	0.02	\pm	0.02
		28	0.58	\pm	0.08
		30	0.13	\pm	0.02
		31	0.04	\pm	0.02
		32	0.14	\pm	0.01
		33	0.02	\pm	0.01
34	0.28	\pm	0.04		
secondary alkanols	pos. 8/9/10/11/12	31	0.06	\pm	0.02
	pos. 9/10/11	32	0.01	\pm	0.00
	pos. 8/9/10/11/12	33	1.35	\pm	0.27
	pos. 8/9/10/11/12	35	0.04	\pm	0.02
alkanoic acids		20	traces		
		22	0.02	\pm	0.00
		23	0.02	\pm	0.00
		24	0.45	\pm	0.09
		25	0.01	\pm	0.00
		26	0.26	\pm	0.23
		28	0.03	\pm	0.02
		30	0.04	\pm	0.02
alkanals		24	0.03	\pm	0.02
		25	0.01	\pm	0.00
		26	0.28	\pm	0.18
		27	0.28	\pm	0.31
		28	0.25	\pm	0.15
		30	0.11	\pm	0.05
		32	0.09	\pm	0.07

(continued)

	carbon chain length	wax coverage ($\mu\text{g cm}^{-2}$)		
methyl esters	22	traces		
	23	0.03	±	0.03
	24	0.15	±	0.02
	25	traces		
	26	0.07	±	0.02
	28	0.02	±	0.01
alkyl esters	38	0.16	±	0.03
	40	0.49	±	0.06
	41	0.03	±	0.00
	42	0.62	±	0.06
	43	0.02	±	0.01
	44	0.39	±	0.09
	45	0.02	±	0.01
	46	0.25	±	0.08
	47	0.01	±	0.00
	48	0.15	±	0.05
	50	0.05	±	0.01
sum acyclic components (80.7%)		18.77	±	3.12
α -amyrin		0.06	±	0.01
β -amyrin		traces		
uvaol		0.04	±	0.01
ursolic acid		1.03	±	0.67
sum cyclic components (5.5%)		1.29	±	0.82
monoglycerides	18	0.01	±	0.00
not identified		3.18	±	0.56
sum acyclic, cyclic and not identified cuticular wax components (100.0%)		23.26	±	4.31

2.4.5 Cuticular leaf wax from *Sesleria albicans*

Total cuticular leaf wax coverage of *Sesleria albicans* was $14.63 \pm 3.48 \mu\text{g cm}^{-2}$ (mean value \pm SD, $n = 5$). The leaf wax composed of very-long-chain acyclic component classes (83.9%, $12.27 \pm 2.95 \mu\text{g cm}^{-2}$).

n-alkanes were the most prominent acyclic component class (38.4%, $5.62 \pm 0.68 \mu\text{g cm}^{-2}$), followed by primary alkanols (26.7%, $3.91 \pm 1.00 \mu\text{g cm}^{-2}$) and alkyl esters (10.5%, $1.54 \pm 0.54 \mu\text{g cm}^{-2}$). Additional component classes detected in the cuticular wax were alkanolic acids, alkanals and alkanol acetates. Carbon chain lengths ranged from C₂₀ to C₅₀, the most abundant chain lengths were C₂₆ and C₂₉ (Figure 38). Hexacosanol (23.9%, $3.50 \pm 0.88 \mu\text{g cm}^{-2}$) and *n*-nonacosane (29.5%, $4.32 \pm 0.50 \mu\text{g cm}^{-2}$) dominated the acyclic components (Table 18). The average carbon chain length (ACL) of the very-long-chain acyclic wax components was 29.83.

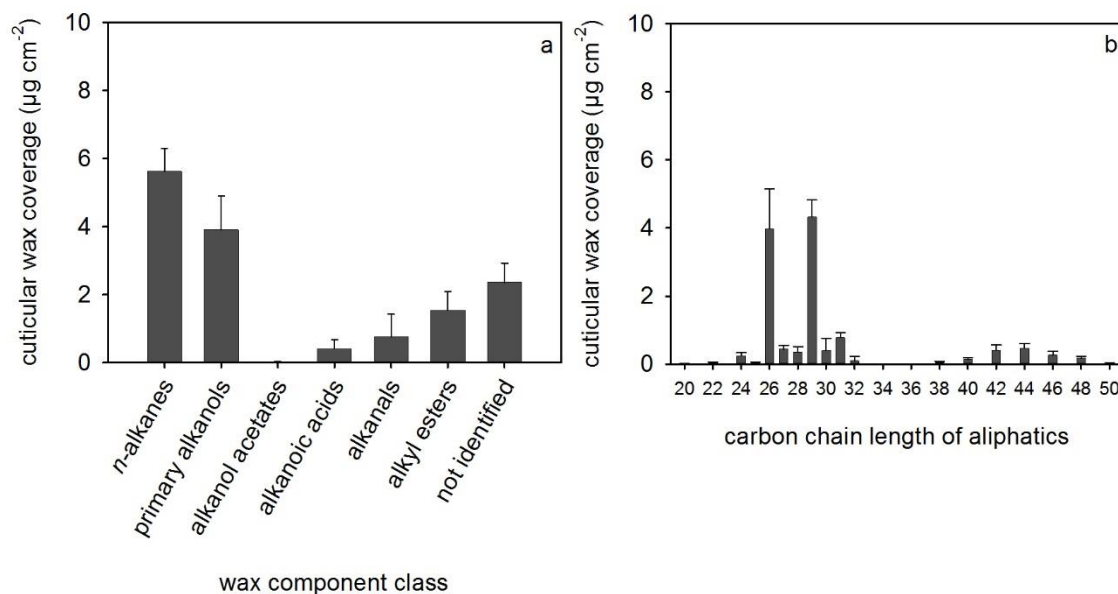


Figure 38. Cuticular wax composition of *Sesleria albicans* leaves. (a) Cuticular wax coverage arranged according to the component classes and (b) the carbon chain length distribution of the acyclic components (mean value \pm SD, $n = 5$).

Table 18. The cuticular wax coverage and components of *Sesleria albicans* leaves (mean value \pm SD, n = 5).

	carbon chain length	wax coverage ($\mu\text{g cm}^{-2}$)		
<i>n</i> -alkanes	27	0.44	\pm	0.12
	28	0.08	\pm	0.01
	29	4.32	\pm	0.50
	31	0.78	\pm	0.14
primary alkanols	22	0.03	\pm	0.01
	24	0.21	\pm	0.08
	25	0.05	\pm	0.02
	26	3.50	\pm	0.88
	28	0.09	\pm	0.03
	30	0.03	\pm	0.01
alkanol acetates	28	0.02	\pm	0.01
alkanoic acids	20	0.01	\pm	0.00
	22	0.02	\pm	0.01
	24	0.04	\pm	0.02
	26	0.07	\pm	0.04
	28	0.09	\pm	0.03
	30	0.16	\pm	0.14
	32	traces		
alkanals	26	0.39	\pm	0.30
	28	traces		
	30	0.22	\pm	0.21
	32	traces		
alkyl esters	38	0.06	\pm	0.03
	40	0.14	\pm	0.05
	42	0.41	\pm	0.16
	44	0.46	\pm	0.14
	46	0.27	\pm	0.10
	48	0.18	\pm	0.05
	50	0.03	\pm	0.02
sum acyclic components (83.9%)		12.27	\pm	2.95
not identified		2.36	\pm	0.57
sum acyclic, cyclic and not identified cuticular wax components (100.0%)		14.63	\pm	3.48

2.4.6 Cuticular leaf wax from *Pulsatilla vulgaris*

Total cuticular leaf wax coverage of *Pulsatilla vulgaris* was $11.99 \pm 1.47 \mu\text{g cm}^{-2}$ (mean value \pm SD, $n = 5$). The leaf wax composed of very-long-chain acyclic component classes (72.0%, $8.63 \pm 0.99 \mu\text{g cm}^{-2}$).

Alkyl esters were the most prominent acyclic component class (38.8%, $4.65 \pm 0.75 \mu\text{g cm}^{-2}$), followed by alkanolic acids (19.3%, $2.32 \pm 0.53 \mu\text{g cm}^{-2}$), primary alkanols (8.1%, $0.97 \pm 0.21 \mu\text{g cm}^{-2}$) and *n*-alkanes (5.8%, $0.69 \pm 0.12 \mu\text{g cm}^{-2}$). Carbon chain lengths ranged from C₂₀ to C₅₂, the most abundant chain lengths were C₄₄, C₄₆ and C₄₈ (Figure 39). C₄₄, C₄₆ and C₄₈ esters dominated the acyclic components with a total amount of $1.14 \pm 0.15 \mu\text{g cm}^{-2}$ (9.5%), $1.08 \pm 0.21 \mu\text{g cm}^{-2}$ (9.0%) and $1.05 \pm 0.29 \mu\text{g cm}^{-2}$ (8.8%), respectively (Table 19). The average carbon chain length (ACL) of the very-long-chain acyclic wax components was 37.66. In addition, minor fractions of coumaric acid esters and phytosterols were detected.

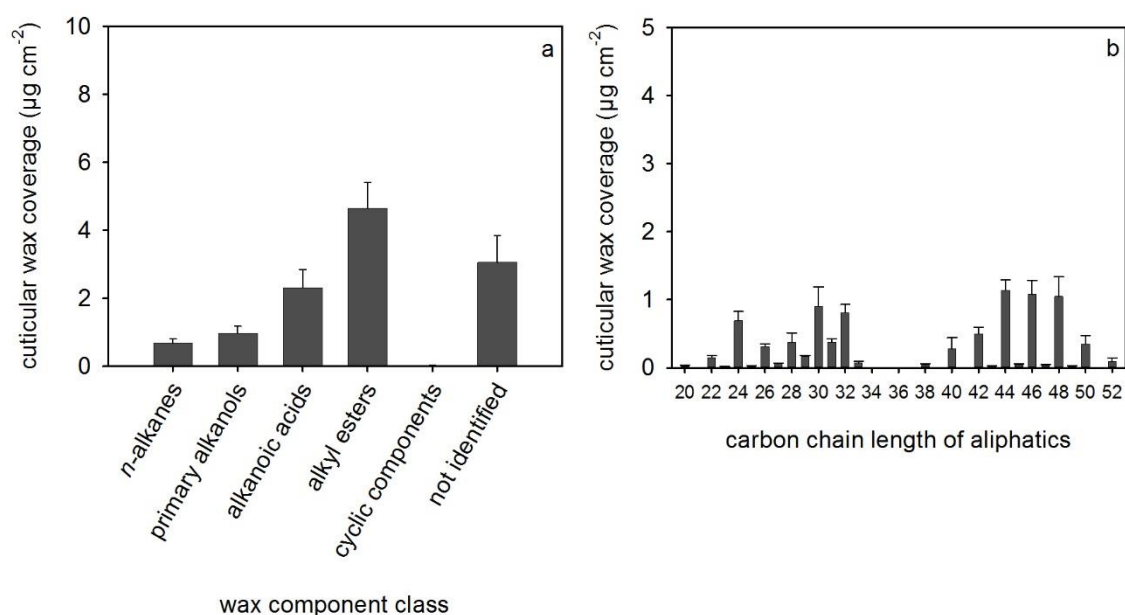


Figure 39. Cuticular wax composition of *Pulsatilla vulgaris* leaves. (a) Cuticular wax coverage arranged according to the component classes and (b) the carbon chain length distribution of the acyclic components (mean value \pm SD, $n = 5$).

Table 19. The cuticular wax coverage and components of *Pulsatilla vulgaris* leaves (mean value \pm SD, n = 5).

	carbon chain length	wax coverage ($\mu\text{g cm}^{-2}$)		
<i>n</i> -alkanes	27	0.05	\pm	0.01
	29	0.16	\pm	0.02
	30	0.02	\pm	0.01
	31	0.35	\pm	0.06
	32	0.03	\pm	0.02
	33	0.07	\pm	0.03
primary alkanols	22	0.11	\pm	0.03
	23	0.01	\pm	0.00
	24	0.41	\pm	0.11
	25	0.01	\pm	0.00
	26	0.17	\pm	0.03
	27	0.01	\pm	0.00
	28	0.08	\pm	0.02
	30	0.06	\pm	0.02
	32	0.12	\pm	0.03
alkanoic acids	20	0.03	\pm	0.01
	22	0.04	\pm	0.00
	23	0.01	\pm	0.00
	24	0.28	\pm	0.04
	25	0.01	\pm	0.00
	26	0.14	\pm	0.04
	28	0.29	\pm	0.14
	29	0.01	\pm	0.00
	30	0.82	\pm	0.28
	31	0.03	\pm	0.01
	32	0.66	\pm	0.13
alkyl esters	38	0.04	\pm	0.01
	40	0.28	\pm	0.16
	42	0.50	\pm	0.10
	43	0.03	\pm	0.00
	44	1.14	\pm	0.15
	45	0.05	\pm	0.01
	46	1.08	\pm	0.21
	47	0.03	\pm	0.01
	48	1.05	\pm	0.29
	49	0.02	\pm	0.01
	50	0.35	\pm	0.12
	52	0.09	\pm	0.05
sum acyclic components (72.0%)		8.63	\pm	0.99
β -sitosterol		0.02	\pm	0.01
cholesterol		traces		
sum cyclic components (0.2%)		0.02	\pm	0.01

(continued)

	carbon chain length	wax coverage ($\mu\text{g cm}^{-2}$)		
coumaric acid esters	20	0.01	±	0.00
	22	0.19	±	0.07
	24	0.09	±	0.03
not identified		3.06	±	0.80
sum acyclic, cyclic and not identified cuticular wax components (100.0%)		11.99	±	1.47

2.4.7 Cuticular leaf wax from *Teucrium chamaedrys*

Total cuticular leaf wax coverage of *Teucrium chamaedrys* was $18.68 \pm 5.90 \mu\text{g cm}^{-2}$ (mean value \pm SD, $n = 3$). The leaf wax composed of a major portion of very-long-chain acyclic component classes (43.4%, $8.11 \pm 1.09 \mu\text{g cm}^{-2}$) and a minor portion of cyclic components (1.6%, $0.29 \pm 0.08 \mu\text{g cm}^{-2}$).

N-alkanes were the most prominent acyclic component class (24.5%, $4.58 \pm 0.73 \mu\text{g cm}^{-2}$), followed by alkyl esters (7.2%, $1.34 \pm 0.81 \mu\text{g cm}^{-2}$), alkanolic acids (6.4%, $1.19 \pm 0.61 \mu\text{g cm}^{-2}$) and primary alkanols (5.1%, $0.96 \pm 0.44 \mu\text{g cm}^{-2}$). Additional components detected in the cuticular wax were alkanals. Carbon chain lengths ranged from C_{20} to C_{50} , the most abundant chain lengths were C_{31} and C_{33} (Figure 40). *N*-hentriacontane (6.0%, $1.13 \pm 0.34 \mu\text{g cm}^{-2}$) and *n*-tritriacontane (9.9%, $1.85 \pm 0.05 \mu\text{g cm}^{-2}$) dominated the acyclic components (Table 20). The average carbon chain length (ACL) of the very-long-chain acyclic wax components was 32.57. In addition, minor fractions of cyclic components and monoglycerides were detected.

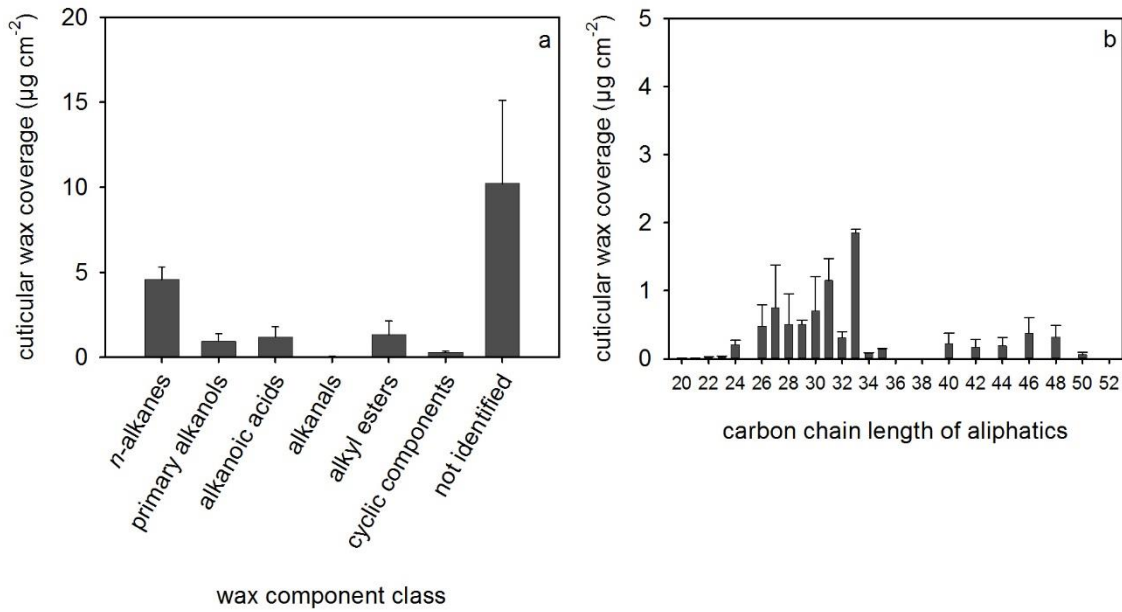


Figure 40. Cuticular wax composition of *Teucrium chamaedrys* leaves. (a) Cuticular wax coverage arranged according to the component classes and (b) the carbon chain length distribution of the acyclic components (mean value \pm SD, $n = 3$).

Table 20. The cuticular wax coverage and components of *Teucrium chamaedrys* leaves (mean value \pm SD, $n = 3$).

	carbon chain length	wax coverage (µg cm ⁻²)		
<i>n</i> -alkanes	26	0.01	\pm	0.01
	27	0.22	\pm	0.13
	29	0.48	\pm	0.04
	30	traces		
	31	1.13	\pm	0.34
	32	0.15	\pm	0.01
	33	1.85	\pm	0.05
	34	0.09	\pm	0.00
	35	0.14	\pm	0.01
	primary alkanols	26	0.27	\pm
28		0.47	\pm	0.44
30		0.12	\pm	0.07
31		0.02	\pm	0.02
32		0.07	\pm	0.05
alkanoic acids	20	0.01	\pm	0.00
	21	0.01	\pm	0.01
	22	0.03	\pm	0.01
	23	0.02	\pm	0.02
	24	0.21	\pm	0.06
	26	0.20	\pm	0.12

(continued)

	carbon chain length	wax coverage ($\mu\text{g cm}^{-2}$)		
alkanoic acids	27	traces		
	28	0.04	±	0.02
	29	0.03	±	0.02
	30	0.07	±	0.04
	32	0.04	±	0.01
alkanals	32	0.04	±	0.02
alkyl esters	40	0.22	±	0.15
	42	0.17	±	0.12
	44	0.19	±	0.12
	46	0.37	±	0.23
	48	0.32	±	0.17
	50	0.06	±	0.04
sum acyclic components (43.4%)		8.11	±	1.09
α -amyrin		0.14	±	0.09
β -amyrin		0.08	±	0.03
oleanolic acid		0.01	±	0.00
β -sitosterol		0.06	±	0.06
sum cyclic components (1.6%)		0.29	±	0.08
monoglycerides	16	0.01	±	0.00
	18	traces		
not identified		10.23	±	4.89
sum acyclic, cyclic and not identified cuticular wax components (100.0%)		18.68	±	5.90

2.4.8 Cuticular leaf wax from *Salvia pratensis*

Total cuticular leaf wax coverage of *Salvia pratensis* was $13.80 \pm 2.09 \mu\text{g cm}^{-2}$ (mesophytic) and $39.43 \pm 17.70 \mu\text{g cm}^{-2}$ (xerophytic; mean value \pm SD, $n = 5$). The mesophytic leaf wax composed of a major portion of cyclic components (69.2%, $9.55 \pm 2.68 \mu\text{g cm}^{-2}$) and a minor portion of very-long-chain acyclic component classes (12.7%, $1.75 \pm 0.42 \mu\text{g cm}^{-2}$). Similarly, the xerophytic leaf wax composed of a major portion of cyclic components (73.1%, $28.82 \pm 14.55 \mu\text{g cm}^{-2}$) and a minor portion of very-long-chain acyclic component classes (9.3%, $3.65 \pm 1.51 \mu\text{g cm}^{-2}$).

N-alkanes were the most prominent acyclic component class, followed by branched alkanes, alkanolic acids and primary alkanols of both the mesophytic and the xerophytic leaf cuticular waxes. Carbon chain lengths ranged from C_{20} to C_{33} , the most abundant chain lengths were C_{29} , C_{31} and C_{33} (Figure 41). The acyclic components of both leaf types were dominated by *n*-hentriacontane. The average carbon chain length

(ACL) of the very-long-chain acyclic wax components was 30.07 (mesophytic) and 30.71 (xerophytic). The main cyclic component was ursolic acid for both mesophytic and xerophytic leaves (Table 21).

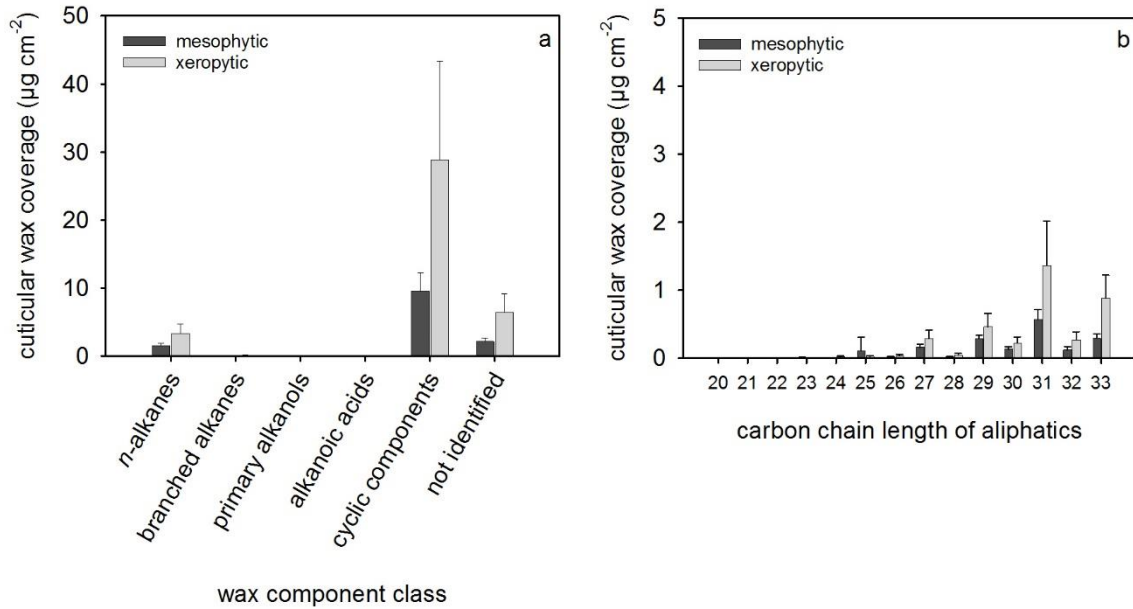


Figure 41. Cuticular wax composition of mesophytic and xerophytic *Salvia pratensis* leaves. (a) Cuticular wax coverage arranged according to the component classes and (b) the carbon chain length distribution of the acyclic components (mean value \pm SD, $n = 5$).

Table 21. The cuticular wax coverage and components of *Salvia pratensis* mesophytic and xerophytic leaves (mean value \pm SD, n = 5).

	carbon chain length	wax coverage ($\mu\text{g cm}^{-2}$)						
		mesophytic			xerophytic			
<i>n</i> -alkanes	23	0.01	\pm	0.01	0.01	\pm	0.00	
	25	traces			0.03	\pm	0.01	
	26	0.01	\pm	0.00	0.01	\pm	0.00	
	27	0.16	\pm	0.04	0.29	\pm	0.12	
	29	0.27	\pm	0.04	0.44	\pm	0.19	
	30	0.09	\pm	0.03	0.18	\pm	0.08	
	31	0.49	\pm	0.12	1.23	\pm	0.57	
	32	0.13	\pm	0.05	0.27	\pm	0.12	
	33	0.29	\pm	0.06	0.88	\pm	0.34	
<i>iso</i> - and <i>anteiso</i> -alkanes	29	0.03	\pm	0.01	0.02	\pm	0.01	
	31	0.08	\pm	0.04	0.13	\pm	0.10	
primary alkanols	20	traces			0.01	\pm	0.00	
	26	0.01	\pm	0.00	0.03	\pm	0.02	
alkanoic acids	24	not detected			0.02	\pm	0.01	
	28	0.02	\pm	0.01	0.05	\pm	0.02	
	30	0.05	\pm	0.01	0.04	\pm	0.04	
sum acyclic components	12.7%	1.75	\pm	0.42	9.3%	3.65	\pm	1.51
α -amyrin		not detected			traces			
erythrodiol		0.05	\pm	0.01	0.14	\pm	0.07	
uvaol		0.07	\pm	0.01	0.24	\pm	0.11	
oleanolic acid		2.68	\pm	0.69	7.92	\pm	4.19	
betulinic acid		0.34	\pm	0.15	1.26	\pm	0.95	
ursolic acid		6.23	\pm	2.01	18.18	\pm	8.95	
echinocystic acid		0.08	\pm	0.02	0.56	\pm	0.47	
hederagenin		0.11	\pm	0.02	0.50	\pm	0.20	
cholesterol		not detected			0.01	\pm	0.00	
sum cyclic components	69.2%	9.55	\pm	2.68	73.1%	28.82	\pm	14.55
monoglycerides	16	0.12	\pm	0.07	0.14	\pm	0.06	
	18	0.25	\pm	0.15	0.33	\pm	0.14	
not identified		2.15	\pm	0.52	6.49	\pm	2.68	
sum acyclic, cyclic and not identified cuticular wax components	100.0%	13.80	\pm	2.09	100.0%	39.43	\pm	17.70

2.4.9 Cuticular leaf wax from *Plantago lanceolata*

Total cuticular leaf wax coverage of *Plantago lanceolata* was $4.15 \pm 0.83 \mu\text{g cm}^{-2}$ (mean value \pm SD, $n = 5$). The leaf wax composed of a major portion of cyclic components (65.3%, $2.71 \pm 0.71 \mu\text{g cm}^{-2}$) and a minor portion of very-long-chain acyclic component classes (24.8%, $1.03 \pm 0.15 \mu\text{g cm}^{-2}$).

N-alkanes were the most prominent acyclic component class (19.8%, $0.82 \pm 0.13 \mu\text{g cm}^{-2}$), followed by primary alkanols (2.9%, $0.12 \pm 0.03 \mu\text{g cm}^{-2}$) and alkyl esters (1.2%, $0.05 \pm 0.04 \mu\text{g cm}^{-2}$). Additional component classes detected in the cuticular wax were branched alkanes, secondary alkanols, alkanol acetates and alkanolic acids. Carbon chain lengths ranged from C_{20} to C_{48} , the most abundant chain lengths were C_{31} and C_{33} (Figure 42). *N*-hentriacontane (10.6%, $0.44 \pm 0.08 \mu\text{g cm}^{-2}$) and *n*-trtriacontane (4.6%, $0.19 \pm 0.04 \mu\text{g cm}^{-2}$) dominated the acyclic components. The average carbon chain length (ACL) of the very-long-chain acyclic wax components was 31.70.

The main cyclic component was ursolic acid with a cuticular wax coverage of $1.89 \pm 0.44 \mu\text{g cm}^{-2}$ (45.5%), followed by oleanolic acid (17.3%, $0.72 \pm 0.26 \mu\text{g cm}^{-2}$; Table 22).

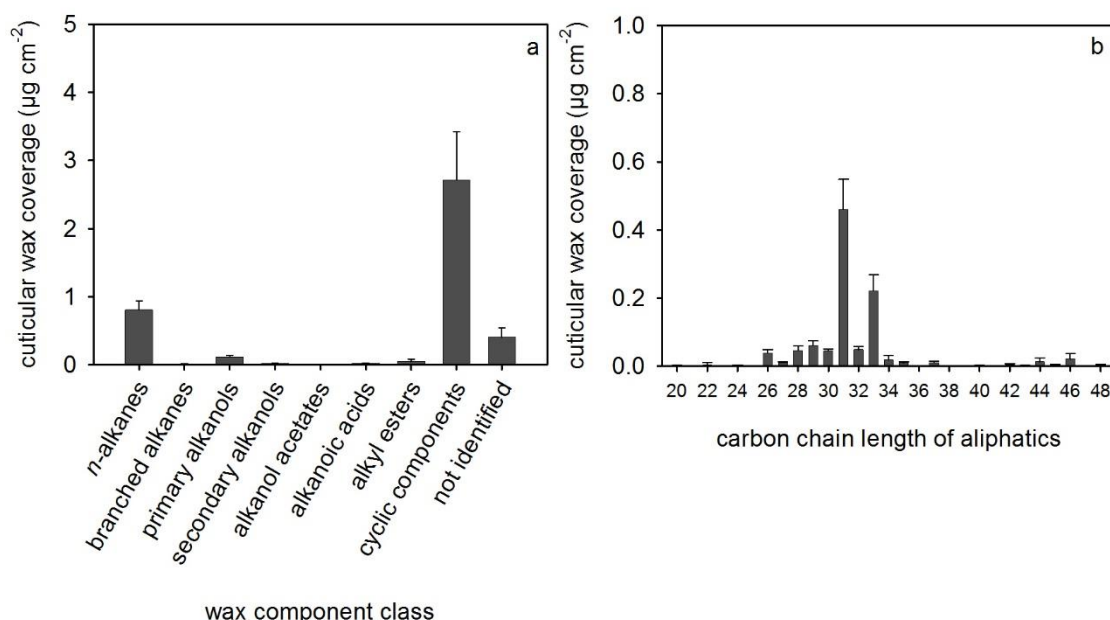


Figure 42. Cuticular wax composition of *Plantago lanceolata* leaves. (a) Cuticular wax coverage arranged according to the component classes and (b) the carbon chain length distribution of the acyclic components (mean value \pm SD, $n = 5$).

Table 22. The cuticular wax coverage and components of *Plantago lanceolata* leaves (mean value \pm SD, n = 5).

		carbon chain length	wax coverage ($\mu\text{g cm}^{-2}$)		
<i>n</i> -alkanes		25	traces		
		26	0.00	\pm	0.00
		27	0.00	\pm	0.00
		28	0.00	\pm	0.00
		29	0.06	\pm	0.01
		30	0.03	\pm	0.01
		31	0.44	\pm	0.08
		32	0.04	\pm	0.00
		33	0.19	\pm	0.04
		34	traces		
		35	0.01	\pm	0.00
		37	0.01	\pm	0.00
	<i>iso</i> - and <i>anteiso</i> -alkanes		31	0.01	\pm
		32	0.00	\pm	0.00
		33	0.01	\pm	0.00
primary alkanols		22	traces		
		24	0.00	\pm	0.00
		25	0.00	\pm	0.00
		26	0.04	\pm	0.01
		27	0.01	\pm	0.00
		28	0.04	\pm	0.01
		30	0.01	\pm	0.00
		31	0.01	\pm	0.01
		32	traces		
		33	0.00	\pm	0.00
		34	traces		
secondary alkanols	pos. 2	31	0.00	\pm	0.00
	pos. 2	33	0.02	\pm	0.01
alkanol acetates		30	0.00	\pm	0.00
alkanoic acids		20	0.00	\pm	0.00
		22	traces		
		24	0.00	\pm	0.00
		26	0.00	\pm	0.00
		27	0.00	\pm	0.00
		28	0.00	\pm	0.00
		30	0.01	\pm	0.00
		32	0.00	\pm	0.00
alkyl esters		40	0.00	\pm	0.00
		42	0.01	\pm	0.00
		43	0.00	\pm	0.00
		44	0.01	\pm	0.01
		45	0.00	\pm	0.00
		46	0.02	\pm	0.02
		48	0.00	\pm	0.00

(continued)

	carbon chain length	wax coverage ($\mu\text{g cm}^{-2}$)	
sum acyclic components (24.8%)		1.03	± 0.15
α -amyrin		0.00	± 0.00
taraxerol		0.02	± 0.01
erythrodiol		0.00	± 0.00
uvaol		0.04	± 0.02
friedelin		0.00	± 0.00
oleanolic acid		0.72	± 0.26
ursolic acid		1.89	± 0.44
β -sitosterol		0.03	± 0.01
stigmasterol		0.00	± 0.00
cholesterol		0.00	± 0.00
campesterol		0.00	± 0.00
sum cyclic components (65.3%)		2.71	± 0.71
not identified		0.40	± 0.14
sum acyclic, cyclic and not identified cuticular wax components (100.0%)		4.15	± 0.83

2.5 Cuticular wax chemistry and minimum water permeability

Correlation analysis was performed in order to evaluate the relationship between the cuticular wax chemistry and the minimum water permeability. The natural logarithm of the minimum conductance did not correlate with the total wax coverage, the very-long-chain acyclic coverage, the cyclic wax coverage or the average carbon chain length of the aliphatics (Figure 43). The plant species with the lowest minimum conductances (*Geranium sanguineum*, *Teucrium chamaedrys* and *Sesleria albicans*) had *n*-alkanes as the most prominent acyclic component class of the cuticular waxes. The most abundant component classes of the very-long-chain acyclic components were separately correlated with the minimum water permeability. The natural logarithm of the minimum conductance did not correlate with the amount of *n*-alkanes, primary alkanols, alkanolic acids or alkyl esters.

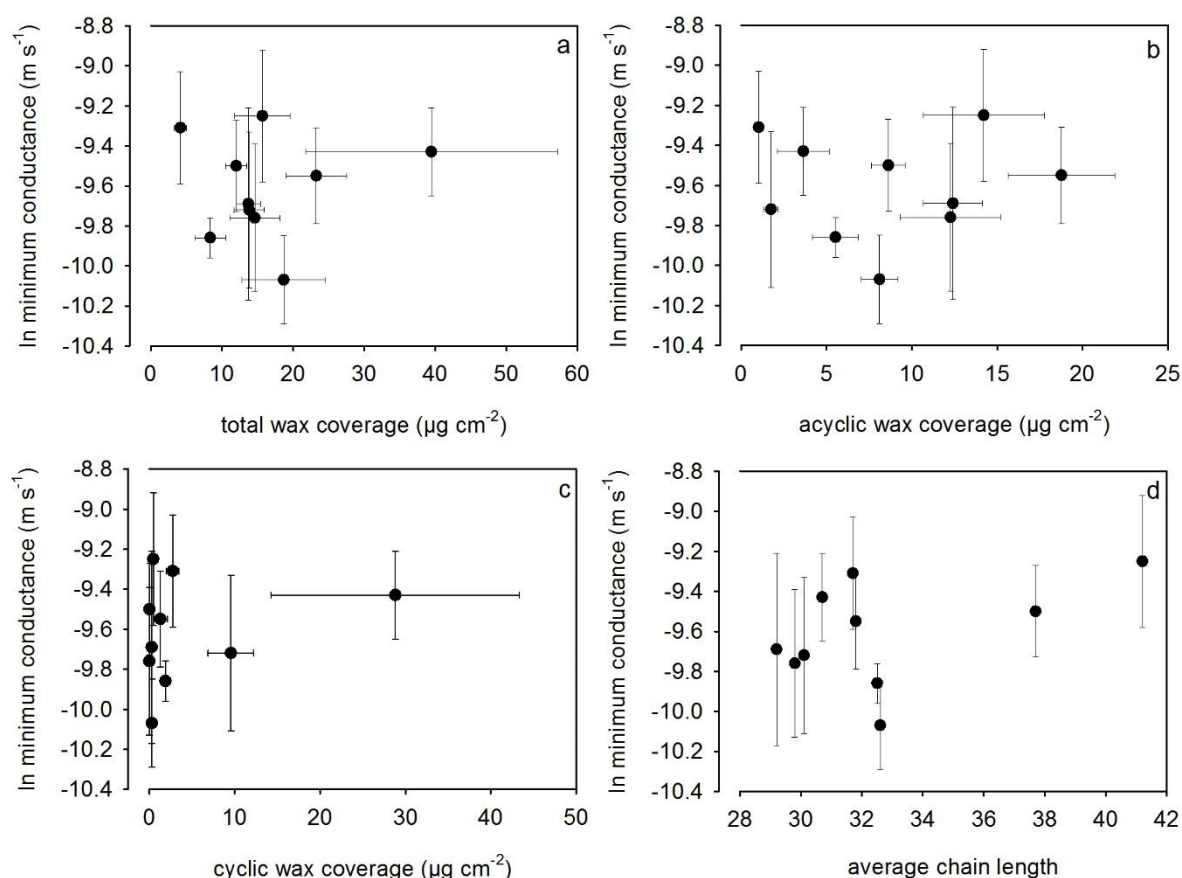


Figure 43. The natural logarithm of the minimum conductance as a function of (a) the total wax coverage, (b) the very-long-chain acyclic wax coverage, (c) the cyclic wax coverage and (d) the average carbon chain length of the aliphatics.

3 Discussion

3.1 Leaf characteristics and minimum conductance

Characteristic plant species from xeric limestone sites naturally located in Franconia (Southern Germany) were chosen for the study (Kraus 1906, Volk 1937, Witschel 1991, Diekmann *et al.* 2014). The growing sites are characterised by hot and dry environmental conditions (Kraus 1906, 1911). Dwarfing of several plant species, such as *Salvia pratensis*, *Sanguisorba minor*, *Teucrium chamaedrys* and *Plantago lanceolata*, has been described as a result of the edaphic dryness. Normal growth of plants from dwarf seeds was observed on garden mould (Kraus 1906). The dwarf form of *Salvia pratensis* from the natural xeric limestone growing site (class Festuco-Brometea) was compared with the mesophytic *Salvia pratensis* (class Molinio-Arrhenatheretea). The double-sided leaf area of the mesophytic *Salvia pratensis* was increased by factor 4.0, the fresh weight by factor 2.9 and the dry weight by factor 2.4 in comparison to the xerophytic dwarf leaves. Although considerable differences of the leaf characteristics were detected, the minimum conductance did not differ significantly ($p = 0.129$) between the xerophytic and mesophytic *Salvia pratensis* leaves. Similar results were obtained by Burghardt *et al.* (2008) analysing *Teucrium chamaedrys*.

The minimum conductances ranged between $4.32 \cdot 10^{-5} \text{ m s}^{-1}$ and $10.10 \cdot 10^{-5} \text{ m s}^{-1}$ (Table 12). The indecious woody chamaephyte *Teucrium chamaedrys* (dwarf-shrub; Ellenberg *et al.* 1991) had the lowest minimum conductance of the analysed species. However, it was still 1.6-fold higher than the literature value for *Teucrium chamaedrys* (Burghardt *et al.* 2008). The given variability might be due to different harvest places, harvest dates and growth conditions. *Helianthemum apenninum* and *Plantago lanceolata* had the highest minimum conductances. *Helianthemum apenninum* is an indecious woody chamaephyte, such as *Teucrium chamaedrys* (dwarf-shrub; Ellenberg *et al.* 1991). The minimum conductance of both plant species was expected to be similarly low, due to the longer leaf life span of chamaephytes in comparison to hemicryptophytes, such as *Plantago lanceolata* (Ellenberg *et al.* 1991, Navas *et al.* 2003). Small leaves are proposed to have a lower transpiration rate (Sandquist 2014). Small leaves with long leaf life spans might be assumed to have low minimum conductances, however, this is not the case for *Helianthemum apenninum*.

Teucrium chamaedrys had a low specific leaf area (SLA) and a low leaf water content (LWC), whereas *Plantago lanceolata* had a high SLA and a high LWC (Table 12). The hemicryptophyte *Plantago lanceolata* is a common plant species of

mesophytic grasslands (class Molinio-Arrhenatheretea). Slow-growing plant species with sclerophyllous leaves were described to have low SLA associated with low LWC. Tender leaves in contrast were associated with high SLA and high LWC (Vendramini *et al.* 2002). A significantly positive correlation between SLA and LWC of the analysed characteristic plant species from xeric limestone sites was calculated (Figure 31). In comparison with a literature survey of 77 plant species (succulent, sclerophyllous and tender-leaved; Vendramini *et al.* 2002), the xeric plant species from this study were tender-leaved and/or sclerophyllous.

The minimum conductance was compared with different leaf characteristics (Figure 32). No correlation between the specific leaf area (SLA) and the minimum conductance was detected. However, the minimum conductance showed a slight, non-significant tendency to increase with leaf water content (LWC) and a significant correlation to increase with degree of succulence (SU). *Teucrium chamaedrys* had the lowest minimum conductance, in addition to low SU and low SLA. In contrast, *Plantago lanceolata* had a high minimum conductance, high SU and high LWC. The tendency that plant species with low specific leaf area (SLA) and low leaf water content (LWC) have low minimum conductances and plant species with high SLA and high LWC have high minimum conductances can be observed.

The difference between the leaf and air temperature ($\Delta T_{\text{leaf}} - T_{\text{air}}$) was measured, when stomata were completely closed as a result of desiccation stress. Higher minimum conductances of leaves showed a non-significant tendency to elevated temperature differences. Under water-limited growth conditions, smaller leaves were proposed to avoid heating up above air temperatures, due to the reduced boundary layer and, thus, quick rate of heat transfer. Consequently, lower transpiration rates are proposed for smaller leaves in comparison to larger leaves (Gates 1980, Gibson 1998, Jones 2014, Sandquist 2014). The dual projected leaf surface area (LA) was neither correlated with the temperature difference between the leaf and air temperature ($\Delta T_{\text{leaf}} - T_{\text{air}}$) nor with the minimum conductance (Figure 44).

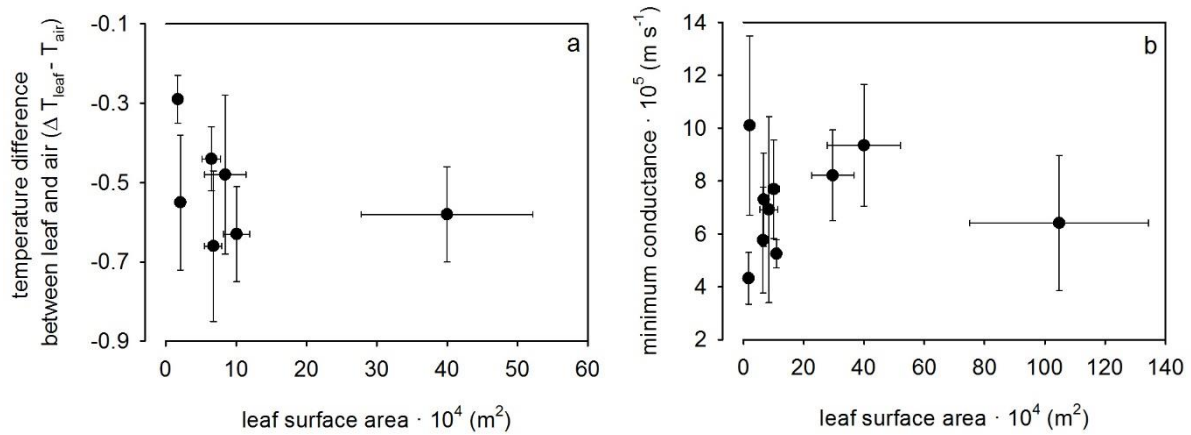


Figure 44. The relationship between the dual projected leaf surface area (LA) with (a) the difference between leaf and air temperature ($\Delta T_{\text{leaf}} - T_{\text{air}}$) and with (b) the minimum conductance.

3.2 Leaf thermal tolerance

Thermal tolerance is frequently determined by the basal fluorescence, the maximum fluorescence or the maximum quantum yield of the photosystem II from dark adapted leaves ($F_v F_m^{-1}$). The basal and maximum fluorescence values might become a source of mistakes due to a strong sample dependence and, thus, a high variability (Brestic and Zivcak 2013). In the conducted experiments $F_v F_m^{-1}$ was used. The critical temperature (T_{crit}) of the maximum quantum yield of photosystem II indicates the temperature at which $F_v F_m^{-1}$ starts to decline. The critical temperature recorded (T_{crit}) from the characteristic xeric limestone plant species ranged from 37.85 °C (*Plantago lanceolata*) up to 43.76 °C (*Teucrium chamaedrys*; Table 13). In general, the critical temperature of plant species, determined as the steep increase of the basal fluorescence, ranged from 38 °C up to 49 °C (Bilger 1984, Froux *et al.* 2004). The measured T_{crit} values are in the lower range compared to published values. For example, the literature values for *Teucrium chamaedrys* are higher (46 - 47 °C, 47.5 °C; Bilger 1984, Burghardt *et al.* 2008) than the measured T_{crit} (44 °C). The $F_v F_m^{-1}$ parameter reduces variability in comparison to the basal and maximum fluorescence. Though, the usage of $F_v F_m^{-1}$ might lead to an underestimation of leaf thermal tolerance. This would indicate a more severe temperature effect than actually occurred, due to an underestimation of $F_v F_m^{-1}$ (Brestic and Zivcak 2013).

A link between the specific leaf area (SLA) and the photosynthetic performance has been suggested (Wright *et al.* 2001, Knight and Ackerly 2003). Plant species with

low SLA had higher thermal tolerances and were able to withstand high temperature stresses. Plant species with higher SLA had lower thermal tolerances (Knight and Ackerly 2003). A slight negative, non-significant tendency was found between SLA and leaf thermal tolerance. Plant species with low SLA tended to higher critical temperatures and plant species with high SLA tended to lower critical temperatures (Figure 45).

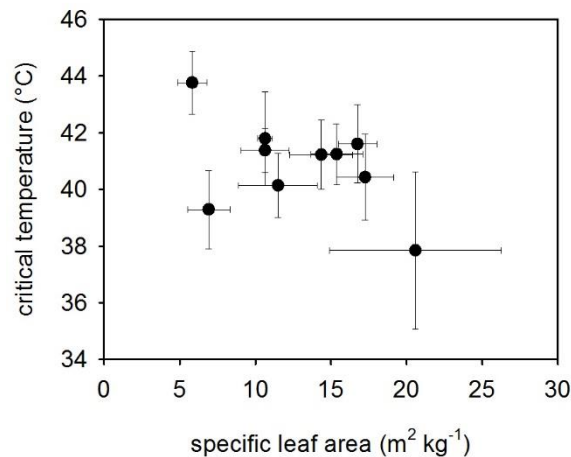


Figure 45. The critical temperature of the maximum quantum yield of photosystem II (T_{crit}) and its relationship with the specific leaf area (SLA).

3.3 Leaf thermal tolerance and minimum conductance

Recently, Feller (2006) demonstrated that heat induces stomatal opening. This is in contrast to the stomatal closure upon dehydration. A trade-off between reducing heat stress through transpirational leaf cooling (enhanced when stomata are open) and reducing drought stress through limited water loss was proposed (Feller 2006, Crawford *et al.* 2012). Low minimum conductance is used as an indicator of efficient cuticular transpiration barriers enabling dehydration avoidance (Muchow and Sinclair 1989, Smith *et al.* 2006). The critical temperature of the maximum quantum yield of photosystem II (T_{crit}) was measured as an indicator of leaf thermal tolerance. Characteristic plant species from xeric limestone sites with efficient transpiration barriers had high leaf thermal tolerances (Figure 33). From the regression equation ($g_{min} = -8.764 \cdot 10^{-6} \cdot T_{crit} + 4.295 \cdot 10^{-4}$) the minimum conductances were predicted (Figure 46).

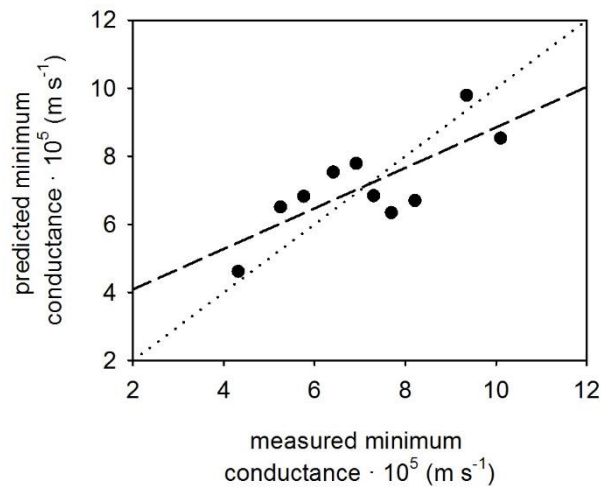


Figure 46. The leaf minimum conductance of characteristic plant species from xeric limestone sites from an equation based on the leaf thermal tolerance. Plot of predicted versus measured minimum conductances ($r^2 = 0.596$; dotted line indicates a slope of 1.0).

Teucrium chamaedrys had the lowest minimum conductance and *Helianthemum apenninum* had the highest minimum conductance of the analysed plant species. The leaf thermal tolerance was highest for the *Teucrium chamaedrys* leaves and a low leaf thermal tolerance was detected for the *Helianthemum apenninum* leaves. *Helianthemum apenninum* and *Teucrium chamaedrys* are indeciduous woody chamaephytes (Ellenberg *et al.* 1991). A low minimum conductance with high leaf thermal tolerances was expected for both plant species. Due to the extreme and very variable microclimatic conditions on the hot and dry xeric limestone sites (Kraus 1911) it is conceivable that both plant species inhabit different vegetation mosaics due to the local heterogeneity in microclimatic conditions. According to this, dry and hot vegetation mosaics would support plant species such as *Teucrium chamaedrys*, being able to save water and endure high temperatures. *Helianthemum apenninum* on the other hand would occur on less extreme vegetation mosaics.

3.4 Cuticular wax chemistry and minimum water permeability

Cuticular wax coverages ranged between $4.15 \mu\text{g cm}^{-2}$ (*Plantago lanceolata*) and $39.43 \mu\text{g cm}^{-2}$ (xerophytic *Salvia pratensis*). Common component classes, such as *n*-alkanes, primary alkanols, alkanolic acids, alkanals and alkyl esters, were present in all analysed cuticular waxes. Other very-long-chain aliphatic component classes were branched alkanes, secondary alkanols, methyl esters and alkanol acetates. The

carbon chain lengths of the aliphatic compounds are ubiquitously found and ranged from C₂₀ to C₅₂ (Jetter *et al.* 2006). The cuticular leaf waxes of the characteristic plant species from xeric limestone sites were analysed for the first time considering the chemical wax quantity and quality.

The main very-long-chain acyclic component class of the analysed plant species were *n*-alkanes. *N*-alkanes are ubiquitous wax components and are present in almost all plant waxes (Bianchi 1995). *Hippocrepis comosa* leaf wax predominantly composed of primary alkanols. In the leaf wax of *Helianthemum apenninum* and *Pulsatilla vulgaris* alkyl esters formed the dominant class of aliphatic components.

Plant species belonging to the family Cistaceae, such as *Helianthemum apenninum*, have plant waxes with the major component classes being alkanolic acids, alkanols, alkyl esters and alkanes (Bianchi 1995). These major component classes were detected in the leaf wax of *Helianthemum apenninum* (Figure 35). The major component classes described for Rosaceae (such as *Sanguisorba minor*) are alkanolic acids, alkanols, alkanals, alkanes, alkyl esters and alkanones (Bianchi 1995). The leaf wax of *Sanguisorba minor* was composed of *n*-alkanes, primary alkanols, alkyl esters, secondary alkanols, alkanolic acids, alkanals and methyl esters (Figure 37). The leaf wax of *Plantago major* has been analysed by Bakker *et al.* (1998). The cuticular leaf wax of *Plantago major* (Plantaginaceae) composed of triterpenoids (57% - 68%) and *n*-alkanes (13% - 19%). Similarly, the leaf wax of *Plantago lanceolata* composed of cyclic components (65.3%) and a smaller fraction of very-long-chain acyclic components, mainly *n*-alkanes (19.8%, Figure 42).

Teucrium chamaedrys and *Salvia pratensis* belong to the family Lamiaceae. Lamiaceae are described to contain both alkanes and pentacyclic triterpenoids as common leaf (Maffei 1994, Jäger *et al.* 2009) and cuticular leaf wax components (Bianchi 1995). The main aliphatic component of the cuticular leaf wax of *Teucrium chamaedrys* were *n*-alkanes and only a minor fraction of cyclic components was detected (Figure 40). *Salvia pratensis* mainly composed of pentacyclic triterpenoids and *n*-alkanes were the main aliphatic component class (Figure 41). All wax extracts had an unidentified fraction, mostly below 20% of the extracted total wax coverage. An exception was the cuticular leaf wax extracted from *Teucrium chamaedrys* leaves. The comparable high amount of unidentified components in the wax extract of *Teucrium chamaedrys* leaves might be solvent-extracted from inner tissues, given that the lower

leaf surface of *Teucrium chamaedrys* was covered by glandular trichomes (Annex, Figure 70).

Cuticular waxes establish the main transport-limiting barrier and, thus, correlation analysis of the minimum conductances with the total wax coverage, the amount of cyclic components, the amount of aliphatic components and the average carbon chain length were conducted (Figure 43). Higher wax amounts did not constitute more efficient transpiration barriers. *Salvia pratensis* had a total leaf wax coverage of 13.80 $\mu\text{g cm}^{-2}$ from the mesophytic leaves and 39.43 $\mu\text{g cm}^{-2}$ from the xerophytic leaves (Table 21). The higher wax coverage did not lead to a more efficient transpiration barrier. It was proposed that very-long-chain aliphatics built more efficient transpiration barriers than cyclic components. This hypothesis was based on the fact that cyclic wax components, such as pentacyclic triterpenoids, form less efficient barriers than for example *n*-alkanes (Oliveira *et al.* 2003). In line with that, it was tested whether the barrier properties depend on the very-long-chain acyclic wax coverage or the cyclic wax coverage. No relationship between the minimum water permeability and the aliphatic wax amount or the cyclic wax amount was found. Higher average carbon chain lengths of the aliphatics were proposed to enhance the crystalline volume fractions of the cuticular waxes and, thus, reduce the cuticular water permeability. The crystal lattices are proposed to be impermeable to water (Riederer and Schneider 1990, Riederer 1991). No correlation between the average carbon chain length and the minimum conductance was calculated.

3.5 Conclusion

The hypothesis that plant species with efficient transpiration barriers have higher photosynthetic leaf thermal tolerances can be confirmed for the characteristic plant species from xeric limestone sites. The minimum conductance was measured as an indicator of efficient cuticular transpiration barriers enabling dehydration avoidance. Low minimum conductances were associated with a higher availability to withstand drought. The critical temperature (T_{crit}) of the maximum quantum yield of photosystem II was measured as an indicator of leaf thermal tolerance. The minimum conductance and the critical temperature (T_{crit}) were significantly positively correlated. Consequently, plant species with efficient transpiration barrier properties had high leaf thermal tolerances.

The minimum conductances of the typical plant species from the hot and dry environment ranged between $4.32 \cdot 10^{-5} \text{ m s}^{-1}$ and $10.10 \cdot 10^{-5} \text{ m s}^{-1}$. The tendency

that plant species with low specific leaf area (SLA) and low leaf water content (LWC) have low minimum conductances and, vice versa, plant species with high SLA and high LWC have high minimum conductances was observed for characteristics plant species of xeric limestone sites.

Given that cuticular waxes establish the main transport-limiting barrier, correlation analysis of the barrier efficiency with the results from the leaf wax analysis was performed. Abundant wax coverages did not yield more efficient transpiration barriers. Neither the amount of cyclic components nor the amount of acyclic components showed a relation to the cuticular barrier function. The average carbon chain length did not influence the efficiency of the transpiration barrier.

Chapter V. Chemical and functional analyses of the plant cuticle as leaf transpiration barrier

1 Introduction

All aerial primary plant surfaces are covered by a thin continuous layer, the plant cuticle. The main function of the plant cuticle is to minimise the uncontrolled non-stomatal water loss from the interior of plants into the surrounding atmosphere. Efficient cuticular transpiration barriers are proposed to prolong plant survival, for example under drought conditions when stomata are closed. An extensive literature survey of cuticular water permeabilities measured from astomatous, isolated leaf cuticles is available (Riederer and Schreiber 2001). The cuticular permeances of 57 plant species range between $0.04 \cdot 10^{-5} \text{ m s}^{-1}$ (*Vanilla planifolia*) and $14.40 \cdot 10^{-5} \text{ m s}^{-1}$ (*Abies alba*). The lowest cuticular water permeabilities are described for evergreen leaves from epiphytic or climbing tropical plant species, such as *Vanilla planifolia* and *Monstera deliciosa*. Leaves of temperate climate plant species, such as *Juglans regia* and *Hedera helix*, have the highest cuticular water permeabilities. Leaves of plant species from Mediterranean type of climates, such as *Olea europaea*, *Nerium oleander* and *Prunus laurocerasus*, have a high variability in cuticular water permeabilities and overlap with both other groups (Schreiber and Riederer 1996, Helbsing *et al.* 2001, Riederer and Schreiber 2001).

Plant cuticles consist of a cutin matrix with cuticular waxes embedded within or deposited on its surface (Pollard *et al.* 2008, Yeats and Rose 2013). The presence of the cuticular waxes almost completely determines the transpiration barrier properties. Extraction of cuticular waxes leads to a considerable increase of the cuticular water permeability (Schönherr 1976, Schönherr and Lenzian 1981). Thickness of cuticular membranes is not correlated with transpiration barrier efficiency (Kamp 1930, Schreiber and Riederer 1996, Riederer and Schreiber 2001, Anfodillo *et al.* 2002). The relation between cuticular wax quantity, quality and the transpiration barrier properties remains unsolved (Schönherr 1982, Kerstiens 2006). Cuticular waxes are heterogeneous in coverage and composition. Cuticular leaf wax quantities are reported to range between $0.4 \mu\text{g cm}^{-2}$ and $160.0 \mu\text{g cm}^{-2}$ (Bouzoubaâ *et al.* 2006, Mamrutha *et al.* 2010). Typically, mixtures of very-long-chain acyclic components, such as *n*-alkanes, primary alkanols, alkanolic acids, alkanals and alkyl esters, constitute the

cuticular waxes. Additionally, pentacyclic triterpenoids mainly of the oleanane, lupane and ursane type are common cyclic components (Kolattukudy 1970, Martin and Juniper 1970, Bianchi 1995, Jetter *et al.* 2006).

Cyclic constituents are proposed to establish less efficient transpiration barriers than very-long-chain aliphatics (Grncarevic and Radler 1967, Oliveira *et al.* 2003, Vogg *et al.* 2004, Leide *et al.* 2011, Buschhaus and Jetter 2012). The average carbon chain length (ACL) of the aliphatic wax components and the ratio between average carbon chain length dispersion (ΔACL) and average carbon chain length were proposed to influence the barrier properties (Riederer and Schneider 1990, Riederer 1991). In this study, the potential influence of the acyclic and cyclic cuticular wax constituents on the efficacy of the transpiration barrier properties was analysed. Furthermore, the impact of average carbon chain length and of the ratio ($\Delta\text{ACL} \text{ ACL}^{-1}$) on structural properties was addressed through analysis of the cuticular barrier function.

In most studies attempting to clarify the relationship between chemistry, structure and function of plant cuticles one plant species was analysed under different environmental aspects such as drought exposure (Cameron *et al.* 2006), developmental stages (Hauke and Schreiber 1998) or growth conditions (Riederer and Schneider 1990). A study involving different plant species from different habitats indicated no correlation between the gravimetrically obtained wax quantity and efficacy of the transpiration barrier (Schreiber and Riederer 1996). In the present work, chemical analyses of cuticular waxes of a wide range of plant species, including tropical (*Vanilla planifolia*), temperate (*Juglans regia*) and Mediterranean (*Olea europaea*) plant species, were proposed to enable new insights allowing to deduce a potential relation between chemistry and function of plant cuticles.

2 Results

2.1 Minimum conductance and cuticular permeance

The minimum conductances (g_{\min}) were obtained from leaf drying curves (*Solanum lycopersicum*, *Solanum surratense*) and the cuticular permeances (P) by sealing the stomatous leaf surface (*Vanilla planifolia*, *Prunus laurocerasus*, *Olea europaea*) and by measuring isolated cuticular membranes in transpiration chambers (*Juglans regia*). The cuticular water permeabilities range between $0.13 \pm 0.03 \cdot 10^{-5} \text{ m s}^{-1}$ (*Vanilla planifolia*) and $11.54 \pm 2.04 \cdot 10^{-5} \text{ m s}^{-1}$ (*Solanum surratense*, Table 23).

Table 23. Leaf minimum conductance (g_{\min}) and cuticular permeance (P) at 25 °C (mean value \pm SD, n = 9 - 23).

plant species (family)		g_{\min} or P $\cdot 10^5$ (m s^{-1})		
<i>Solanum lycopersicum</i> (Solanaceae)	g_{\min}	3.31	\pm	0.78
<i>Solanum surratense</i> (Solanaceae)	g_{\min}	11.54	\pm	2.04
<i>Vanilla planifolia</i> (Orchidaceae)	P	0.13	\pm	0.03
<i>Juglans regia</i> (Juglandaceae)	P	4.25	\pm	2.17
<i>Prunus laurocerasus</i> (Rosaceae)	P	1.04	\pm	0.37
<i>Olea europaea</i> (Oleaceae)	P	2.11	\pm	1.18

2.2 Chemical analysis of the cuticular leaf wax

2.2.1 Cuticular leaf wax from *Solanum lycopersicum*

The cuticular waxes were analysed quantitatively by gas chromatograph equipped with a flame ionisation detector and the qualitative analysis by gas chromatograph equipped with a mass spectrometric detector. Total cuticular leaf wax coverage of *Solanum lycopersicum* was $3.90 \pm 0.77 \mu\text{g cm}^{-2}$ (mean value \pm SD, $n = 5$). The leaf wax composed of a major portion of very-long-chain acyclic component classes (81.3%, $3.17 \pm 0.63 \mu\text{g cm}^{-2}$) and a minor portion of cyclic components (12.1%, $0.47 \pm 0.02 \mu\text{g cm}^{-2}$).

N-alkanes were the most prominent acyclic component class (52.8%, $2.06 \pm 0.35 \mu\text{g cm}^{-2}$), followed by branched alkanes (21.8%, $0.85 \pm 0.10 \mu\text{g cm}^{-2}$). Additional component classes detected in the cuticular wax were primary alkanols, alkanolic acids and alkyl esters. Carbon chain lengths ranged from C_{20} to C_{50} , the most abundant chain lengths were C_{31} , C_{32} and C_{33} (Figure 47). *N*-hentriacontane dominated the acyclic components (33.1%, $1.29 \pm 0.19 \mu\text{g cm}^{-2}$). The average carbon chain length (ACL) of the very-long-chain acyclic wax components was 31.48.

The main cyclic component was lupeol with a cuticular wax coverage of $0.19 \pm 0.05 \mu\text{g cm}^{-2}$ (4.9%), followed by β -amyrin (3.1%, $0.12 \pm 0.04 \mu\text{g cm}^{-2}$; Table 24).

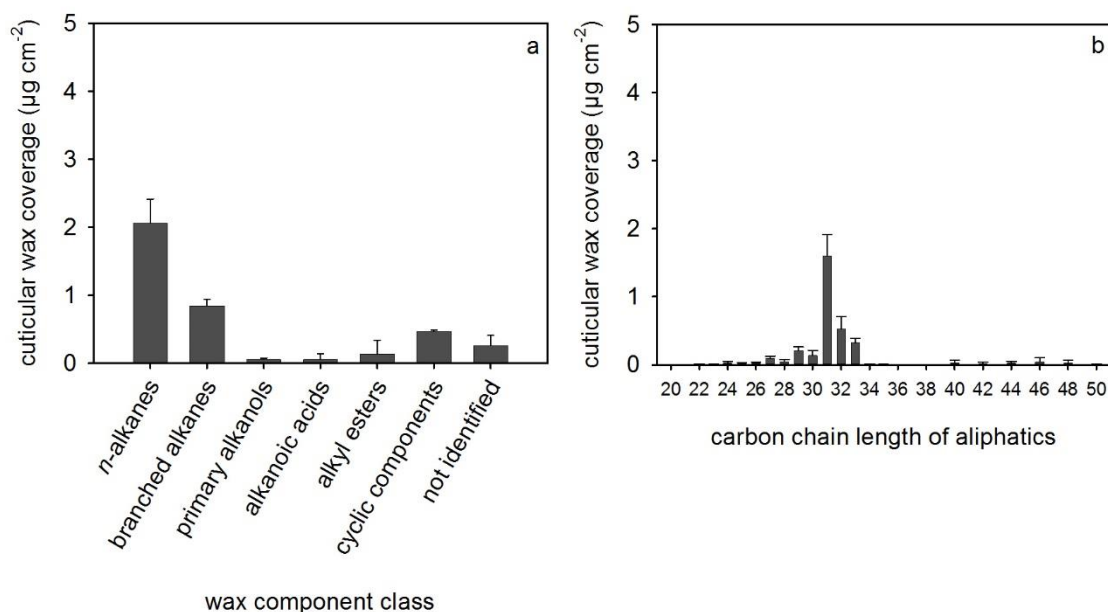


Figure 47. Cuticular wax composition of *Solanum lycopersicum* leaves. (a) Cuticular wax coverage arranged according to the component classes and (b) the carbon chain length distribution of the acyclic components (mean value \pm SD, $n = 5$).

Table 24. The cuticular wax coverage and components of *Solanum lycopersicum* leaves (mean value \pm SD, n = 5).

	carbon chain length	wax coverage ($\mu\text{g cm}^{-2}$)		
<i>n</i> -alkanes	25	0.02	\pm	0.01
	26	0.01	\pm	0.00
	27	0.09	\pm	0.04
	28	0.03	\pm	0.02
	29	0.18	\pm	0.05
	30	0.06	\pm	0.01
	31	1.29	\pm	0.19
	32	0.12	\pm	0.02
	33	0.25	\pm	0.09
	34	0.01	\pm	0.00
<i>iso</i> - and <i>anteiso</i> -alkanes	35	0.01	\pm	0.00
	28	traces		
	29	0.02	\pm	0.01
	30	0.06	\pm	0.06
	31	0.31	\pm	0.15
primary alkanols	32	0.39	\pm	0.20
	33	0.07	\pm	0.02
	20	0.00	\pm	0.00
	22	0.00	\pm	0.00
	24	0.00	\pm	0.00
	25	0.00	\pm	0.00
	26	0.01	\pm	0.00
	27	0.00	\pm	0.00
	28	0.01	\pm	0.00
	29	traces		
	30	0.01	\pm	0.00
	31	0.00	\pm	0.00
	32	0.01	\pm	0.01
	33	0.00	\pm	0.00
	34	0.00	\pm	0.00
alkanoic acids	20	0.00	\pm	0.00
	21-26,28,30,31,32	traces		
alkyl esters	38	0.00	\pm	0.00
	40,42,44,46,48,50	traces		
sum acyclic components (81.3%)		3.17	\pm	0.63
α -amyrin		0.05	\pm	0.01
β -amyrin		0.12	\pm	0.04
δ -amyrin		0.09	\pm	0.01
lupeol		0.19	\pm	0.05
β -sitosterol		0.02	\pm	0.02
stigmasterol		0.00	\pm	0.00
cholesterol		0.00	\pm	0.00

(continued)

	carbon chain length	wax coverage ($\mu\text{g cm}^{-2}$)	
sum cyclic components (12.1%)		0.47	± 0.02
not identified		0.26	± 0.15
sum acyclic, cyclic and not identified cuticular wax components (100.0%)		3.90	± 0.77

2.2.2 Cuticular leaf wax from *Solanum surratense*

Total cuticular leaf wax coverage of *Solanum surratense* was $7.41 \pm 1.21 \mu\text{g cm}^{-2}$ (mean value \pm SD, $n = 5$). The leaf wax composed of a major portion of very-long-chain acyclic component classes (76.1%, $5.64 \pm 1.05 \mu\text{g cm}^{-2}$) and a minor portion of cyclic components (7.0%, $0.52 \pm 0.17 \mu\text{g cm}^{-2}$).

N-alkanes were the most prominent acyclic component class (57.8%, $4.28 \pm 0.70 \mu\text{g cm}^{-2}$), followed by alkyl esters (6.7%, $0.50 \pm 0.42 \mu\text{g cm}^{-2}$) and alkanolic acids (4.7%, $0.35 \pm 0.11 \mu\text{g cm}^{-2}$). Additional component classes detected in the cuticular wax were branched alkanes and primary alkanols. Carbon chain lengths ranged from C_{20} to C_{50} , the most abundant chain lengths were C_{31} , C_{32} and C_{33} (Figure 48). *N*-hentriacontane (8.5%, $0.63 \pm 0.15 \mu\text{g cm}^{-2}$) and *n*-tritriacontane (36.2%, $2.68 \pm 0.38 \mu\text{g cm}^{-2}$) dominated the acyclic components. The average carbon chain length (ACL) of the very-long-chain acyclic wax components was 33.09. In addition, minor fractions of phytosterols and phenyl methyl esters were detected (Table 25).

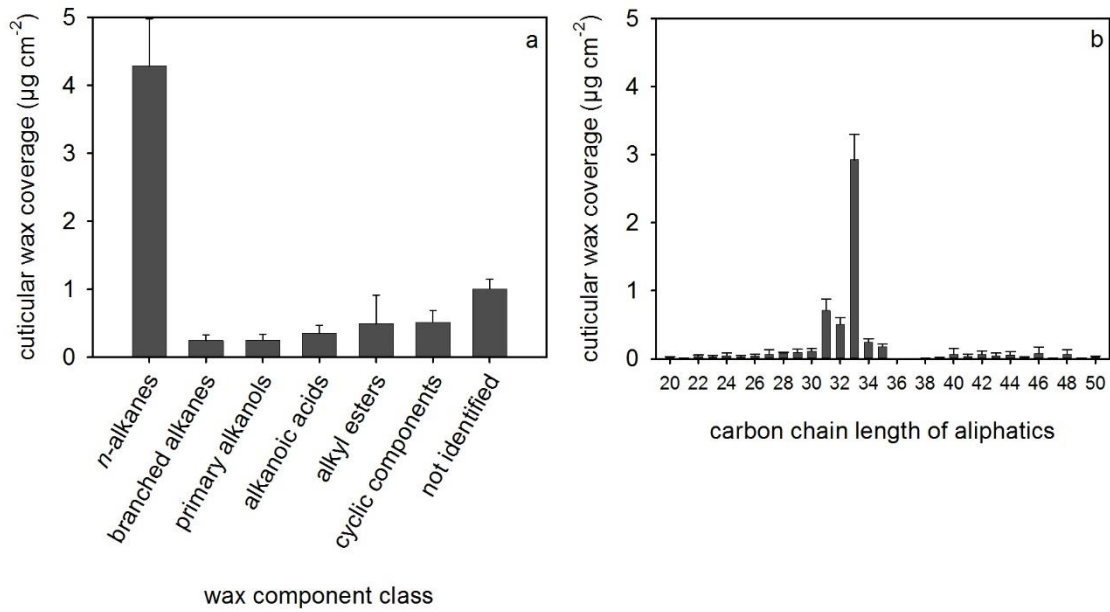


Figure 48. Cuticular wax composition of *Solanum surratense* leaves. (a) Cuticular wax coverage arranged according to the component classes and (b) the carbon chain length distribution of the acyclic components (mean value \pm SD, $n = 5$).

Table 25. The cuticular wax coverage and components of *Solanum surratense* leaves (mean value \pm SD, $n = 5$).

	carbon chain length	wax coverage (µg cm ⁻²)		
<i>n</i> -alkanes	23	0.02	\pm	0.01
	25	0.02	\pm	0.02
	26	0.01	\pm	0.00
	27	traces		
	28	0.01	\pm	0.00
	29	0.08	\pm	0.05
	30	0.04	\pm	0.02
	31	0.63	\pm	0.15
	32	0.37	\pm	0.09
	33	2.68	\pm	0.38
	34	0.19	\pm	0.04
<i>iso</i> - and <i>anteiso</i> -alkanes	29	traces		
	31	0.02	\pm	0.01
	32	0.02	\pm	0.00
primary alkanols	33	0.20	\pm	0.09
	20	0.01	\pm	0.00
	22	0.03	\pm	0.01
	23	traces		
	24	0.01	\pm	0.01

(continued)

	carbon chain length	wax coverage ($\mu\text{g cm}^{-2}$)		
primary alkanols	26	0.01	±	0.01
	28	0.03	±	0.01
	30	0.03	±	0.02
	31	0.05	±	0.01
	32	0.05	±	0.02
	33	0.03	±	0.01
	34	0.02	±	0.00
alkanoic acids	20	0.02	±	0.00
	21	0.01	±	0.00
	22,23	0.01	±	0.01
	24	0.04	±	0.04
	25	0.01	±	0.00
	26	0.02	±	0.01
	27	0.01	±	0.00
	28	0.04	±	0.02
	29	0.01	±	0.00
	30	0.04	±	0.01
	31	0.01	±	0.01
	32	0.07	±	0.02
	33	0.01	±	0.00
	34	0.04	±	0.02
alkyl esters	38	0.01	±	0.00
	39,40	traces		
	41	0.04	±	0.03
	42	0.06	±	0.05
	43	0.05	±	0.04
	44	0.06	±	0.05
	45,46,47,48,49,50	traces		
sum acyclic components (76.1%)		5.64	±	1.05
β-sitosterol		0.15	±	0.04
stigmasterol		0.34	±	0.13
cholesterol		0.01	±	0.00
campesterol		0.02	±	0.01
sum cyclic components (7.0%)		0.52	±	0.17
phenyl methyl esters	30	0.07	±	0.03
	31	0.02	±	0.00
	32	0.10	±	0.02
	33	0.02	±	0.00
	34	0.04	±	0.01
not identified		1.01	±	0.14
sum acyclic, cyclic and not identified cuticular wax components (100.0%)		7.41	±	1.21

2.2.3 Cuticular leaf wax from *Vanilla planifolia*

Total cuticular adaxial leaf wax coverage of *Vanilla planifolia* was $45.79 \pm 6.87 \mu\text{g cm}^{-2}$ (mean value \pm SD, $n = 4$). The leaf wax composed of a major portion of very-long-chain acyclic component classes (81.1%, $37.12 \pm 6.37 \mu\text{g cm}^{-2}$) and a minor portion of cyclic components (5.0%, $2.30 \pm 0.50 \mu\text{g cm}^{-2}$).

Primary alkanols were the most prominent acyclic component class (32.6%, $14.91 \pm 2.18 \mu\text{g cm}^{-2}$), followed by *n*-alkanes (21.3%, $9.75 \pm 1.69 \mu\text{g cm}^{-2}$) and alkanolic acids (17.0%, $7.77 \pm 1.53 \mu\text{g cm}^{-2}$). Additional component classes detected in the cuticular wax were branched alkanes, secondary alkanols, alkanol acetates, alkanals and alkyl esters. Carbon chain lengths ranged from C₂₀ to C₅₄, the most abundant chain lengths were C₃₀, C₃₁ and C₃₂ (Figure 49). *N*-hentriacontane (8.6%, $3.92 \pm 0.78 \mu\text{g cm}^{-2}$) and dotriacontanoic acid (21.6%, $9.87 \pm 1.39 \mu\text{g cm}^{-2}$) dominated the acyclic components. The average carbon chain length (ACL) of the very-long-chain acyclic wax components was 31.57.

The main cyclic component was δ -tocopherol with a cuticular wax coverage of $1.45 \pm 0.22 \mu\text{g cm}^{-2}$ (3.2%). In addition, a minor fraction of coumaric acid esters was detected (Table 26).

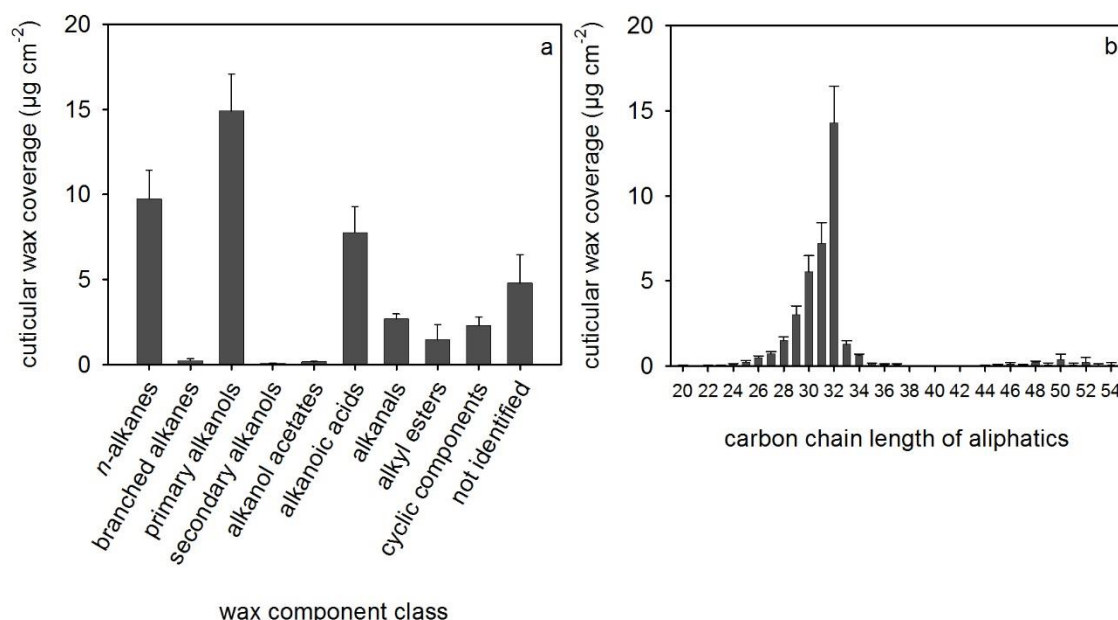


Figure 49. Adaxial cuticular wax composition of *Vanilla planifolia* leaves. (a) Cuticular wax coverage arranged according to the component classes and (b) the carbon chain length distribution of the acyclic components (mean value \pm SD, $n = 4$).

Table 26. The cuticular wax coverage and components of isolated adaxial cuticular membranes of *Vanilla planifolia* leaves (mean value \pm SD, n = 4).

		carbon chain length	wax coverage ($\mu\text{g cm}^{-2}$)		
<i>n</i> -alkanes		25	0.19	\pm	0.07
		26	0.15	\pm	0.03
		27	0.56	\pm	0.10
		28	0.36	\pm	0.06
		29	2.21	\pm	0.38
		30	1.24	\pm	0.24
		31	3.92	\pm	0.78
		32	0.31	\pm	0.05
		33	0.32	\pm	0.07
		34	0.16	\pm	0.06
		35	0.15	\pm	0.05
		36	0.10	\pm	0.03
		37	0.08	\pm	0.06
<i>iso</i> - and <i>anteiso</i> -alkanes		32	0.13	\pm	0.06
		34	0.12	\pm	0.10
primary alkanols		22	0.01	\pm	0.00
		23	0.01	\pm	0.01
		24	0.02	\pm	0.00
		25	0.02	\pm	0.01
		26	0.06	\pm	0.00
		27	0.03	\pm	0.01
		28	0.20	\pm	0.04
		29	0.23	\pm	0.05
		30	1.67	\pm	0.30
		31	1.58	\pm	0.26
		32	9.87	\pm	1.39
		33	0.84	\pm	0.13
	34	0.35	\pm	0.06	
secondary alkanols	pos. 2	29	0.02	\pm	0.00
	pos. 2	31	0.07	\pm	0.02
alkanol acetates		26	0.01	\pm	0.01
		27	0.02	\pm	0.00
		28	0.05	\pm	0.01
		29	0.03	\pm	0.02
		30	0.07	\pm	0.01
alkanoic acids		20	0.06	\pm	0.01
		21	0.01	\pm	0.01
		22	0.05	\pm	0.02
		23	0.05	\pm	0.01
		24	0.12	\pm	0.03
		25	0.04	\pm	0.01
		26	0.28	\pm	0.05
	27	0.12	\pm	0.03	

(continued)

	carbon chain length	wax coverage ($\mu\text{g cm}^{-2}$)		
alkanoic acids	28	0.88	±	0.14
	29	0.47	±	0.11
	30	2.14	±	0.41
	31	1.06	±	0.24
	32	2.37	±	0.55
	33	0.12	±	0.07
	34	traces		
alkanals	26	0.02	±	0.01
	28	0.03	±	0.02
	29	0.07	±	0.05
	30	0.43	±	0.07
	31	0.57	±	0.08
	32	1.59	±	0.18
alkyl esters	44	traces		
	45	0.06	±	0.06
	46	0.14	±	0.06
	47	0.09	±	0.02
	48	0.23	±	0.07
	49	traces		
	50	0.40	±	0.30
51,52,53,54		traces		
sum acyclic components (81.1%)		37.12	±	6.37
δ-tocopherol		1.45	±	0.22
γ-tocopherol		0.09	±	0.06
β-sitosterol		0.58	±	0.15
stigmasterol		traces		
cholesterol		0.05	±	0.05
sum cyclic components (5.0%)		2.30	±	0.50
coumaric acid esters	28	0.06	±	0.02
	29	0.07	±	0.06
	30	0.40	±	0.09
	31	0.42	±	0.07
	32	0.60	±	0.15
not identified		4.81	±	1.64
sum acyclic, cyclic and not identified cuticular wax components (100.0%)		45.79	±	6.87

2.2.4 Cuticular leaf wax from *Juglans regia*

Total cuticular adaxial leaf wax coverage of *Juglans regia* was $29.63 \pm 2.59 \mu\text{g cm}^{-2}$ (mean value \pm SD, $n = 5$). The leaf wax composed of a major portion of very-long-chain acyclic component classes (90.3%, $26.75 \pm 2.30 \mu\text{g cm}^{-2}$) and a minor portion of cyclic components (2.2%, $0.64 \pm 0.49 \mu\text{g cm}^{-2}$).

Primary alkanols were the most prominent component class (68.1%, $20.18 \pm 2.43 \mu\text{g cm}^{-2}$), followed by alkyl esters (13.3%, $3.93 \pm 0.78 \mu\text{g cm}^{-2}$) and alkanolic acids (4.5%, $1.33 \pm 0.26 \mu\text{g cm}^{-2}$). Additional component classes detected in the cuticular wax were *n*-alkanes, alkanals and methyl esters. Carbon chain lengths ranged from C₂₀ to C₅₄, the most abundant chain lengths were C₂₄, C₂₆ and C₂₈ (Figure 50). Tetracosanol (12.2%, $3.59 \pm 0.77 \mu\text{g cm}^{-2}$) and hexacosanol (38.0%, $11.26 \pm 1.69 \mu\text{g cm}^{-2}$) dominated the acyclic components. The average carbon chain length (ACL) of the very-long-chain acyclic wax components was 29.28.

The main cyclic component was α -amyrin with a cuticular wax coverage of $0.30 \pm 0.23 \mu\text{g cm}^{-2}$ (1.0%; Table 27).

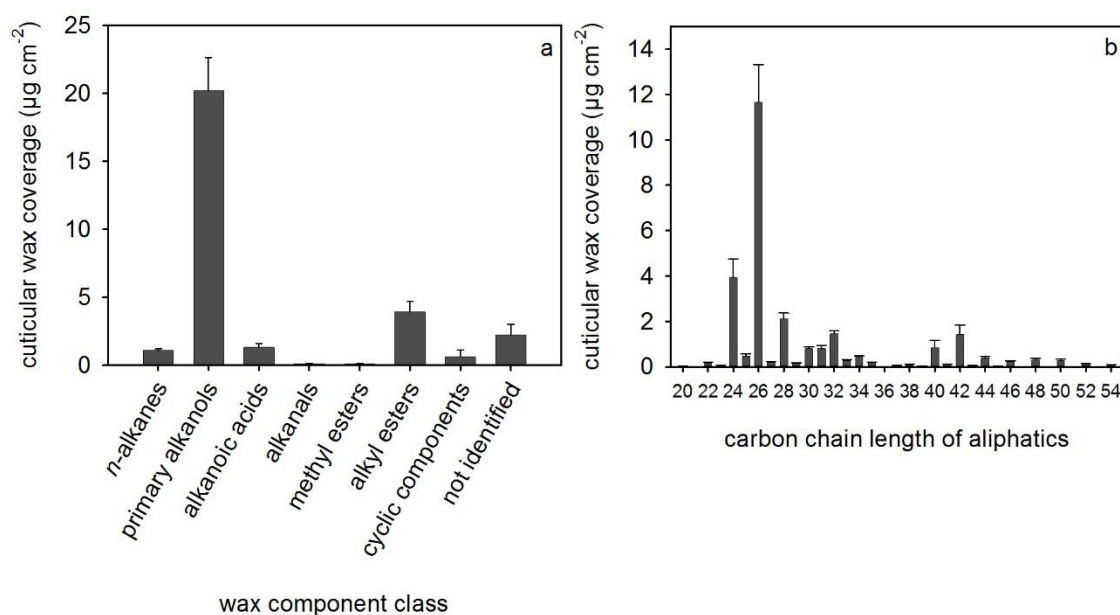


Figure 50. Adaxial cuticular wax composition of *Juglans regia* leaves. (a) Cuticular wax coverage arranged according to the component classes and (b) the carbon chain length distribution of the acyclic components (mean value \pm SD, $n = 5$).

Table 27. The cuticular wax coverage and components of isolated adaxial cuticular membranes of *Juglans regia* leaves (mean value \pm SD, n = 5).

	carbon chain length	wax coverage ($\mu\text{g cm}^{-2}$)		
<i>n</i> -alkanes	25	0.03	\pm	0.02
	26	0.02	\pm	0.01
	27	0.05	\pm	0.02
	28	0.03	\pm	0.02
	29	0.08	\pm	0.02
	31	0.41	\pm	0.11
	32	0.09	\pm	0.02
	33	0.15	\pm	0.02
	35	0.18	\pm	0.03
	37	0.05	\pm	0.01
primary alkanols	22	0.07	\pm	0.03
	23	0.02	\pm	0.01
	24	3.59	\pm	0.77
	25	0.38	\pm	0.05
	26	11.26	\pm	1.69
	27	0.13	\pm	0.02
	28	1.98	\pm	0.29
	29	0.05	\pm	0.01
	30	0.76	\pm	0.07
	31	0.31	\pm	0.18
	32	1.11	\pm	0.09
	33	0.11	\pm	0.03
	34	0.41	\pm	0.03
	alkanoic acids	20	0.03	\pm
21		0.01	\pm	0.00
22		0.09	\pm	0.02
23		0.03	\pm	0.02
24		0.31	\pm	0.06
25		0.07	\pm	0.03
26		0.22	\pm	0.03
27		0.02	\pm	0.01
28		0.08	\pm	0.02
29		0.01	\pm	0.00
30		0.04	\pm	0.01
31		0.08	\pm	0.02
32		0.27	\pm	0.05
33		0.02	\pm	0.00
34	0.07	\pm	0.01	
alkanals	26	0.08	\pm	0.04
	28	0.02	\pm	0.01
methyl esters	24	0.05	\pm	0.02
	26	0.07	\pm	0.02

(continued)

	carbon chain length	wax coverage ($\mu\text{g cm}^{-2}$)		
alkyl esters	38	0.09	±	0.02
	39	0.02	±	0.00
	40	0.84	±	0.33
	41	0.10	±	0.02
	42	1.43	±	0.42
	43	0.05	±	0.01
	44	0.38	±	0.06
	45	0.02	±	0.01
	46	0.23	±	0.04
	48	0.29	±	0.07
	50	0.27	±	0.08
	52	0.13	±	0.02
54	0.07	±	0.01	
sum acyclic components (90.3%)		26.75	±	2.30
α -amyrin		0.30	±	0.23
lupeol		0.03	±	0.02
β -sitosterol		0.31	±	0.25
sum cyclic components (2.2%)		0.64	±	0.49
not identified		2.24	±	0.79
sum acyclic, cyclic and not identified cuticular wax components (100.0%)		29.63	±	2.59

2.2.5 Cuticular leaf wax from *Prunus laurocerasus*

Total cuticular adaxial leaf wax coverage of *Prunus laurocerasus* was $107.50 \pm 6.52 \mu\text{g cm}^{-2}$ (mean value \pm SD, $n = 6$). The leaf wax composed of a major portion of cyclic components (66.3%, $71.24 \pm 4.14 \mu\text{g cm}^{-2}$) and a minor portion of very-long-chain acyclic component classes (22.8%, $24.51 \pm 3.17 \mu\text{g cm}^{-2}$).

N-alkanes were the most prominent component class (14.2%, $15.26 \pm 2.28 \mu\text{g cm}^{-2}$), followed by alkanolic acids (5.6%, $6.00 \pm 1.65 \mu\text{g cm}^{-2}$) and primary and secondary alkanols (1.9%, $2.05 \pm 0.34 \mu\text{g cm}^{-2}$). Additional component classes detected in the cuticular wax were alkyl esters, alkanals and alkanol acetates. Carbon chain lengths ranged from C_{20} to C_{48} , the most abundant chain lengths were C_{29} , C_{30} and C_{31} (Figure 51). *N*-nonacosane (7.3%, $7.86 \pm 1.19 \mu\text{g cm}^{-2}$), triacontanoic acid (2.3%, $2.51 \pm 0.70 \mu\text{g cm}^{-2}$) and *n*-hentriacontane (4.9%, $5.27 \pm 0.86 \mu\text{g cm}^{-2}$) dominated the acyclic components. The average carbon chain length (ACL) of the very-long-chain acyclic wax components was 29.98.

The main cyclic component was ursolic acid with a cuticular wax coverage of $57.44 \pm 3.19 \mu\text{g cm}^{-2}$ (53.4%), followed by oleanolic acid (8.7% , $9.33 \pm 0.53 \mu\text{g cm}^{-2}$; Table 28).

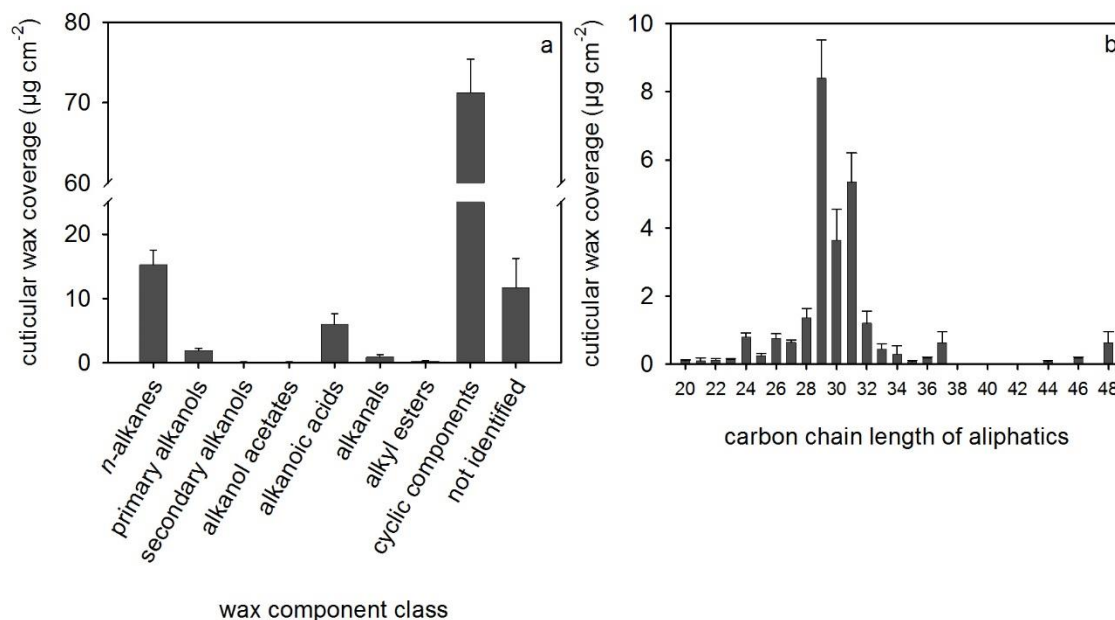


Figure 51. Adaxial cuticular wax composition of *Prunus laurocerasus* leaves. (a) Cuticular wax coverage arranged according to the component classes and (b) the carbon chain length distribution of the acyclic components (mean value \pm SD, $n = 6$).

Table 28. The cuticular wax coverage and components of isolated adaxial cuticular membranes of *Prunus laurocerasus* leaves (mean value \pm SD, $n = 6$).

	carbon chain length	wax coverage ($\mu\text{g cm}^{-2}$)		
<i>n</i> -alkanes	22	0.01	\pm	0.01
	23	0.08	\pm	0.04
	25	0.11	\pm	0.04
	26	0.08	\pm	0.02
	27	0.46	\pm	0.07
	28	0.27	\pm	0.04
	29	7.86	\pm	1.19
	30	0.51	\pm	0.08
	31	5.27	\pm	0.86
	32	0.17	\pm	0.05
	33	0.45	\pm	0.16
primary alkanols	21	traces		
	22	0.03	\pm	0.03
	23	0.01	\pm	0.01
	24	0.25	\pm	0.06
	25	0.05	\pm	0.03

(continued)

		carbon chain length	wax coverage ($\mu\text{g cm}^{-2}$)		
primary alkanols		26	0.43	±	0.06
		27	0.06	±	0.02
		28	0.38	±	0.05
		29	0.13	±	0.02
		30	0.43	±	0.11
		31	0.01	±	0.01
		34	traces		
secondary alkanols	pos. 2	29	0.05	±	0.02
	pos. 2	31	0.06	±	0.02
alkanol acetates		28	0.07	±	0.02
		30	0.04	±	0.02
alkanoic acids		20	0.10	±	0.03
		21	0.04	±	0.03
		22	0.08	±	0.02
		23	0.06	±	0.03
		24	0.56	±	0.10
		25	0.09	±	0.02
		26	0.25	±	0.11
		27	0.12	±	0.05
		28	0.66	±	0.20
		29	0.30	±	0.11
		30	2.51	±	0.70
		32	1.03	±	0.33
		34	0.18	±	0.13
alkanals		29	traces		
		30	0.15	±	0.08
alkyl esters		44	0.07	±	0.04
		46	0.18	±	0.04
		48	0.64	±	0.33
sum acyclic components (22.8%)			24.51	±	3.17
α -amyrin			0.10	±	0.02
taraxerol			0.57	±	0.10
erythrodiol			0.16	±	0.03
uvaol			0.80	±	0.14
oleanolic acid			9.33	±	0.53
betulinic acid			0.83	±	0.37
ursolic acid			57.44	±	3.19
hederagenin			2.01	±	0.48
β -sitosterol			0.02	±	0.04
sum cyclic components (66.3%)			71.24	±	4.14
not identified			11.73	±	4.52
sum acyclic, cyclic and not identified cuticular wax components (100.0%)			107.50	±	6.52

2.2.6 Cuticular leaf wax from *Olea europaea*

Total cuticular adaxial leaf wax coverage of *Olea europaea* was $320.41 \pm 39.54 \mu\text{g cm}^{-2}$ (mean value \pm SD, $n = 6$). The leaf wax composed of a major portion of cyclic components (83.4%, $267.11 \pm 39.22 \mu\text{g cm}^{-2}$) and a minor portion of very-long-chain acyclic component classes (3.4%, $10.86 \pm 3.51 \mu\text{g cm}^{-2}$).

N-alkanes were the most prominent component class (2.6%, $8.47 \pm 2.95 \mu\text{g cm}^{-2}$), followed by alkanolic acids (0.7%, $2.14 \pm 0.64 \mu\text{g cm}^{-2}$) and primary alkanols (0.1%, $0.25 \pm 0.05 \mu\text{g cm}^{-2}$). Carbon chain lengths ranged from C_{20} to C_{33} , the most abundant chain lengths were C_{28} , C_{31} and C_{33} (Figure 52). *N*-hentriacontane (0.8%, $2.71 \pm 0.97 \mu\text{g cm}^{-2}$) and *n*-tritriacontane (1.1%, $3.49 \pm 1.60 \mu\text{g cm}^{-2}$) dominated the acyclic components. The average carbon chain length (ACL) of the very-long-chain acyclic wax components was 30.31.

The main cyclic component was oleanolic acid with a cuticular wax coverage of $191.92 \pm 45.63 \mu\text{g cm}^{-2}$ (59.9%), followed by ursolic acid (8.9%, $28.50 \pm 2.85 \mu\text{g cm}^{-2}$; Table 29).

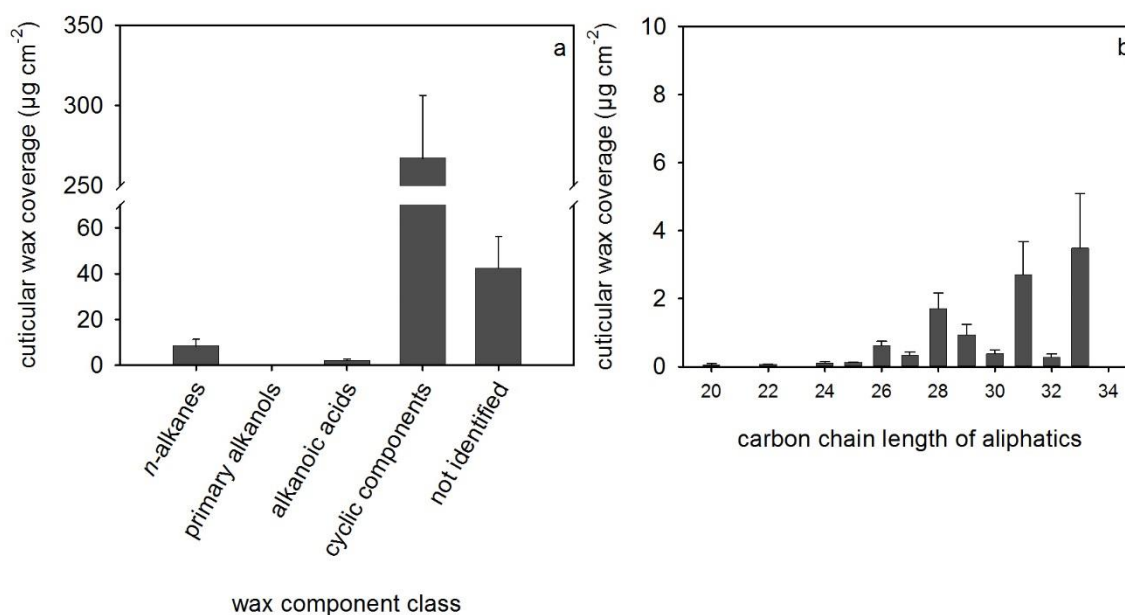


Figure 52. Adaxial cuticular wax composition of *Olea europaea* leaves. (a) Cuticular wax coverage arranged according to the component classes and (b) the carbon chain length distribution of the acyclic components (mean value \pm SD, $n = 6$).

Table 29. The cuticular wax coverage and components of isolated adaxial cuticular membranes of *Olea europaea* leaves (mean value \pm SD, n = 6).

	carbon chain length	wax coverage ($\mu\text{g cm}^{-2}$)		
<i>n</i> -alkanes	26	0.13	\pm	0.05
	27	0.24	\pm	0.05
	28	0.27	\pm	0.05
	29	0.94	\pm	0.31
	30	0.39	\pm	0.11
	31	2.71	\pm	0.97
	32	0.28	\pm	0.09
	33	3.49	\pm	1.60
primary alkanols	26	0.13	\pm	0.04
	28	0.12	\pm	0.04
alkanoic acids	20	0.06	\pm	0.04
	22	0.07	\pm	0.01
	24	0.12	\pm	0.03
	25	0.13	\pm	0.01
	26	0.35	\pm	0.14
	27	0.09	\pm	0.08
	28	1.32	\pm	0.40
sum acyclic components (3.4%)		10.86	\pm	3.51
β -amyrin		0.48	\pm	0.09
taraxerol		0.76	\pm	0.25
erythrodiol		20.15	\pm	7.01
uvaol		22.26	\pm	6.17
oleanolic acid		191.92	\pm	45.63
ursolic acid		28.50	\pm	2.85
hederagenin		3.05	\pm	0.53
sum cyclic components (83.4%)		267.11	\pm	39.22
not identified		42.43	\pm	13.79
sum acyclic, cyclic and not identified cuticular wax components (100.0%)		320.41	\pm	39.54

2.3 Cuticular wax chemistry and minimum or cuticular water permeability

In total 17 plant species were analysed concerning their leaf cuticular wax quantity and quality. The corresponding leaf minimum conductance or cuticular permeance was determined (Table 30). Total cuticular wax coverages ranged between $3.90 \mu\text{g cm}^{-2}$ (*Solanum lycopersicum*) and $336.93 \mu\text{g cm}^{-2}$ (*Nerium oleander*). Aliphatic cuticular wax quantities varied between $1.03 \mu\text{g cm}^{-2}$ (*Plantago lanceolata*) and $37.12 \mu\text{g cm}^{-2}$ (*Vanilla planifolia*). Average carbon chain lengths ranged between 28.52 (*Rhazya stricta*) and 41.15 (*Helianthemum apenninum*). Minimum conductances or cuticular permeances ranged between $0.13 \cdot 10^{-5} \text{ m s}^{-1}$ (*Vanilla planifolia*) and $11.54 \cdot 10^{-5} \text{ m s}^{-1}$ (*Solanum surratense*).

Minimum or cuticular water permeability was correlated with the cuticular wax chemistry to detect potential relationships. The water permeability did neither correlate with the total wax coverage nor with the cyclic wax coverage. However, the natural logarithm of the minimum conductances or cuticular permeances were significantly negatively correlated with the very-long-chain acyclic wax coverage (Figure 53).

Table 30. Total leaf wax coverage, very-long-chain acyclic wax coverage, leaf minimum conductances (g_{\min}) or cuticular permeances (P) and the natural logarithm of g_{\min} or P of the 17 plant species (mean value \pm SD).

plant species (family)	total wax coverage ($\mu\text{g cm}^{-2}$)	acyclic wax coverage ($\mu\text{g cm}^{-2}$)	g_{\min} (g) or P (P) $\cdot 10^5$ (m s^{-1})	In g_{\min} or In P
<i>Rhazya stricta</i> (Apocynaceae)	251.41 \pm 38.97	8.56 \pm 2.93	g 5.41 \pm 1.36	-9.82
<i>Nerium oleander</i> (Apocynaceae)	336.93 \pm 63.73	34.08 \pm 5.87	P 1.77 \pm 0.30	-10.94
<i>Hippocrepis comosa</i> (Fabaceae)	13.71 \pm 1.71	12.41 \pm 1.73	g 6.92 \pm 3.52	-9.58
<i>Helianthemum apenninum</i> (Cistaceae)	15.68 \pm 3.91	14.22 \pm 3.56	g 10.10 \pm 3.39	-9.20
<i>Geranium sanguineum</i> (Geraniaceae)	8.35 \pm 2.13	5.45 \pm 1.31	g 5.25 \pm 0.54	-9.85
<i>Sanguisorba minor</i> (Rosaceae)	23.26 \pm 4.31	18.77 \pm 3.12	g 7.30 \pm 1.77	-9.53
<i>Sesleria albicans</i> (Poaceae)	14.63 \pm 3.48	12.27 \pm 2.95	g 5.76 \pm 2.00	-9.76
<i>Pulsatilla vulgaris</i> (Ranunculaceae)	11.99 \pm 1.47	8.63 \pm 0.99	g 7.69 \pm 1.86	-9.47
<i>Teucrium chamaedrys</i> (Lamiaceae)	18.68 \pm 5.90	8.11 \pm 1.09	g 4.32 \pm 0.97	-10.05
<i>Salvia pratensis</i> (Lamiaceae, xerophytic)	39.43 \pm 17.70	3.65 \pm 1.51	g 8.21 \pm 1.72	-9.41
<i>Salvia pratensis</i> (Lamiaceae, mesophytic)	13.80 \pm 2.09	1.75 \pm 0.42	g 6.41 \pm 2.55	-9.66
<i>Plantago lanceolata</i> (Plantaginaceae)	4.15 \pm 0.83	1.03 \pm 0.15	g 9.35 \pm 2.30	-9.28
<i>Solanum lycopersicum</i> (Solanaceae)	3.90 \pm 0.77	3.17 \pm 0.63	g 3.31 \pm 0.78	-10.32
<i>Solanum surratense</i> (Solanaceae)	7.41 \pm 1.21	5.64 \pm 1.05	g 11.54 \pm 2.04	-9.07
<i>Vanilla planifolia</i> (Orchidaceae)	45.79 \pm 6.87	37.12 \pm 6.37	P 0.13 \pm 0.03	-13.55
<i>Juglans regia</i> (Juglandaceae)	29.63 \pm 2.59	26.75 \pm 2.30	P 4.25 \pm 2.17	-10.07
<i>Prunus laurocerasus</i> (Rosaceae)	107.50 \pm 6.52	24.51 \pm 3.17	P 1.04 \pm 0.37	-11.47
<i>Olea europaea</i> (Oleaceae)	320.41 \pm 39.54	10.86 \pm 3.51	P 2.11 \pm 1.18	-10.77

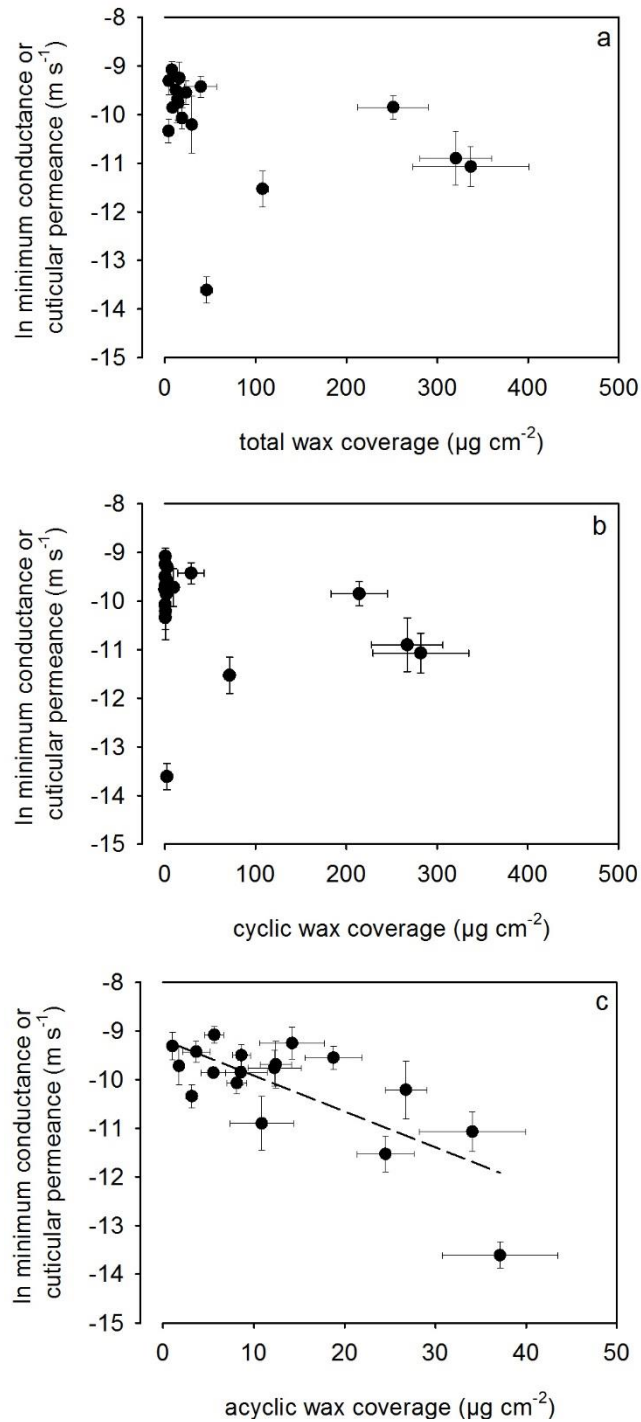


Figure 53. The natural logarithm of the minimum conductance or cuticular permeance as a function of (a) the total cuticular wax coverage, (b) the cyclic wax coverage and (c) the very-long-chain acyclic wax coverage ($r^2 = 0.546$; Pearson correlation coefficient (PCC) = -0.739 , $p < 0.001$).

The most dominant component classes of the very-long-chain acyclic components (*n*-alkanes, primary alkanols, alkanolic acids and alkyl esters) were separately correlated with the minimum or cuticular water permeability. The natural logarithm of the minimum conductance or cuticular permeance did neither correlate with the cuticular wax coverage of primary alkanols nor with the coverage of alkyl esters. The minimum or cuticular water permeability was significantly negatively correlated with the cuticular wax coverage of *n*-alkanes and the coverage of alkanolic acids (Figure 54).

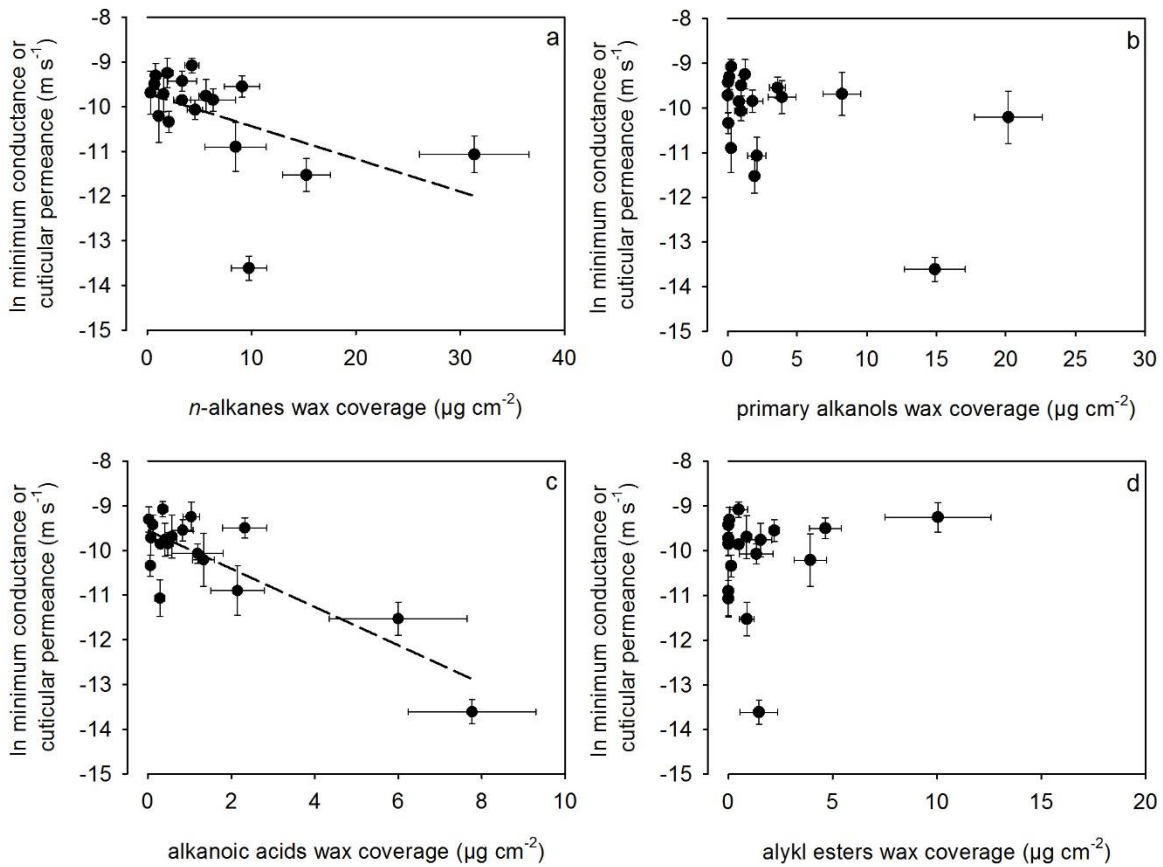


Figure 54. The natural logarithm of the minimum conductance or cuticular permeance as a function of cuticular wax coverage of the component classes (a) *n*-alkanes ($r^2 = 0.251$; PCC = -0.501, $p = 0.034$), (b) primary alkanols, (c) alkanolic acids ($r^2 = 0.703$; PCC = -0.839, $p < 0.001$) and (d) the alkyl esters.

The average carbon chain length (ACL) of aliphatics was calculated based on the wax amount coverage ($\mu\text{g cm}^{-2}$) and based on the molar wax coverage ($\mu\text{mol m}^{-2}$; Annex, Table 31). No correlation of ACL with the minimum or cuticular water permeability was detected. In addition, the ratio between average carbon chain length dispersion (ΔACL) and average carbon chain length ($\Delta\text{ACL ACL}^{-1}$) did not correlate with the natural logarithm of the minimum conductance or cuticular permeance (Figure 55). Due to the slight variance between ACL based on the wax amount coverage and based on the molar wax coverage, for further investigations ACL based on the wax amount coverage was used.

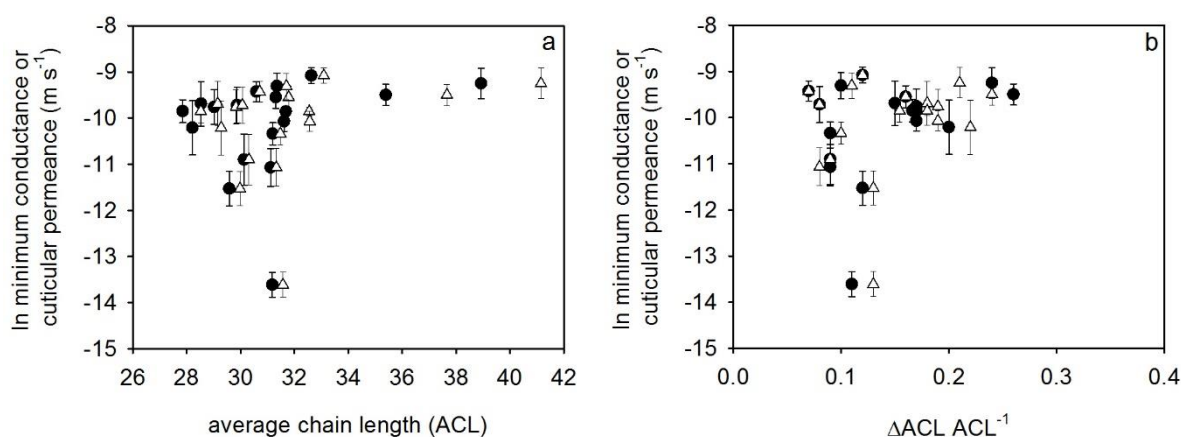


Figure 55. The natural logarithm of the minimum conductance or cuticular permeance as a function of (a) the average carbon chain length (ACL) and (b) the ratio between average carbon chain length dispersion (ΔACL) and average carbon chain length ($\Delta\text{ACL ACL}^{-1}$; molar wax coverage, ●; wax amount coverage, Δ).

The average carbon chain length (ACL) of aliphatics based on the wax amount coverage ($\mu\text{g cm}^{-2}$) and its relation to the minimum or cuticular water permeability was analysed in the low carbon chain length range ($\leq \text{C}_{37}$) and the high carbon chain length range ($\geq \text{C}_{38}$, alkyl esters in this study). The ACL of aliphatic components with carbon chain lengths of C_{38} and higher appeared to significantly negatively correlate with the natural logarithm of the minimum conductance or cuticular permeance. However, excluding the extreme cuticular permeance value of *Vanilla planifolia* proved a non-significant correlation. No relationship between the ratio $\Delta\text{ACL ACL}^{-1}$ and the minimum or cuticular water permeability was calculated (Figure 56).

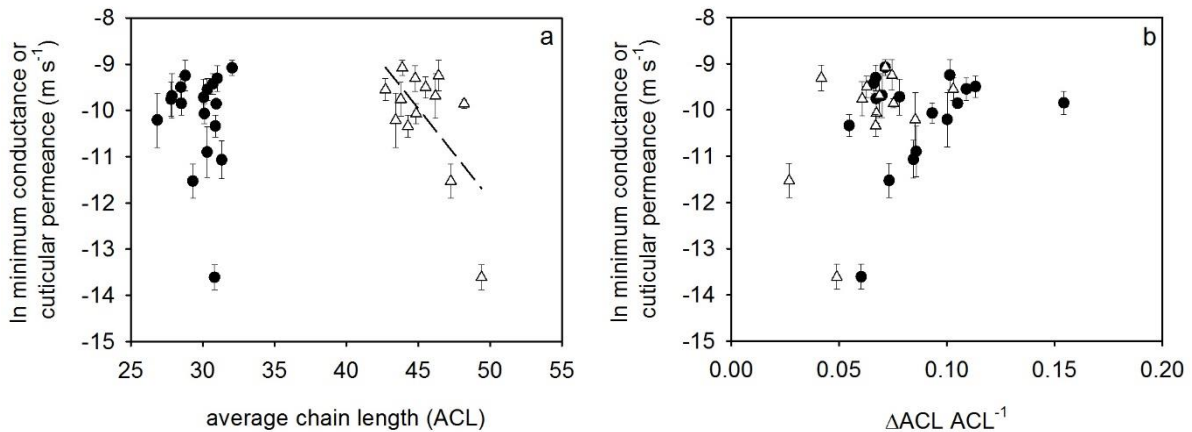


Figure 56. The natural logarithm of the minimum conductance or cuticular permeance as a function of (a) the average carbon chain length (ACL) and (b) the ratio between average carbon chain length dispersion (ΔACL) and average carbon chain length ($\Delta ACL \text{ ACL}^{-1}$; $\leq C_{37}$, ●; $\geq C_{38}$, Δ). A significant negative correlation between the minimum or cuticular water permeability and the ACL ($\geq C_{38}$) was calculated ($r^2 = 0.403$; PCC = -0.634, $p = 0.020$). However, without the extreme value the relationship was not significant (PCC = -0.289, $p = 0.362$).

3 Discussion

3.1 Classification of the minimum conductance and the cuticular permeance

The minimum conductance and cuticular permeance of leaves ranged between $0.13 \cdot 10^{-5} \text{ m s}^{-1}$ (*Vanilla planifolia*) and $11.54 \cdot 10^{-5} \text{ m s}^{-1}$ (*Solanum surratense*; Table 30). In comparison, a wide literature survey of cuticular permeances from astomatous leaf cuticles of 57 plant species indicated a range between $0.04 \cdot 10^{-5} \text{ m s}^{-1}$ and $14.40 \cdot 10^{-5} \text{ m s}^{-1}$ (Riederer and Schreiber 2001). In the present study, minimum conductances (stomatous leaves) and cuticular permeances (astomatous leaf surface) were within the range of literature values and, thus, intact stomatous leaves were considered as appropriate measurement systems. In addition, for leaves of *Acer campestre*, *Fagus sylvatica*, *Quercus petraea*, *Ilex aquifolium*, *Teucrium chamaedrys* (Burghardt and Riederer 2003, Burghardt *et al.* 2008) and *Nerium oleander* (Chapter II) the residual stomatal transpiration after complete stomatal closure was negligible. Currently, only one plant species, *Hedera helix*, is described to have a significantly higher minimum conductance than cuticular permeance due to residual stomatal transpiration (Burghardt and Riederer 2003). However, potential residual stomatal transpiration due to incomplete stomatal closure cannot be excluded when measuring the minimum water permeability of stomatous leaves. Wherever applicable the abaxial, stomatous leaf surface was sealed and/or isolated, astomatous cuticles were used to determine the cuticular permeance of hypostomatic leaves.

The lowest cuticular water permeabilities are described for evergreen leaves from epiphytic or climbing plants naturally growing in tropical climates (Schreiber and Riederer 1996, Helbsing *et al.* 2001, Riederer and Schreiber 2001). This observation can be confirmed with the cuticular permeance of *Vanilla planifolia*. The measured value ($0.13 \cdot 10^{-5} \text{ m s}^{-1}$; Table 23) was 1.6-fold and 3.3-fold higher than literature data (Schreiber and Riederer 1996, Riederer and Schreiber 2001). The isolated cuticular membranes of *Juglans regia* had a cuticular permeance of $4.25 \cdot 10^{-5} \text{ m s}^{-1}$ (Table 23). *Juglans regia* leaves with comparable values of minimum conductance and cuticular permeance have been reported ($3.5 \cdot 10^{-5} \text{ m s}^{-1}$; Burghardt and Riederer 2006). The reported and measured cuticular permeances of *Juglans regia* and *Prunus laurocerasus* leaves are in the same order of magnitude (Schreiber and Riederer 1996, Schreiber 2001). The cuticular permeance of *Olea europaea* leaves was 3.8-fold higher than the literature value ($0.55 \cdot 10^{-5} \text{ m s}^{-1}$; Schreiber and Riederer 1996).

3.2 Chemistry of the plant cuticle

Cuticular wax coverages of leaves ranged between $3.90 \mu\text{g cm}^{-2}$ (*Solanum lycopersicum*) and $320.41 \mu\text{g cm}^{-2}$ (*Olea europaea*). Common component classes, such as *n*-alkanes, primary alkanols, alkanolic acids, alkanals and alkyl esters, composed the cuticular waxes. Additional very-long-chain aliphatic component classes were branched alkanes, secondary alkanols, methyl esters and alkanol acetates. Carbon chain lengths of the aliphatic constituents ranged from C₂₀ to C₅₄ and are ubiquitously found (Jetter *et al.* 2006).

Solanum lycopersicum leaf cuticular wax coverage was $3.90 \mu\text{g cm}^{-2}$. *N*-alkanes, branched alkanes and triterpenoids established the major component classes (Figure 47). In literature leaf wax coverages of $3.50 \mu\text{g cm}^{-2}$ and $4.24 \mu\text{g cm}^{-2}$ have been described, the dominant component classes are in good accordance (Vogg *et al.* 2004, Leide 2008). *Solanum surratense*, a prickly Solanaceae common in Iran, India and Saudi Arabia, has a leaf wax composition with similar major component classes as *Solanum lycopersicum* (Figure 48). The total wax coverage was by factor 2 higher ($7.41 \mu\text{g cm}^{-2}$) than the wax coverage of *Solanum lycopersicum* leaves. *Vanilla planifolia* wax coverage was $45.79 \mu\text{g cm}^{-2}$ (Figure 49). Gravimetrically reported wax quantities were $29.6 \mu\text{g cm}^{-2}$ (Gouret *et al.* 1993) and $122.0 \mu\text{g cm}^{-2}$ (Schreiber and Riederer 1996). In the conducted analysis 81.1% of the total wax coverage were aliphatic components, 5.0% cyclic components and 10.5% not identified. Merk (1998) reported 65.0% aliphatic components, < 0.5% cyclic components and 35.0% of the wax extract as not identified. The component classes are in good accordance as well as the main component (dotriacontanoic acid) and the average carbon chain length (31.2 compared to 31.6). The predominant cuticular wax component classes of *Juglans regia* leaves have been similarly described in literature (Figure 50; Prasad and Gülz 1990, Merk *et al.* 1998). The main component class were primary alkanols with hexacosanol as dominant component, the average carbon chain length was 29.3. Merk (1998) obtained the same main component class, main constituent and an average carbon chain length of 28.1. The total leaf wax coverage of *Prunus laurocerasus* was $107.50 \mu\text{g cm}^{-2}$. Mainly cyclic components, such as ursolic acid and oleanolic acid, composed 66.3% of the leaf wax (Figure 51). The reported wax amount of *Prunus laurocerasus* leaves was $61.8 \mu\text{g cm}^{-2}$, with 70.0% of the wax being pentacyclic triterpenoids (Zeisler and Schreiber 2015). Merk (1998) described 56.0% of the cuticular wax as cyclic components, mainly ursolic acid. The average carbon chain

length was 29.4 compared to 30.0 in this study. Mechanical removal of the epicuticular waxes proved that the intracuticular waxes were mainly composed of pentacyclic triterpenoids (Jetter *et al.* 2000, Zeisler and Schreiber 2015). The leaf wax of *Olea europaea* composed of 83.4% cyclic components, mainly oleanolic acid, and 3.4% very-long-chain acyclic components (Figure 52). The average carbon chain length was 30.3. These results are in good agreement with the data set obtained by Merk (1998; 87.0% cyclic components, 4.0% acyclic components, main component oleanolic acid, average carbon chain length 31.0).

In general, it can be concluded that literature data is in conformity with the analysed wax quantity and quality. However, the percentage merely is often specified and, thus, wax quantities were not comparable. Slight variances might be due to different cultivars, developmental stages and environmental growth conditions as well as extraction and analysis methods (Riederer and Schneider 1990, Riederer and Markstädter 1996, Hauke and Schreiber 1998, Jetter and Schäffer 2001, Anfodillo *et al.* 2002, Leide *et al.* 2007, Mamrutha *et al.* 2010, Szakiel *et al.* 2012, Pensec *et al.* 2014).

3.3 Cuticular wax chemistry and minimum or cuticular water permeability

Plant cuticular membranes are composed of two major hydrophobic components, the cutin polymer and the cuticular waxes. Separate functional analysis of the two major components, conducted with enzymatically isolated cuticular membranes, proved the establishment of the main transport-limiting barrier by the cuticular waxes. Removal of the cuticular waxes with organic solvents leads to an increased cuticular water permeability (Schönherr 1982, Schreiber 2002). However, the relationship between the wax quality and the cuticular water permeability remains unsolved (Schönherr 1982, Kerstiens 2006). Chemical and functional analyses of the leaf cuticular waxes and the permeability did not reveal a correlation between the total wax coverage and the minimum or cuticular water permeability (Figure 53). Abundant wax coverages did not yield more efficient transpiration barriers.

A study conducted by Schreiber and Riederer (1996), comparing the wax amount (determined by weight loss before and after extraction) of plant species from different habitats with cuticular permeances, showed a similar result. One problem when determining the gravimetric wax amount is that these values are generally larger than the wax coverages obtained by chemical analysis (Schreiber and Schönherr 2009). This might be due to a limited resolution of the analytical measurements, especially

when determining the amount of very-long-chain alkyl esters approaching the detection limits. However, most of the typical component classes in the common chain length range are detectable and identifiable. In addition, weighing does not distinguish between wax components and substances that are not part of the cuticular waxes (Santos *et al.* 2007, Schreiber and Schönherr 2009). Furthermore, when determining the gravimetric wax amount, a differentiation between cyclic and acyclic components is not possible. Aliphatic components are proposed to form more efficient transpiration barriers, while the cyclic wax components seem to establish less efficient barriers (Oliveira *et al.* 2003, Vogg *et al.* 2004, Leide *et al.* 2007, 2011, Buschhaus and Jetter 2012). In this study, the detailed chemical analyses enabled the differentiation between cyclic and acyclic components.

The minimum or cuticular permeability and the amount of cyclic wax components were not correlated. However, a significant negative correlation with the very-long-chain aliphatic wax coverage was detected. About 54.6% of the transpiration barrier properties were determined by the aliphatic wax amount. This strengthens the hypothesis put forward by Jetter and Riederer (2015), stating that the majority of the barrier properties is formed by the very-long-chain acyclic components rather than the cyclic wax components.

The minimum or cuticular water permeability was predicted from the very-long-chain acyclic wax coverage. The prediction equation was gained from the regression line fitted to the plot of the natural logarithm of the minimum conductance (g_{\min}) and cuticular permeance (P) as a function of very-long-chain acyclic wax coverage ($r^2 = 0.546$; Figure 53; \pm SE of regression).

$$\ln g_{\min} \text{ or } P = -9.182 (\pm 0.284) - (0.074 (\pm 0.017) \cdot \text{acyclic wax coverage})$$

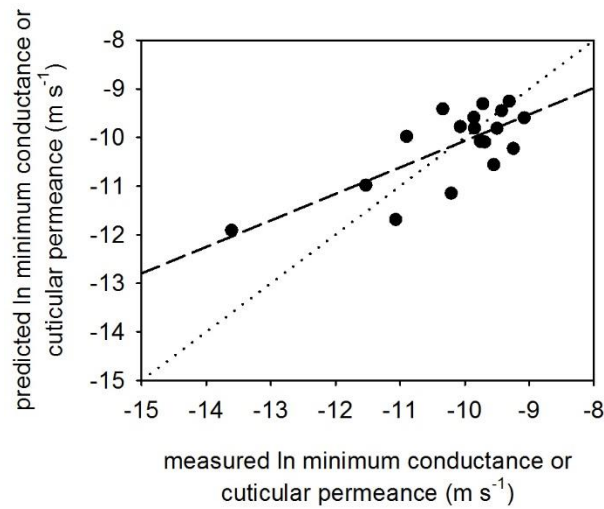


Figure 57. The natural logarithm of the minimum conductance (g_{\min}) or cuticular permeance (P) of leaves from an equation based on the acyclic wax coverage. Plot of predicted versus measured $\ln g_{\min}$ or $\ln P$ ($r^2 = 0.546$; dotted line indicates a slope of 1.0).

The influence of high average carbon chain lengths, which are proposed to enhance crystalline volume fractions and reduce the cuticular water permeability (Riederer and Schneider 1990, Riederer 1991), was analysed. It was suggested that waxes with high average carbon chain lengths form more efficient transpiration barriers. However, no significant correlation between the average carbon chain length (ACL) and the minimum conductance (g_{\min}) or cuticular permeance (P) was detected (Figure 55). Nevertheless, the cuticular water permeability was predicted with a prediction equation including the acyclic wax coverage and the ACL (x-axis: very-long-chain acyclic wax coverage, y-axis: ACL and z-axis: $\ln g_{\min}$ or $\ln P$; $r^2 = 0.581$; \pm SE of regression).

$$\ln g_{\min} \text{ or } P = -11.316 (\pm 1.912) - (0.072 (\pm 0.017) \cdot \text{acyclic wax coverage}) \\ + (0.066 (\pm 0.059) \cdot \text{average carbon chain length})$$

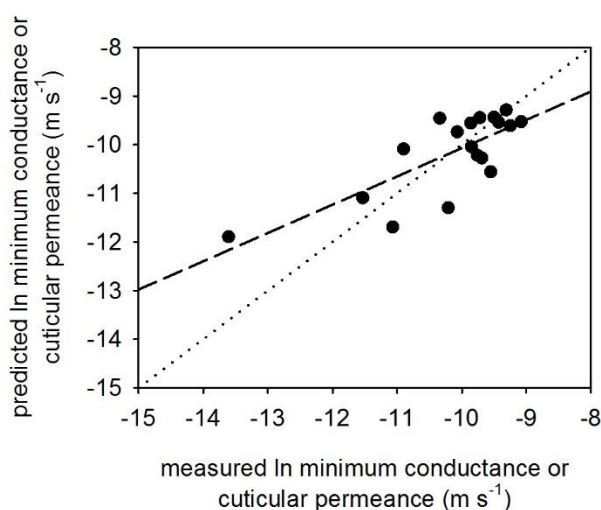


Figure 58. The natural logarithm of the minimum conductance (g_{\min}) or cuticular permeance (P) of leaves from an equation based on the acyclic wax coverage and the average carbon chain length. Plot of predicted versus measured $\ln g_{\min}$ or $\ln P$ ($r^2 = 0.581$; dotted line indicates a slope of 1.0).

The very-long-chain acyclic wax coverage was suitable to predict the minimum conductance or cuticular permeance with a slope of 0.546. Including the average carbon chain length in the prediction equation, a slope of 0.581 was obtained. Multiple linear regression indicated that the acyclic wax coverage accounts for the ability to predict the natural logarithm of the minimum conductance or cuticular permeance ($p < 0.001$), whereas the average carbon chain length had a non-significant influence ($p = 0.277$).

Given that 54.6% of the transpiration barrier properties were determined by the aliphatic wax coverage, the main component classes of the cuticular waxes were correlated separately with the minimum or cuticular water permeability (Figure 54). Common component classes were *n*-alkanes, alkanolic acids, primary alkanols and alkyl esters. Both, the wax coverage of *n*-alkanes and alkanolic acids, were significantly negatively correlated with the natural logarithm of minimum conductance and cuticular permeance, respectively (Figure 54). The cuticular wax coverage of *n*-alkanes and alkanolic acids affected the efficiency of the cuticular barrier function. These component classes might play a pivotal role in determining the barrier properties.

The proposed influence of average carbon chain lengths on the barrier efficiency was not confirmed with the 17 analysed plant species. The ratio of $\Delta ACL \text{ ACL}^{-1}$ was proposed to enable insights concerning the structural properties of plant cuticular waxes. The middle portions of the very-long-chain acyclic wax components align

(orthorhombic crystal lattice) with the vertical orientation towards the leaf surface. These crystalline fractions form flakes with probable parallel orientation to the outer surface of the cuticle. The chain ends of the very-long-chain acyclic wax components form a second, less ordered amorphous fraction. The highly ordered orthorhombic crystalline fractions of the cuticular waxes are impermeable to water molecules. Water diffuses through the intercrystalline amorphous fractions (Riederer and Schreiber 1995). High ratios $\Delta\text{ACL} \text{ACL}^{-1}$ indicate a wide scattering of the chain ends of the very-long-chain acyclic wax components. This was proposed to reflect in enhanced amorphous volume fractions (Riederer 1991). An impact of the ratio $\Delta\text{ACL} \text{ACL}^{-1}$ on the permeability was not confirmed with the 17 analysed plant species (Figure 55, Figure 56).

Multiplying the cuticular permeance (P) with the membrane thickness (l) yields the permeability coefficient of a membrane having 1 m thickness (\mathcal{P}). The permeability coefficient was described as useful tool to compare the water permeability of hypothetical homogeneous plant cuticles (Schreiber and Schönherr 2009).

$$P \cdot l = \mathcal{P}$$

The thickness of the wax layer can be calculated by dividing the wax coverage per area by the wax density (0.9 g cm^{-3}). The thickness of the membrane (l) does not reflect the length of the diffusion path for water. The diffusion path can be enhanced strongly due to the tortuosity factor (Schreiber and Schönherr 2009). Hence, the crystalline fractions are impermeable to water and higher average carbon chain lengths were proposed to enhance the crystalline volume fractions. A correlation of the average carbon chain length with cuticular permeance or minimum conductance normalised to the thickness is proposed. The permeability coefficient was calculated for the total wax coverage and the acyclic wax coverage and the obtained values were plotted against the average carbon chain length (ACL). The cuticular permeance or minimum conductance normalised to the thickness did not correlate with the average carbon chain length (Figure 59).

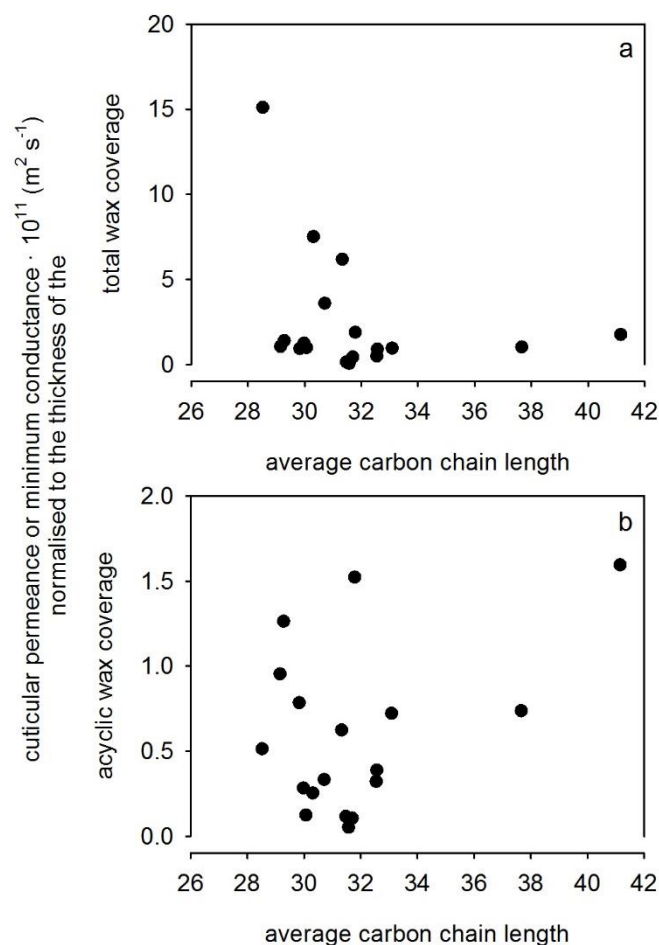


Figure 59. The cuticular permeance or minimum conductance normalised to the thickness of (a) the total wax coverage and (b) the acyclic wax coverage plotted against the average carbon chain length.

3.4 Conclusion

Minimum conductances and cuticular permeances of the analysed plant species ranged between $0.13 \cdot 10^{-5} \text{ m s}^{-1}$ and $11.54 \cdot 10^{-5} \text{ m s}^{-1}$. The measured values are within the similar range as literature data (between $0.04 \cdot 10^{-5} \text{ m s}^{-1}$ and $14.40 \cdot 10^{-5} \text{ m s}^{-1}$; Riederer and Schreiber 2001). In the present study, the minimum and cuticular water permeabilities were determined from stomatous leaves and astomatous leaf surfaces, respectively, and were used to deduce a relation between chemistry and function of plant cuticles.

Higher cuticular wax amounts did not constitute more efficient transpiration barriers. The amount of cyclic components showed no relation to the cuticular barrier function. However, the coverage of aliphatic components influenced the efficiency of

the transpiration barrier. About 54.6% of the transpiration barrier properties were determined by the coverage of very-long-chain aliphatic constituents. These new findings provide evidence that the acyclic wax coverage plays a pivotal role establishing efficient transpiration barriers. *N*-alkanes and alkanolic acids were two aliphatic wax classes whose amount affected the barrier properties. Both were significantly negatively correlated with the minimum or cuticular water permeability.

The average carbon chain length of the wax components, the dispersion around the average value and the ratio were hypothesised to influence the wax structure and, consequently, the barrier properties (Riederer and Schneider 1990, Riederer 1991). A relation between the cuticular water permeability and average carbon chain length was not evident in the analysed plant species.

Summarising discussion

1 Temperature effect on the minimum or cuticular water permeability

When analysing the temperature effect on the cuticular water permeability, all astomatous and isolated plant cuticles that have been investigated so far are characterised by a phase transition, which is indicated by a steep increase of cuticular permeances above 35 °C (Schönherr *et al.* 1979, Schreiber 2001, Riederer 2006b). The cuticular waxes form the main transport-limiting barrier (Schönherr 1982, Schreiber 2002) and, accordingly, Eckl and Gruler (1980) attributed the phase transition to the cuticular waxes. Extended melting ranges of the cuticular waxes have been described when analysing the phase behaviour (Merk *et al.* 1998). Tightly packed aliphatic carbon chains, which form orthorhombic crystalline zones, change into the hexagonal state or the solid state disappears completely (Schönherr *et al.* 1979, Merk *et al.* 1998). For example, the melting range of the cuticular leaf wax of *Prunus laurocerasus* occurred in the temperature range between 50.0 °C to 83.0 °C, with an orthorhombic endpoint at 58.0 °C (Merk 1998). The lethal limit of heat stress of *Prunus laurocerasus* leaves was 53.2 °C (Chapter III), which indicates that the orthorhombic endpoint occurred at temperatures that are not ecologically relevant. On the other hand, the phase transition has been explained by a divergent thermal volume expansion of the cutin polymer, the wax-free matrix membrane and the associated waxes, leading to micro-defects of the waxy transpiration barrier (Schönherr *et al.* 1979, Schreiber and Schönherr 1990). The phase transition has also been attributed to swelling of the polysaccharide material, which extends through plant cuticles. This was suggested to open up new regions of the polysaccharides for the water diffusion (Riederer 2006b).

The temperature effect on cuticular water permeability of intact leaf material, in comparison to the frequently analysed enzymatically isolated plant cuticles, is an ecophysiological question still unanswered (Kerstiens 2006). The minimum conductance, analysed of intact and stomatous *Rhazya stricta* (Apocynaceae) leaves, is the lowest conductance a leaf can reach with completely closed stomata as a result of desiccation stress (Körner 1995). The temperature-dependent minimum conductance of *Rhazya stricta* leaves did not increase steeply up to physiology relevant temperatures, which would indicate a phase transition and, thus, structural changes of the plant cuticle (Chapter I). In order to determine whether the desert plant is especially adapted to high temperatures and/or has an efficient transpiration barrier

at high temperatures, the temperature-dependent minimum conductance of *Nerium oleander* (Apocynaceae) leaves served as comparison. The Mediterranean sclerophyll *Nerium oleander* replaces *Rhazya stricta* in less arid conditions (Deil and Al-Gifri 1998). As for *Rhazya stricta*, no steep increase at elevated temperatures of the temperature-dependent minimum conductance of intact *Nerium oleander* leaves was detected (Chapter II).

The cuticle of intact, stomatous leaves might be stabilised by the cell wall. The volume expansion causing micro-defects or cracks in the barrier and, thus, enhancing the permeability, was merely determined for enzymatically isolated cuticular membranes (Schreiber and Schönherr 1990). The cell wall might act stabilising on the cuticular membrane and suppress the steep increase of the water permeability at elevated temperatures. In addition, the assumption of complete stomatal closure is described as highly uncertain (Kerstiens 1996, 2006). To exclude the influence of residual stomatal transpiration, which might influence the minimum conductance, the cuticular water permeability of astomatous, isolated cuticular membranes of *Nerium oleander* leaves as comparative system was determined. No sharp increase of the cuticular permeances up to physiology relevant temperatures was detected (Chapter II).

In order to classify and validate these new findings, *Prunus laurocerasus* was used as model plant (Chapter III; Schreiber 2001, Riederer 2006b). The temperature effect on the cuticular permeance of isolated cuticles, leaf discs and leaf envelopes was compared. Leaf discs and leaf envelopes represented the intact leaf. The cuticular permeance of the intact leaf systems did not indicate a steep increase at elevated temperatures. However, the cuticular permeance of isolated cuticles increased steeper at elevated temperatures in comparison to the intact leaf system. In addition, the cuticular permeances of isolated cuticles of *Prunus laurocerasus* are in good accordance with literature data (Riederer 2006b). The steep increase of the cuticular permeances of intact *Prunus laurocerasus* leaves might be suppressed, due to the cell wall stabilising the cuticle. Correspondingly, a smaller volume expansion of the cuticular membrane might prevent an enhancement of the permeability (Schreiber and Schönherr 1990).

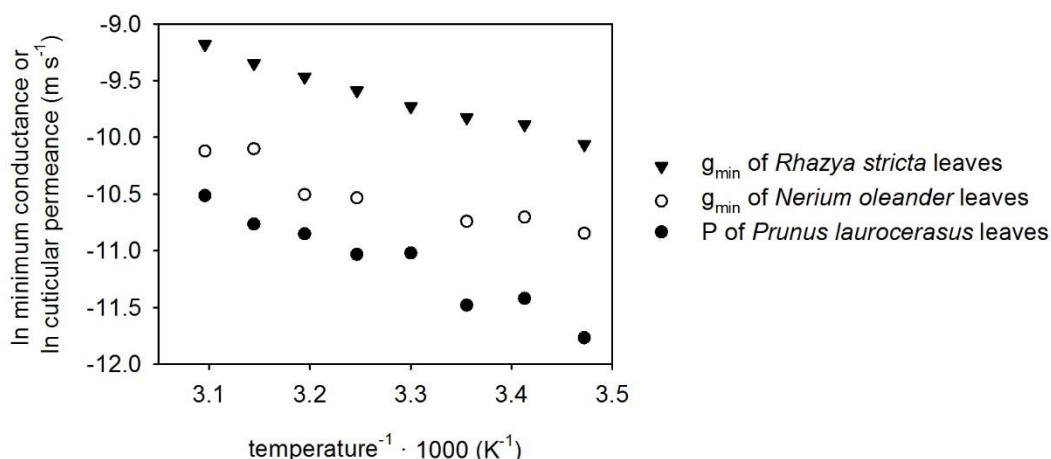


Figure 60. Arrhenius plot of the natural logarithm of the minimum conductance (g_{\min}) or cuticular permeance (P) and the inverse absolute temperature. The minimum conductance of *Rhazya stricta* (▼) and *Nerium oleander* (○) was determined for leaves and the cuticular permeance of *Prunus laurocerasus* (●) for leaf envelopes.

The role of the cuticle as a structural stabilisation component is determined by the mechanical properties, which in turn influence the transport properties. The mechanical properties are affected by factors such as the polymer density and composition, water as a plasticiser and temperature (Wiedemann and Neinhuis 1998, Marga *et al.* 2001, Edelmann *et al.* 2005, Matas *et al.* 2005, Bargel *et al.* 2006). Cutin monomer composition is proposed to influence the rigidity of plant cuticles (Marga *et al.* 2001). Upon hydration a lowered stiffness and an increased extensibility is reported for enzymatically isolated cuticles (Wiedemann and Neinhuis 1998). Similarly, elevated temperatures increased the extensibility and reduced the stiffness of isolated plant cuticles. This might influence the transport properties of isolated cuticular membranes.

Additionally, intracuticular waxes are described to serve as supporting fillers, reducing free volume within matrix membranes, increasing the rigidity and stiffness and decreasing the extensibility (Petracek and Bukovac 1995, Domínguez *et al.* 2009, Khanal *et al.* 2013). Triterpenoids are nearly exclusively localised in the intracuticular wax layer within the cutin polymer (Jetter *et al.* 2000, Buschhaus *et al.* 2007). Cutin and triterpenoids have a high compatibility and embedded triterpenoids are proposed to increase the density of the cuticle and the maximum strain and improve the mechanical strength. Pentacyclic triterpenoids endow the toughness of the cuticle by functioning as nanofillers in the cutin matrix (Tsubaki *et al.* 2013). Such a function can be assumed for *Rhazya stricta* and *Nerium oleander* due to the presence of high

amounts of triterpenoids in relation to the amounts of cutin monomers. Triterpenoids have high melting points (for example 285 °C - 288 °C for ursolic acid; Windholz *et al.* 1983) and the structural arrangement remains unaffected up to temperatures of 100 °C (Casado and Heredia 1999). Accordingly, strengthening of the cutin matrix by triterpenoids potentially reduces the extensibility of the cuticle and, therefore, prevents cuticular cracks and the occurrence of a phase transition. Although the leaf wax of *Prunus laurocerasus* composed of a major portion of cyclic components, the ratio between the cyclic wax components and the total amount of cutin monomers (0.3, 240 $\mu\text{g cm}^{-2}$ cutin monomers; Graça *et al.* 2002) is much smaller than the obtained ratio from *Rhazya stricta* and *Nerium oleander* leaves (0.6), which might explain the temperature influence on the cuticular permeances of isolated cuticles from *Prunus laurocerasus*.

2 The plant cuticle as leaf transpiration barrier

The most prominent function of plant cuticles is the reduction of uncontrolled water loss from plant organs, such as leaves, into the surrounding atmosphere. The cuticular waxes establish the main transport-limiting barrier of the plant cuticles. An extraction of the cuticular waxes with organic solvents leads to a considerable increase of the cuticular water permeability (Schönherr 1976, Schönherr and Lenzian 1981). However, the relation between the wax composition and the cuticular water permeability remains unsolved (Schönherr 1982, Kerstiens 2006). Due to this fact, chemical analysis of the cuticular wax components and the corresponding cuticular water permeability of a wide range of plant species were conducted.

In this study, the chemical composition of the cuticular waxes was heterogeneous in wax quantity and quality. The wax quantity ranged from very small amounts of 3.90 $\mu\text{g cm}^{-2}$ up to very high wax coverages of 336.93 $\mu\text{g cm}^{-2}$ (Chapter II, Chapter IV, Chapter V). Very-long-chain acyclic component classes, such as *n*-alkanes, primary alkanols, alkanolic acids, alkanals and alkyl esters, and cyclic components, such as pentacyclic triterpenoids, were common constituents of the cuticular waxes.

The cuticular water permeabilities were determined from astomatous and stomatous leaf surfaces. The minimum conductance of leaves with fully closed stomata and the astomatous cuticular permeance are often considered to be equal (Nobel 2009). However, incomplete stomatal closure and, thus, residual stomatal transpiration probably exceeding cuticular permeances might influence the minimum conductance

of leaves (Kerstiens 1996b). For leaves of *Acer campestre*, *Fagus sylvatica*, *Quercus petraea*, *Ilex aquifolium*, *Teucrium chamaedrys* (Burghardt and Riederer 2003, Burghardt *et al.* 2008) and *Nerium oleander* (Chapter II) the residual stomatal conductance after complete stomatal closure was negligible. Currently, only one plant species, *Hedera helix*, is described to have a significantly higher minimum conductance than cuticular permeance due to residual stomatal transpiration (Burghardt and Riederer 2003). Hence, in this study the minimum conductance was measured from stomatous leaves and, if applicable, the cuticular permeance was measured from hypostomatic leaves. The lower, stomatous leaf surface was either sealed and/or isolated plant cuticles were used. The minimum conductances and cuticular permeances of all analysed plant species ranged from $0.13 \cdot 10^{-5} \text{ m s}^{-1}$ (*Vanilla planifolia*) to $11.54 \cdot 10^{-5} \text{ m s}^{-1}$ (*Solanum surratense*; Chapter IV - V). A wide literature survey of cuticular permeances measured from astomatous, isolated leaf cuticles of 57 plant species indicated a range from $0.04 \cdot 10^{-5} \text{ m s}^{-1}$ to $14.40 \cdot 10^{-5} \text{ m s}^{-1}$ (Riederer and Schreiber 2001).

The minimum or cuticular water permeability (as natural logarithm of the minimum conductance or cuticular permeance, respectively) of the analysed plant species did not decrease with increasing total wax coverage. Higher cuticular wax amounts did not constitute more efficient transpiration barriers. Cyclic wax components were proposed to establish less efficient transpiration barriers than very-long-chain acyclic components (Oliveira *et al.* 2003, Vogg *et al.* 2004, Leide *et al.* 2007, 2011, Buschhaus and Jetter 2012). Consequently, an influence of the very-long-chain aliphatics on the barrier properties was suggested. Aliphatic wax compounds are arranged in highly ordered, crystalline zones representing excluded volumes for permeating water molecules. The crystalline zones increase the tortuosity of the diffusion pathway for water. Permeation is restricted to amorphous zones made up by chain ends, functional groups and short-chain aliphatics. The structural arrangement of cyclic wax compounds is characterised by a low molecular ordering (Casado and Heredia 1999, Tsubaki *et al.* 2013). Triterpenoids form amorphous zones, which are accessible to permeating water molecules (Riederer and Schreiber 1995).

Higher amounts of aliphatic components established more efficient barriers. A significant negative correlation between the very-long-chain aliphatic wax coverage and the natural logarithm of the minimum conductances or cuticular permeances was calculated. A relationship between the cuticular wax composition and the water

permeability was deduced, 54.6% of the transpiration barrier properties were determined by the aliphatic wax coverage. Cutin and the corresponding ester-linkage are proposed to play a major role in establishing barrier properties by providing the framework in which the cuticular waxes are arranged (Goodwin and Jenks 2005, Kosma and Jenks 2007). In addition to the role of acyclic components, the cutin composition and the cyclic components influence the cuticular barrier function. It has to be considered, that the specific leaf surface area has been shown to exceed the projected leaf surface area (Schreiber and Schönherr 1992, Riederer and Schreiber 1995). Not only wax crystals but also leaf surface structures, such as trichomes (Annex, Figure 61 - Figure 77), might influence the specific leaf area. In addition, in some plant species the epicuticular waxes do not contribute to the barrier properties (Jetter and Riederer 2015, Zeisler and Schreiber 2015). In this study, the total leaf cuticular waxes were analysed and correlated with the minimum or cuticular water permeability.

The common aliphatic component classes *n*-alkanes and alkanolic acids indicate the formation of more efficient barriers when present in high amounts. They might play a pivotal role in determining the barrier properties of plant cuticles. The proposed influence of high average carbon chain lengths, which enhance crystalline volume fractions and reduce the cuticular water permeability (Riederer and Schneider 1990, Riederer 1991), was not confirmed. Additionally, Riederer (1991) proposed that the ratio of the average carbon chain length dispersion (ΔACL) and the average carbon chain length (ACL) indicates structural properties of the amorphous volume fractions. According to this, it was hypothesised that cuticular waxes with low ratios of $\Delta\text{ACL}/\text{ACL}^{-1}$ have less amorphous volume fractions and, thus, an enhanced cuticular water permeability. This relationship between structure and function was not confirmed in this study.

So far, a relation between the wax composition and the cuticular water permeability has not been established (Schönherr 1982, Kerstiens 2006). The new findings of the present work provide insight into the chemistry-function analysis of plant cuticles. Given that the plant cuticle enables plant survival by conserving water during drought, the fundamental knowledge of the functioning of the barrier properties is especially important.

Summary

Cuticles cover all above-ground primary plant organs and are lipoid in nature consisting of a cutin matrix with cuticular waxes embedded within or deposited on its surface. The foremost function of the plant cuticle is the limitation of transpirational water loss into the surrounding atmosphere. Transpiration of water vapour from plants differs between stomatal and cuticular transpiration. Stomatal closure minimises the stomatal water loss and the remaining, much lower water transpiration occurs through the plant cuticle.

Temperature influence on the transpiration barrier properties of intact leaves is not yet known, despite the importance of the cuticular transpiration especially under drought and heat conditions. The present study focuses on the temperature-dependent minimum water permeability of whole leaves, in comparison to the temperature effect on the cuticular permeance of isolated, astomatous cuticles (Chapter I - III).

The minimum water permeability was determined gravimetrically from leaf drying curves and represents the cuticular water permeability of intact, stomatous leaves under conditions of complete stomatal closure. The temperature effect on the transpiration barrier of the desert plant *Rhazya stricta* and the Mediterranean sclerophyll *Nerium oleander* exposed a continuous increase of minimum water permeabilities with an increase in temperature. In contrast to other published studies, no abrupt and steep increase of the water permeability at high temperatures was detected. This steep increase indicates structural changes of the barrier properties of isolated cuticular membranes with a drastic decrease of efficiency. A stabilising impact of the cell wall on the plant cuticle of intact leaves was proposed. This steadying effect was confirmed with different experimental approaches measuring the cuticular water permeability of *Prunus laurocerasus* intact leaves.

Physiological analysis of water transport on isolated, astomatous leaf cuticles indicated a drastic decline of the barrier properties at elevated temperatures for *Prunus laurocerasus* but not for *Nerium oleander*. Cuticular components were quantitatively and qualitatively analysed by gas chromatography with a flame ionisation detector and a mass spectrometric detector, respectively. A high accumulation of pentacyclic triterpenoids as cuticular wax components in relation to the cutin monomer coverage was detected for *Nerium oleander* and for *Rhazya stricta* leaves, too. Accordingly, reinforcing of the cutin matrix by triterpenoids was proposed to improve the mechanical strength and to reduce the extensibility of plant cuticles. Thus, structural changes of the cuticular barrier properties were potentially suppressed at elevated temperatures.

The function of the cuticular wax amount and/or wax composition and its relation with the cuticular water permeability remains to be elucidated. In the second part of this work the cuticular wax quantity and quality as well as its impact on the transpiration barrier properties was analysed in order to deduce a potential relation between chemistry and function of plant cuticles (Chapter IV - V).

Chemical analyses of the cuticular wax components of a wide range of plant species, including one tropical (*Vanilla planifolia*), temperate (*Juglans regia*, *Plantago lanceolata*), Mediterranean (*Nerium oleander*, *Olea europaea*) and one desert (*Rhazya stricta*) plant species, were conducted. The cuticular wax compositions of nine characteristic plant species from xeric limestone sites naturally located in Franconia (Southern Germany) were determined for the first time. The corresponding minimum or cuticular water permeabilities of both stomatous and astomatous leaf surfaces were measured to detect a potential relationship between the cuticular wax amount, wax composition and the cuticular barrier properties.

It was demonstrated that abundant cuticular wax amounts did not constitute more efficient transpiration barriers. However, 55% of the cuticular barrier function can be attributed to the very-long-chain aliphatic wax coverages. These new findings provide evidence that the acyclic wax constituents play a pivotal role establishing efficient transpiration barriers. Additionally, these findings strengthen the hypothesis that cyclic components, such as pentacyclic triterpenoids, do not hinder the water diffusion through plant cuticles as effectively as acyclic constituents. For the first time a relationship between the cuticular wax composition and the transpiration barrier properties of a wide range of plant species proved insights into the potential relation between chemistry and function of plant cuticles.

Zusammenfassung

Die Kutikula bedeckt die Epidermis aller primären oberirdischen Pflanzenorgane. Diese lipophile Membran besteht aus dem Polymer Kutin und ein- bzw. aufgelagerten kutikulären Wachsen. Die wichtigste Aufgabe der Kutikula ist der Schutz der Pflanze vor Austrocknung, indem der unkontrollierte Wasserverlust in die Atmosphäre reduziert wird. Spaltöffnungen unterbrechen die kontinuierliche Schutzschicht, wobei die stomatäre Transpiration durch Spaltenschluss minimiert wird und die verbleibende, stark reduzierte Transpiration ausschließlich durch die pflanzliche Kutikula erfolgt.

Der Temperatureinfluss auf die Transportbarriere intakter Blätter ist bislang unerforscht, obwohl die kutikuläre Transpiration vor allem an trockenen und heißen Standorten eine wichtige Rolle spielt. Im Rahmen dieser Dissertation wurde die temperaturabhängige kutikuläre Wasserpermeabilität ganzer Blätter und isolierter Kutikularmembranen verglichen (Kapitel I - III).

Die minimale Wasserpermeabilität wurde gravimetrisch mittels Blattaustrocknungskurven bestimmt. Sie ist ein Maß für die kutikuläre Wasserdurchlässigkeit intakter, stomatärer Blätter bei geschlossenen Spaltöffnungen. Die minimale Wasserpermeabilität intakter Blätter von *Rhazya stricta* und *Nerium oleander* zeigte einen kontinuierlichen Anstieg mit zunehmender Temperatur. Im Gegensatz zu anderen Veröffentlichungen wurde kein abrupter, steiler Anstieg der Wasserpermeabilität bei erhöhten Temperaturen detektiert, welcher auf strukturelle Veränderungen der Transpirationsbarriere isolierter Kutikularmembranen und auf eine damit einhergehende, stark verminderte Effizienz hindeutet. Dies kann auf einen stabilisierenden Einfluss der Zellwand auf die pflanzliche Kutikula zurückgeführt werden. Verschiedene experimentelle Ansätze zur Bestimmung der temperaturabhängigen kutikulären Wasserpermeabilität von *Prunus laurocerasus* Blättern konnten dies bestätigen.

Bei erhöhten Temperaturen wiesen die isolierten, astomatären Kutikularmembranen von *Prunus laurocerasus* Blättern eine starke Abnahme der Barrierefunktion auf, die isolierten Kutikularmembranen von *Nerium oleander* Blättern jedoch nicht. Die kutikulären Wachs- und Kutinkomponenten wurden quantitativ mittels Gaschromatograph mit Flammenionisationsdetektor und qualitativ mittels Gaschromatograph gekoppelt mit Massenspektrometer analysiert. Ein sehr hoher Gehalt an pentazyklischen Triterpenoiden im kutikulären Wachs in Bezug auf den Kutingehalt wurde sowohl für die Blätter von *Nerium oleander* als auch für *Rhazya*

stricta bestimmt. Triterpenoide erhöhen möglicherweise die mechanische Festigkeit und reduzieren die Dehnbarkeit der Kutikula, indem sie die Kutinmatrix verstärken. Hierdurch könnten strukturelle Veränderungen der Transpirationsbarriere bei erhöhten Temperaturen herabgesetzt werden.

Die weit verbreitete Ansicht, dass die Wasserpermeabilität von der kutikulären Wachsmenge und/oder der Wachszusammensetzung bestimmt wird, konnte bislang nicht bestätigt werden. Im zweiten Teil der vorliegenden Arbeit wurden chemisch-analytische Methoden angewandt, um den Einfluss der Wachskomponenten auf die Transpirationsbarriere zu ermitteln, und somit einen potentiellen Zusammenhang zwischen der Chemie und der Funktion der pflanzlichen Kutikula abzuleiten (Kapitel IV - V).

Um Hinweise auf die Auswirkung der chemischen Zusammensetzung der Kutikula auf die Transpirationsbarriere zu erhalten, wurden die kutikulären Wachse eines breiten Artenspektrums analysiert, darunter eine tropische Pflanzenart (*Vanilla planifolia*), mediterrane Arten (*Nerium oleander*, *Olea europaea*), Pflanzenarten der gemäßigten Zone (*Juglans regia*, *Plantago lanceolata*) und eine Wüstenpflanze (*Rhazya stricta*). Zusätzlich wurde die kutikuläre Wachszusammensetzung von neun charakteristischen Pflanzenarten des Mainfränkischen Trockenrasens erstmals untersucht. Die entsprechende minimale oder kutikuläre Wasserpermeabilität von stomatären und astomatären Blattoberflächen dieser Pflanzenarten wurde bestimmt, um einen möglichen Zusammenhang zwischen der Wachschemie mit der Barrierefunktion aufzuklären.

Es konnte gezeigt werden, dass hohe Wachsmengen keine effizienteren Transpirationsbarrieren bilden. Jedoch konnten rund 55% der Barrierefunktion dem Anteil an langkettigen aliphatischen Komponenten zugeordnet werden. Diese neuen Erkenntnisse erbringen den Nachweis, dass die kutikuläre Transpirationsbarriere entscheidend von azyklischen Wachskomponenten beeinflusst wird. Zudem konnte bestätigt werden, dass zyklische Wachskomponenten die Wasserpermeabilität weniger stark beeinflussen als azyklische Bestandteile. Diese Ergebnisse zeigen zum ersten Mal einen Zusammenhang zwischen der chemischen Zusammensetzung der kutikulären Wachse und der kutikulären Transportbarriere anhand eines breiten Artenspektrums.

References

- Abd El-Ghani MM (1997) Phenology of ten common plant species in western Saudi Arabia. *Journal of Arid Environments* 35, 673-683
- Aharoni A, Dixit S, Jetter R, Thoenes E, van Arkel G, Pereira A (2004) The SHINE clade of AP2 domain transcription factors activates wax biosynthesis, alters cuticle properties, and confers drought tolerance when overexpressed in *Arabidopsis*. *The Plant Cell* 16, 2463-2480
- Al-Khamis HH, Al-Hemaid FM, Ibrahim ASS (2012) Diversity of perennial plants at Ibex Reserve in Saudi Arabia. *The Journal of Animal and Plant Sciences* 22, 484-492
- Almazroui M, Islam MN, Jones PD, Athar H, Rahman MA (2012) Recent climate change in the Arabian Peninsula: Seasonal rainfall and temperature climatology of Saudi Arabia for 1979-2009. *Atmospheric Research* 111, 29-45
- Anfodillo T, Pasqua di Bisceglie D, Urso T (2002) Minimum cuticular conductance and cuticle features of *Picea abies* and *Pinus cembra* needles along an altitudinal gradient in the Dolomites (NE Italian Alps). *Tree Physiology* 22, 479-487
- Badger MR, Björkman O, Armond PA (1982) An analysis of photosynthetic response and adaptation to temperature in higher plants: temperature acclimation in the desert evergreen *Nerium oleander* L. *Plant, Cell and Environment* 5, 85-99
- Baker EA (1974) The influence of environment on leaf wax development in *Brassica oleracea* var. *gemmifera*. *New Phytologist* 73, 955-966
- Bakker MI, Baas WJ, Sijm DTHM, Kollöffel C (1998) Leaf wax of *Lactuca sativa* and *Plantago major*. *Phytochemistry* 47, 1489-1493
- Bargel H, Koch K, Cerman Z, Neinhuis C (2006) Structure-function relationships of the plant cuticle and cuticular waxes - a smart material? *Functional Plant Biology* 33, 893-910
- Barkman JJ (1988) Some reflections on plant architecture and its ecological implications. A personal view demonstrated on two species of *Quercus*. In: Werger MJA, van der Aart PJM, During HJ, Verhoeven JTA (eds) *Plant form and vegetation structure*. Academic Publishing, The Hague, Netherlands, 1-7
- Barthlott W, Neinhuis C (1997) Purity of the sacred lotus, or escape from contamination in biological surfaces. *Planta* 202, 1-8
- Barthlott W, Neinhuis C, Cutler D, Ditsch F, Meusel I, Theisen I, Wilhelmi H (1998) Classification and terminology of plant epicuticular waxes. *Botanical Journal of the Linnean Society* 126, 237-260
- Bartlett MK, Scoffoni C, Sack L (2012) The determinants of leaf turgor loss point and prediction of drought tolerance of species and biomes: a global meta-analysis. *Ecology Letters* 15, 393-405
- Basson I, Reynhardt EC (1988) An investigation of the structures and molecular dynamics of natural waxes: II. Carnauba wax. *Journal of Physics D, Applied Physics* 21, 1429-1433

References

- Baur P (1997) Lognormal distribution of water permeability and organic solute mobility in plant cuticles. *Plant, Cell and Environment* 20, 167-177
- Becker M, Kerstiens G, Schönherr J (1986) Water permeability of plant cuticles: permeance, diffusion and partition coefficients. *Trees* 1, 54-60
- Belge B, Llovera M, Comabella E, Graell J, Lara I (2014) Fruit cuticle composition of a melting and a nonmelting peach cultivar. *Journal of Agricultural and Food Chemistry* 62, 3488-3495
- Bianchi G (1995) Plant Waxes. In: Hamilton RJ (ed) *Waxes: chemistry, molecular biology and functions*. The Oily Press, Dundee, Scotland, 175-222
- Bianchi G, Murelli C, Vlahov G (1992) Surface waxes from olive fruits. *Phytochemistry* 31, 3503-3506
- Bilger HW, Schreiber U, Lange OL (1984) Determination of leaf heat resistance: comparative investigation of chlorophyll fluorescence changes and tissue necrosis methods. *Oecologia* 63, 256-262
- Bourdenx B, Bernard A, Comergue F, Pascal S, Léger A, Roby D, Pervent M, Vile D, Haslam RP, Napier JA, Lessire R, Joubès J (2011) Overexpression of *Arabidopsis* ECERIFERUM1 promotes wax very-long-chain alkane biosynthesis and influences plant response to biotic and abiotic stresses. *Plant Physiology* 156, 29-45
- Bouzoubaâ Z, El Mousadik A, Belahsen Y (2006) Variation in amounts of epicuticular wax on leaves of *Argania spinosa* (L). *Skeels. Acta Botanica Gallica* 153, 167-177
- Brestic M, Zivcak M (2013) PSII fluorescence techniques for measurement of drought and high temperature stress signal in crop plants: protocols and applications. In: Rout GR, Das AB (eds) *Molecular stress physiology of plants*. Springer, India, 87-131
- Brodribb TJ, Holbrook NM (2003) Stomatal closure during leaf dehydration, correlation with other leaf physiological traits. *Plant Physiology* 132, 2166-2173
- Brodribb TJ, Holbrook NM, Edwards EJ, Gutiérrez MV (2003) Relations between stomatal closure, leaf turgor and xylem vulnerability in eight tropical dry forest trees. *Plant, Cell and Environment* 26, 443-450
- Brunner U, Eller MB (1974) Öffnen der Stomata bei hoher Temperatur im Dunkeln. *Planta* 121, 293-302
- Buchholz A (2006) Characterization of the diffusion of non-electrolytes across plant cuticles: properties of the lipophilic pathway. *Journal of Experimental Botany* 57, 2501-2513
- Burghardt M, Riederer M (2003) Ecophysiological relevance of cuticular transpiration of deciduous and evergreen plants in relation to stomatal closure and leaf water potential. *Journal of Experimental Botany* 54, 1941-1949
- Burghardt M, Riederer M (2006) Cuticular transpiration. In: Riederer M, Müller C (eds) *Biology of the plant cuticle*. Blackwell Publishing, Oxford, UK, 292-311

- Burghardt M, Burghardt A, Gall J, Rosenberger C, Riederer M (2008) Ecophysiological adaptations of water relations of *Teucrium chamaedrys* L. to the hot and dry climate of xeric limestone sites in Franconia (Southern Germany). *Flora* 203, 3-13
- Buschhaus C, Herz H, Jetter R (2007a) Chemical composition of the epicuticular and intracuticular wax layers on adaxial sides of *Rosa canina* leaves. *Annals of Botany* 100, 1557-1564
- Buschhaus C, Herz H, Jetter R (2007b) Chemical composition of the epicuticular and intracuticular wax layers on the adaxial side of *Ligustrum vulgare* leaves. *New Phytologist* 176, 311-316
- Buschhaus C, Jetter R (2011) Composition differences between epicuticular and intracuticular wax substructures: How do plants seal their epidermal surface? *Journal of Experimental Botany* 62, 841-853
- Buschhaus C, Jetter R (2012) Composition and physiological function of the wax layers coating Arabidopsis leaves: β -amyrin negatively affects the intracuticular water barrier. *Plant Physiology* 160, 1120-1129
- Cameron KD, Teece MA, Smart LB (2006) Increased accumulation of cuticular wax and expression of lipid transfer protein in response to periodic drying events in leaves of tree tobacco. *Plant Physiology* 140, 176-183
- Casado CG, Heredia A (1999) Structure and dynamics of reconstituted cuticular waxes of grape berry cuticle (*Vitis vinifera* L.). *Journal of Experimental Botany* 50, 175-182
- Chen X, Goodwin SM, Boroff VL, Liu X, Jenks MA (2003) Cloning and characterization of the *WAX2* gene of Arabidopsis involved in cuticle membrane and wax production. *The Plant Cell* 15, 1170-1185
- Cordeiro SZ, Simas NK, Arruda RCO, Sato A (2011) Composition of epicuticular wax layer of two species of *Mandevilla* (Apocynoideae, Apocynaceae) from Rio de Janeiro, Brazil. *Biochemical Systematics and Ecology* 39, 198-202
- Cornelissen JHC, Lavorel S, Garnier E, Díaz S, Buchmann N, Gurvich DE, Reich PB, ter Steege H, Morgan HD, van der Heijden MAG, Pausas JG, Poorter H (2003) A handbook of protocols for standardised and easy measurement of plant functional traits worldwide. *Australian Journal of Botany* 51, 335-380
- Crawford AJ, McLachlan DH, Hetherington AM, Franklin KA (2012) High temperature exposure increases plant cooling capacity. *Current Biology* 22, R396-R397
- Curtis EM, Knight CA, Petrou K, Leigh A (2014) A comparative analysis of photosynthetic recovery from thermal stress: a desert plant case study. *Oecologia* 175, 1051-1061
- Diekmann M, Jandt U, Alard D, Bleeker A, Corcket E, Gowing DJG, Stevens CJ, Duprè C (2014) Long-term changes in calcareous grassland vegetation in North-western Germany - No decline in species richness, but a shift in species composition. *Biological Conservation* 172, 170-179
- De Micco V, Aronne G (2012) Morpho-anatomical traits for plant adaptation to drought. In: Aroca R (ed) *Plant responses to drought stress, from morphological to molecular features*. Springer, Berlin Heidelberg, Germany, 37-61

References

- Deil U, Al-Gifri AN (1998) Montane and wadi vegetation. In: Ghazanfar SA, Fisher M (eds) *Vegetation of the Arabian Peninsula*. Kluwer Academic Publishers, Dordrecht, Netherlands, 125-174
- Deshmukh AP, Simpson AJ, Hatcher PG (2003) Evidence for cross-linking in tomato cutin using HR-MAS NMR spectroscopy. *Phytochemistry* 64, 1163-1170
- Eckl K, Gruler H (1980) Phase transitions in plant cuticles. *Planta* 150, 102-113
- Edelmann HC, Neinhuis C, Bargel H (2005) Influence of hydration and temperature on the rheological properties of plant cuticles and their impact on plant organ development. *Journal of Plant Growth Regulation* 24, 116-126
- Eigenbrode SD, Espelie KE (1995) Effects of plant epicuticular lipids on insect herbivores. *Annual Review of Entomology* 40, 171-94
- Ellenberg H, Weber HE, Düll R, Wirth V, Werner W, Paulißen D (1991) *Zeigerwerte von Pflanzen in Mitteleuropa*. *Scripta Geobotanica* 18, 1-248
- Emad El-Deen HM (2005) Population ecology of *Rhazya stricta* Decne. in Western Saudi Arabia. *International Journal of Agriculture and Biology* 7, 932-938
- Feller U (2006) Stomatal opening at elevated temperature: An underestimated regulatory mechanism? *General and Applied Plant Physiology, Special Issue* 19-31
- Franke R, Briesen I, Wojciechowski T, Faust A, Yephremov A, Nawrath C, Schreiber L (2005) Apoplastic polyesters in *Arabidopsis* surface tissues - a typical suberin and a particular cutin. *Phytochemistry* 66, 2643-2658
- Froux F, Ducrey M, Epron D, Dreyer E (2004) Seasonal variations and acclimation potential of the thermostability of photochemistry in four Mediterranean conifers. *Annals of Forest Science* 61, 235-241
- Gabr DG, Khafagi AAF, Mohamed AH, Mohamed FS (2015) The significance of leaf morphological characters in the identification of some species of Apocynaceae and Asclepiadaceae. *Journal of American Science* 11, 61-70
- Galassi M, Davies J, Theiler J, Gough B, Jungman G, Alken P, Booth M, Rossi F, Ulerich R (2015) *GNU Scientific Library Reference Manual*. 2.1, Network Theory Limited, United Kingdom
- Garnier E (1992) Growth analysis of congeneric annual and perennial grass species. *Journal of Ecology* 80, 665-675
- Garnier E, Laurent G (1994) Leaf anatomy, specific mass and water content in congeneric annual and perennial grass species. *New Phytologist* 128, 725-736
- Garnier E, Shipley B, Roumet C, Laurent G (2001) A standardized protocol for the determination of specific leaf area and leaf dry matter content. *Functional Ecology* 15, 688-695
- Gates DM (1980) *Biophysical Ecology*. Springer, Berlin Heidelberg, Germany
- Gentry GL, Barbosa P (2006) Effects of leaf epicuticular wax on the movement, foraging behavior, and attack efficacy of *Diaeretiella rapae*. *Entomologia Experimentalis et Applicata* 121, 115-122

- Geyer U, Schönherr J (1990) The effect of the environment on the permeability and composition of *Citrus* leaf cuticles. I. Water permeability of isolated cuticular membranes. *Planta* 180, 147-153
- Gibson AC (1996) Structure-function relations of warm desert plants. Springer, Berlin Heidelberg, Germany
- Gibson AC (1998) Photosynthetic organs of desert plants. *BioScience* 48, 911-920
- Giese BN (1975) Effects of light and temperature on the composition of epicuticular wax of barley leaves. *Phytochemistry* 14, 921-929
- Goodwin SM, Jenks MA (2005) Plant cuticle function as a barrier to water loss. In: Jenks MA, Hasegawa PM (eds) *Plant abiotic stress*. Blackwell Publishing, Oxford, UK, 14-36
- Graça J, Schreiber L, Rodrigues J, Pereira H (2002) Glycerol and glyceryl esters of ω -hydroxyacids in cutins. *Phytochemistry* 61, 205-215
- Grcarevic M, Radler F (1967) The effect of wax components on cuticular transpiration - Model experiments. *Planta* 75, 23-27
- Grubešić RJ, Vladimir-Knežević S, Kremer D, Kalodera Z, Vuković J (2007) Trichome micromorphology in *Teucrium* (Lamiaceae) species growing in Croatia. *Biologia Bratislava* 62, 148-156
- Gülz PG, Markstädter C, Riederer M (1994) Isomeric alkyl esters in *Quercus robur* leaf cuticular wax. *Phytochemistry* 35, 79-81
- Gupta NS, Collinson ME, Briggs DEG, Evershed RP, Pancost RD (2006) Reinvestigation of the occurrence of cutan in plants: implications for the leaf fossil record. *Paleobiology* 32, 432-449
- Haas K, Schönherr J (1979) Composition of soluble cuticular lipids and water permeability of cuticular membranes from *Citrus* leaves. *Planta* 146, 399-403
- Hansjakob A, Bischof S, Bringmann G, Riederer M, Hildebrandt U (2010) Very-long-chain aldehydes promote *in vitro* prepenetration processes of *Blumeria graminis* in a dose- and chain length-dependent manner. *New Phytologist* 188, 1039-1054
- Hansjakob A, Riederer M, Hildebrandt U (2011) Wax matters: absence of very-long-chain aldehydes from the leaf cuticular wax of the *glossy11* mutant of maize compromises the prepenetration processes of *Blumeria graminis*. *Plant Pathology* 60, 1151-1161
- Hauke V, Schreiber L (1998) Ontogenetic and seasonal development of wax composition and cuticular transpiration of ivy (*Hedera helix* L.) sun and shade leaves. *Planta* 207, 67-75
- Helbsing S, Riederer M, Zotz G (2000) Cuticles of vascular epiphytes: Efficient barriers for water loss after stomatal closure? *Annals of Botany* 86, 765-769
- Hoad SP, Grace J, Jeffree CE (1996) A leaf disc method for measuring cuticular conductance. *Journal of Experimental Botany* 47, 431-437

- Holloway PJ (1982a) Structure and histochemistry of plant cuticular membranes: an overview. In: Cutler DF, Alvin KL, Price CE (eds) *The plant cuticle*. Academic Press, London, UK, 1-32
- Holloway PJ (1982b) The chemical constitution of plant cutins. In: Cutler DF, Alvin KL, Price CE (eds) *The plant cuticle*. Academic Press, London, UK, 45-85
- Holloway PJ (1994) Plant cuticles: physicochemical characteristics and biosynthesis. In: Percy KE, Cape JN, Jagels R, Simpson CJ (eds) *Air pollutants and the leaf cuticle*. Springer, Berlin Heidelberg, Germany, 1-13
- Holmes MG, Keiller DR (2002) Effects of pubescence and waxes on the reflectance of leaves in the ultraviolet and photosynthetic wavebands: a comparison of a range of species. *Plant, Cell and Environment* 25, 85-93
- Isaacson T, Kosma DK, Matas AJ, Buda GJ, He Y, Yu B, Pravitasari A, Batteas JD, Stark RE, Jenks MA, Rose JKC (2009) Cutin deficiency in the tomato fruit cuticle consistently affects resistance to microbial infection and biomechanical properties, but not transpirational water loss. *The Plant Journal* 60, 363-377
- Jäger S, Trojan H, Kopp T, Laszczyk MN, Scheffler A (2009) Pentacyclic triterpene distribution in various plants - rich sources for a new group of multi-potent plant extracts. *Molecules* 14, 2016-2031
- Jeffree CE (1996) Structure and ontogeny of plant cuticles. In: Kerstiens G (ed) *Plant cuticles: an integrated functional approach*. BIOS Scientific, Oxford, UK, 33-82
- Jeffree CE (2006) The fine structure of the plant cuticle. In: Riederer M, Müller C (eds) *Biology of the plant cuticle*. Blackwell Publishing, Oxford, UK, 11-125
- Jenks MA, Joly RJ, Peters PJ, Rich PJ, Axtell JD, Ashworth EN (1994) Chemically induced cuticle mutation affecting epidermal conductance to water vapor and disease susceptibility in *Sorghum bicolor* (L.) Moench. *Plant Physiology* 105, 1239-1245
- Jenks MA, Andersen L, Teusink RS, Williams MH (2001) Leaf cuticular waxes of potted rose cultivars as affected by plant development, drought and paclobutrazol treatments. *Physiologia Plantarum* 112, 62-70
- Jetter R, Schäffer S, Riederer M (2000) Leaf cuticular waxes are arranged in chemically and mechanically distinct layers: evidence from *Prunus laurocerasus* L. *Plant, Cell and Environment* 23, 619-628
- Jetter R, Schäffer S (2001) Chemical composition of the *Prunus laurocerasus* leaf surface. Dynamic changes of the epicuticular wax film during leaf development. *Plant Physiology* 126, 1725-1737
- Jetter R, Kunst L, Samuels AL (2006) Composition of plant cuticular waxes. In: Riederer M, Müller C (eds) *Biology of the plant cuticle*. Blackwell Publishing, Oxford, UK, 146-181
- Jetter R, Riederer M (2016) Localization of the transpiration barrier in the epi- and intracuticular waxes of eight plant species: water transport resistances are associated with fatty acyl rather than alicyclic components. *Plant Physiology* 170, 921-934

References

- Ji X, Jetter R (2008) Very long chain alkylresorcinols accumulate in the intracuticular wax of rye (*Secale cereale* L.) leaves near the tissue surface. *Phytochemistry* 69, 1197-1207
- Jones HG (2014) *Plants and microclimate, a quantitative approach to environmental plant physiology*. 3th edn. Cambridge University Press, Cambridge, United Kingdom
- Joubès J, Raffaele S, Bourdenz B, Garcia C, Laroche-Traineau J, Moreau P, Domergue F, Lessire R (2008) The VLCFA elongase gene family in *Arabidopsis thaliana*: phylogenetic analysis, 3D modelling and expression profiling. *Plant Molecular Biology* 67, 547-566
- Kamp H (1930) Untersuchungen über Kutikularbau und kutikuläre Transpiration von Blättern. *Jahrbuch für wissenschaftliche Botanik* 72, 403-465
- Kerstiens G (1996a) Signalling across the divide: a wider perspective of cuticular structure-function relationships. *Trends in plant science* 1, 125-129
- Kerstiens G (1996b) Cuticular water permeability and its physiological significance. *Journal of Experimental Botany* 47, 1813-1832
- Kerstiens G (2006) Water transport in plant cuticles: an update. *Journal of Experimental Botany* 57, 2493-2499
- Kerstiens G, Lenzian KJ (1989) Interactions between ozone and plant cuticles II. Water permeability. *New Phytologist* 112, 21-27
- Khanal BP, Grimm E, Finger S, Blume A, Knoche M (2013) Intracuticular wax fixes and restricts strain in leaf and fruit cuticles. *New Phytologist* 200, 134-143
- Kim H, Lee SB, Kim HJ, Min MK, Hwang I, Suh MC (2012) Characterization of glycosylphosphatidylinositol-anchored lipid transfer protein 2 (LTPG2) and overlapping function between LTPG/LTPG1 and LTPG2 in cuticular wax export or accumulation in *Arabidopsis thaliana*. *Plant and Cell Physiology* 53, 1391-1403
- Kim KS, Park SH, Jenks MA (2007) Changes in leaf cuticular waxes of sesame (*Sesamum indicum* L.) plants exposed to water deficit. *Journal of Plant Physiology* 164, 1134-1143
- Kirsch T, Kaffarnik F, Riederer M, Schreiber L (1997) Cuticular permeability of the three tree species *Prunus laurocerasus* L., *Ginkgo biloba* L. and *Juglans regia* L.: comparative investigation of the transport properties of intact leaves, isolated cuticles and reconstituted cuticular waxes. *Journal of Experimental Botany* 48, 1035-1045
- Knight CA, Ackerly DD (2003) Evolution and plasticity of photosynthetic thermal tolerance, specific leaf area and leaf size: congeneric species from desert and coastal environments. *New Phytologist* 160, 337-347
- Koch K, Bhushan B, Barthlott W (2009) Multifunctional surface structures of plants: An inspiration for biomimetics. *Progress in Materials Science* 54, 137-178
- Kolattukudy PE (1970) Plant waxes. *Lipids* 5, 259-275
- Kolattukudy PE (1980) Biopolyester membranes of plants: cutin and suberin. *Science* 208, 990-1000

References

- Körner C (1994) Scaling from species to vegetation: the usefulness of functional groups. In: Schule ED, Mooney HA (eds) Biodiversity and ecosystem function. Springer, Berlin Heidelberg, Germany, 117-140
- Körner C (1995) Leaf diffusive conductances in the major vegetation types of the globe. In: Schulze ED, Caldwell M (eds) Ecophysiology of photosynthesis. Springer, Berlin Heidelberg, Germany, 463-490
- Kosma DK, Bourdenx B, Bernard A, Parsons EP, Lü S, Joubès J, Jenks MA (2009) The impact of water deficiency on leaf cuticle lipids of *Arabidopsis*. *Plant Physiology* 151, 1918-1929
- Kosma DK, Jenks MA (2007) Eco-physiological and molecular-genetic determinants of plant cuticle function in drought and salt stress tolerance. In: Jenks MA, Hasegawa PM, Jain SM (eds) Advances in molecular breeding toward drought and salt tolerant crops. Springer, Dordrecht, Netherlands, 91-210
- Kraus G (1906) Über den Nanismus unserer Wellenkalkpflanzen. *Verhandlungen der Physikalisch-Medizinischen Gesellschaft zu Würzburg* 38, 193-224
- Kraus G (1911) *Boden und Klima auf kleinstem Raum*. Gustav Fischer, Jena, Germany
- Krauss P, Markstädter C, Riederer M (1997) Attenuation of UV radiation by plant cuticles from woody species. *Plant, Cell and Environment* 20, 1079-1085
- Krishna LV (2014) Long term temperature trends in four different climatic zones of Saudi Arabia. *International Journal of Applied Science and Technology* 4, 233-242
- Kummerow J (1973) Comparative anatomy of sclerophylls of Mediterranean climatic areas. In: Di Castri F, Mooney HA (eds) Mediterranean type ecosystems. Springer, Berlin Heidelberg, Germany, 157-170
- Kurdyukov S, Faust A, Nawrath C, Bär S, Voisin D, Efremova N, Franke R, Schreiber L, Saedler H, Métraux JP, Yephremov (2006) The epidermis-specific extracellular BODYGUARD controls cuticle development and morphogenesis in *Arabidopsis*. *The Plant Cell* 18, 321-339
- Lambers H, Poorter H (1992) Inherent variation in growth rate between higher plants: a search for physiological causes and ecological consequences. *Advances in Ecological Research* 34, 283-362
- Lawson T, Davey PA, Yates SA, Bechtold U, Baeshen M, Baeshen N, Mutwakil MZ, Sabir J, Baker NR, Mullineaux PM (2014) C3 photosynthesis in the desert plant *Rhazya stricta* is fully functional at high temperatures and light intensities. *New Phytologist* 201, 862-873
- Lee Sb, Suh MC (2013) Recent advances in cuticular wax biosynthesis and its regulation in *Arabidopsis*. *Molecular Plant* 6, 246-249
- Leide J (2008) Cuticular wax biosynthesis of *Lycopersicon esculentum* and its impact on transpiration barrier properties during fruit development. Graduate thesis, Würzburg, Germany

References

- Leide J, Hildebrandt U, Reussing K, Riederer M, Vogg G (2007) The developmental pattern of tomato fruit wax accumulation and its impact on cuticular transpiration barrier properties: effects of a deficiency in a β -ketoacyl-coenzyme A synthase (LeCER6). *Plant Physiology* 144, 1667-1679
- Leide J, Hildebrandt U, Vogg G, Riederer M (2011) The positional sterile (ps) mutation affects cuticular transpiration and wax biosynthesis of tomato fruits. *Journal of Plant Physiology* 168, 871-877
- Leveau JHJ (2006) Microbial communities in the phyllosphere. In: Riederer M, Müller C (eds) *Biology of the plant cuticle*. Blackwell Publishing, Oxford, UK, 334-367
- Levizou W, Drilias P, Psaras GK, Manetas Y (2005) Nondestructive assessment of leaf chemistry and physiology through spectral reflectance measurements may be misleading when changes in trichome density co-occur. *New Phytologist* 165, 463-472
- Li-Beisson Y, Pollard M, Sauveplane V, Pinot F, Ohlrogge J, Beisson F (2009) Nanoridges that characterize the surface morphology of flowers require the synthesis of cutin polyester. *Proceedings of the National Academy of Sciences* 106, 22008-22013
- Lichtenthaler HK, Buschmann C, Knapp M (2005) How to correctly determine the different chlorophyll fluorescence parameters and the chlorophyll fluorescence ratio R_{Fd} of leaves with the PAM fluorometer. *Photosynthetica* 43, 379-393
- Lösch R (1978) Veränderungen im stomatären Kaliumgehalt bei Änderungen von Luftfeuchte und Umgebungstemperatur. *Berichte der Deutschen Botanischen Gesellschaft* 91, 645-656
- Lösch R (1980) Die Ökologie der mainfränkischen Kalktrockenrasen. *Abhandlungen des Naturwissenschaftlichen Vereins Würzburg* 21/22, 72-85
- Lösch R (2001) *Wasserhaushalt der Pflanzen*. Quelle & Meyer, Wiebelsheim, Germany
- López-Casado G, Matas AJ, Domínguez E, Cuartero J, Heredia A (2007) Biomechanics of isolated tomato (*Solanum lycopersicum* L.) fruit cuticles: the role of the cutin matrix and polysaccharides. *Journal of Experimental Botany* 58, 3875-3883
- Loza-Cornejo S, Terrazas T (2003) Epidermal and hypodermal characteristics in North American Cactoideae (Cactaceae). *Journal of Plant Research* 116, 27-35
- Macková J, Vašková M, Macek P, Hronková M, Schreiber L, Šantrůček J (2013) Plant response to drought stress simulated by ABA application: changes in chemical composition of cuticular waxes. *Environmental and Experimental Botany* 86, 70-75
- Maffei M (1994) Discriminant analysis of leaf wax alkanes in the Lamiaceae and four other plant families. *Biochemical Systematics and Ecology* 22, 711-728
- Maguire Km, Banks NH (2000) Harvest date, cultivar, orchard, and tree effects on water vapor permeance in apples. *Journal of the American Society for Horticultural Science* 125, 100-104

References

- Mamrutha HM, Mogili T, Lakshmi KJ, Rama N, Kosma D, Kumar MU, Jenks MA, Nataraja KN (2010) Leaf cuticular wax amount and crystal morphology regulate post-harvest water loss in mulberry (*Morus species*). *Plant Physiology and Biochemistry* 48, 690-696
- Marga F, Pesacreta TC, Hasenstein KH (2001) Biochemical analysis of elastic and rigid cuticles of *Cirsium horridulum*. *Planta* 213, 841-848
- Martin JT, Juniper BE (1970) *The cuticles of plants*. Edward Arnold, London, UK
- Matas AJ, Cobb ED, Bartsch JA, Paolillo DJ, Niklas KJ (2004) Biomechanics and anatomy of *Lycopersicon esculentum* fruit peels and enzyme-treated samples. *American Journal of Botany* 91, 352-360
- Matas AJ, López-Casado G, Cuartero J, Heredia A (2005) Relative humidity and temperature modify the mechanical properties of isolated tomato fruit cuticles. *American Journal of Botany* 93, 462-468
- Maximov NA (1931) The physiological significance of the xeromorphic structure of plants. *Journal of Ecology* 19, 273-282
- Maxwell K, Johnson GN (2000) Chlorophyll fluorescence - a practical guide. *Journal of Experimental Botany* 51, 659-668
- McFarlane HE, Shin JJH, Bird DA, Samuels AL (2010) *Arabidopsis* ABCG transporters, which are required for export of diverse cuticular lipids, dimerize in different combinations. *The Plant Cell* 22, 3066-3075
- McKinney DE, Bortiatynski JM, Carson DM, Clifford DJ, de Leeuw JW, Hatcher PG (1996) Tetramethylammonium hydroxide (TMAH) thermochemolysis of the aliphatic biopolymer cutan: insights into the chemical structure. *Organic Geochemistry* 24, 641-650
- Meletiyou-Christou MS, Rhizopoulou S (2012) Constraints of photosynthetic performance and water status of four evergreen species co-occurring under field conditions. *Botanical Studies* 53, 325-334
- Merk S (1998) FTIR-spektroskopische Untersuchungen zum Phasenverhalten und zur Kristallinität pflanzlicher kutikularer Wachse. Graduate thesis, Würzburg, Germany
- Merk S, Blume A, Riederer M (1998) Phase behavior and crystallinity of plant cuticular waxes studied by Fourier transform infrared spectroscopy. *Planta* 204, 44-53
- Millar AA, Clemens S, Zachgo S, Giblin EM, Taylor DC, Kunst L (1999) *CUT1*, an *Arabidopsis* gene required for cuticular wax biosynthesis and pollen fertility, encodes a very-long-chain fatty acid condensing enzyme. *The Plant Cell* 11, 825-838
- Muchow RC, Sinclair TR (1989) Epidermal conductance, stomatal density and stomatal size among genotypes of *Sorghum bicolor* (L.) Moench. *Plant, Cell and Environment* 12, 425-431
- Müller C (2006) Plant-insect interactions on cuticular surfaces. In: Riederer M, Müller C (eds) *Biology of the plant cuticle*. Blackwell Publishing, Oxford, UK, 398-422

References

- Navas ML, Ducout B, Roumet C, Richarte J, Garnier J, Garnier E (2003) Leaf life span, dynamics and construction cost of species from Mediterranean old-fields differing in successional status. *New Phytologist* 159, 213-228
- Niederl S, Kirsch T, Riederer M, Schreiber L (1998) Co-permeability of ³H-labeled water and ¹⁴C-labeled organic acids across isolated plant cuticles. *Plant Physiology* 116, 117-123
- Nip M, Tegelaar EW, de Leeuw J, Schenck PA, Holloway PJ (1986) A new non-saponifiable highly aliphatic and resistant biopolymer in plant cuticles. Evidence from pyrolysis and ¹³C-NMR analysis of present-day and fossil plants. *Naturwissenschaften* 73, 579-585
- Nobel PS (2009) *Physicochemical and environmental plant physiology*. 4th edn. Elsevier Academic Press, San Diego
- Ohlrogge J, Browse J (1995) Lipid biosynthesis. *The Plant Cell* 7, 957-970
- Oliveira AFM, Salatino A (2000) Major constituents of the foliar epicuticular waxes of species from the Caatinga and Cerrado. *Zeitschrift für Naturforschung* 55c, 688-692
- Oliveira AFM, Meirelles ST, Salatino A (2003) Epicuticular waxes from caatinga and cerrado species and their efficiency against water loss. *Annals of the Brazilian Academy of Sciences* 75, 431-439
- Oppenheimer HR (1960) Adaptation to drought: xerophytism. In: *Arid zone research, Plant-water relationships in arid and semi-arid conditions. Review of Research*, Unesco, Paris, France, 105-138
- Pearcy RW, Schulze ED, Zimmermann R (1989) Measurement of transpiration and leaf conductance. In: *Pearcy RW, Ehleringer JR, Mooney HA, Rundel PW (eds) Plant physiological ecology, field methods and instrumentation*. Chapman and Hall, London, UK, 137-160
- Peel MC, Finlayson BL, McMahon TA (2007) Updated world map of the Köppen-Geiger climate classification. *Hydrology and Earth System Sciences* 11, 1633-1644
- Pensec F, Pączkowski C, Grabarczyk M, Woźniak A, Bénard-Gellon M, Bertsch C, Chonh J, Szakiel A (2014) Changes in the triterpenoid content of cuticular waxes during fruit ripening of eight grape (*Vitis vinifera*) cultivars grown in the Upper Rhine Valley. *Journal of Agricultural and Food Chemistry* 62, 7998-8007
- Peschel S, Knoche M (2012) Studies on water transport through the sweet cherry fruit surface: XII. Variation in cuticle properties among cultivars. *Journal of the American Society for Horticultural Science* 137, 367-375
- Petracek PD, Bukovac MJ (1995) Rheological properties of enzymatically isolated tomato fruit cuticle. *Plant Physiology* 109, 675-679
- Pisek A, Berger E (1938) Kutikuläre Transpiration und Trockenresistenz isolierter Blätter und Sprosse. *Planta* 28, 124-155
- Pisek A, Winkler E (1953) Die Schliessbewegung der Stomata bei ökologisch verschiedenen Pflanzentypen in Abhängigkeit vom Wassersättigungszustand der Blätter und vom Licht. *Planta* 42, 253-278

References

- Pollard M, Beisson F, Li Yonghua, Ohlrogge B (2008) Building lipid barriers: biosynthesis of cutin and suberin. *Trends in Plant Science* 13, 236-246
- Post-Beittenmiller D (1996) Biochemistry and molecular biology of wax production in plants. *Annual Review of Plant Physiology and Plant Molecular Biology* 47, 405-430
- Prasad RBN, Gülz PG (1990) Surface structure and chemical composition of leaf waxes from *Quercus robur* L., *Acer pseudoplatanus* L. and *Juglans regia* L.. *Zeitschrift für Naturforschung* 45, 813-817
- Proctor MCF (2012) Adaptive differences related to water availability and shading in *Helianthemum* and *Koeleria*. *New Journal of Botany: Journal of the Botanical Society of Britain & Ireland* 2, 26-36
- Quets JJ, Temmerman S, El-Bana MI, Al-Rowaily SL, Assaeed AM, Nijs I (2014) Use of spatial analysis to test hypotheses on plant recruitment in a hyper-arid ecosystem. *PLOS ONE* 9.3, e91184
- Reisberg EE, Hildebrandt U, Riederer M, Hentschel U (2013) Distinct phyllosphere bacterial communities on *Arabidopsis* wax mutant leaves. *PLOS ONE* 8.11, e78613
- Reynhardt EC, Riederer M (1991) Structure and molecular dynamics of the cuticular wax from leaves of *Citrus aurantium* L. *Journal of Physics D, Applied Physics* 24, 478-486
- Reynhardt EC, Riederer M (1994) Structures and molecular dynamics of plant waxes. II. Cuticular waxes from leaves of *Fagus sylvatica* L. and *Hordeum vulgare* L. *European Biophysics Journal* 23, 59-70
- Reynolds-Henne CE, Langenegger A, Mani J, Schenk N, Zumsteg A, Feller U (2010) Interactions between temperature, drought and stomatal opening in legumes. *Environmental and Experimental Botany* 68, 37-43
- Riederer M (1991) Die Kutikula als Barriere zwischen terrestrischen Pflanzen und der Atmosphäre. Die Bedeutung der Wachsstruktur für die Permeabilität der Kutikula. *Naturwissenschaften* 78, 201-208
- Riederer M (2006a) Introduction: Biology of the plant cuticle. In: Riederer M, Müller C (eds) *Biology of the plant cuticle*. Blackwell Publishing, Oxford, UK, 1-10
- Riederer M (2006b) Thermodynamics of the water permeability of plant cuticles: characterization of the polar pathway. *Journal of Experimental Botany* 27, 2937-2942
- Riederer M, Schneider G (1990) The effect of the environment on the permeability and composition of *Citrus* leaf cuticles. II. Composition of soluble cuticular lipids and correlation with transport properties. *Planta* 180, 154-165
- Riederer M, Schreiber L (1995). Waxes: the transport barriers of plant cuticles. In: Hamilton RJ (ed) *Waxes. Chemistry, molecular biology and functions*. The Oily Press, Dundee, Scotland, 131-156
- Riederer M, Markstädter C (1996) Cuticular waxes: a critical assessment of current knowledge. In: Kerstiens G (ed) *Plant cuticles: an integrated functional approach*. BIOS Scientific, Oxford, UK, 189-200

References

- Riederer M, Schreiber L (2001) Protecting against water loss: analysis of the barrier properties of plant cuticles. *Journal of Experimental Botany* 52, 2023-2032
- Ristic Z, Jenks MA (2002) Leaf cuticle and water loss in maize lines differing in dehydration avoidance. *Journal of Plant Physiology* 159, 645-651
- Sánchez FJ, Manzanares M, de Andrés EF, Tenorio JL, Ayerbe L (2001) Residual transpiration rate, epicuticular wax load and leaf colour of pea plants in drought conditions. Influence on harvest index and canopy temperature. *European Journal of Agronomy* 15, 57-70
- Sandquist DR (2014) Plants in deserts. In: Monson RK (ed) *Ecology and the environment, The plant sciences*. Springer Reference, New York, 297-326
- Samuels L, Kunst L, Jetter R (2008) Sealing plant surfaces: cuticular wax formation by epidermal cells. *Annual Review of Plant Biology* 59, 683-707
- Schnurr JA, Shockey JM, de Boer GJ, Browse JA (2002) Fatty acid export from the chloroplast. Molecular characterization of a major plastidial acyl-coenzyme A synthetase from *Arabidopsis*. *Plant Physiology* 129, 1700-1709
- Schnurr J, Shockey J, Browse J (2004) The acyl-CoA synthetase encoded by *LACS2* is essential for normal cuticle development in *Arabidopsis*. *The Plant Cell* 16, 629-642
- Schönherr J (1976) Water permeability of isolated cuticular membranes: the effect of cuticular waxes on diffusion of water. *Planta* 131, 159-164
- Schönherr J (1982) Resistance of plant surfaces to water loss: transport properties of cutin, suberin and associated lipids. In: Lange OL, Nobel PS, Osmond CB, Ziegler H (eds) *Physiological plant ecology II*, Springer, Berlin Heidelberg, Germany, 153-179
- Schönherr J (2000) Calcium chloride penetrates plant cuticles via aqueous pores. *Planta* 212, 112-118
- Schönherr J (2006) Characterization of aqueous pores in plant cuticles and permeation of ionic solutes. *Journal of Experimental Botany* 57, 2471-2491
- Schönherr J, Eckl K, Gruler H (1979) Water permeability of plant cuticles: the effect of temperature on diffusion of water. *Planta* 147, 21-26
- Schönherr J, Lenzian K (1981) A simple and inexpensive method of measuring water permeability of isolated plant cuticular membranes. *Zeitschrift für Pflanzenphysiologie* 102, 321-327
- Schönherr J, Mérida T (1981) Water permeability of plant cuticular membranes: the effects of humidity and temperature on the permeability of non-isolated cuticles of onion bulb scales. *Plant, Cell and Environment* 4, 349-354
- Schreiber L (2001) Effect of temperature on cuticular transpiration of isolated cuticular membranes and leaf discs. *Journal of Experimental Botany* 52, 1893-1900
- Schreiber L (2002) Co-permeability of ³H-labelled water and ¹⁴C-labelled organic acids across isolated *Prunus laurocerasus* cuticles: effect of temperature on cuticular paths of diffusion. *Plant Cell Environment* 25, 1087-1094

References

- Schreiber L (2005) Polar paths of diffusion across plant cuticles: new evidence for an old hypothesis. *Annals of Botany* 95, 1069-1073
- Schreiber L (2006) Review of sorption and diffusion of lipophilic molecules in cuticular waxes and the effects of accelerators on solute mobilities. *Journal of Experimental Botany* 57, 2515-2523
- Schreiber L, Schönherr J (1990) Phase transitions and thermal expansion coefficients of plant cuticles, the effects of temperature on structure and function. *Planta* 182, 186-193
- Schreiber L, Schönherr J (1992) Uptake of organic chemicals in conifer needles: surface adsorption and permeability of cuticles. *Environmental Science & Technology* 26, 153-159
- Schreiber L, Riederer M (1996) Ecophysiology of cuticular transpiration: comparative investigation of cuticular water permeability of plant species from different habitats. *Oecologia* 107, 426-432
- Schreiber L, Schorn K, Heimbürg T (1997) ^2H NMR study of cuticular wax isolated from *Hordeum vulgare* L. leaves: identification of amorphous and crystalline wax phases. *European Biophysics Journal* 26, 371-380
- Schreiber L, Skrabs M, Hartmann KD, Diamantopoulos, Simanova E, Santrucek J (2001) Effect of humidity on cuticular water permeability of isolated cuticular membranes and leaf disks. *Planta* 214, 274-282
- Schreiber L, Schönherr J (2009) Water and solute permeability of plant cuticles, measurement and data analysis. Springer, Berlin Heidelberg, Germany
- Schreiber U, Bilger W, Neubauer C (1995). Chlorophyll fluorescence as a noninvasive indicator for rapid assessment of in vivo photosynthesis. In: Schulze ED, Caldwell M (eds) *Ecophysiology of photosynthesis*. Springer, Berlin Heidelberg, Germany, 49-70
- Scoffoni C, Vuong C, Diep S, Cochard H, Sack L (2014) Leaf shrinkage with dehydration: coordination with hydraulic vulnerability and drought tolerance. *Plant Physiology* 164, 1772-1788
- Shepherd T, Griffiths DW (2006) The effects of plant stress on plant cuticular waxes. *New Phytologist* 171, 469-499
- Shouten S, Moerkerken P, Gelin F, Baas M, de Leeuw J, Sinninghe Damsté JS (1997) Structural characterization of aliphatic, non-hydrolyzable biopolymers in freshwater algae and a leaf cuticle using ruthenium tetroxide degradation. *Phytochemistry* 49, 987-993
- Smirnova A, Leide J, Riederer M (2013) Deficiency in a very-long-chain fatty acid β -ketoacyl-coenzyme A synthase of tomato impairs microgametogenesis and causes floral organ fusion. *Plant Physiology* 161, 196-209
- Smith SE, Fendenheim DM, Halbrook K (2006) Epidermal conductance as a component of dehydration avoidance in *Digitaria californica* and *Eragrostis lehmanniana*, two perennial desert grasses. *Journal of Arid Environments* 64, 238-250

References

- Smith WK (1978) Temperatures of desert plants: another perspective on adaptability of leaf size. *Science* 201, 614-616
- Soper DS (2016) Significance of the difference between two slopes calculator, Software. Available from www.danielsoper.com/statcalc
- Szafranek BM, Synak EE (2006) Cuticular waxes from potato (*Solanum tuberosum*) leaves. *Phytochemistry* 67, 80-90
- Szakiel A, Pączkowski C, Huttunen S (2012) Triterpenoid content of berries and leaves of bilberry *Vaccinium myrtillus* from Finland and Poland. *Journal of Agricultural and Food Chemistry* 60, 11839-11849
- Szakiel A, Nizyński, Pączkowski C (2013) Triterpenoid profile of flower and leaf cuticular waxes of heather *Calluna vulgaris*. *Natural Product Research* 27, 1404-1407
- Turner NC (1988) Measurement of plant water status by the pressure chamber technique. *Irrigation Science* 9, 289-308
- Tsubaki S, Sugimura K, Teramoto Y, Yonemori K, Azuma JI (2012) Cuticular membrane of *Fuyu* persimmon fruit is strengthened by triterpenoid nano-fillers. *PLOS ONE* 8.9, e75275
- Van Gardingen PR, Grace J (1992) Vapour pressure deficit response of cuticular conductance in intact leaves of *Fagus sylvatica* L. *Journal of Experimental Botany* 43, 1293-1299
- Vendramini F, Díaz S, Gurvich DE, Wilson PJ, Thompson K, Hodgson JG (2002) Leaf traits as indicators of resource-use strategy in floras with succulent species. *New Phytologist* 154, 147-157
- Villena JF, Domínguez E, Stewart D, Heredia A (1999) Characterization and biosynthesis of non-degradable polymers in plant cuticles. *Planta* 208, 181-187
- Vogg G, Fischer S, Leide J, Emmanuel E, Jetter R, Levy AA, Riederer M (2004) Tomato fruit cuticular waxes and their effects on transpiration barrier properties: functional characterization of a mutant deficient in a very-long-chain fatty acid β -ketoacyl-CoA synthase. *Journal of Experimental Botany* 55, 1401-1410
- Volk OH (1937) Über einige Trockenrasengesellschaften des Würzburger Wellenkalkgebietes. *Beihefte zum Botanischen Centralblatt* 57, 577-598
- Walden-Coleman AE, Rajcan I, Earl HJ (2013) Dark-adapted leaf conductance, but not minimum leaf conductance, predicts water use efficiency of soybean (*Glycine max* L. Merr.). *Canadian Journal of Plant Science* 93, 13-22
- Wiedemann P, Neinhuis C (1998) Biomechanics of isolated plant cuticles. *Botanica Acta* 111, 28-34
- Windholz M, Budavari S, Blumetti RF, Otterbein ES (1983) *The Merck Index*. Merck & Co, Rahway, New York
- Witschel M (1991) Die *Trinia glauca*-reichen Trockenrasen in Deutschland und ihre Entwicklung seit 1880. *Berichte der Bayerischen Botanischen Gesellschaft* 62, 189-219

References

- Woo NS, Badger MR, Pogson BJ (2008) A rapid, non-invasive procedure for quantitative assessment of drought survival using chlorophyll fluorescence. *Plant Methods* 4, 27
- Woods CL (2013) Functional traits explain vascular epiphyte distributional patterns along environmental gradients in tropical canopies. 98th ESA Annual Convention, Conference Paper, Minneapolis, United States
- Wright IJ, Reich PB, Westoby M (2001) Strategy shifts in leaf physiology, structure and nutrient content between species of high- and low-rainfall and high- and low-nutrient habitats. *Functional Ecology* 15, 423-434
- Yang W, Pollard M, Li-Beisson Y, Beisson F, Feig M, Ohlrogge J (2010) A distinct type of glycerol-3-phosphate acyltransferase with *sn*-2 preference and phosphatase activity producing 2-monoacylglycerol. *Proceedings of the National Academy of Sciences* 107, 12040-12045
- Yang W, Simpson JP, Li-Beisson Y, Beisson F, Pollard M, Ohlrogge JB (2012) A land-plant-specific glycerol-3-phosphate acyltransferase family in *Arabidopsis*: substrate specificity, *sn*-2 preference, and evolution. *Plant Physiology* 160, 638-652
- Yates SA, Chernukhin I, Alvarez-Fernandez R, Bechtold U, Baeshen M, Baeshen N, Mutwakil MZ, Sabir J, Lawson T, Mullineaux PM (2014) The temporal foliar transcriptome of the perennial C3 desert plant *Rhazya stricta* in its natural environment. *BMC Plant Biology* 14, 2
- Yeats TH, Martin LBB, Viart HMF, Isaacson T, He Y, Zhao L, Matas AJ, Buda GJ, Domozych DS, Clausen MH, Rose JKC (2012) The identification of cutin synthase: formation of the plant polyester cutin. *Nature Chemical Biology* 8, 609-611
- Yeats TH, Rose JKC (2013) The formation and function of plant cuticles. *Plant Physiology* 163, 5-20
- Zeisler V, Schreiber L (2015) Epicuticular wax on cherry laurel (*Prunus laurocerasus*) leaves does not constitute the cuticular transpiration barrier. *Planta*, 1-17
- Zhang JZ, Broeckling CD, Blancaflor EB, Sledge MK, Summer LW, Wang ZY (2005) Overexpression of *WXP1*, a putative *Medicago truncatula* AP2 domain-containing transcription factor gene, increases cuticular wax accumulation and enhances drought tolerance in transgenic alfalfa (*Medicago sativa*). *The Plant Journal* 42, 689-707

Annex

Table 31. The average carbon chain length of the aliphatic wax components (ACL) and the standard deviation (Δ ACL) as a measure of dispersion either based on the wax amount or based on the molar wax coverage. ACL and Δ ACL based on the wax amount were additionally calculated for the low chain length range ($\leq C_{37}$) and the high chain length range ($\geq C_{38}$).

	based on wax amount coverage							based on molar wax coverage		
	ACL	Δ ACL	$\frac{\Delta\text{ACL}}{\text{ACL}^{-1}}$	ACL low chain length range	Δ ACL high chain length range	ACL	Δ ACL	$\frac{\Delta\text{ACL}}{\text{ACL}^{-1}}$	ACL	Δ ACL
<i>Rhazya stricta</i>	28.52	4.40	0.15	28.52	4.40	-	-	27.85	4.63	0.17
<i>Nerium oleander</i>	31.33	2.65	0.08	31.33	2.65	-	-	31.12	2.66	0.09
<i>Prunus laurocerasus</i>	29.98	3.98	0.13	29.33	2.15	47.27	1.27	29.58	3.48	0.12
<i>Hippocrepis comosa</i>	29.15	5.15	0.18	27.86	1.95	46.21	3.18	28.54	4.25	0.15
<i>Helianthemum apenninum</i>	41.15	8.76	0.21	28.79	2.92	46.42	3.46	38.93	9.31	0.24
<i>Geranium sanguineum</i>	32.55	6.02	0.18	30.95	3.25	48.20	3.63	31.68	5.30	0.17
<i>Sanguisorba minor</i>	31.79	5.17	0.16	30.33	3.31	42.72	4.40	31.31	5.06	0.16
<i>Sesleria albicans</i>	29.83	5.69	0.19	27.81	1.87	43.79	2.66	29.02	4.80	0.17
<i>Pulsatilla vulgaris</i>	37.66	9.06	0.24	28.49	3.23	45.52	2.86	35.39	9.11	0.26
<i>Teucrium chamaedrys</i>	32.57	6.19	0.19	30.13	2.81	44.86	3.02	31.61	5.53	0.17
<i>Salvia pratensis</i>	30.71	2.03	0.07	30.71	2.03	-	-	30.58	2.10	0.07
<i>S. pratensis, mesophytic</i>	30.07	2.35	0.08	30.07	2.35	-	-	29.87	2.44	0.08
<i>Plantago lanceolata</i>	31.70	3.63	0.11	31.02	2.08	44.79	1.87	31.35	3.28	0.10
<i>Solanum lycopersicum</i>	31.48	3.27	0.10	30.89	1.69	44.29	2.97	31.19	2.91	0.09
<i>Solanum surratense</i>	33.09	4.12	0.12	32.05	2.29	43.89	3.14	32.63	3.86	0.12
<i>Vanilla planifolia</i>	31.57	4.09	0.13	30.84	1.86	49.40	2.42	31.18	3.50	0.11
<i>Juglans regia</i>	29.28	6.56	0.22	26.85	2.69	43.43	3.71	28.21	5.57	0.20
<i>Olea europaea</i>	30.31	2.60	0.09	30.31	2.60	-	-	30.13	2.69	0.09

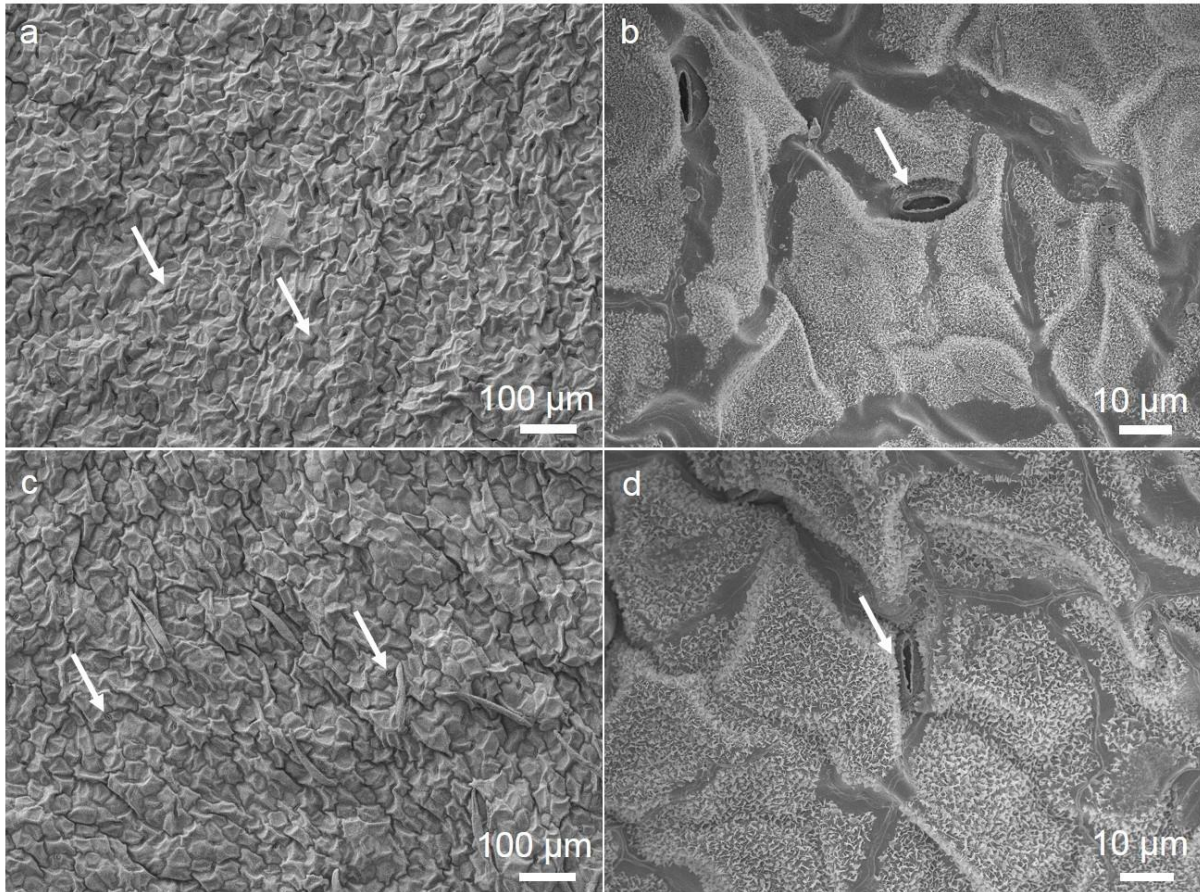


Figure 61. The native adaxial (a,b) and abaxial (c,d) leaf surface of *Hippocrepis comosa*. Stomata occurred on both leaf surfaces and are indicated by arrows. The abaxial leaf surface showed foliar trichomes. The epicuticular wax structure were platelets, the main component class of the cuticular wax were primary alkanols dominated by hexacosanol. Platelets are a common wax type and the dominating component described are primary alkanols, such as hexacosanol (Koch *et al.* 2009).

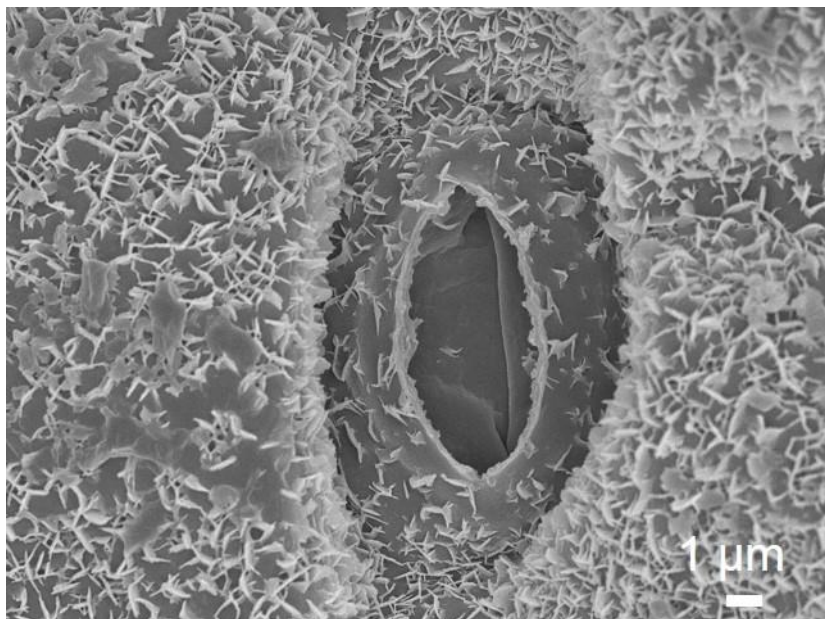


Figure 62. Detailed view of the epicuticular wax structures on the adaxial leaf surface of *Hippocrepis comosa*.

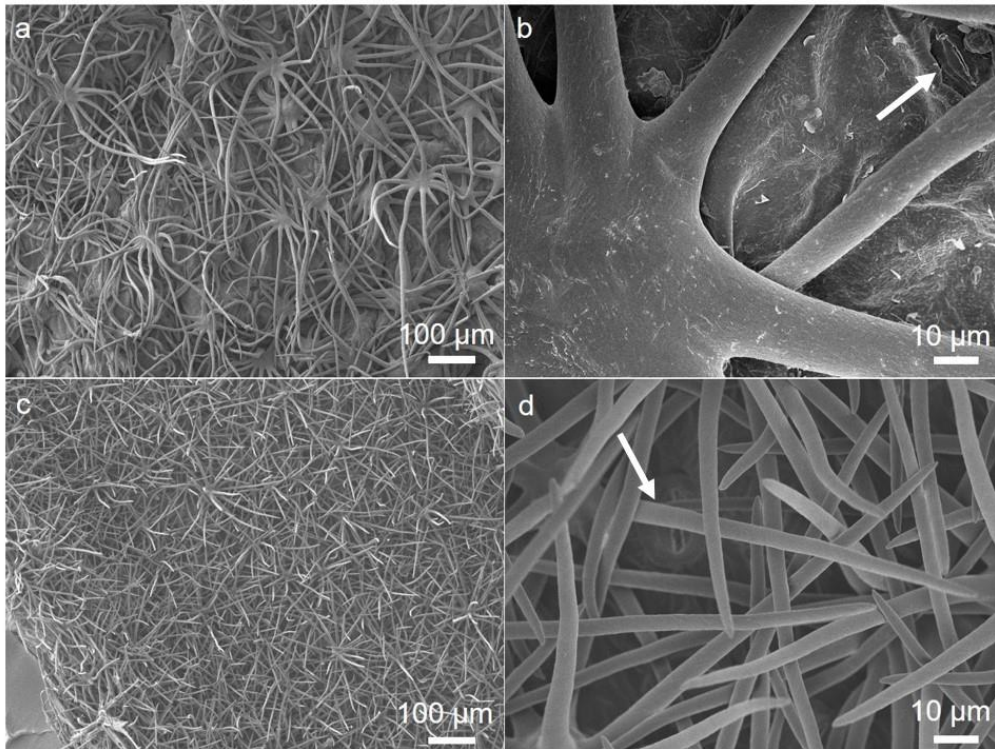


Figure 63. The native adaxial (a,b) and abaxial (c,d) leaf surface of *Helianthemum apenninum*. Stomata occurred on both leaf surfaces and are indicated by arrows. Both leaf surfaces were covered by stellate indumentum (Proctor 2012). The upper leaf surface was covered by stellate hairs and the lower leaf surface by a dense stellate tomentum.

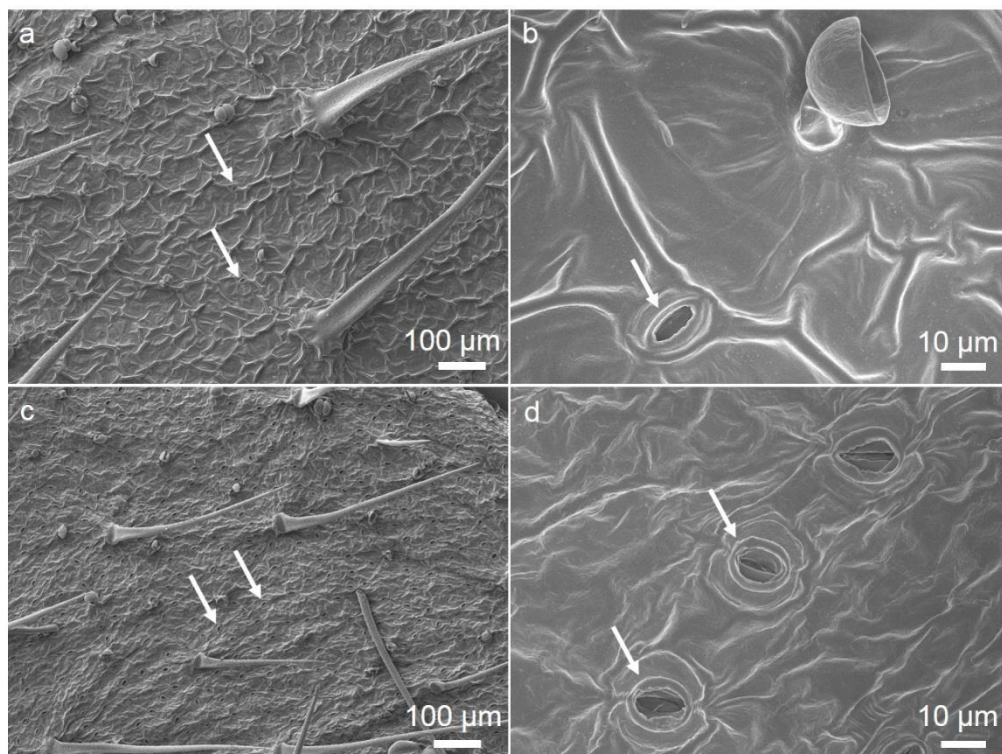


Figure 64. The native adaxial (a,b) and abaxial (c,d) leaf surface of *Geranium sanguineum*. Stomata occurred on both leaf surfaces and are indicated by arrows. Both leaf surfaces showed foliar trichomes. A wax film covered the leaf surface.

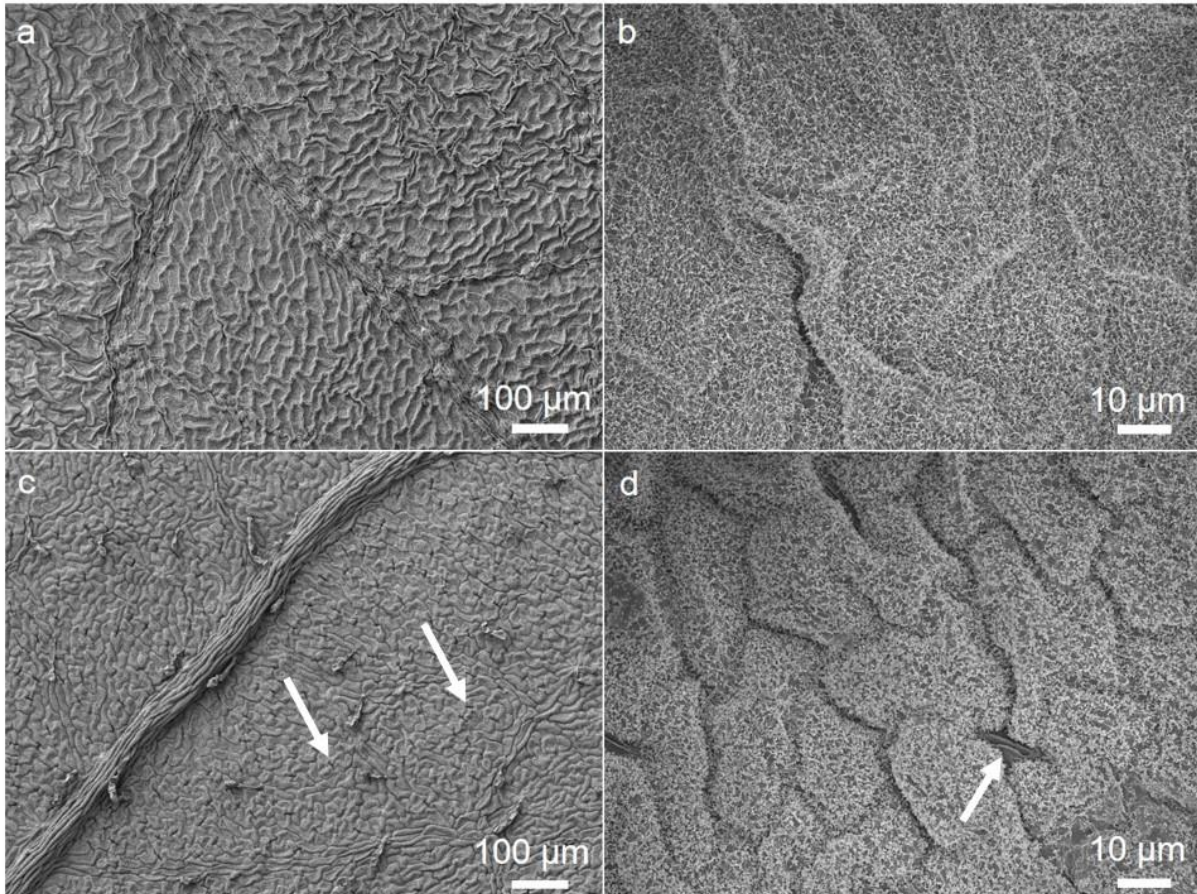


Figure 65. The native adaxial (a,b) and abaxial (c,d) leaf surface of *Sanguisorba minor*. Stomata occurred on the abaxial leaf surface and are indicated by arrows. The abaxial leaf surface showed foliar trichomes. The epicuticular waxes have a distinguishable structure, the main component class of the cuticular wax were *n*-alkanes dominated by *n*-hentriacontane.

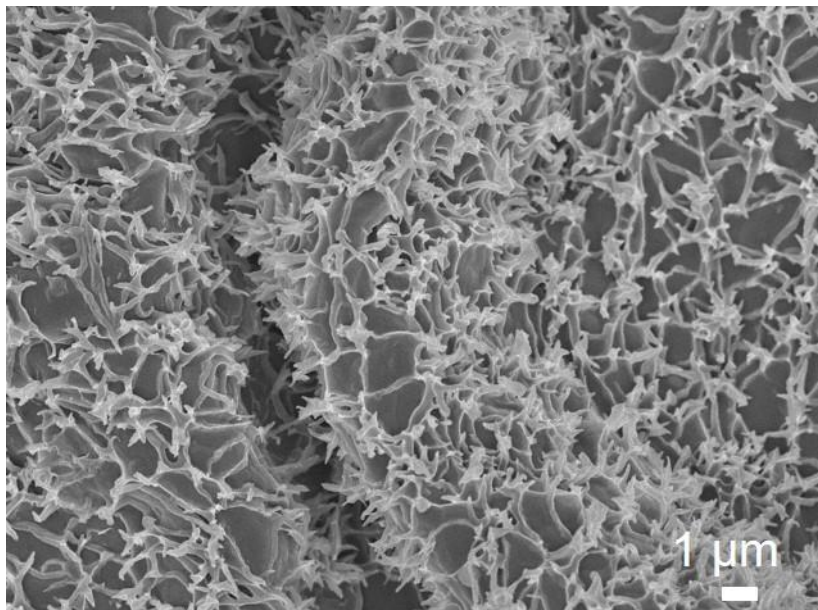


Figure 66. Detailed view of the epicuticular wax structures on the adaxial leaf surface of *Sanguisorba minor*.

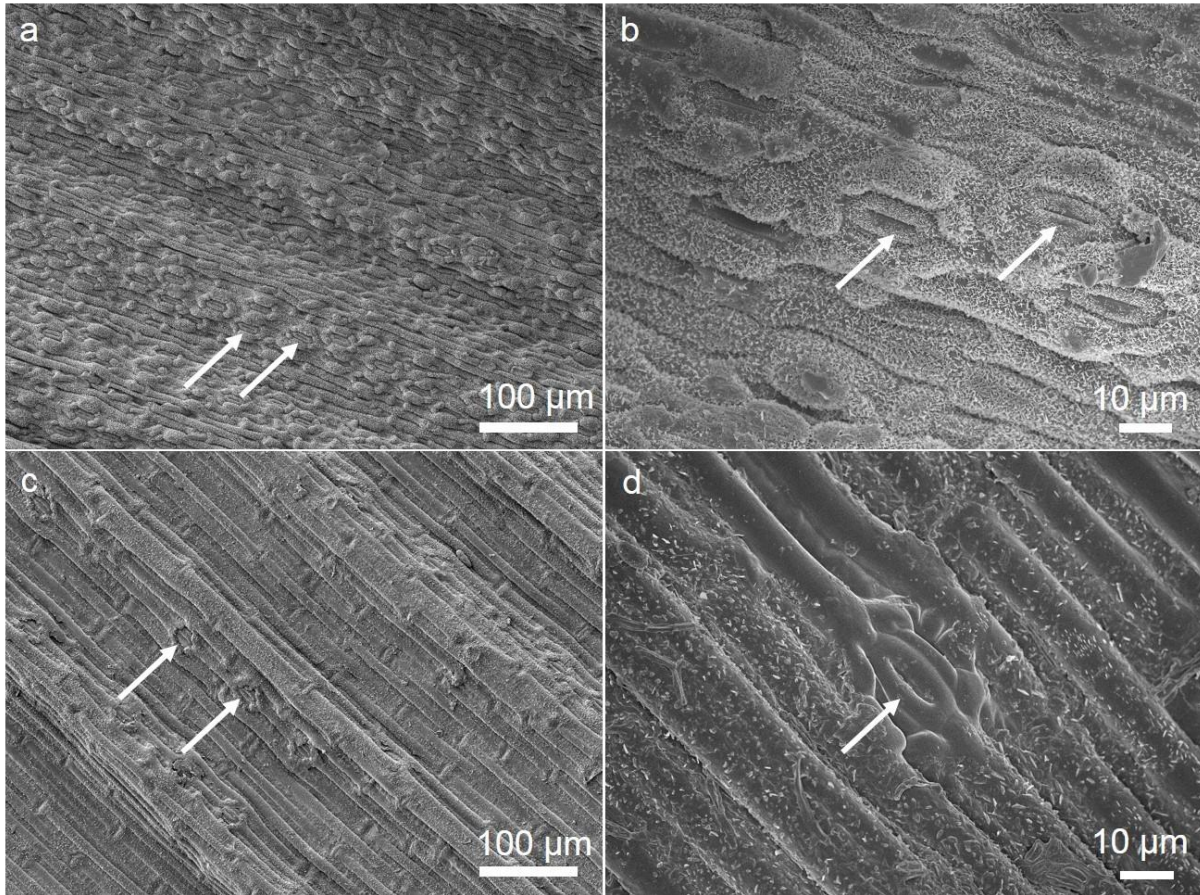


Figure 67. The native adaxial (a,b) and abaxial (c,d) leaf surface of *Sesleria albicans*. Stomata occurred on both leaf surfaces and are indicated by arrows. The epicuticular wax structure were platelets, the main component class of the cuticular wax were *n*-alkanes (*n*-nonacosane) followed by primary alkanols (hexacosanol). Platelets are a common wax type and the dominating component described are primary alkanols, such as hexacosanol (Koch *et al.* 2009).

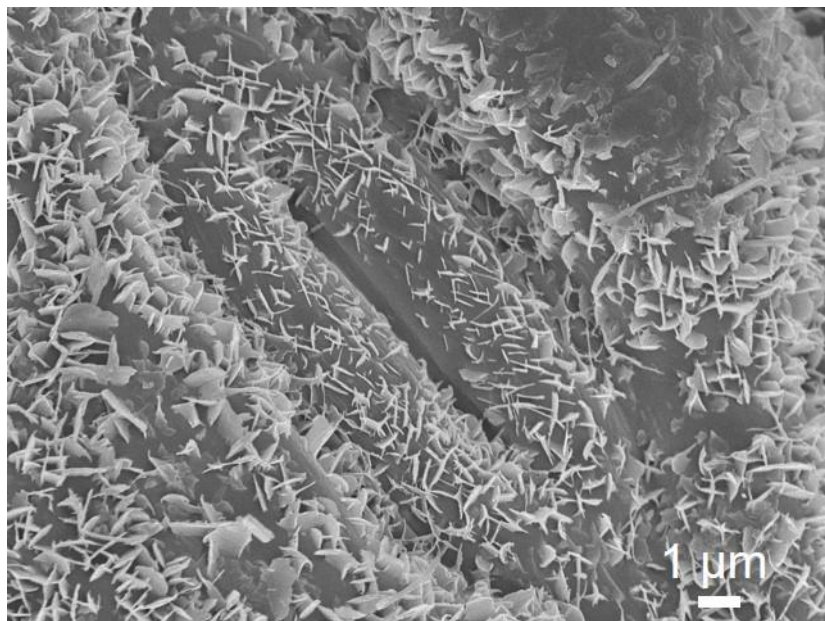


Figure 68. Detailed view of the epicuticular wax structures on the adaxial leaf surface of *Sesleria albicans*.

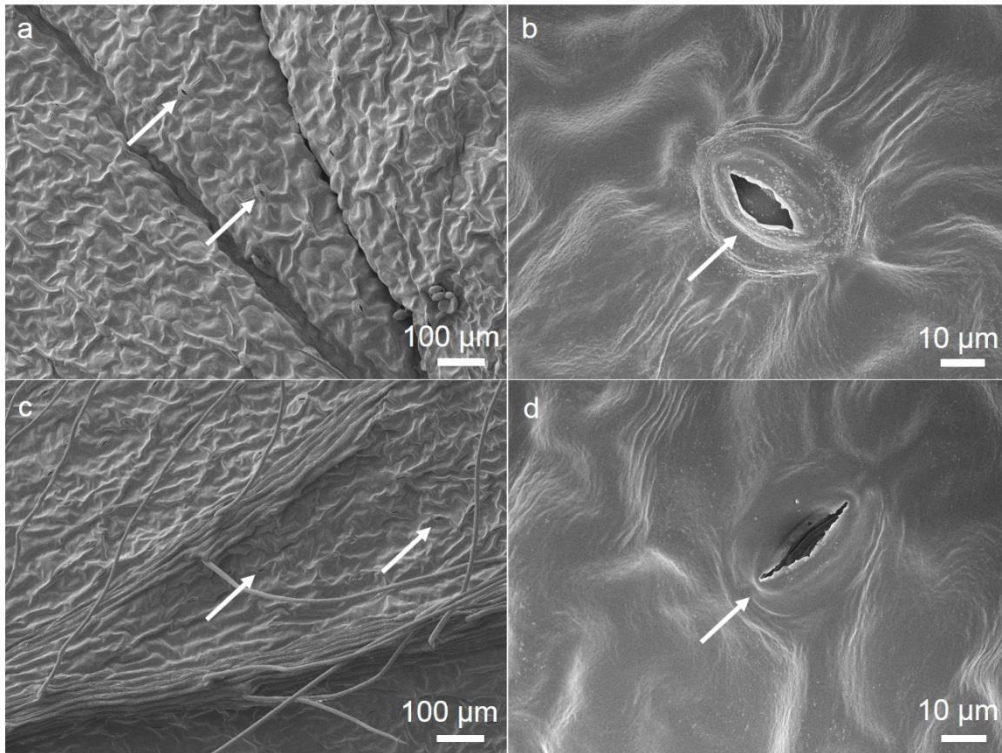


Figure 69. The native adaxial (a,b) and abaxial (c,d) leaf surface of *Pulsatilla vulgaris*. Stomata occurred on both leaf surfaces and are indicated by arrows. The abaxial leaf surface showed foliar trichomes. A wax film covered the leaf surface.

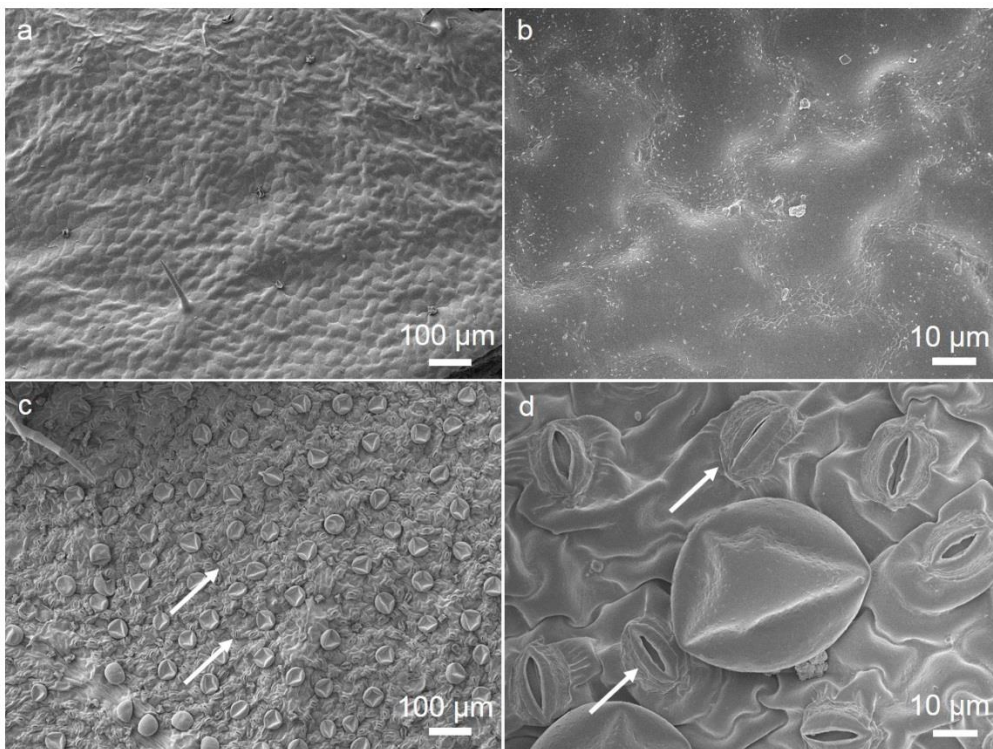


Figure 70. The native adaxial (a,b) and abaxial (c,d) leaf surface of *Teucrium chamaedrys*. Stomata occurred on the abaxial leaf surface and are indicated by arrows. The lower leaf surface is covered by glandular trichomes (Grubešić *et al.* 2007) and both leaf surfaces showed foliar trichomes.

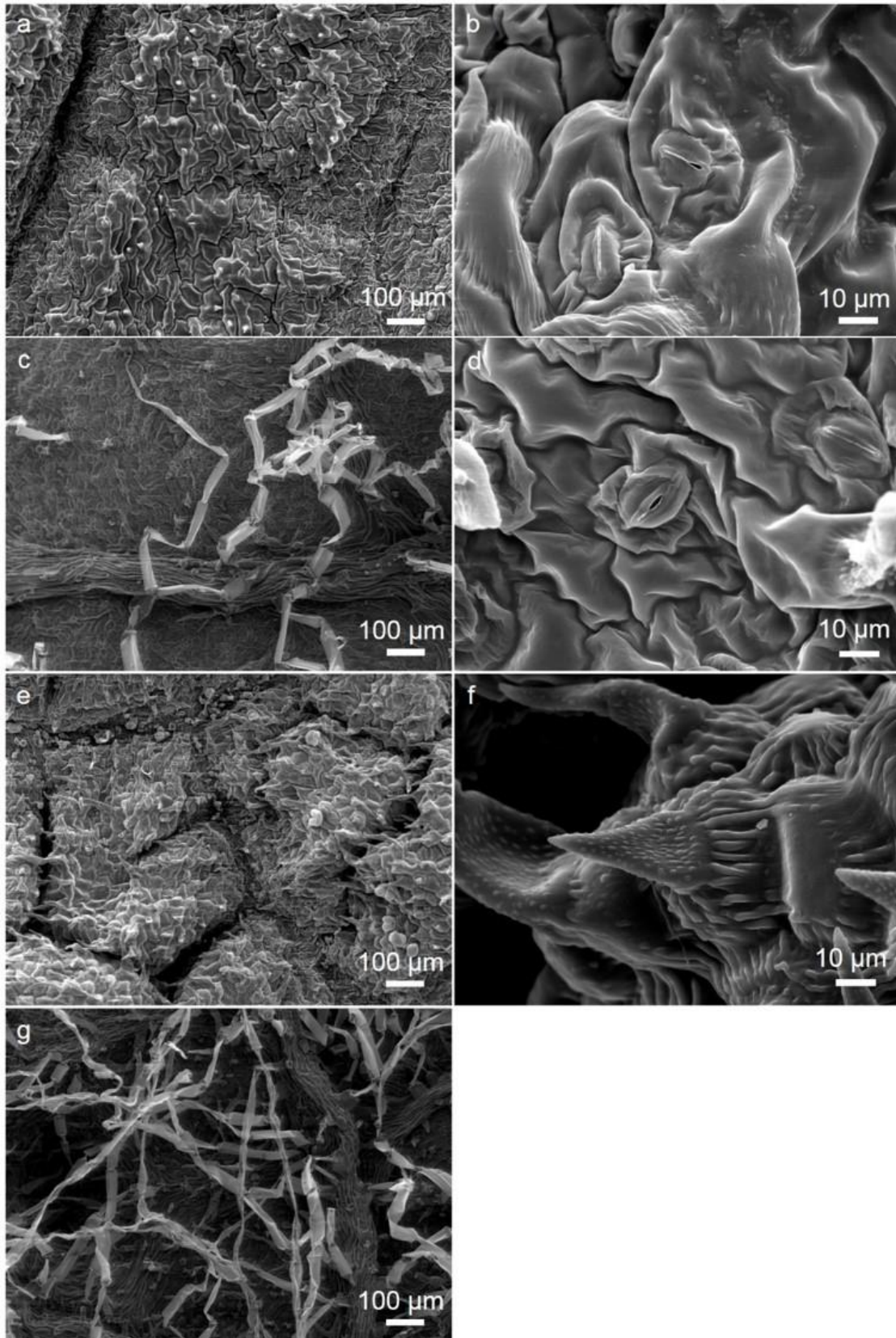


Figure 71. The native (a,b) adaxial and (c,d) abaxial leaf surface of the mesophytic *Salvia pratensis* and the native (e,f) adaxial and (g) abaxial leaf surface of the xerophytic *Salvia pratensis*. Stomata occurred on both leaf surfaces. The abaxial leaf surfaces showed foliar trichomes. A wax film covered the leaf surface.

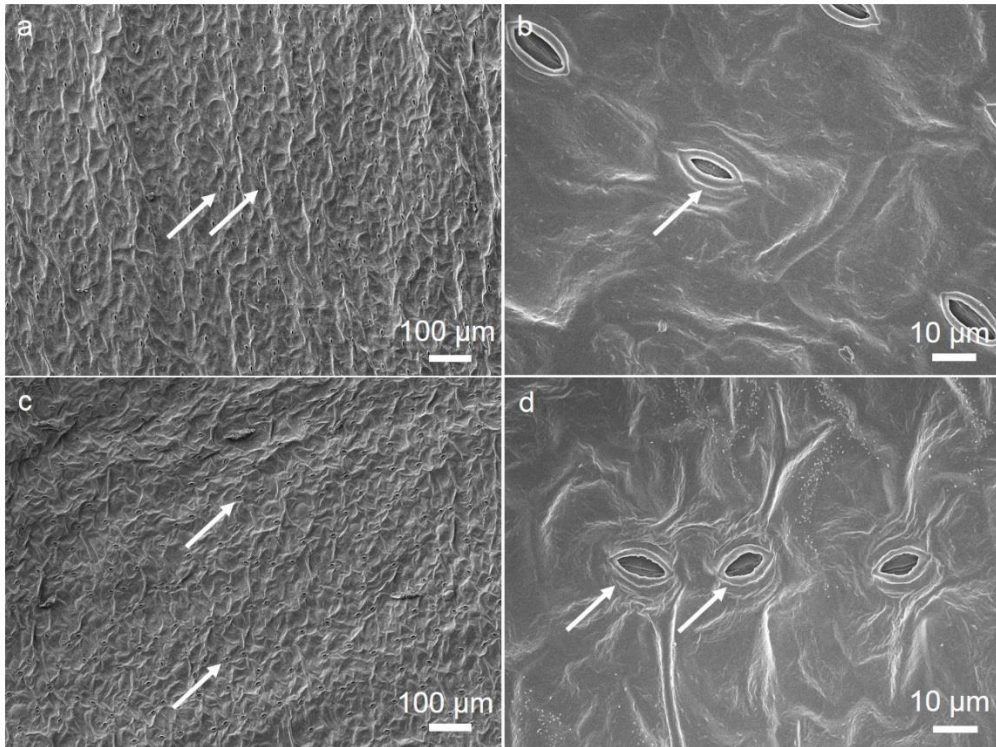


Figure 72. The native adaxial (a,b) and abaxial (c,d) leaf surface of *Plantago lanceolata*. Stomata occurred on both leaf surfaces and are indicated by arrows. A wax film covered the leaf surface.

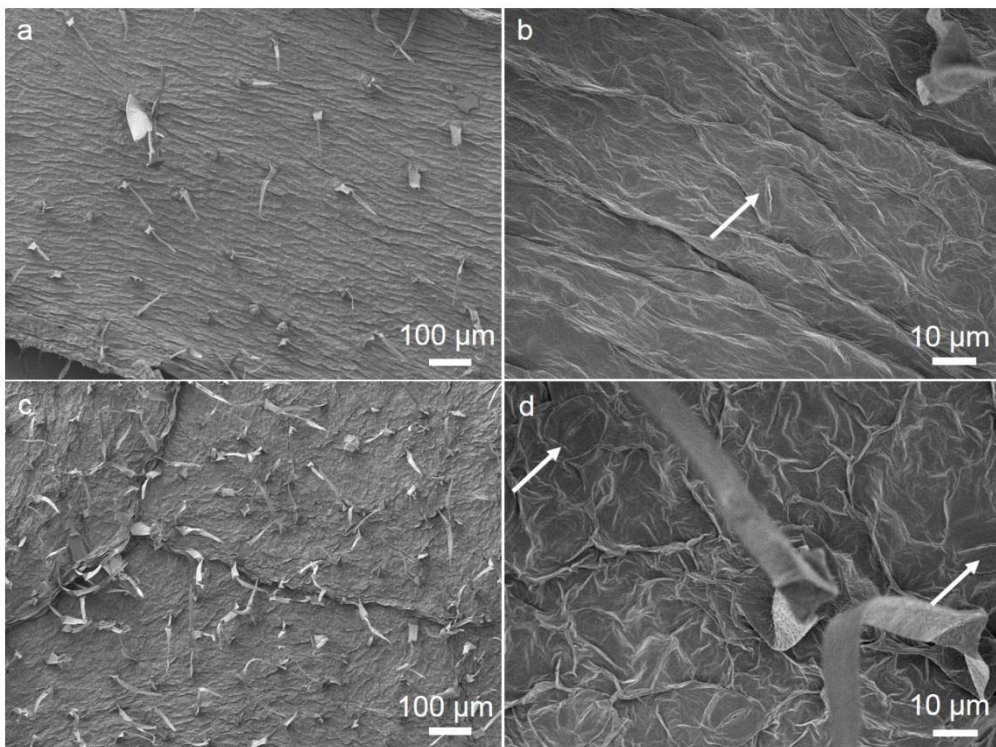


Figure 73. The native adaxial (a,b) and abaxial (c,d) leaf surface of *Solanum lycopersicum*. Stomata occurred on both leaf surfaces and are indicated by arrows. Both leaf surfaces showed foliar trichomes. A wax film covered the leaf surface.

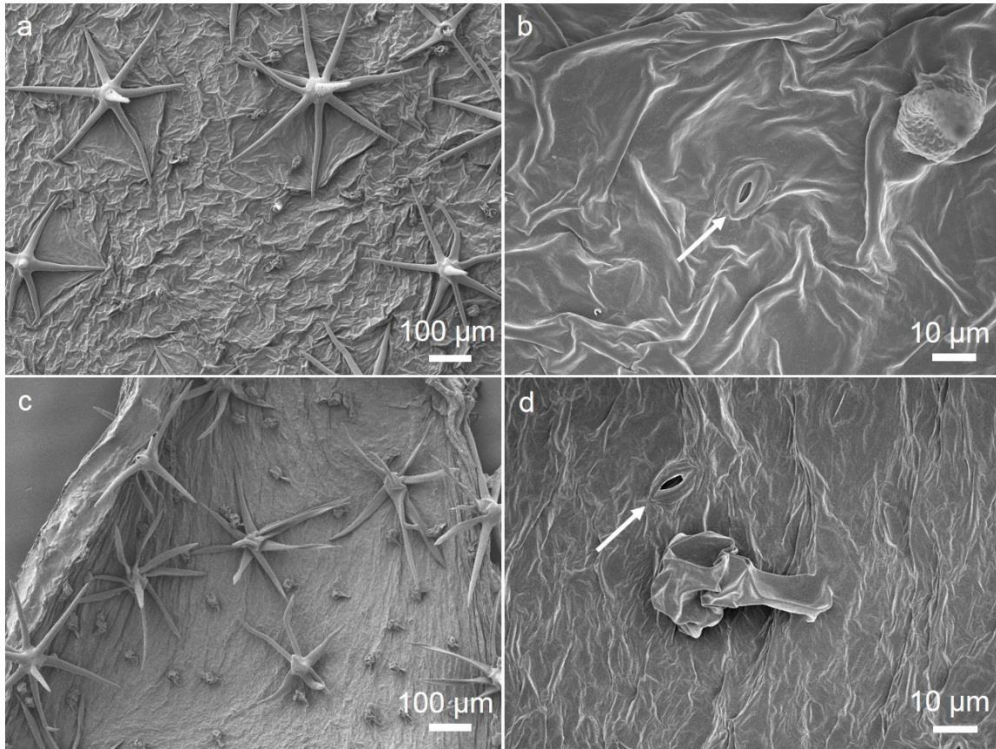


Figure 74. The native adaxial (a,b) and abaxial (c,d) leaf surface of *Solanum surratense*. Stomata occurred on both leaf surfaces and are indicated by arrows. Both leaf surfaces showed foliar stellate trichomes. A wax film covered the leaf surface.

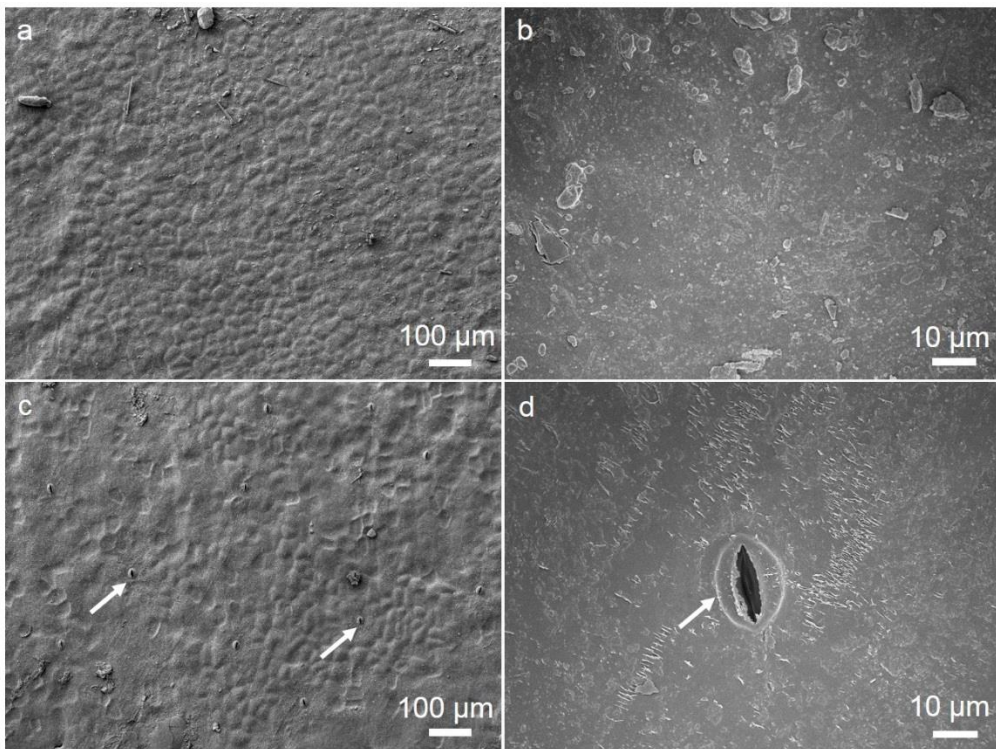


Figure 75. The native adaxial (a,b) and abaxial (c,d) leaf surface of *Vanilla planifolia*. Stomata occurred on the abaxial leaf surface and are indicated by arrows. The adaxial epicuticular waxes had an irregularly granulated structure. The abaxial epicuticular waxes showed platelets.

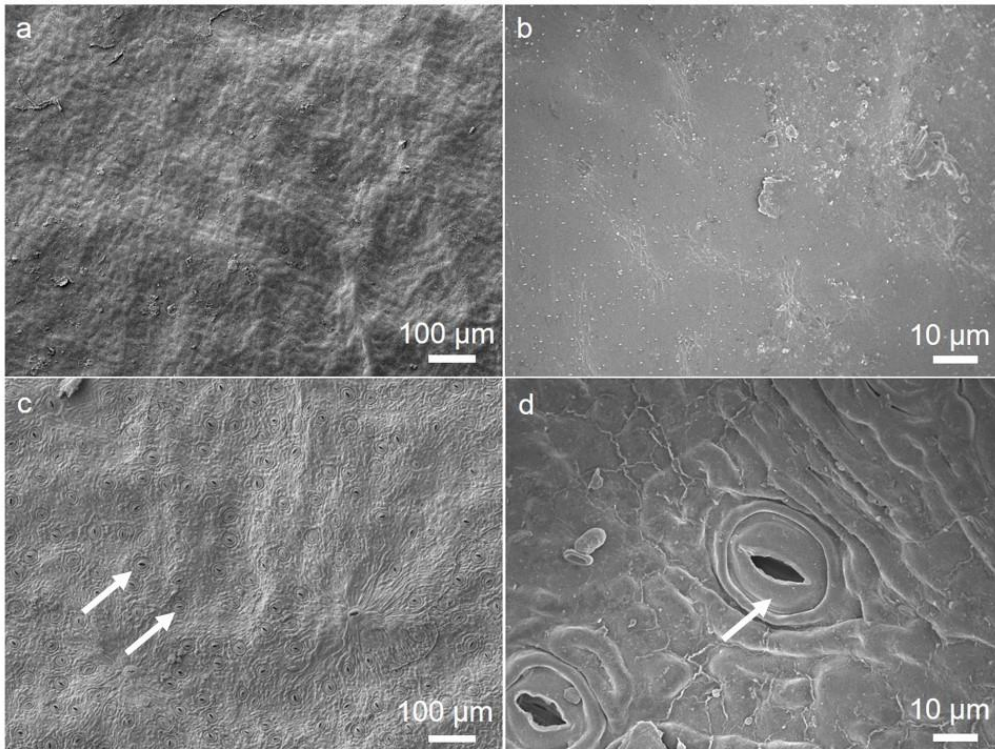


Figure 76. The native adaxial (a,b) and abaxial (c,d) leaf surface of *Prunus laurocerasus*. Stomata occurred on the abaxial leaf surface and are indicated by arrows. The epicuticular waxes had an irregularly granulated structure (Jetter *et al.* 2000) and were described as wax films (Koch *et al.* 2009).

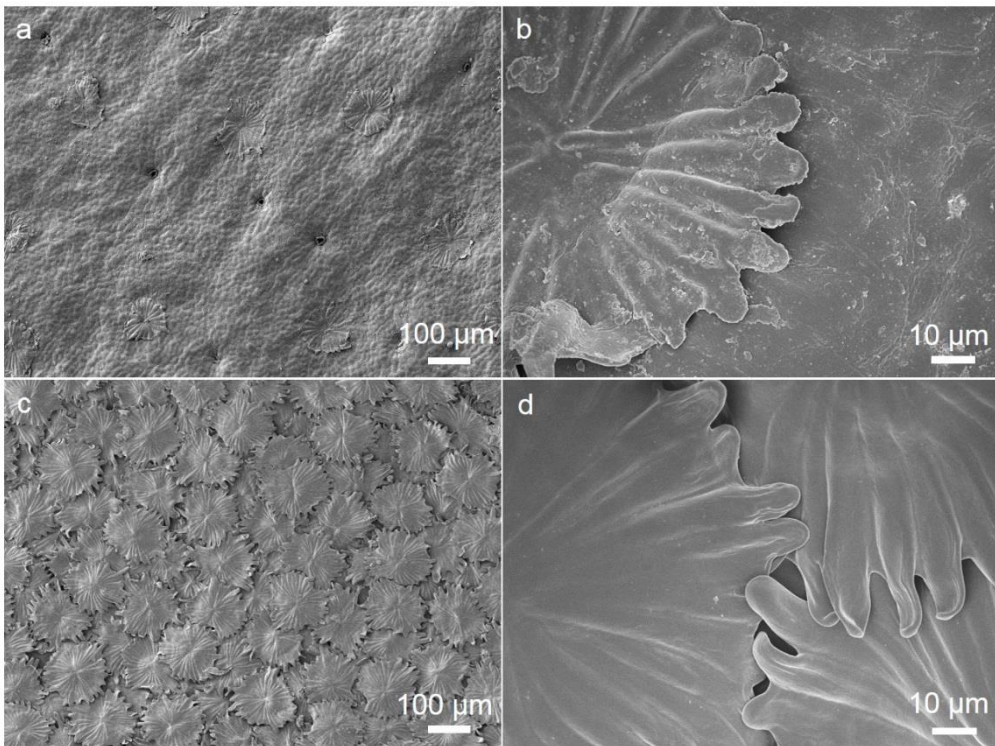


Figure 77. The native adaxial (a,b) and abaxial (c,d) leaf surface of *Olea europaea*. Stomata occurred on the abaxial leaf surface, the leaves are hypostomatic. Both leaf surfaces showed peltate hairs, the abaxial leaf surface is completely covered (Levizou *et al.* 2004).

Publications and presentations

Publications

Riederer M, Arand K, Burghardt M, Huang H, Riedel M, Schuster AC, Smirnova A, Jiang Y (2015) Water loss from litchi (*Litchi chinensis*) and longan (*Dimocarpus longan*) fruits is biphasic and controlled by a complex pericarpal transpiration barrier. *Planta* 242, 1207-1219

Schuster AC, Burghardt M, Alfarhan A, Bueno A, Hedrich R, Leide J, Thomas J, Riederer M (2016) Effectiveness of cuticular transpiration barriers in a desert plant at controlling water loss at high temperatures. *AoB Plants*, under revision.

Presentations at conferences

Schuster AC, Burghardt M, Thomas J, Alfarhan A, Riederer M (2013) Cuticular transpiration control of *Rhazya stricta* Decne. in the hot and dry climate of Saudi Arabia. Deutsche Botanikertagung in Tübingen, Deutschland

Schuster AC, Burghardt M, Thomas J, Alfarhan A, Riederer M (2013) Cuticular transpiration control of *Rhazya stricta* Decne. in the hot and dry climate of Saudi Arabia. Scientific Crosstalk Symposium in Würzburg, Deutschland

Schuster AC, Burghardt M, Thomas J, Alfarhan A, Riederer M (2015) Cuticular wax composition of *Rhazya stricta* leaves growing in a hot and dry desert climate. „Plant Waxes: From Biosynthesis to Burial“ Tagung in Ascona, Schweiz

Curriculum vitae

Acknowledgements

Affidavit

I hereby confirm that my thesis entitled “Chemical and functional analyses of the plant cuticle as leaf transpiration barrier“ is the result of my own work. I did not receive any help or support from commercial consultants. All sources and/or materials applied are listed and specified in the thesis.

Furthermore, I confirm that this thesis has not yet been submitted as part of another examination process neither in identical nor in similar form.

Würzburg,

Place, Date

Signature

Eidesstattliche Erklärung

Hiermit erkläre ich an Eides statt, die Dissertation „Chemie-Funktionsanalysen der pflanzlichen Kutikula als Transpirationsbarriere“ eigenständig, d.h. insbesondere selbstständig und ohne Hilfe eines kommerziellen Promotionsberaters, angefertigt und keine anderen als die von mir angegebenen Quellen und Hilfsmittel verwendet zu haben.

Ich erkläre außerdem, dass die Dissertation weder in gleicher noch in ähnlicher Form bereits in einem anderen Prüfungsverfahren vorgelegen hat.

Würzburg,

Ort, Datum

Unterschrift